DISSERTATION

Submitted to the
Combined Faculties for the Natural Science and for Mathematics
of the Ruperto-Carola University of Heidelberg, Germany
for the degree of
Doctor of Natural Science

Presented by
M.Sc. Firat Nebioglu
Born in Izmir, Turkey
Oral-examination 02.12.2021

HOST FACTORS ASSOCIATED WITH HEPATITIS B VIRUS LIFE-CYCLE: INSIDE AND OUT

Referees:

Prof. Dr. Ralf Bartenschlager

Prof. Dr.Stephan Urban

The applicant, Firat Nebioglu, declares that he is the sole author of the submitted dissertation and no other sources or help from those specifically referred to have been used. Additionally, the applicant declares that he has not applied for permission to enter examination procedure at another institution and this dissertation has not been presented to other faculty and not used in its current or in any other form in another examination.

……..... ……

Date Signature

I. Acknowledgement

First of all, I would like to thank Prof. Dr. Ralf Bartenschlager for allowing me to pursue an exciting Ph.D project in his lab. Since the first day, I could feel the trust and the confidence he put in me which has been instrumental for my scientific development. There are not many places in the world where your mentor gives you the freedom to follow your ideas in a Ph.D study. I am grateful for having this privilege.

I want to thank Prof. Dr. Stephan Urban and his lab members for accepting me to their internal lab meetings and the most importantly, for the great scientific discussions I have been exposed in these meetings.

I would like to give my sincere thanks to Dr.Stephan Seitz for sharing his vast knowledge in HBV biology with me. His support let me build my resilience in difficult situations.

I would like to thank Prof. Dr. Martin Müller and Dr.Viet Loan Dao Thi for accepting to be part of my Ph.D defense committee.

Next, I would like thank to former and current colleagues in the department for contributing to the great teamwork atmosphere. I would especially thank the following people for their helps in experiment, proof-reading of my thesis, or the time we spent together outside of the lab: Pascal Mutz, Nadine Gillich, Agnieszka Plociennikowska, Julita Mikulec, Aditi Dhawan, Anastasia Demshina, Anna-Clara Franke, Josef Vaas, Shangqing Yang, Michael Bonadonna, and Berati Cerikan.

Basta esim ve ulkemdeki ailem olmak uzere, benden desteklerini esirgemeyen ve hep yanimda olan ailemin butun fertlerine tesekkur ederim. Sart kosmadan ve cikar gutmeden daima yanimda olacak insanlarin oldugunu bilmek en buyuk mutlulugum.

II. Abstract

An estimated 257 million people are chronically infected with hepatitis B virus (HBV), which is a major cause of mortality among viral hepatitis related deaths despite the availability of a safe and effective vaccine. Current antiviral therapies against HBV focus on the suppression of viral replication and although improving the quality of life and long-term survival of patients this therapy only rarely leads to functional cure. To comply with the goals of WHO (summarized in "Global Health Sector Strategy on viral hepatitis"), more potent HBV therapeutics are needed and thus, a better understanding of the basics of HBV biology is essential to explore novel antiviral strategies. Hepatocytes infected with HBV contain highly stable episomal viral genomes, called covalently closed circular DNA (cccDNA), acting as a template for the synthesis of all viral transcripts. In addition, genomic integration of replication-defective, partial HBV genomes is frequently observed early after infection, which is thought to contribute to the chronicity of hepatitis B by providing a stable reservoir for the production HBV antigens.

The aim of my thesis was to delineate host cell factors contributing to the HBV replication cycle. To this end, I addressed two specific aspects: First, to identify host factors modulating the secretion of subviral particles (SVPs) that originate from sub-genomic HBV integrates; second, to determine host factors incorporated into HBV virions and subviral particles in the course of particle morphogenesis.

With respect to the first aim, I conducted an RNAi-based mini-screen using a custom-made library. I found that the neddylation pathway components Nedd8 and Ube2m are required for hepatitis B surface antigen (HBsAg). Knock-down of these components or pharmacological inhibition with the small molecule neddylation inhibitor MLN4924 inhibited the secretion of HBsAg. Previously, MLN4924 was reported to re-instate an epigenetic cccDNA silencing complex called Smc5/6 (structural maintenance of chromosomes complex 5/6) by preventing its HBx dependent degradation. I found that in addition, neddylation also contributes to the secretion of HBsAg from integrated HBV genome sequences in an HBx-independent manner.

To sum up, my siRNA screen identified a previously unknown role of the neddylation pathway on HBsAg secretion that is independent of cccDNA.

In the second part of my thesis, I established a protocol combining affinity chromatography, size exclusion chromatography, isopycnic centrifugation, and HBsAg immune-precipitation to enrich HBV particles and SVPs derived from two independent cell lines. Obtained particles

were analyzed by mass spectrometry to determine their proteome. In this way, we identified approximately 160 proteins associated with both particle fractions, 6 of them exclusively detected in HBV virions. In addition to the previously published HBV associated proteins, we could identify numerous novel host factors, laying the ground for mechanistic follow-up studies and the possible use of identified host factors as targets for novel antiviral therapy.

III. Zusammenfassung

Schätzungsweise 257 Millionen Menschen sind chronisch mit dem Hepatitis-B-Virus (HBV) infiziert, das trotz der Verfügbarkeit eines sicheren und wirksamen Impfstoffs eine der Hauptursachen für Todesfälle im Zusammenhang mit viraler Hepatitis ist. Die derzeitigen antiviralen Therapien gegen HBV konzentrieren sich auf die Unterdrückung der viralen Replikation, und obwohl sie die Lebensqualität und das langfristige Überleben der Patienten verbessern, führt diese Therapie nur selten zu einer funktionellen Heilung. Um die Ziele der WHO (zusammengefasst in der "Global Health Sector Strategy on viral hepatitis") zu erreichen, werden wirksamere HBV-Therapeutika benötigt, und daher ist ein besseres Verständnis der Grundlagen der HBV-Biologie für die Erforschung neuer antiviraler Strategien unerlässlich. HBV-infizierte Hepatozyten enthalten hochstabile episomale virale Genome, so genannte kovalent geschlossene zirkuläre DNA (cccDNA), die als Vorlage für die Synthese aller viralen Transkripte dienen. Darüber hinaus wird die genomische Integration von replikationsdefekten, partiellen HBV-Genomen häufig schon früh nach der Infektion beobachtet, was vermutlich zur Chronizität von Hepatitis B beiträgt, da es als stabiles Reservoir für die Produktion von HBV-Antigenen dient.

Ziel meiner Arbeit war es, die Wirtszellfaktoren zu beschreiben, die zum HBV-Replikationszyklus beitragen. Zu diesem Zweck habe ich zwei spezifische Aspekte untersucht: Erstens, die Identifizierung von Wirtsfaktoren, die die Sekretion subviraler Partikel (SVPs) modulieren, die aus subgenomischen HBV-Integraten entstehen; zweitens, die Bestimmung von Wirtsfaktoren, die im Verlauf der Partikelmorphogenese in HBV-Virionen und subvirale Partikel eingebaut werden.

Im Hinblick auf das erste Ziel habe ich einen RNAi-basierten Mini-Screen mit einer maßgeschneiderten Bibliothek durchgeführt. Ich fand heraus, dass die Komponenten des Neddylierungsweges Nedd8 und Ube2m für das Hepatitis-B-Oberflächenantigen (HBsAg) erforderlich sind. Der Knock-down dieser Komponenten oder die pharmakologische Hemmung mit dem niedermolekularen Neddylierungsinhibitor MLN4924 hemmte die Sekretion von HBsAg. Zuvor wurde berichtet, dass MLN4924 einen epigenetischen cccDNA-Silencing-Komplex namens Smc5/6 (structural maintenance of chromosomes complex 5/6) wiederherstellt, indem es dessen HBx-abhängigen Abbau verhindert. Ich fand heraus, dass die Neddylierung auch zur Sekretion von HBsAg aus integrierten HBV-Genomsequenzen auf HBx-unabhängige Weise beiträgt.

Zusammenfassend lässt sich sagen, dass mein siRNA-Screen eine bisher unbekannte Rolle des Neddylierungsweges bei der HBsAg-Sekretion identifiziert hat, die unabhängig von cccDNA ist.

Im zweiten Teil meiner Arbeit habe ich ein Protokoll entwickelt, das Affinitätschromatographie, Größenausschlusschromatographie, isopyknische Zentrifugation und HBsAg-Immunpräzipitation kombiniert, um HBV-Partikel und SVPs aus zwei unabhängigen Zelllinien anzureichern. Die so gewonnenen Partikel wurden mittels Massenspektrometrie analysiert, um ihr Proteom zu bestimmen. Auf diese Weise identifizierten wir etwa 160 Proteine, die mit beiden Partikelfraktionen assoziiert sind, wobei 6 von ihnen ausschließlich in HBV-Virionen nachgewiesen wurden. Zusätzlich zu den bereits veröffentlichten HBV-assoziierten Proteinen konnten wir zahlreiche neue Wirtsfaktoren identifizieren, die die Grundlage für mechanistische Folgestudien und die mögliche Verwendung identifizierter Wirtsfaktoren als Ziele für neue antivirale Therapien bilden.

IV. Content

V. Figures

VI. Tables

VII. Abbreviations

aa	Amino acids
AASLD	American Association for the Study of Liver Diseases
AGL	Antigenic loop
ALIX	ALG-2 interacting protein X
ALT	Alanine amino transferase
anti-HBc	Hepatitis B core antibody
Apo	Apolipoprotein
APS	Ammonium persulfate
ASGPR	Asialoglycoprotein receptor
ASO	Anti-sense oligonucleotide
BFA	Brefeldin A
bp	Base pair
BSA	Bovine serum albumin
CAD	Cytosolic anchorage site
CASP14	Caspase14
cccDNA	Covalently closed circular DNA
cDNA	Complementary deoxyribonucleic acid
CHB	Chronic hepatitis B
CHMP3	Charged MVB protein 3
CME	Clathrin mediated endocytosis
CpAMs	Capsid protein assembly modulators
CRISPR	Clustered regularly interspaced short palindromic repeats
CRLs	Cullin ring ubiquitin ligases
CTD	C-terminal domain
CWF19L2	CWF19 Like Cell Cycle Control Factor 2
CYL-I	cytosolic loop-I
Da	Dalton
DAAs	Direct acting antivirals
DNA	Deoxyribonucleic acid
DCAF	DDB1 and CUL4 associated factor
DDB1	DNA damage-binding protein 1
ddH2O	Double distilled water
DHBV	Duck hepatitis B virus
DIG	Digoxigenin
DMEM	Dulbecco's Modified Eagle Medium
DMSO	Dimethyl sulfoxide
DNMTs	DNA methyltransferases
dNTP	Deoxynucleoside triphosphate
DOX	Doxycycline
DR	Direct repeat
dslDNA	Double stranded linear DNA
EASL	European Association for the Study of the Liver
ECL	Enhanced chemiluminescence
EDTA	Ethylenediaminetetraacetic acid
EGFR	Epidermal growth factor receptor
EGTA	Egtazic acid
ELISA	Enzyme-linked immunosorbent assay
EM	Electron microscopy
Enh	Enhancer
ER	Endoplasmic reticulum

ERGIC	ER-Golgi intermediate compartment
ESCRT	Endosomal sorting complexes required for transport
ETV	Entecavir
FCS	Fetal calf serum
FEN1	Flap structure specific endonuclease 1
FLUC	Firefly luciferase
FXR	farnesoid X receptor
GAG	Glycosaminoglycan
Gapdh	Glyceraldehyde 3-phosphate dehydrogenase
GenD	Genotype D
H1	HiTrap Heparin HP affinity columns (5mL)
H5	HiTrap Heparin HP affinity columns (5mL)
HAPs	Heteroarylpyrimidines
HAV	Hepatitis A virus
HBc	HBV core protein
HBcrAg	HBV core related antigen
HBDSP	Hepatitis B doubly spliced protein
HBeAg	hepatitis B e-antigen
HBsAg	Hepatitis B surface antigen
HBSP	Hepatitis B spliced protein
HBV	Hepatitis B virus
HBx	HBV X protein
HCl	Hydrochloric acid
HCV	Hepatitis C virus
HDAC1	Histone deacetylates 1
HDV	Hepatitis D virus
HEV	Hepatitis E virus
HIV	Human immunodeficiency virus
HNRNPC	Heterogeneous Nuclear Ribonucleoprotein C
HRP	Horseradish peroxidase
HSP90AB1	Heat Shock Protein 90 Alpha Family Class B Member 1
HSPGs	Heparan sulfate proteoglycans
IAV	Influenza A virus
iBAQ	Intensity based absolute quantification
IFNa	Interferon-α
IgG	Immunoglobulin G
IGL	Immuno-gold Labeling
IP	Immuno-precipitation
ISGs	Interferon stimulating genes
IU/mL	International unit/milliliter
k	kilo
LB	Luria-Bertani medium
LC-MS/MS	Liquid Chromatography with tandem mass spectrometry
LFQ	Label-free quantitation
LIG1	DNA ligase 1
LIG3	DNA ligase 3
LMO7	LIM Domain 7
MOA	Mode of action
MVB	Multivesicular body
NAE1	Nedd8 E1 activating enzyme

NAPs	Nucleic acid polymers	PRC	Polycomb repressive complex
NAs	Nucleos(t)ide analogs	P-S FP	Polymerase-surface fusion protein
Nedd4	Neural Precursor Cell Expressed, Developmentally Down-Regulated 4	qPCR	Quantitative PCR
Nedd8	Neural Precursor Cell Expressed, Developmentally Down-Regulated 8	rcDNA	Relaxed circular DNA
NH4Cl	Ammonium chloride	RFC	Replication factor C
NK	Natural killer	RING	Really Interesting New Gene
NTCP	Sodium taurocholate cotransporting polypeptide	RNA	Ribonucleic acid
ºC	Celsius	RNAi	RNA interference
OD	Optical density	RRL	Rabbit reticulocyte lysate
ORFs	Open reading frames	RT	Room temperature/Reverse transcription/Reverse transcriptase
PAGE	Polyacrylamide gel electrophoresis	RXRα	retinoid X receptor alpha
PBS	Phosphate Buffered Saline	S6	Superose 6
PCNA	Proliferating cell nuclear antigen	SBSN	Suprabasin
PCR	Polymerase chain reaction	SD	Standard deviation
PDI	Protein disulfide isomerase	SDS	Sodium dodecyl sulfate
PFA	Paraformaldehyde	SEC	Size exclusion chromatography
pgRNA	Pregenomic RNA	siRNAs	Small interfering RNAs
pH	Power of hydrogen	SMC5	Structural maintenance of chromosome 5
PHH	Primary human hepatocytes	ssDNA	Single-stranded DNA
POLA1	DNA polymerase alpha	SVPs	Subviral lipoprotein particles
POLH	DNA polymerase eta	SVR	Sustained virological response
POLK	DNA polymerase kappa	TAE	Tris-Acetate-EDTA
POLL	DNA polymerase lambda	TAF	Tenofovir alafenamide
PPARα	Peroxisome proliferator-activated receptor alpha	TALENs	Transcription-activator like effector nucleases

TDF	Tenofovir disoproxil fumarate	TP	Terminal protein
TEMED	Tetramethylethylenediamine	TP53	Tumor protein 53
TfB	Transformation buffer	TRIM	Tipartite motif
TGS	Tris-Glycine-SDS	UA	Uranyl-Acetate
TM	Transmembrane domain	WB	Western Blot
TN	Tris-NaCl	WHO	World Health Organization
TOP1	DNA topoisomerase I	WST-1	Water-soluble tetrazolium salts 1
TOP2	DNA topoisomerase II	ε	Epsilon

1 Introduction

1.1 Global Burden of Hepatitis Viruses

Viral hepatitis is one of the major causes of liver-related death worldwide. The studies of global burden of disease revealed viral hepatitis as the seventh leading cause of death with; liver cirrhosis and liver cancer accounting for the majority of the mortality[1] . The global death toll of viral hepatitis is estimated as 1.4 million in 2017, exceeding the number of deaths from malaria (0.62 million), tuberculosis (1.18 million), and human immunodeficiency virus (HIV) infections (0.95 million)[2]. The projectile of viral hepatitis mortality surpasses the cumulative mortality of tuberculosis, malaria, and HIV in 2040[3], urging to implement elimination strategies of viral hepatitis. In May 2016, the global health sector strategy on the elimination of viral hepatitis by 2030 was accepted, aiming to reduce mortality by 65% and incidence rate by 90% relative to the 2015 baseline. The common sources of viral hepatitis are five hepatotropic viruses: hepatitis A virus (HAV), hepatitis B virus (HBV), hepatitis C virus (HCV), hepatitis D virus (HDV), and hepatitis E virus (HEV). According to 2015 baseline estimates of the WHO, 96% of the viral hepatitis mortality is due to HBV- and HCV-associated long-term complications such as cirrhosis and hepatocellular carcinoma[4]. The minority of deaths results from acute hepatitis by HAV and HEV infection, which account for 4% of the viral hepatitis deaths.

Hepatitis A virus (HAV) is a single-stranded, positive sense RNA virus that transmits through the fecal-oral route or person-person contact in places with poor sanitary conditions and high density of housing[5]. 15 million people are estimated to be infected annually, with 1.5 million symptomatic patients and 11,000 death cases due to acute liver failure[4,6]. HAV infections are mostly asymptomatic, making the current epidemiologic data likely an underestimate. Endemic regions of the HAV are categorized into levels of low, medium, and high according to the prevalence rate of anti HAV-IgG in human serum of the population. South Asia and Sub-Saharan Africa have high endemicity to HAV with more than 50% seropositivity[7]. Development in socioeconomic status, adequate sanitation, and hygiene conditions decreases HAV endemicity to low levels of <15% as in Northern America and most of the European countries. This poses a potential issue of lack of population immunity that can increase the rate of symptomatic sequela of HAV among infected people, especially in older persons[8,9]. An HAV

vaccine is available on the market in both attenuated live and formalin-inactivated forms, protectecting against HAV infections at least for 8 years[6,10]. HAV particles are resistant to inactivation by low pH, freezing, drying, or moderate heat which is conferring easy transmission on the surface of food products and contaminated water supplies[11]. With the globalization of the world food supply and enhanced mobility of the travelers, transmission, and spread of HAV in low-endemic regions poses public health threat.

Another foodborne virus, HEV, is an RNA virus having a positive sense, single-stranded genome. Infections with HEV are generally asymptomatic, only rarely resulting in acute hepatitis that accounted for 44,000 death in 2015[4]. HEV infections can lead to serious consequences in certain risk groups, such as pregnant women and immune-compromised patients. The fatality rate of HEV infections is 0.1% in healthy individuals but increases to 25% for women infected during the 3rd trimester of pregnancy[12]. As an enteric virus, a common transmission way of HEV in developing countries is contaminated water supplies due to poor sanitation. On the other hand, the zoonotic nature of certain HEV genotypes can cause sporadic cases in developed/industrialized countries. Pigs, wild boar, deer, rabbit, sheep, and goat have been shown to be a reservoir for HEV. HEV infection from animal products has been reported. High seroprevalence of the virus was observed as high as 90% in pig farms, where the viremia detected ranging between 0.5% to 3.8% during slaughtering[13-16]. HEV infections in immuno-compromised patients, generally recipients of organ transplants, can develop into chronic infections[17,18]. Ribavirin is the treatment of choice in most of the chronic HEV cases. Currently, the only vaccine against HEV is licensed in China[19].

One of the major causative agents of viral hepatitis is HCV that is an RNA virus with positive sense, single-stranded genome. According to WHO viral hepatitis report, it is estimated that 71 million persons were chronically infected with HCV in 2015 and of which just 20% (14 million) was aware of their disease and, only 7% of those diagnosed (1.1 million) were treated with antiviral therapy[4]. HCV prevalence is heterogeneously distributed around the world, which is around 1.1% globally[20]. HCV is a bloodborne virus, acute infections of it are generally asymptomatic, and the rate of conversion to chronic state is high after 6 months. Approximately, 75% of the infected persons older than 20 years develop chronic HCV infection[21]. The chronic inflammation caused by HCV accounted for 400,000 death in 2015 due to cirrhosis and hepatocellular carcinoma. 1.7 million persons are estimated to be chronically infected annually[4]. A vaccine against HCV is not yet available but direct acting antivirals (DAAs) are highly effective with a very high rate of sustained virological response (SVR) in more than 90% of the patients. Compared to previously used less effective interferon treatments, DAAs are

accompanied with fewer side effects[22]. In general, the treatment duration lies between 8-12 weeks, however even shorter treatment strategies are already in clinical trials[23]. To comply with WHO's 2030 goals, prevention of the new incidences by harm reduction interventions, decreased unsafe health-care associated injections and surveillance in HCV risk groups are crucial.

Among the hepatitis viruses, the heaviest burden is posed by HBV with 257 million chronically infected people globally in 2015[4]. The estimated number of people under antiviral treatment was just 1.72 million people in 2015[4]. The prevalence rate is estimated by seropositivity for HBsAg, which globally approximated as 3.6%. The most affected regions of the world are Western Pacific and Africa, where prevalences are as high as 5.3% and 8.8% of the population[24]. HBV transmission differs between highly endemic and low endemic regions of the world. In the high endemic regions, prevalence rate exceed 8% of the population, where perinatal and horizontal transmission of the disease is widespread[25,26]. However, in low endemic areas with prevalence rate lower than 2%, horizontal transmissions are predominant [27,28]. The progression rate of HBV infections from acute to chronic state is age dependent. Infants below 1 year age develop chronic HBV infection in >90% of the cases, while that rate decreases to 5% in HBV infected adults[29]. HBV-associated mortality usually results from late complications such as cirrhosis and liver cancer, being responsible for approximately 890,000 death cases in 2015[4]. Infections of HBV can cause acute liver failure in the minority of cases (1%), which is a life-threatening condition that necessitates liver transplantation as a medical treatment[30]. An efficient vaccine against HBV is available for a long time and integration of the global vaccination program increased the amount of vaccinated infants to 84% in 2015. It is estimated that 83% of new cases have been prevented by the vaccine between 1990 and 2020, corresponding to approximately 310 million HBV incidences[31]. According to WHO, the prevalence rate of chronic HBV under 5 years of age diminished to 1.3% in 2015 from 4.7% in the pre-vaccine era of 1980s to the beginning of the 2000s[4]. One effective mean of prevention for perinatal HBV transmission is birth dose vaccination within the first 24 hours of delivery, therefore it was recommended by WHO in 2009. However, the rate of birth-dose vaccination was estimated to be only 39% by 2015[2,4]. The WHO's viral hepatitis elimination plan aims for reaching 90% for the birth dose vaccination globally. Unlike HCV, there is no curative treatment available for HBV. The current antiviral therapy's goal is prevention of disease progression, improvement of survival rate and life quality of the patient[32].

One of the smallest viruses that can infect humans is HDV, which contains negative sense RNA as genetic material. It is a satellite virus that depends on HBV for its propagation and

transmission to another person. It hijacks HBsAg as an outer layer of the virus, thus sharing the same entry receptors with HBV for infection[33]. Propagation of HDV life-cycle requires co-infection with HBV or superinfection on HBsAg carrier patients to sustain production of progeny viruses and transmission. Similar to HBV infections, HDV/HBV co-infection can lead to fulminant hepatitis in the minority of acute hepatitis cases[34]. Recovery from acute hepatitis usually clears both HBV and HDV from the patients. Most of the chronic HDV cases are established in the settings of HDV superinfection on chronic HBV patients. It is estimated that 12 million patients worldwide are chronically infected with HDV, constituting 5% prevalence in HBsAg carriers[35]. HDV and HBV co-infections aggravate the progression of the disease with an increased risk for hepatocellular carcinoma and cirrhosis development[33,36-38]. Recent meta-analysis showed differences in the HDV prevalence in different regions of the world. To illustrate this, in Mongolia, 36.9% of the HBsAg positive patients are also positive for HDV, while HDV prevalence exceeds 10% among HBsAg positive people for the Republic of Moldova, Western and Middle Africa[35]. The HBV vaccine is an effective and safe way of prevention from HDV infection[4]. However, the antiviral strategies against HBV with nucleos(t)ide analogs are not effective on HDV that made the interferon-based treatment the only treatment option for HDV until the recent approval of the Bulevirtide in Europe[4,39]. Bulevirtide can inhibit *de novo* infections of HDV and HBV by blocking the entry receptor NTCP which alleviates liver inflammation and decreases HDV RNA levels in the serum of infected patients[39]. The general features of the described hepatitis viruses are summarized on the table below.

Table 1.1 Hepatitis viruses

	HAV	HBV	HCV	HDV	HEV
Genome	RNA	DNA	RNA	RNA	RNA
Family	Picornaviridae	Hepadnaviridae	Flaviviridae	Incertae sedis	Hepeviridae
Genus	Hepatovirus	Orthohepadnavirus	Hepacivirus	Deltavirus	Orthohepevirus
Transmission	Fecal to oral	Perinatal, Blood	Perinatal, Blood	Perinatal, Blood	Fecal to oral
Incubation	15-45 days	30-180 days	15-150 days	30-180 days	15-60 days
Chronicity	Acute	Acute & Chronic	Acute & Chronic	Acute & Chronic	Acute & Rarely Chronic
Prevention	Vaccine	Vaccine	Not available	Vaccine	Vaccine+
Antiviral Drugs	Not available	Available	Available	Available	Not available

+ Only in China.

Adapted from Sinn, H.D. *et al*. 2017[40].

1.2 Natural History of HBV Infection

The outcome of an HBV infections, as can be acute or chronic, is highly dependent on the age of the infected patient[29,41]. Acute infections of infants are generally asymptomatic while 70% of the adults display hepatitis with subclinical symptoms and the rest might have icteric hepatitis. In very rare cases, around 1%, fulminant hepatitis might develop. It is a severe condition with poor survival rate and requires liver transplantation as the only treatment in most of the cases[29,42]. The diagnosis of the acute infection requires biochemical and serological characterization in addition to clinical symptoms such as jaundice, right upper quadrant discomfort, anorexia, and nausea. In general, HBsAg elevates in the serum of infected patients

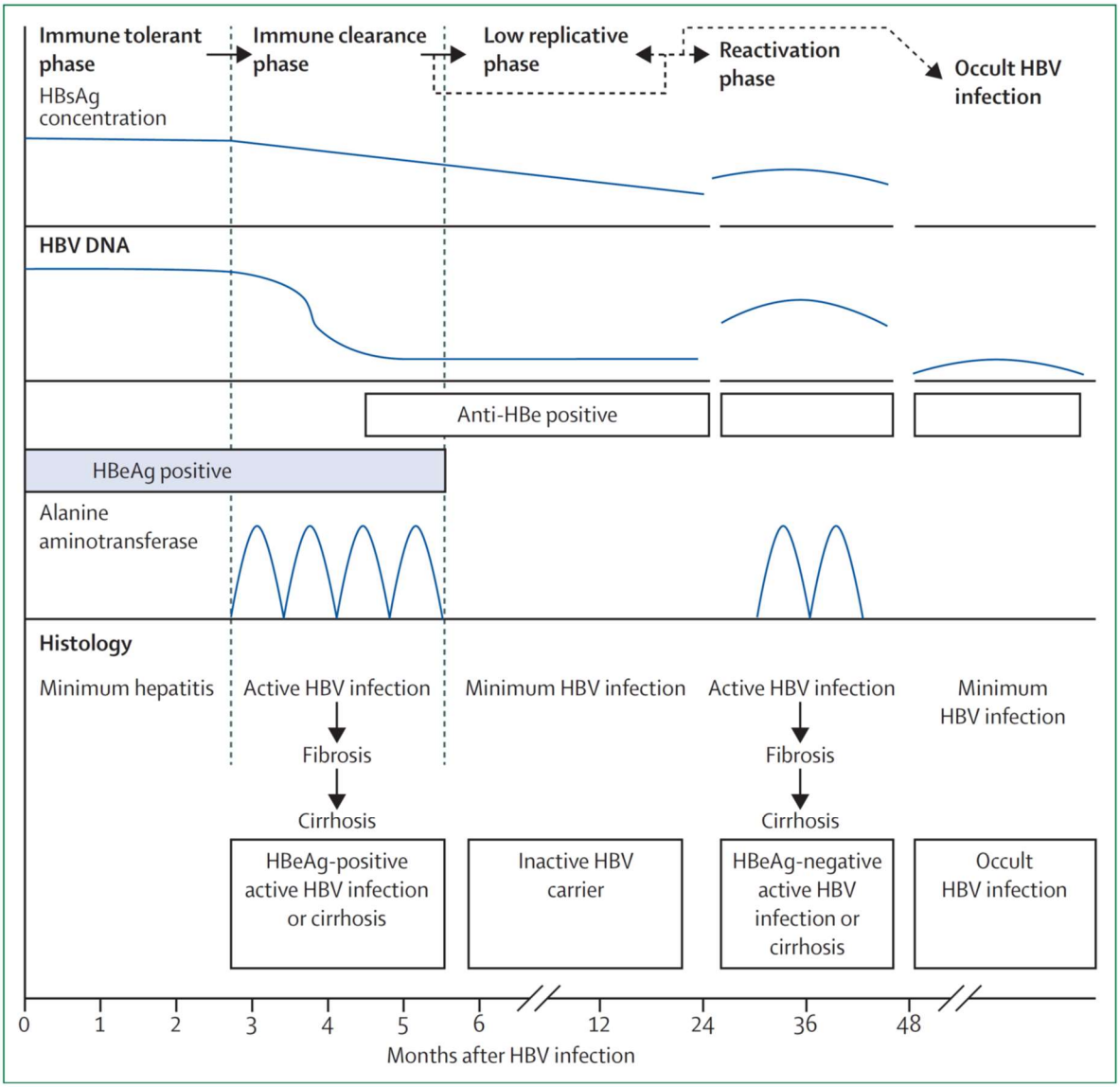

Figure 1.1. **The natural history of HBV infection**

Assessment of the stage of the HBV infection by serological, biochemical and viral parameters. The image is taken from Trépo, c. *et al.*[29]

during 2-10 weeks after infection followed by an increase in anti-HBc IgM and IgGs as well as biochemical markers - alanine amino transferase (ALT) and bilirubin[43]. The infection is generally resolved after 4-6 months with seroconversion of HBeAg and HBsAg by concerted action of innate and adaptive immune systems[32]. Antiviral cytokines, neutralizing antibodies secreted by B cells and cytolytic T cells prevent the spread of the virus and eliminate the persistent cccDNA genome of HBV in the infected hepatocyte by cell death. In persistent HBsAg positive cases, that is longer than 6 months, the infection is defined as chronic.

Most of the perinatal infections progress into the chronic phase in which the virus replicates efficiently with high DNA levels (>10^7 IU/mL), sero-positivity for HBeAg and HBsAg without any liver damage assessed by normal ALT levels and lack of fibrosis[44]. This initial stage of chronic HBV infection is called immuno-tolerant phase or recently re-named to HBeAg-positive chronic HBV infection by the EASL in 2017-clinical practice guideline. The immune-tolerant phase can last 20-40 years with high viremia but without any symptoms of disease or pathophysiology[29,45]. Recent reports showed that even in this early phase of the chronic infection, HBV integration and clonal hepatocyte expansion might initiate and set the conditions for disease progression to hepatocellular carcinoma[46]. The induction of cytotoxic T cells and increase in liver inflammation initiates the second phase of the chronic HBV named immune active or HBeAg positive hepatitis phase[29,32,47]. The immune reactions mediate a decrease in the HBV parameters HBV DNA and HBsAg, while causing necroinflammation and an increase in ALT levels[48]. Spontaneous seroclearance of HBeAg is achieved in 10-20% of the patients annually[49] with a significant drop of HBV DNA and lower serum HBsAg levels (10^3-10^4 IU/mL)[29,43]. The prolongation of the immune active state with flares of ALT results in moderate to severe liver damage that hasten the fibrosis progression[32,50].

Seroconversion of HBeAg and presence of anti-HBeAg points towards the initiation of inactive carrier or HBeAg negative HBV infection phase[29,32]. This phase is characterized with low to undetectable levels of ALT and low levels of HBV DNA (<2000 IU/mL). The levels of HBsAg decreases as well. In patients having HBsAg below 1000 IU/mL, the chance of HBsAg seroconversion is higher, 1-3%, compared to 0.5-1% annual seroconversion rate of those in the inactive carrier phase[51,52]. The elevated HBsAg concentrations are associated with a higher risk of hepatocellular carcinoma and cirrhosis. In 20-30% of the patients, relapse of the HBV infection and ALT elevation occurs, mostly due to the selection of basal core promoter or precore mutant variants of the virus[29,32,43,53]. The viral DNA levels raise back above 2000 IU/mL with intermediate levels of HBsAg concentration. This phase is named reactivation

phase or HBeAg negative hepatitis. Re-initiation of the necroinflammation results in higher likelihood of cirrhosis and hepatocellular carcinoma compared to the inactive carrier phase[50].

In the natural course of acute and chronic infections, occult HBV infection might develop characterized by HBsAg negativity in the presence of anti-HBc IgGs[54]. In most of these cases, cccDNA is still existing in the nucleus of hepatocytes[55] and HBV DNA levels detected in the blood are usually below 200 IU/mL[54]. Occasionally, HBsAg mutations in the HBV envelope gene can cause negativity in the detection assay. The ALT levels remain normal and loss of HBsAg before the onset of late stage liver complications are an indicator of better outcome for these patients[32]. The natural history of HBV infections is summarized in Figure 1.1.

1.3 Genomic Organization

Hepatitis B virus has a small partially double stranded DNA genome, approximately 3.2kb in length and belongs to the Hepadnaviridae family. As a characteristic feature of this family, the small genome accommodates wealth of genetic information by possessing overlapping open reading frames (ORFs) and cis-acting elements (Figure1.2). This tight and economic design of the HBV genome attributes coding information to each nucleotide at least for one ORF[56]. The partially double stranded DNA has a full length minus strand with the viral polymerase covalently linked to the 5' end. The positive strand DNA varies in length, carrying an approximately 15-18nt long RNA primer sequence at its 5' end that is derived from pgRNA. The RNA primer is used for the initiation of positive strand DNA synthesis[57,58]. The genome within the viral particles is found in the relaxed circular DNA (rcDNA) form, where the ends of the HBV genome are not covalently closed but the complementarity at 5' ends ensures the circularity of the genome[59]. In a small fraction of HBV virions, double stranded linear DNA (dslDNA) is synthesized by alternative priming of the positive strand DNA synthesis[58]. Upon infection of hepatocytes, the gap of the positive strand DNA is filled by host polymerases in the nucleus apart from the removal of the HBV polymerase protein and RNA oligomer from the 5' end of the negative and positive strands, respectively[60]. The end of the HBV genome is sealed by the actions of host factors which create a very stable form of DNA named covalently closed circular DNA (cccDNA) [61-63].

Reverse transcription and synthesis of the HBV genome by the polymerase protein is an error-prone process that can lead to variability and quasi-species generation. The compact genome

organization of HBV restricts and thus decreases the probability of mutagenesis on the HBV genome which is around 10^{-3} to 10^{-6} nucleotide substitutions/site/year[64]. There have been 10 HBV genotypes (A-I) phylogenetically classified based on >7.5% divergence in nucleotide sequence, including the newest putative genotype J isolated in 2009 from a single individual in Japan. Moreover, it is estimated that more than 35 HBV sub-genotypes are present with approximately 4-8% nucleotide difference[64,65]. The HBV genotypes and the genomic variants have been associated with the specific clinical implications during the natural course of infection.

The cccDNA genome in the infected hepatocytes serves as a transcriptional template for four RNAs differing in length- 3.5kb, 2.4kb, 2.1kb and 0.7 kb - and coding for seven HBV proteins[66]. The viral transcription is regulated by two enhancer elements (EnhI and EnhII) and four promoters – Core/preCore promoter for 3.5kb RNAs, PreS1 promoter for 2.4kb RNA, PreS2/S promoter for 2.1kb RNA and X promoter for 0.7kb RNA. All of the HBV transcripts are products of RNA polymerase II[67] and contain 5'cap while alternative X transcripts were recently reported without 5'cap and with non-canonical lengths[68]. The transcripts of all lengths share the same polyadenylation signal at the 3' end. The 3.5kb transcripts are larger than the size of the HBV genome which encompass the polyadenylation signal and important sequences for the HBV replication such as direct repeat 1 (DR1) and a stem loop structure termed as epsilon, 'ε', two times at both 5' and 3' ends. These overlength 3.5kb transcripts are namely pregenomic RNA (pgRNA) and preCore RNAs, the former encodes core and polymerase proteins and the latter is translated to HBeAg precursor precore (p22) protein. The other subgenomic RNAs are translated into large (2.4kb), middle and small envelope (2.1kb) proteins and X (0.7kb) proteins [66]. Besides that, transcripts of the cccDNA can be alternatively spliced and were shown to produce at least sixteen splice variant transcripts across different HBV genotypes in different experimental settings[69]. Some of the spliced isoforms carry coding capacity for novel proteins; hepatitis B spliced protein (HBSP) from SP1 transcript, hepatitis B doubly spliced protein (HBDSP) from SP7 transcript and the polymerase-surface fusion protein (P-S FP) from SP13 transcripts[70-72]. Moreover, some of the spliced RNA isoforms are reported to be incorporated into the viral particles and reverse transcribed into ssDNA and linear DNA species which might contribute to HBV DNA integration into the host genome[58].

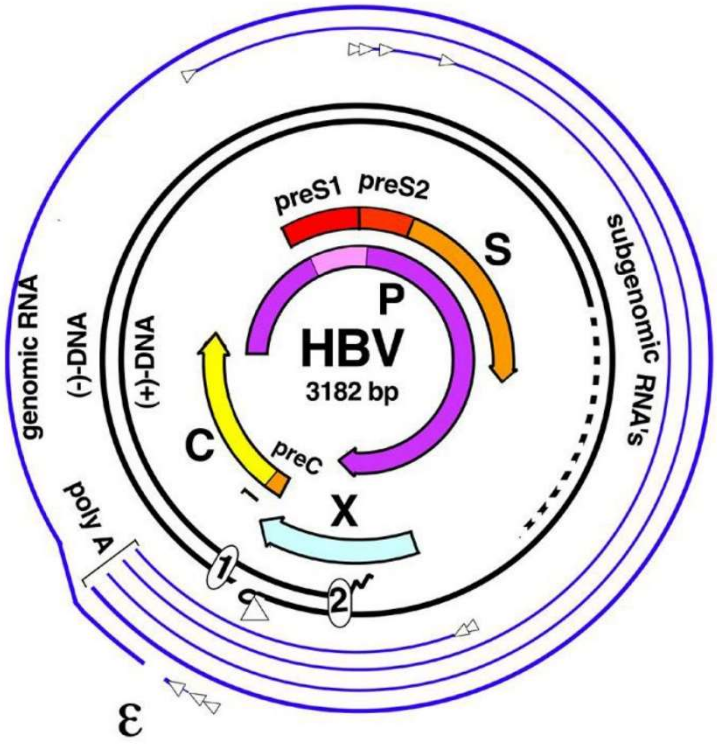

Figure 1.2 **Genome Organisation of HBV**

The rcDNA of the HBV is depicted as black line and the genomic and subgenomic RNAs are in blue lines. Dashed lines on the (+) DNA indicates the partial double stranded nature of rcDNA. At the 5' end of the (-) strand of rcDNA HBV polymerase protein is covalently attached and shown as triangle whereas the 5' end (+) strand is with zigzag line indicating RNA primer sequence. Epsilon stem-loop structure and poly-adenylation sites are indicated at the ends of the pgRNA. The inner part of the rcDNA shows ORFs of the HBV genome and their relative positions.

The image is provided by Dr.Christa Kuhn and Dr.Michael Nassal.

1.4 **HBV Lifecycle**

1.4.1 Entry of HBV into cells

The initiation of the infection is similar for plenty of viruses and relies on binding to the target cell surface in a sequential manner before internalization. The attachment process of HBV depends on low affinity interactions of the viral envelope proteins with the glycosaminoglycan (GAG) moieties of heparan sulfate proteoglycans (HSPGs) [73,74]. Heparan sulfate is consisting of repetitive units of 1→4 linked disaccharides of hexuronic acid and D-glucosamine. The

modifications of the disaccharides by epimerases and sulfotransferases produce plenty of variety among heparin sulfate proteoglycans with different structural properties[75]. Experiments suggested that HBV and heparan sulfate proteoglycan attachment depends on the electrostatic interaction between negatively charged GAGs and HBV envelope proteins, in which the sulfation level of the proteoglycan positively correlates with the binding affinity. Heparin is a highly sulfated derivate of heparan sulfate. It is shown to inhibit HBV attachment to the cell surface upon co-incubation with HBV, hence the infection is blocked in an effective manner at the entry step[74]. Biochemical analysis of cell culture derived HBV and HDV revealed that the HSPG interactions are dependent on both HBV large and small envelope proteins[74,75]. The conserved positively charged residues R122 and K141 in the antigenic loop (AGL) of the HBV envelope proteins' S domain are shown to be important for attachment of the viral particles on hepatocytes[76]. Moreover, a targeted siRNA knock-down screen demonstrated preferential binding of HDV and HBV virions on glypican-5 heparan sulfate proteoglycan[77]. For a successful HBV entry, the initial binding of the virus is followed by a specific interaction with the viral entry receptor, sodium taurocholate cotransporting polypeptide (NTCP) [78,79]. Identification of the viral receptor, which interacts with the PreS1 region of the L envelope protein, enabled susceptibility to the HUH7 and HepG2 permissive cell lines. The expression of NTCP is shown to be upregulated upon differentiation of HepaRG cells and rapidly downregulated in cultured primary human hepatocytes after isolation and seeding[80]. NTCP is located at the basolateral membrane of hepatocytes and is responsible for the transport of sodium taurocholate conjugates[81]. The role of additional cell surface proteins are demonstrated in the HBV entry. To illustrate that, the cell adhesion molecule e-cadherin has recently been reported as a novel host factor playing a role at the entry of HBV by affecting the distribution of glycosylated NTCP on the cell[82]. Likewise, the importance of cell polarization has been known for efficient HBV infection of HepaRG cells[83]. Another host factor, epidermal growth factor receptor (EGFR), has been described lately for the internalization of HBV virions, acting as a co-receptor by interacting with the NTCP protein[84]. The intake of HBV to the endosomes is followed by a trafficking from early endosome to late endosome before the release of the HBV nucleocapsids to the cytoplasm[85]. The mechanism of the internalization of HBV and the type of the hijacked endocytosis pathway has been vague until now, however new studies started to accumulate more information for understanding of the process. The initial studies described an important role of caveolin-1 during the entry process on HepaRG cells[86]. However, the subsequent investigations on HepG2-NTCP, HUH7-NTCP[87,88] and immortalized primary human hepatocytes[89] have demonstrated that clathrin mediated endocytosis (CME) is the major

route for HBV entry. Some of the components of clathrin coated vesicles, adaptor protein-2 and clathrin heavy chains were found in complex with HBV L protein and depletion of these proteins inhibits HBV infection[89]. An independent study confirmed the role of adaptor protein-2 during the endocytosis besides the EPS15 adaptor proteins[90]. The clathrin coated vesicles are pinched off by the action of dynamin-2 protein from the plasma membrane with concerted action of actin filaments and knockdown of Dynamin-2 expression inhibits the infection of HBV likely at the internalization step[88,91]. Investigation of pharmacological inhibitors against different internalization/trafficking pathways further supports the role of CME for HBV internalization[87]. Analyses of the HBV infected cells by transmission electron microscopy captured HBV virions in the clathrin coated pits and vesicles which is corroborated by immune-gold co-labeling of HBV core antigen and clathrin proteins[88]. The HBV containing vesicles follow the route of Rab5+ early endosomes to Rab7+ late endosomes before the escape of nucleocapsid into the cytosol. Experiments using RNA silencing of Rab5 and Rab7 small GTPases or a small molecule inhibitor of the vacuolar proton ATPase, named Bafilomycin A1, for inhibition of acidification and maturation of early to late endosomes, revealed that successful HBV infection needs cues presented by the endolysosomal system before the fusion of the viral membrane with the host vesicles[92-95]. Entry of many enveloped viruseses depend on the pH gradient established in the endosomes[96]. In contrast to the reports above, HBV infection experiments in the presence of ammonium chloride (NH_4Cl), a chemical compound raising the pH of endosomes, revealed pH-independency of duck hepatitis B virus (DHBV) and HBV entry[92,97,98]. Moreover, Macovei *et al.* showed that Bafilomycin A1 treatment of HepaRG cells does not inhibit HBV entry, which is contradicting with other's findings[92]. There are some HBV envelope protein domains postulated as acid responsive fusogenic elements located at the PreS1 and N-terminus of S[99-101]. The fusion of the viral envelope with the endosomal membranes and the cues triggering this process is currently not well known. The ion flux in the endolysosomal system is complex[102] and waiting to be investigated in the context of HBV entry. The internalization of HBV virions is summarized in Figure 1.3.

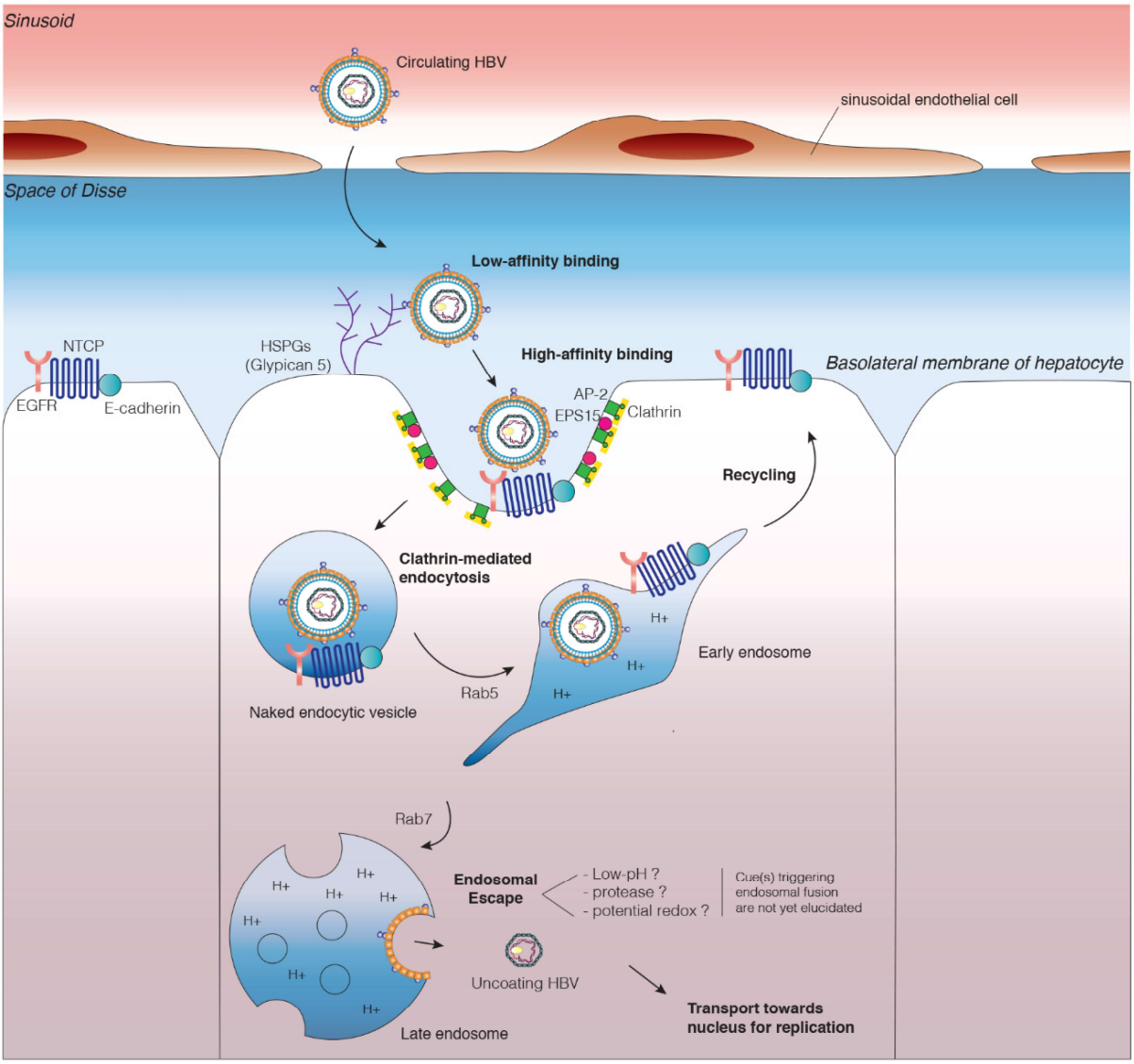

Figure 1.3 **HBV Internalization**

Hepatitis B virus binds to heparan sulfate proteoglycans with low-affinity at the surface of hepatocytes before establishment of specific interactions with the NTCP receptor. EGFR is shown to be an important co-receptor for HBV intake via clathrin-mediated endocytosis. The luminal cues along the endosomal maturation via Rab5+ to Rab7+ vesicle might be important for the release of the viral nucleocapsid to the cytoplasm and thus for a productive entry.

Source: The image is taken from Herrscher *et al* [85].

Similar to the majority of DNA viruses and retroviruses, the HBV genome containing capsids are imported into the nucleus to minimize the chance of innate immunity induction[103]. The active nuclear transport of the HBV nucleocapsids is dependent on the cytoskeletal motor proteins on microtubules; interaction between dynein light chain LL1 and HBV capsids was

reported recently[104]. Moreover, interfering with polymerization of microtubules by nocodazole (Paclitaxel) diminishes the nuclear transport and consequently the infection of HBV[105]. The retrograde transport is also mediated by the importin-α and importin-β proteins[106] which recognize the nuclear localization signal and the importin-beta-binding domain, respectively, located at the c-terminal domain (CTD) of HBV core protein[106,107]. Analysis of the core protein has shown that the genomic maturation and phosphorylation state of the CTD regulates the exposure of the CTD, presenting the NLS signal for the nuclear import process[103,108,109]. The mature HBV capsids interact with the nuclear pore complex and release the rcDNA genomic content for establishment of cccDNA[110]. The rcDNA comprises of DNA damage signals like gaps and nicks on its structure and needs fixation by the host factors for the formation of cccDNA. The conversion of rcDNA to cccDNA is a very inefficient process in the HepG2-NTCP infection system, only 0.6% of the attached viral particles can generate cccDNA, albeit, 22% of the particles are detected in the nucleus[87]. The mechanism behind this conversion is not fully understood yet, so far a handful of host factors has been reported. The completion of the missing sequences on the (+) strand of rcDNA is independent of the viral polymerase. Early studies have demonstrated that nucleoside analogs are unable to inhibit formation of cccDNA[111,112]. Moreover, a targeted siRNA screen on HepG2-NTCP identified DNA polymerase kappa (POLK) as a key polymerase for the filling of the gap in the positive (+) strand of rcDNA together with polymerase eta (POLH) and polymerase lambda (POLL), which decreased the formation of cccDNA during *de novo* infection[62]. In a non-susceptible but permissive cell line, HepAD38, DNA polymerase alpha (POLA1) is a crucial host factor during the intracellular cccDNA formation, taking part in the repair process of the minus (-) strand of cccDNA[63]. Moreover, the covalently attached viral polymerase can be cleaved and removed from the rcDNA by the cellular DNA repair enzyme, tyrosyl-DNA phosphodiesterase 2 (TDP2) *in vitro*[113,114]. Besides that, the flap structure at the minus strand has to be removed. Flap structure specific endonuclease 1 (FEN1), which is an important protein during the synthesis of DNA lagging strand, is responsible for this process[115]. Recent investigations added more to the number of proteins taking part during cccDNA conversion; DNA ligase 1 and 3 (LIG1 and LIG3), DNA topoisomerase I and II (TOP1 and TOP2), proliferating cell nuclear antigen (PCNA), DNA polymerase delta and the replication factor C (RFC) complex are reported[61,116,117].

1.4.2 Regulation of cccDNA Transcription

The repair and generation of episomal cccDNA initiates the association of histone and non-histone proteins onto the viral DNA and the formation of mini-chromosomal structures in the nucleus. Under electron microscope, the cccDNA minichromose displays beads on a string appearance by the presence of nucleosomes with a repeat length of 180bp which is shorter than the 200bp bulk chromosomal repeats of the host cell[118]. The association of HBc protein with cccDNA is thought to be responsible for this difference in nucleosome repeat length. *In vitro* experiments showed a reduction by 10% in the nucleosomal repeat lengths upon HBc protein binding onto the HBV sequences[119]. The interaction of HBc protein with the cccDNA might have a regulatory role in the transcription process. Clinical observations associate high viral load and minor hepatitis with nuclear localization of the HBc protein, whereas the low viremia and active hepatitis condition is found when the majority of HBc is located in the cytoplasm[103,120,121].

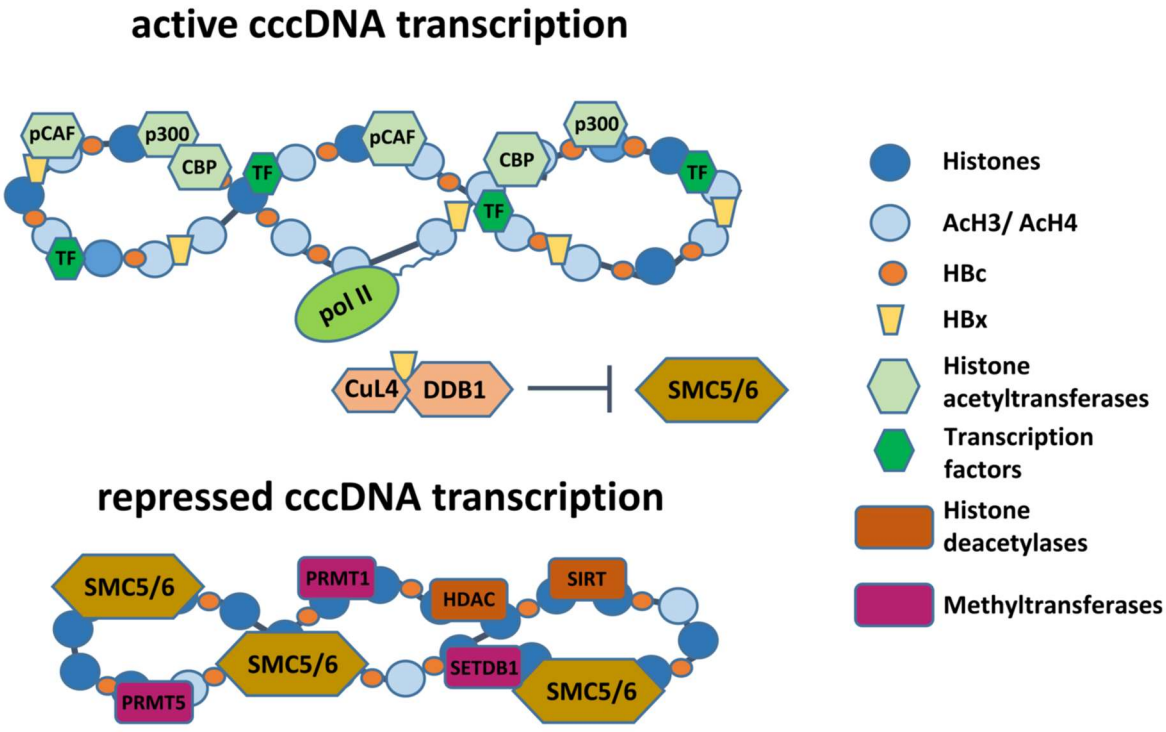

Figure 1.4 **HBV mini-chromosome associated factors and signatures**

Active and repressive states of the HBV mini-chromosome are recognized by recruitment of specific enzymes and non-histone proteins onto the cccDNA. Decoration of the histones with activator or repressive post-translational modifications and the composition of the cccDNA determine the transcriptional activity. Acetylated histones are associated with the active cccDNA state and HBx protein ensures that by counteracting diverse restriction factors posed on cccDNA transcription.

Source: The schematic is taken from Dandri, M. 2020[137].

The accessibility of HBV sequences by epigenetic mechanisms is crucial for the regulation of RNA transcription. The research on cccDNA epigenetics revealed numerous modifications at specific locations. Some histone modifications are generally linked to actively transcribed genes such as H3K4me3, H3K27ac, H3K36me3 and H3K122ac, while some are associated with repression of transcription like H3K9me3 and H3K27me3. Analysis of infected HepG2-NTCP, PHH and HBV(+) liver tissues demonstrates only active histone modifications on the cccDNAs, mainly H3K4me3, H3K27ac and, a lesser extent, H3K122ac. Intriguingly, the repressive histone marks are underrepresented on cccDNA[122]. Distribution of the active marks shows enrichment on the upstream part of Enhancer I for all of the examined cell lines. However, PHH infection displays active histone signatures along the HBV genome with the intesification of active histone marks around X ORF and PreS1 transcription start sites[122]. Previously, a similar observation has been made by cccDNA examination from chronic HBV patients; an increase in the acetylation level of H3 and H4 correlates well with the viremia, while higher expression of histone deacetylase 1 (HDAC1) causes hypoacetylation and low viremia[123]. A link between HBx protein and the recruitment of p300, CBP and PCAF/GCN5 histone acetyltransferase on cccDNA is known. Mutations on the HBx protein cause hypoacetylation of cccDNA by recruitment of deacetylating HDAC1 and Sirtuin1 enzymes[124]. On the other hand, interferon treatment of HBV plasmid transfected cells can cause translocation of polycomb repressive complex 2 (PRC2) components, EZH2 and YY1, to the hypomethylated cccDNAs[125]. In addition, methylation of H4R3 by protein arginine methyltransferase 5 (PRMT5) has been identified as a repressive marker and the presence of H4R3me2 is inversely correlated with the transcriptional activity of cccDNA[126]. In the same line, PRMT1 is a negative regulator of HBV transcription and it is counteracted by HBx by direct interaction[127]. Repression of the cccDNA by SET domain bifurcated 1 (SETDB1) accompanied accumulations of H3K9m2 and H3K9me3 is illustrated in the absence of HBx protein[128].

Decorsiere *et al.* found that structural maintenance of chromosomes (Smc) complex proteins 5/6 act as restriction factors for extrachromosomal DNAs including cccDNA[129]. Independent studies confirmed their findings that HBx protein hijacks E3 ubiquitin ligase component DNA damage-binding protein 1 (DDB1) and exploits Cullin4-RING-Ligases for the ubiquitination and degradation of Smc5/6 complex and therefore removes the transcriptional repression on cccDNA[130,131].

An additional layer of transcriptional regulation on cccDNA is imposed by DNA methylation on position 5’ of cytosine ring structures (5mC) by DNA methyltransferases (DNMTs). The

5mC modification usually takes place in CpG islands and leads to silencing of the gene expression[132]. *In silico* analysis of patient derived HBV genomes from 10 different genotypes revealed 2 or 3 sites of CpG islands depending on the genotype. The sites are located near the start codon of the S envelope protein (IslandI), enhancer1 / X gene promoter (IslandII) and near the beginning of the Polymerase (IslandIII) gene[133,134]. Investigation of clinical samples showed an inverse correlation between cccDNA methylation in IslandII and pgRNA transcription. Moreover, the level of HBsAg in the chronic patient serum tends to be lower probably due to the methylation of IslandIII on the cccDNA[135].

HBV plasmid transfection experiments into hepatocarcinoma cell lines revealed upregulation of DNMTs, which are repressing viral transcripts, particularly pgRNA, and host cell factors by causing hypermethylation[136]. In contrast to cccDNA or integrated HBV genomes, DNA of the progeny HBV viruses in cytoplasm or in the patient sera do not contain methylated cytosines[133,137]. Investigation of HBV infection in humanized mice showed a time-dependent effect of the infection in the methylation status of around 160 genes, some of which overlap with the methylation profile changes associated with HCC samples[138].

As mentioned earlier, the promoters and enhancers in the HBV genome are crucial for the expression of viral structural and non-structural proteins including the 3.5kb pgRNA which is the replication template for rcDNA generation. Various transcription factors are deployed to the transcription regulatory regions of the viral genome, some of them are ubiquitously expressed in many cell types and some are liver specific transcription factors[60,139]. Among the hepatocyte enriched factors, the most important ones for the HBV viral transcription are hepatocyte nuclear factors (HNF1,3,4α)[140-146], farnesoid X receptor (FXR)[147-149], retinoid X receptor alpha (RXRα)[150-153], and peroxisome proliferator-activated receptor alpha (PPARα)[150,154,155]. Some of the ubiquitous transcription factors binding to the HBV genome are as follows; nuclear transcription factor Y (NF-Y)[156], nuclear factor kappa B (NF-κB)[157], specificity protein 1 (Sp1)[158], zinc-finger E-Box binding homeobox 2 (ZEB2)[159], tumor protein 53 (TP53)[160,161], CCAAT Enhancer binding protein family (C/EBP)[162,163], chicken ovalbumin upstream promoter transcription factor (COUP-TF)[152,164], cAMP response element-binding transcription factor (CREB)[165], TATA box protein (TBP)[166], activator protein 1 (AP-1)[167,168], signal transducer and activator of transctription1,3 (STAT1,3)[125,169] and Yin Yan1 (YY1)[125,170]. Those transcription factors can act as activator or repressor of HBV transcription or both, depending on the context. For example, while low expression of C/EBP facilitates transcription, high expression results in an opposite effect[162].

1.4.3 Replication of HBV

The transcripts expressed from cccDNA vary in terms of their length and proteins encoded as mentioned earlier in section 1.2. As a human para-retrovirus, HBV uses pregenomic RNA intermediates for the reverse transcription of its partially double stranded DNA genome. All HBV transcripts share a common 3'end consisting of epsilon secondary structures and poly-A signals. The replication of the HBV genome necessitates the proper propagation of the genome without information loss, thus discrimination of the pregenomic RNA over the excessive amount of subgenomic RNAs and preCore RNA is required. The only HBV protein having enzymatic activity is a multidomain polymerase protein which comprises four parts: the N-terminal protein domain (TP), the spacer, the reverse transcriptase (RT) and the RNase H domain located at the C-terminus[171]. The hairpin structures called epsilon (ε) are present at the 5' and 3' proximal sites of pgRNA and a recent study demonstrated that these sites are subjected to N6-methyladenosine modifications[172]. The epigenetic modification on the 5'ε is essential for the replication of HBV. The epsilon stem-loop RNA element is an evolutionarily conserved structure existing even in the non-enveloped nackednaviruses, highlighting the significance of this structure for the replication process[173]. Initiation of the replication requires formation of a ribonucleoprotein complex between polymerase, pgRNA and possibly with dimeric core proteins; the 5'cap structure and its close proximity to the ε structure is essential[174-177], thus the 5' ε RNA is the specific binding site for the pgRNA encapsidation and initiation of the viral replication[178]. Noteworthy, the preCore RNA is not packaged into the capsids although it contains the same encapsidation signals as pgRNA[178]. A likely explanation for the exclusion of preCore RNA is the ribosome mediated destabilization of the Pol-ε RNA complex during the translation of preCore protein. In contrast to retroviruses, the hepadnavirus family members employ a protein-priming reaction for the initiation of replication. A short DNA primer on the terminal domain of the polymerase protein is synthesized by using the bulge region of epsilon RNA as a template[57,179,180]. *In vitro* experiments on insect cells revealed that tyrosine Y63 residue is the site for the phosphotyrosyl covalent attachment of the DNA primer[181]. A short oligonucleotide with 5'-GAA-3' sequence on the polymerase is transferred to the complementary DR1* region in the 3' region of the pgRNA[182], that initiates negative-strand DNA synthesis with concomitant degradation of pgRNA by RNase H domain of the polymerase until the DR1 sequence near the 5'-cap of pgRNA[60,183]. The end product has a unit length of the HBV genome, and the ends have around 10nt redundant sequences (r) which is crucial during plus-strand synthesis. The leftover 5'capped pgRNA sequence, around 18nt, is transferred to the DR2 sequence on the negative-strand DNA and used as an RNA primer during

the synthesis of plus-strand DNA towards the 5' end of the negative-strand[184]. Rarely, the template switch for pgRNA is by-passed by in situ priming on DR1 sequences that results in double stranded linear DNA genome[58]. Further elongation of the rcDNA plus-strand necessitates another round of template switch for circularization of the genome. The short redundant sequences 5'r and 3'r on the negative-strand DNA are essential for this process[184]. In mammalian hepatitis B viruses, the polymerization of the positive-strand is not complete, unlike the negative strand, it has a rather heterogeneous length. The reason for the incomplete plus-strand synthesis is not clear, however experiments on Hepadnaviruses suggest that it might be due to the spatial limitations posed during the capsid assembly or depletion of dNTP pools during the plus–strand polymerization reaction. Unlike HBV, duck hepatitis B virus possesses a complete positive-strand DNA and genetic manipulation on the capsid such as removal of the CTD or implementing phosphomimic substitutions have shown to be affecting plus-strand DNA synthesis[185,186]. However, treatment of HBV with non-ionic detergent, which removes the envelope layer, and supplementing the capsid with dNTPs allows completion of DNA synthesis on the plus-strand[187,188].

Early studies on duck hepatitis B virus polymerase using in vitro initiation complex demonstrated that the DNA priming reaction in rabbit reticulocyte lysate (RRL) is more efficient compared to wheat germ extract systems; likely due to the presence of specific host factors facilitating priming in the RRL setup. In the same study, heat shock protein 90 was identified as a component of the polymerase and ε RNA ribonucleoprotein complex enhancing the in vitro priming reaction[189]. Subsequent findings proposed that the formation of a multi-component chaperone complex, which includes Hsp90, Hsp70, Hsp40 and p23 proteins, hydrolyzes ATP and induces conformational changes on the polymerase-ε RNA complex for the initiation of reverse transcription[190]. In a simpler approach by another group, the Hsp70/Hsp40 complex and ATP are shown to be sufficient to bring the viral polymerase in an active priming state, though addition of Hsp90 and Hop proteins increase the reaction efficiency[191]. Truncation of the duck hepatitis B virus polymerase from the C-terminal end, being equivalent to a loss of the entire RNaseH domain and some sequences from the RT domain, diminishes the chaperone dependence of the *in vitro* priming reaction[192]. This observation indicates that the C terminal part of the polymerase is in a closed state in the absence of chaperones, inhibiting the priming reaction, whereas transition to an energetically unfavorable meta-state or open state is induced by chaperone complex activities[57,59].

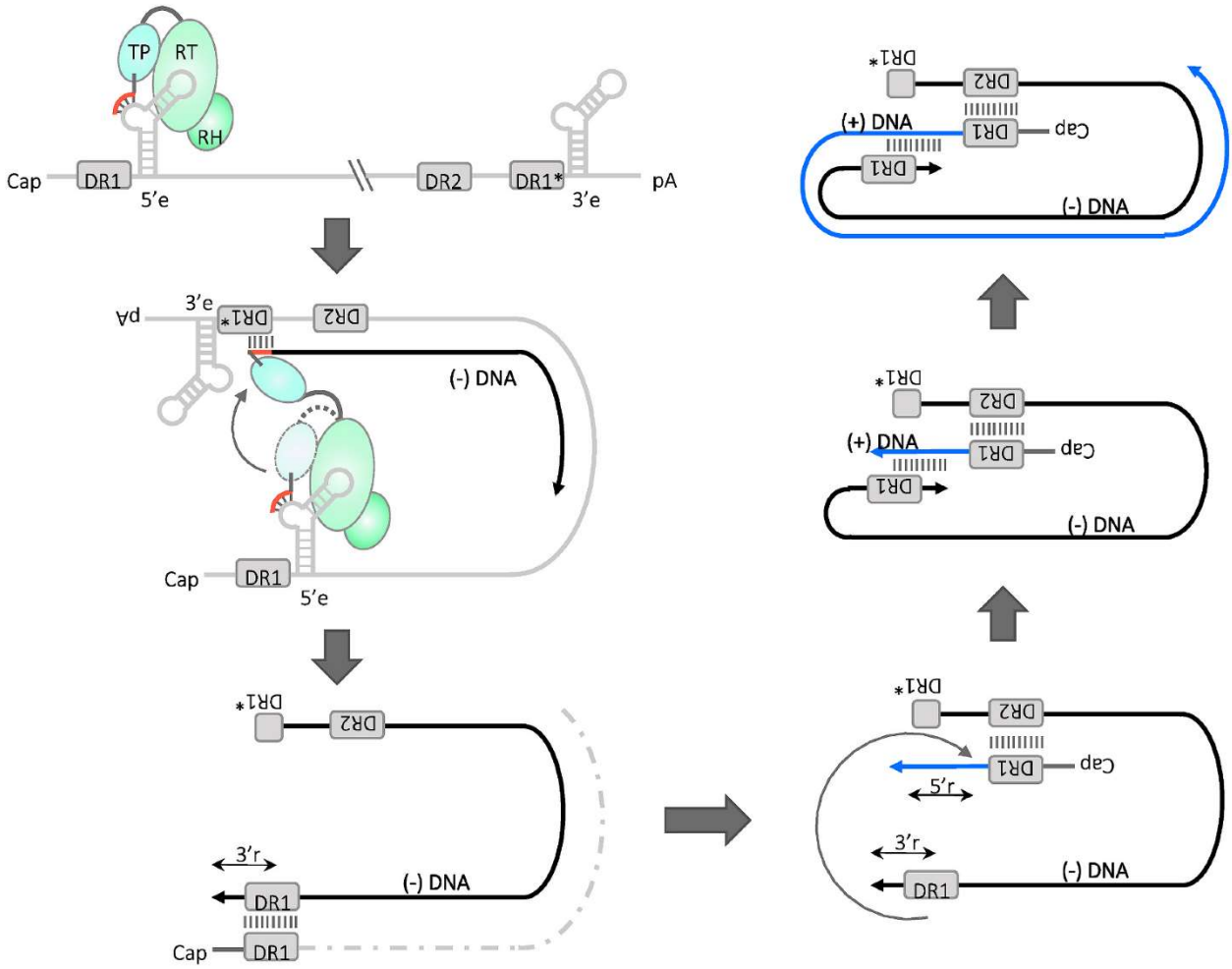

Figure 1.5 **HBV DNA Reverse Transcription**

The schematic represents the steps of rcDNA generation from pregenomic RNA (pgRNA). The polymerase protein recognizes the epsilon secondary structure at the 5' end of the pgRNA for initiation of reverse transcription. Protein-priming on the bulge of epsilon generates a 3-4 nucleotide DNA primer for the negative-strand synthesis. The short DNA primer is transferred onto the DR1* sequence on the 3' end of pgRNA, and negative strand synthesis is completed with simultaneous degradation of pgRNA. The 5' cap containing pgRNA stays intact and is used as primer during the synthesis of the plus-strand. A second template switch reaction takes place, the RNA primer binds to the DR2 sequence and is extended towards the 5' end of negative strand. Terminal redundancies on the minus-strand DNA are utilized for the third template switch reaction and continuation of rcDNA synthesis by circularization.

The image is taken from Tsukuda, S. and Watashi, K., 2020.[60]

1.4.4 Virus Egress and HBV Particles

After replication, the fate of the partially double stranded rcDNA containing capsids can differ; the nucleocapsid can be re-imported to the nucleus or subjected to envelopment by host lipid membranes studded with viral envelope proteins for release out of the infected cells. Besides that, *in vitro* experiments, mainly with DNA-transfected cells have shown that nucleocapsids without any outer lipid layer, which are called naked capsids, can be released from the transfected cells as well. However, *in vivo* analysis of sera from HBV infected chimpanzees and patients could not demonstrate the presence of naked capsids[193,194]. Consistently, *in vitro* infection experiments on hepatic cells shows secretion of progeny virions into the culture medium but barely naked capsids. The phenomenon of nuclear re-import is well-described in DHBV infection systems. Stop codon insertion into the envelope protein ORF resulted in accumulation of cccDNA in the infected cell nucleus, from 22 copies in wild-type to as high as 630 copies in mutant forms[195]. Quantification of cccDNA from single nuclei of DHBV hepatocytes revealed 1-17 copies of cccDNA per cell. However, 10% of the cell population showed more than 17 cccDNA/cell[196]. It is very likely that the amount of the envelope proteins available for the assembly of the virus and their ratio to the nucleocapsids determines the fate of nucleocapsid and eventual cccDNA amount. Analogous approaches showed a disparity between HBV and DHBV that ablation of envelope proteins led to only marginal or no effect on HBV cccDNA amount[197,198]. Egress of the infectious virions entails incorporation of rcDNA containing capsids, referred to as mature nucleocapsids, into the budding sites decorated with the HBV envelope proteins. The immature forms of nucleocapsids contain ssDNA or pgRNA, and are excluded from envelopment and secretion out of the cells[199-202]. How the genomic content maturation and envelopment event are coupled and the switch signal exerting this process are not well understood. Surprisingly, in great excess to the mature virions, empty virions are found in the blood of infected patients. This indicates that the capsids without genomic content are competent for the envelopment[200-202]. To explain the observations on the HBV genomic maturity and release, the so-called single strand blocking hypothesis was postulated; the immature forms containing single stranded nucleic acids are excluded from the egress pathway due to negative signals transmitted via the nucleocapsids, while the genomic maturation imposes an extra layer of regulation by presenting a positive signal for the envelopment[201,202]. Genetic mapping on the core protein suggested that several crucial sites at the base of the capsid spike are crucial for association of the rcDNA containing mature capsids with viral envelope proteins[203]. Moreover, ultrastructural analysis of patient derived nucleocapsids displayed subtle differences in the hydrophobic pocket of the capsid spike

compared to the recombinant capsids derived from *E.coli*, which might as well be associated with the envelopment process[204].

The viral envelope proteins are synthesized from one ORF, which contains three translation start sites, with a common S domain at the C-terminus of middle (M) and large (L) envelope proteins. An additional PreS2 sequences at the N terminus of the S domain constitutes M and a further N-terminal extension with the PreS1 sequences generates L envelope proteins. In the following information, the numbering of the aa positions of HBV envelope proteins is provided according to HBV subtype *ayw* and genotype D. The interaction between HBV nucleocapsids and the L and S envelope proteins is essential during the morphogenesis process, while the M protein is not necessary[205]. Early experiments on envelope proteins have shown four transmembrane helices on the S domain resulting in both N- and C- terminus facing into the ER lumen[206]. The PreS2 domain of the M protein resides in the luminal side as well, whereas the the L protein topology possesses a complex duality to accomplish its function on the entry and assembly[207-209]. The genetic mapping of the PreS1 domain led to the identification of a short patch of sequences at the C-terminus of the PreS1 and beginning of PreS2 domain which is crucial for the capsid interaction. The capsid interacting element or so-called matrix domain (MD) resides at aa position 92-113[210]. Intracellular distribution of core protein exhibits strong colocalization with L protein, except in the case of MD deleted version, further supporting the role of the MD sequence for capsid interaction[211]. Next to the MD, the cytosolic anchorage site (CAD) resides at aa70-94, where the heat shock protein HSC70 binds. Deletion of HSC70 binding element causes co-translational translocation of the PreS1 domain into the luminal side of endoplasmic reticulum (ER) and it is manifested as an abnormal glycosylation pattern on L protein[212-214]. The anchorage of the PreS1 domain to the cytoplasmic side of the ER allows envelopment of nucleocapsids via the interaction with the MD domain and subsequent budding into intracellular vesicles. In addition to that, the S domain residues between the transmembrane domains (TM) I and II, termed cytosolic loop-I (CYL-I), contribute to the envelope-capsid interaction mainly in the context of S but not L protein[215]. The N-terminal end of the PreS1 contains infectivity determinants; removal of the contiguous 5 aa starting from aa position 3 to 77 impairs infectivity of the HBV virions[216]. Myristoylation is a lipidic modification on the glycine residue at aa position 2 of PreS1 that is an essential infectivity factor for many hepadnaviruses, but not necessary for the assembly[217,218]. Moreover, the entry receptor NTCP interacting motif is mapped in the PreS1 domain, 9-NPLGF/LP-15, is highly conserved in mammalian hepadnaviruses[219,220].

The envelope proteins are not only incorporated into the virions. Subviral lipoprotein particles (SVPs) comprise only envelope proteins and are secreted as surplus from the infected cells in 100-10,000 fold relative to the virion number[202,221,222]. The ratio of the L to S proteins differs between the SVP types; the sphere-shaped SVPs with 20-22 nm diameter contain mainly the small envelope proteins (S) and very low amounts of the large isoform (L) while filamentous SVPs, which have the same 20-22 nm diameter but various lengths, the ratio of L:S is higher[223]. The L incorporation into the infectious viral particles is even higher[223]. Overexpression of only S protein is adequate to produce sphere SVPs, which forms the basis of the first recombinant HBV vaccine generated in yeast[224]. The SVP sphere particles contain approximately 48 dimers arranged in octahedral symmetry[225]. The SVP particles are protein enriched entities having only 25% lipids by weight[221,226]. A recent cryo-EM study demonstrated that the lipid membrane of the HBV particles is organized in a bilayer structure[227]. Based on early biochemical analysis, SVPs derived from patient serum comprise phosphatidylcholine as the main lipid component (≈60%) followed by cholesteryl ester (≈14%), cholesterol (≈15%) and triglycerides (≈3%)[226]. *In vitro* experiments are partially congruent with the *in vivo* results that phosphotidlycholine is the main lipid component of the SVPs (≈90%), whereas the percentage of cholesterol and cholesterol ester are greatly reduced in *in vitro* settings, ≈4,5% and ≈1,5% respectively[228,229]. Hitherto, there is not any information available on the lipid composition of HBV virions.

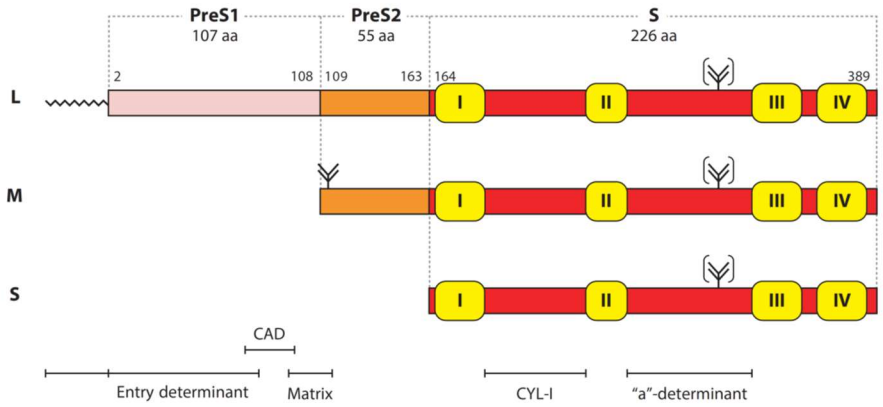

Figure 1.6 **Organization of HBV Envelope Proteins**

Large (L), Middle (M) and Small (S) envelope proteins are illustrated with their respective domains and the positions of amino acids (aa) according to subtype *ayw*, genotype D. The transmembrane segments are in yellow and the N-myristoylation modification of the L protein is illustrated as zigzag line at the N terminus. The antigenic loop (a-determinant) between transmembrane segment II and III carries an N-glycosylation site indicated with an arrow nock. PreS2 of the M protein contains an additional N-glycosylation site. CAD: Cytosolic anchorage domain; CYL-I: cytosolic loop-I

The image is taken from Seitz, S. *et al*.[202]

There are fourteen conserved cysteine residues present in the S domain, eight of which are on the antigenic loop between TMI and TMII[230]. Upon synthesis on ER membranes, the envelope proteins form homo- or heterodimers with disulfide-linkage in a short time, however complex oligomerization is suggested to be prevented by the action of protein disulfide isomerase enzymes (PDIs) [230,231]. Therefore, transport of the dimers to the PDI depleted ER-Golgi intermediate compartment (ERGIC) is required for further stabilization and assembly of the SVPs[231]. Investigations on host factors for the ER exit process of the HBV envelope proteins demonstrated the role of Sec24A and Sec23B on the cargo capture during the COPII vesicle formation and subsequent anterograde transport[232]. This interaction between COPII machinery and S domain is mapped to the di-arginine motif (R78, R79) in CYL-I close to the TM-II segment[232]. The notion of SVPs budding into the ERGIC is supported by pharmacological studies on SVP secretion; Brefeldin A (BFA) treatment of SVP secreting cells led to the accumulation of assembled SVPs intracellularly, while additional H-89 drug treatment, which inhibits COP-II vesicle formation, reverts the BFA dependent intracellular SVPs accumulation[233]. On the contrary, Patient *et al.* reported that the budding process of SVPs takes place in ER membranes by the formation of tightly packed SVP filaments at the perinuclear space, even in the absence of L protein. Subsequently, sphere SVPs are generated by the conversion or relaxation of the filaments in the post-ER compartments[234,235].

In about half of the HBV surface proteins, the S domain is glycosylated at Asn-146 in the antigenic loop or a-determinant region at which the disulfide-bridges between the cysteine residues are crucial for the HBsAg antigenicity but not for the release of the particles[230,236-238]. The PreS2 sequence of the M protein has an additional N-glycosylation site at position Asn4 which is constitutively modified. It gives rise to mono- and di-glycosylated isoforms of M envelope proteins[239]. In HBV genotype D and E, there is an additional O-glycosylation site residing at Thr37 of the PreS2 domain[240]. The glycosylation on Asn146 in the S-domain is indispensable for HBV virion secretion, while SVPs are secreted normally[241,242]. Similar to SVPs, the production of HDV particles is not affected by the lack of Asn146 glycosylation[242]. Inhibition of the glycan processing machinery by the α-glucosidase inhibitor, NB-DNJ, prevents secretion of M protein containing virions and SVPs into the medium[243,244]. The sugar moiety on Asn4 of the PreS2 domain is recognized by the lectin protein calnexin but the carbohydrates on Asn146 of the S domain are not[213,245]. Intracellular SVPs are modified with high-mannose sugars which are sensitive to endoglycosidase H. This suggests accumulation of the high mannose SVPs in either ER or ERGIC or cis-golgi before the further processing of the sugar moieties to more complex forms found in secreted SVPs[246-248].

Consistent with the early studies, lectin-microarray results point out to complex oligosaccharide modifications on the HBV particles as well[249]. Glycosylation level in the highly immunogenic a-determinant region is crucial for the antigenicity of the particles. Hyper-glycosylated isoforms are found in immune-escape variants preventing recognition of the epitopes by polysaccharide shielding[242,250].

The egress of the HBV particles was presumed to follow the constitutive secretory pathway until the identification of new host factors that are shown to act specifically on HBV virion secretion. Yeast-two hybrid experiments revealed the γ2-adaptin protein as an interaction partner of L envelope protein[251] and subsequent studies by the same research group demonstrated that HBV core and γ2-adaptin can interacts with each others as well[252]. The ubiquitin interacting motif of γ2-adaptin is shown to be important for the γ2-adaptin-capsid association and the Nedd4 E3 ubiquitin ligase protein is postulated to recognize PPXY-like late domain on core protein; inhibition of Nedd4 decreases the amount of secreted virus[252]. Several studies investigated the endosomal sorting complexes required for transport (ESCRT) machinery components during the budding of HBV virions into the multivesicular body (MVB) compartment. It has been demonstrated that the sole perturbations of the proteins; vacuolar protein sorting-associated protein 4 (Vps4), ALG-2 interacting protein X (ALIX), charged MVB protein 3, 4B and 4C (CHMP3, 4B, 4C) can block the release of virions without any significant phenotype on the secretion of SVPs comprised of only S proteins[253,254]. In another study, biochemical experiments revealed that the α-taxilin protein is interacting with the ESCRT-I complex protein tsg101 and HBV L envelope protein along with an increase of the α-taxilin expression in HBV replicating cells. Silencing of α-taxilin abolished the secretion of HBV yet, tsg101 knockdown failed to reduce HBV particle release[255,256]. It is likely that the similar sorting and trafficking route via MVBs is exploited by the L enriched filamentous SVPs. Recently, Jiang *et al* examined the role of the ESCRT components by overexpression of dominant negative versions of Vps4 and CHMP3 proteins on the cells transfected with a core-deficient HBV genome[257]. The results were comparable to the previous reports on HBV virion release that the ESCRT components are crucial for L-enriched filamentous SVPs exocytosis.

As mentioned earlier, L protein has a dual topology; one is required to establish the interaction with the capsid for envelopment (interior part of the virus) and the other for the exterior part of the virus which allows binding to the host cell surface during the infection process[202,208,258]. It is assumed that the L topology is present on the virus in a 1:1 ratio between the interior (i-PreS1) and the exterior (e-PreS1) versions[202]. Cryo-EM imaging of HBV virions revealed a distinct binary distribution of morphologies, namely gapped (≈45%) and compact forms

(≈45%). The remaining particles (≈10%) contain features of both sorts[259]. The compact version of HBV is thought to have the PreS1segment on the interior side, whereas the extracellularly relocated PreS1 leads to the gapped version by the maturation of the particles[259]. Switch and maturation processes by i-PreS1 to e-PreS1 conversion are demonstrated to be crucial for productive hepatocyte infection of HBV *in vivo*, which is preventing extrahepatic adsorption of the virions by HSPGs interactions[260].

1.5 Antivirals

1.5.1 Current Therapy Strategies and Targets

The main goal of the HBV antiviral therapy is to increase life-expectancy and quality of the patients by viral suppression and prevention of the disease progression. There is a limited number of licensed therapeutics available for the treatment of CHB disease. Licensed in 1991, interferon-α2b is used as anti-HBV agent, which is a low molecular weight cytokine acting via the Jak-Stat signaling pathway and thereby inducing a plethora of interferon stimulating genes (ISGs) [261,262]. It shows dual effect on the disease by immunomodulatory and antiviral activities[262]. Polyethylene conjugation to the interferon-α increases the pharmacokinetic profile and half-life of the drug with better treatment response thus, peginterferon-α2a (Pegasys, Roche) and interferon-α2b (PegIntron, Merck) are currently in clinical use[263,264]. The response rate or HBeAg sero-conversion of 48 weeks peginterferon-α (pegIFNα) treatment is around 30% for HBeAg-positive patients 6 months post-treatment[32,265-267]. Loss of HBsAg is rarely observed (appx. 5%). The percentage of the HBsAg loss is similar (4%) for the HBeAg-negative CHB patients at 6 months following 48 weeks pegIFNα therapy[32,265]. Interestingly, the percentage of HBsAg loss increases to 8-9% at 3-4 years after cessation of pegIFNα therapy for both HBeAg-positive and HBeAg-negative CHB patients[32,265]. The genotype of HBV is an important variable for the prediction of the response rate that genotype C and D are less sensitive to the interferon treatment than A and B which have a better HBeAg seroconversion rate[268-270]. Moreover, compared to the nucleos(t)ide analogs (NAs), the interferon-α therapy results in inferior efficacy on the HBV DNA suppression[265].

The antiviral effects of interferon-α (IFNα) are diverse, inhibiting the HBV life-cycle at various steps. Experiments on HepaRG cells revealed that IFNα treated cells secrete antiviral products preventing binding of HBV to the cell surface proteoglycans[271]. Moreover, an epigenetic regulatory role of IFNα has been described; a decrease in the level of active post-translational

modifications on cccDNA associated histones is reported[122,125]. Similarly, IFNα treatment of humanized mice for 6 weeks and quantification of cccDNAs at the end of the treatment demonstrated reappearance of the Smc5/6 complex in the nucleus of the infected hepatocytes, that in turn suppresses the transcriptional activity of cccDNA and decrease the level of cccDNA[272]. Induction of the DNA cytidine deaminase protein APOBEC3A/B by IFNα treatment causes cccDNA deamination and apurinic/apyrimidinic site formation, ultimately leading to cccDNA degradation[273]. Another member of APOBEC protein family, APOBEC3G can be induced by IFNα and has been shown to inhibit HBV replication[274]. HBV RNAs are degraded by an exonuclease protein named interferon-stimulated gene 20 (ISG20) which binds to the epsilon stem loop structure at the 3' end of the viral transcripts[275]. Another interferon inducible gene, Mx2, has recently been described to impede HBV transcription and increase the decay rate[276]. Some of the ISGs in tripartite motif (TRIM) protein family, TRIM22, TRIM25, Trim5γ and TRIM31 hamper HBV in a diverse manner ranging from HBx degradation to suppression of viral promoter activity[277-280].

The immunomodulatory role of IFNα is likely the primary anti-HBV mechanism in CHB patients since the short-term activation of ISGs in HBeAg+ patients did not lead to a reduction in HBV DNA levels[281]. Natural killer (NK) cells ($CD56^{bright}$) starts proliferating and are activated by the IFNα therapy in both HBeAg+ and HBeAg- patient cohorts[282,283]. The response rate of pegIFNα has been shown to correlate with the presence of certain subsets of NK cells ($NKp30^{+}$, $NKG2A^{-}$) while the non-responders possess higher expression of the inhibitory receptor NKG2A[284]. Experiments in woodchuck HBV animal model illustrated the concerted role of NK and T cells during the antiviral action of woodchuck IFNα[285]. The impact of IFNα treatment on adaptive immunity is not clear yet. A significant reduction in $CD8^{+}$ T cells was reported by Micco *et al.* in the course of 48 week therapy[282]. In the same line, *ex vivo* cultured T cells produce less interferon-gamma from HBeAg- patients treated with IFNα[286]. On the contrary, NK cell mediated killing of T cells can be evaded by the protection provided by interferon-α signaling[287,288].

Another treatment option for CHB is using nucleos(t)ide analogs (NA) that offer a good safety profile and high antiviral efficacy in long-term treatments. There are six approved NAs available for CHB treatment in Europe, which can be categorized as high or low barrier against HBV resistance. Low resistance NAs, lamivudine, adefovir dipivoxil and, telbivudine, are not recommended in the clinical practice guideline of the EASL to prevent the development of multidrug resistant strains while tenofovir disoproxil fumarate (TDF), tenofovir alafenamide (TAF) and entecavir (ETV) are the preferred NAs displaying high barrier to resistance in long-

term[32,262]. The rate of resistance is around 1 % for ETV after 5 years and without any incidence of resistance for TDF after 8 years of treatment[32,289]. The suppression rate for HBV DNA is superior to IFNα monotherapy; at the end of 48 or 52 weeks, in 64 to 76% of the HBeAg+ patients HBV DNA levels decrease below 60-80 IU/mL, while the DNA suppression rate reaches to more than 90% in the HBeAg- patients[32,265]. In the same setup, NAs rarely result in HBsAg loss[32,265]. Antiviral therapy using NAs is the only treatment option that can be used in the severe liver disease conditions like decompensated liver[32,290,291]. The treatment is often life-long, well-tolerated and associated with normalization of ALT levels which further associated with better outcome for fibrosis and cirrhosis patients along with a reduced risk for HCC development[291-293]. The episomal genome of HBV is not directly targeted by the NA therapy which brings about viral persistence and high relapse rate of NAs upon discontinuation[294].

1.5.2 Novel Therapeutics for Treatment of HBV

The current treatment strategies against CHB result in a low rates of functional cure which is described as HBsAg loss with or without seroconversion. Research on new strategies focuses on various steps of the HBV life-cycle or on augmentation the immune system against HBV.

The entry inhibitors aim to block replenishment of cccDNA by *de novo* infections of the hepatocytes, thus in combination with NAs or pegIFNα, they might reduce the amount of cccDNA in the nucleus of infected hepatocytes. A promising entry inhibitor is Bulevirtide (Myrcludex B) which is an N-myristoylated viral lipopeptide derived from the PreS1 domain of L envelope protein. Bulevirtide interacts with the viral entry receptor NTCP and blocks the entry of HBV or HDV in a picomolar range[219]. In the phase II clinical trial (MYR203) conducted for 48 weeks in 60 HBV/HDV co-infected patients, 2mg Bulevirtide and pegIFNα therapy demonstrated reduction of HBsAg >1log or to undetectable levels in 40% of the patients at 24 weeks off-treatment. Neither Bulevirtide nor pegIFNα monotherapies resulted in HBsAg loss (0%) [295,296]. The synergism between pegIFNα and Bulevirtide allows suppression of HDV RNA around 3 log compared to 0.26 and 1.16 in IFNα and Bulevirtide monotherapies, respectively[295]. Furthermore, ezetimibe and cyclosporin derivatives have been investigated as entry inhibitors of HBV in preclinical studies. The direct interaction between cyclopsporin A and NTCP precludes entry of HBV with an IC_{50} of 350 nM[297]. Currently, HBV immunoglobulin is the only approved HBV entry blocker which is used to prevent mother-to-child transmission and in acute exposure cases[298].

Capsid protein assembly modulators (CpAMs) offer an alternative strategy by targeting critical steps in the HBV biology. By accelerating the assembly of the capsid structure, the CpAMs

prevent encapsidation of pgRNA and subsequent rcDNA synthesis for progeny virus production[299,300]. The treatment with class I mode of action (MOA) CpAMs generates empty, morphologically normal capsid structures; sulfamoyl-benzamide and phenylpropenamide derivatives constitute the members of this category[301,302]. Heteroarylpyrimidine derivatives (HAPs) are in class II MOA CpAMs which lead to aberrant capsid structures[301,302]. Characterization of the CpAM compounds *in vitro* achieved not only the reduction of HBV DNA but also the inhibition of viral uncoating at the entry, thus cccDNA establishment was inhibited[303]. There are several CpAMs tested in early phase clinical trials and demonstrated promising antiviral efficiency. One of them is the phase I clinical study of JNJ-6379 that was conducted on naive HBeAg+ and HBeAg- Asian and Caucasian CHB patients for 28 days. The study demonstrated a decline in HBV replication by causing more than 2 log decrease in HBV DNA relative to the mean baseline value[304]. RO 7049389 is another capsid inhibitor, which showed a robust decline in HBV DNA at the end of the 28 days of treatment of HBeAg+/- patients[305]. Combination therapy with pegIFNα was tested in phase I trial of NVR3-778 and was compared to monotherapy regimens in HBeAg+ patients for 4 weeks. The combination therapy displayed better antiviral action compared to the monotherapies by causing reduction in HBV DNA and RNA levels, while HBsAg was without significant change[306]. Nucleos(t)ide analog treatment might not completely suppress the replication of HBV that allows replenishment of the cccDNA either via *de novo* infection or re-shuttling of nucleocapsids back to nucleus[307,308]. Therefore, NAs and CpAMs combination therapy is an attractive strategy to inhibit the cccDNA persistence. In this line, the ABI-H0732 nucleocapsid inhibitor and entecavir combination therapy reduced HBV DNA in the sera of HBeAg+ patient greater than entecavir alone at week 24 post-treatment[309].

Direct targeting of cccDNA by programmable endonucleases can be used to reach complete cure of CHB. With the recent advances in genetic editing tools, several research groups examined the possibility of cccDNA elimination/inhibition in preclinical settings. Cleavage of cccDNA by transcription-activator like effector nucleases (TALEN) and CRISPR/Cas9 systems generated frameshift mutations on the HBV ORFs and led to a decrease in cccDNA pool[310,311]. However, integrated HBV sequences are the main concern for endonuclease technology in clinical settings due to the potential double-stranded break formation in the chromosomal DNA which might cause severe consequences. Permanent silencing of cccDNA is an additional curative option; as in cases of occult HBV, the stable cccDNA mini-chromosomes can be epigenetically inactivated and converted to a latent state[54,312]. As described in Section 1.4.1,

interferon-α treatment can epigenetically alter the cccDNA and repress the viral transcription[122,125,272]. Upregulation of the Smc5/6 complex and restricting the expression from cccDNA is a promising therapeutic strategy recently tested *in vitro* and in animal model systems[313-315]. MLN4924 is a specific inhibitor of the Nedd8 E1 activating enzyme (NAE). Upon MLN4924 treatment, cullin ring ubiquitin ligases (CRLs) are inactivated due to the loss of Nedd8 conjugation[316]. CRL4a/b-DDB1-HBx mediated degradation of the Smc5/6 complex was shown to be inhibited by MLN4924 drug, leading to a repression of viral transcription from cccDNA in infected primary human hepatocytes[313]. Moreover, the number of HBcAg(+) hepatocytes significantly decreased in the HBV hydrodynamic injection mice model after MLN4924 treatment for 13 days[314]. As a complementary approach, HBx and DDB1-CRL4a/b interaction was targeted by another drug called nitazoxanide and reduction in HBV transcripts were observed in an infection setting[315].

Specific antiviral approaches against HBV transcripts involve RNA interference and anti-sense oligonucleotide (ASO) therapies which are dependent on sequence complementarity. It is a widely accepted view in the HBV field that lowering HBV antigens in patient's circulation might lead to the restoration of adaptive immunity system against HBV[307]. The activity of the siRNA-based therapeutic drug ARC520 has been tested in pre-clinical and clinical studies and demonstrated an effective reduction in HBV parameters[317]. Conjugation of N-aceltylgalactosamine to the ARC-520 siRNAs confers a better delivery profile to liver cells using asialoglycoprotein receptor (ASGPR) as an uptake receptor[318]. Clinical studies revealed that CHB patients under nucleoside treatment or HBeAg(-) state were less responsive to the ARC520, probably due to the integrated HBV sequences which were not targeted by the therapeutic siRNAs. Investigations on chronically HBV infected chimpanzees supported this notion and showed that the HBV integrates were the main source of viral transcripts in HBeAg(-) chimpanzees[317]. The interim results of a clinical phase II study (AROHBV1001) of another siRNA therapeutic agent, JNJ-3989, illustrated that more than 1 log decrease in HBsAg levels was achieved in all patients independent of HBeAg status[319]. Degradation of HBV transcripts via RNaseH activity of ASO is a mechanistically different approach which was studied in preclinical settings against HBV infection and shown to be safe and tolerable in healthy individuals[320,321]. Post-transcriptional control of HBV RNAs by destabilization is another strategy; the orally bioavailable small-molecule inhibitor RG7834 interacts with the host factors PAPD5/7 and inhibits HBV expression[322,323]. Experiments on humanized mice revealed the potency of RG7834 by decreasing HBsAg expression significantly with a concomitant inhibition of viraemia[322]. On the contrary to siRNAs and ASOs, nucleic acid polymers (NAPs)

are amphipathic, single stranded nucleic acids which accomplish antiviral effect regardless of their sequence[324]. One of the important feature of NAPs based drugs is HBsAg assembly/release inhibition besides the blocking of viral entry[324]. The mode of action of anti-HBV NAPs is still not clear, though in the AASLD 2020 meeting, the host protein Hsp40 chaperone DNAJB12 was reported as the target of a NAP(REP2139) which showed promising results in Phase II clinical studies by leading to high rates of functional cure in combination therapy settings with pegIFNα and TDF[325].

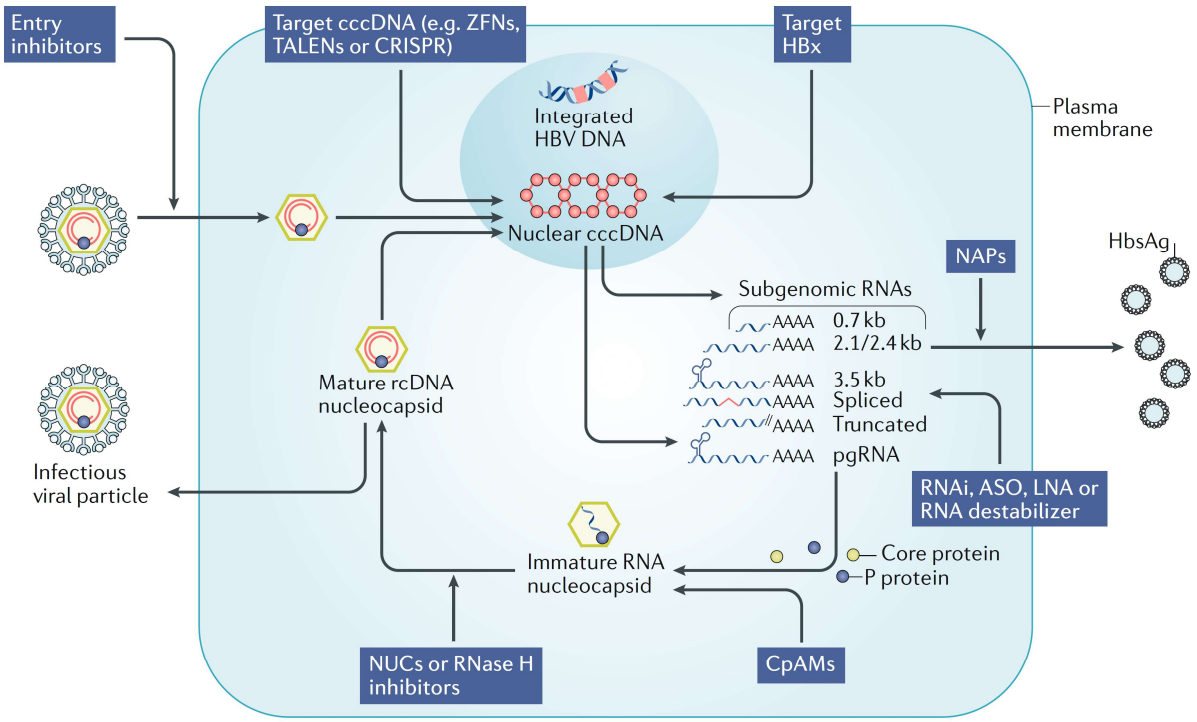

Figure 1.7 **Summary of Antiviral Strategies**

The antiviral approaches are targeting different stages of HBV life-cycle ranging from entry to assembly. NUC,nucleoside or nucleotide drugs; TALEN, transcription-activator like effector nucleases; CRISPR, clustered regularly interspaced short palindromic repeats; ZFN, zinc finger nucleases; RNAi, RNA interference; ASO, anti-sense oligonucleotide; LNA, locked nucleic acid; CpAM,capsid protein assembly modulators; NAPs, nucleic acid polymers.

The image is taken from Fanning, G.C. *et al.*[307]

1.6 Objective of the Study

Viruses are well-known for their reliance on host cells by interacting and manipulating cellular factors. Investigations on the interplay between viral proteins and host cells might open new avenues for the development of novel antiviral agents. As a small DNA virus, HBV alters the host cell transcriptome and proteome and makes use of host factors for all steps of the replication cycle from entry into the hepatocytes to egress[326,327]. Unfortunately, the knowledge on the host factors exploited in the course of HBV infection is quite limited, which hinders the progress to develop novel concepts towards functional cure of CHB.

Therefore, in this study, we pursued two complementary projects aiming to identify novel host factors in HBV biology, which can be exploited for potential therapeutic application:

- First, the excessive number of SVPs in the sera of CHB patients overwhelms the immune system by displaying extreme amounts of immunogenic HBsAg epitopes, thus driving immune tolerance [328]. In order to understand and identify the factors mediating HBsAg secretion, we aimed to conduct an siRNA mini-screen on a cell line expressing HBV envelope proteins from authentic promoters. Identified factors should be functionally characterized and probed as possible therapeutic targets by using, if available, small molecule inhibitor(s) to lower the production and secretion of HBsAg.

- Second, host factors incorporated into virus particles and SVPs might play an important role during assembly and release of these structures and therefore, strategies interfering with such host factors might by a way to lower virion and SVP production, the latter helping to break immune tolerance. For that reason, we aimed to identify host proteins incorporated into HBV virions and SVPs by establishing a purification pipeline suitable to separate both particle species and to obtain highly purified fractions. These should be analyzed by using a highly sensitive LC-MS/MS method. Identified factors should be characterized for their possible role in the production and release of these particle species.

By addressing both of the aims, better elucidation of HBV - host cell interaction might become possible for the development of novel concepts in HBV antiviral therapy.

2 Material & Methods

2.1 Materials

2.1.1 Antibodies

Table 2.1. Primary Antibodies

Antibody	Species	Provider-Catolog#	Application
anti-HBsAG (HBD87)	Human-monoclonal	Humabs Biomed	WB (1:5000)
anti-HBsAg (HBC34)	Human-monoclonal	Humabs Biomed	IGL (1:200) & IP
anti-HBsAg (10-1323)	Mouse-monoclonal	Fitzgerald	ELISA
anti-HBsAg (10-1324)	Mouse-monoclonal	Fitzgerald	ELISA
anti-PreS1 (AP1)	Mouse-monoclonal	Santa-Cruz (sc57761)	IGL(1:50)
anti-HBcAg (H746)	rabbit-polyclonal	Christa Kuhn	WB (1:2000)
anti-HBcAg (M312)	Mouse-monoclonal	Christa Kuhn	WB (1:1000)
anti-HBcAg (H709)	rabbit-polyclonal	Christa Kuhn	WB (1:3000)
anti-HBx (#644)	rabbit-polyclonal	Christa Kuhn	WB (1:500)
anti-HBx	rabbit-monoclonal	Gilead Sciences	WB (1:250)
anti-HBx	mouse-monoclonal	Gilead Sciences	WB (1:250)
anti-Gapdh	mouse-monoclonal	OriGene (TA802519)	WB (1:3000)
anti-β-actin	mouse-monoclonal	Sigma-Aldrich (A5441)	WB (1:5000)
anti-Nedd8	rabbit-polyclonal	Cell Signaling (#2745)	WB (1:1000)
Anti-ApoE	Goat-polyclonal	Sigma-Aldrich (AB947)	WB 1(1:1000) & IGL (1:100)
anti-Ubiquitin	mouse-monoclonal	Cell Signaling (3936S)	WB (1:5000)
Goat-IgG Isotype Control	Goat-polyclonal	Santa Cruz (sc-2028)	IGL (1:100)

Human-IgG1 Isotype Control	Human-polyclonal	Novus Biologicals DDXCH01P-100	IP

**WB: Western Blot; IGL: Immuno-gold Labeling; IP: Immuno-precipitation; ELISA: Enzyme-linked immunosorbent assay

Table 2.2. Secondary Antibodies

Antibody	Species	Provider-Catalog#	Application
anti-human-HRP	Goat	Abcam (ab97165)	WB (1:10000)
anti-rabbit-HRP	Goat	Sigma-Aldrich (A6154)	WB (1:10000)
anti-mouse-HRP	Goat	Sigma-Aldrich (A4416)	WB (1:5000)
anti-goat-HRP	Rabbit	Santa-Cruz (sc2768)	WB (1:2000)
anti-goat	Rabbit		IGL-Linker (1:150)
High Sensitivity Streptavidin-HRP		Pierce Biotechnology	ELISA (1:10,000)

**WB: Western Blot; IGL: Immuno-gold Labeling

2.1.2 Buffers and Solutions

Table 2.3. Buffers and solutions

Name	Composition/Supplier
10x PBS	1369 mM NaCl, 27 mM KCl, 17,6 mM KH2PO4, 100 mM Na2HPO4·2 H2O
10x TGS	250 mM Tris pH 8.3, 1.92 M Glycine, 1% w/v SDS
10x WB Transfer Buffer	250 mM Tris base, 1,5 M glycine pH 8.3
16% Paraformaldehyde for Electron Microscopy	Electron Microscopy Sciences (15710)
20x SSC	3.0 M NaCl, 0.3 M Na3C6H5O7 (sodium citrate) pH 7.0
50x TAE Buffer	2M Tris, 1M Acetic Acid, 50 mM EDTA, pH 8.3
6x Laemmli Sample Buffer	108 mM Tris pH 6.8, 33.6% glycerol, 2.4% SDS, 8.4% β-mercaptoethanol, 0.03% (w/v) bromophenol blue
Coomassie Gel Fixation Solution	40% methanol and 10% acetic acid in ddH_2O

ELISA Blocking Buffer	PBS-T, 2%BSA
ELISA Coating Buffer	0.1 M Carbonate-Bicarbonate, pH 9.5
ELISA Stop Solution	1 M H_2SO_4
LB Agar	300 mL LB medium supplemented with 4.5 g agar
LB Ampicilin Solution	LB medium supplemented with 100 µg/mL ampicillin
LB Medium	100 g LB powder in 5L ddH2O (50 g tryptone, 25 g yeast extract, 25 g NaCl)
Luciferase Assay Buffer	25 mM KPO4 buffer, 15 mM Glycyl-Glycin, 15 mM MgSO4, 4 mM EGTA (pH 7.6)
Luciferase Lysis Buffer	15 mM MgSO4, 25 mM Glycyl-Glycin, 1% Triton X-100, 10% Glycerol, 4 mM EGTA (pH 7.6)
PBS-T (ELISA and WB Washing Buffer)	PBS (1x). 0.1%(v/v) Tween-20
Resolving Gel Buffer	1.5 M Tris base, 0.4% SDS (w/v), pH 8.8
Silver Stain Fixation Solution	30% ethanol and 10% acetic acid in ddH_2O
Silver Stain Stop Solution	5% acetic acid in ddH_2O
Silver Stain Wash Solution	30% ethanol in ddH_2O
Soak I	1.5 M NaCl, 0.5 M NaOH
Soak II	0.3 M Tris, 3 M NaCl
Stacking Gel Buffer	1 M Tris base, 0.8% SDS (w/v), pH 6.8
TfB I	1.5 g KAc, 5.99 g MnCl2·4 H2O (or 7.29 g MnCl2·6 H2O), 3.75 g KCl, 8 mL CaCl2 (1 M), 67 mL glycerol (100%) to 500 mL with ddH2O, pH 5.8 (adjusted with HCl), sterile filtered
TfB II	1.0 g MOPS, 0.375 g KCl, 38 mL CaCl2 (1 M), 67 mL glycerol (100%) to 500 mL with ddH2O, pH 7.0 (adjusted with KOH), sterile filtered
TN Buffer	20 mM Tris-HCl, 140 mM NaCl
TN2140 Buffer	20 mM Tris-HCl, 2140 mM NaCl
WB Blocking Buffer	PBS-T, 5%BSA

**WB: Western Blot; LB: Luria-Bertani medium; PBS: Phosphate Buffered Saline; SSC: Saline-Sodium Citrate; TAE: Tris-Acetate-EDTA; TfB: Transformation buffer; TGS: Tris-Glycine-SDS; TN: Tris-NaCl

2.1.3 Cell lines and cell culture media

Table 2.4. Cell Lines

Name	Characteristics	Resistance
HepG2	Human hepatoma cell line isolated from a 15 year-old Caucasian male patient	
HUH7	Human hepatoma cell line derived from a 57-year old Japanese male patient suffering from HCC [Nakabayashi et al., 1982]	
HepaRG	Human hepatoma cell line isolated from an HCV-infected woman suffering from HCC [Gripon et al., 2002]	
HepAD38	HepG2-derived cell line carrying a tetracycline-inducible HBV integrate of genotype D subtype ayw [Ladner et al., 1997]	G418
HEK 293T	Human embryonic kidney cell line [DuBridge et al., 1987]	
HeLa-Kyoto	Human epithelia cell line from a 31 year old African American patient suffering from cervical carcinoma	
HepG2-HB2.7	HepG2 cell with 2.7kb partial HBV genotype D genome integrate	Blasticidin
HepG2-FLUC-HB2.7	HepG2-HB2.7 cell line harboring firefly luciferase cDNA under EF1a promoter	Blasticidin G418
HepaRG-HB2.7	HepaRG cell with 2.7kb partial HBV genotype D genome integrate	Blasticidin
HepaRG-HB2.7(X-)	HepaRG cell with 2.7kb partial HBV genotype D genome integrate with two stop codons on X ORFs	Blasticidin
HepaRG-LXEmpty	HepaRG cell harboring blasticidin resistance	Blasticidin

Table 2.5. Cell culture media

Name	Composition
$DMEM_{cult}$	500 ml DMEM, 10% FCS (heat inactivated), 100 U/ml penicillin, 100 µg/ml streptomycin and 1x non-essential amino acids
William's E_{HepaRG}	500 ml William's E medium, 10% FCS (heat inactivated), 2 mM L-glutamine, 100 U/ml penicillin, 100 µg/ml streptomycin, 50 µM hydrocortisone-hemisuccinate, 5 µg/ml insulin.
HepAD38	500 mL DMEM/F-12, 10% FCS (non-heatinactivated), 100 U/mL penicillin, 100 µg/mL streptomycin,1x MEM-non-essential amino acids, 2 mM L-glutamine,1 mM sodium pyruvate, 1ug/mL doxycycline For virus production/induction: Remove doxycycline
2x Cell freezing medium	FCS (heat-inactivated) supplemented with 20%DMSO

2.1.4 Chemicals and Reagents

Table 2.6. Chemicals and Reagents

Chemical/Reagent	Supplier
(Di)Sodium hydrogen phosphate (Na2HPO4)	Carl Roth, Karlsruhe, GER
1X TMB Solution	Thermo Fisher Scientific
Acetic acid (Rotipuran; 100% p.a.)	Carl Roth, Karlsruhe, GER
Acrylamide solution (Rotiphorese Gel 40 (29:1))	Carl Roth, Karlsruhe, GER
Agar	Sigma-Aldrich, St. Louis, USA
AGK2	Enzo Lifesciences, USA
Ammonium peroxodisulfate (APS)	Carl Roth, Karlsruhe, GER
Ampicillin sodium salt	Sigma-Aldrich, St. Louis, USA
Blasticidin	MP Biomedicals, Graffenstaden, FR
Bovine serum albumin (BSA) heat shock fraction, protease-free, pH 7	Sigma-Aldrich, St. Louis, USA
Bromophenol blue	AppliChem, Darmstadt, GER
Calcium chloride dihydrate (CaCl2·2 H2O)	AppliChem, Darmstadt, GER

cOMPLETE EDTA-free protease inhibitor	Roche-Diagnostics, Mannheim, GER
DIG Easy Hyb buffer	Roche Diagnostics, Mannheim, GER
Dimethyl sulfoxide (DMSO)	VWR International, Fontenay-sous-Bois, FR
D-Luciferin	PJK Biotech, GER
DMEM, high glucose (Cat.No.:41965)	Life Technologies, Paisley, UK
DMEM/F-12 (1:1), HEPES (Cat. No.: 31330)	Life Technologies, Paisley, UK
dNTPs (10 mM)	PEQLAB Biotechnologie, Erlangen, GER
Doxycycline hyclate	Sigma-Aldrich, St. Louis, USA
DTT (dithiothreitol)	Thermo Fisher Scientific,Vilnius, LT
Dynabeads Protein G for Immunoprecipitation	Life Technologies, Carlsbad, USA
EDTA disodium salt	AppliChem, Darmstadt, GER
EGTA	AppliChem
Ethanol absolute	VWR International, Fontenay-sous-Bois, FR
EZBlue Gel Staining Reagent	Sigma-Aldrich, St. Louis, USA
EZ-Link Sulfo-NHS-LC-Biotin	Pierce Biotechnology, *Illinois*, USA
Fetal Bovine Serum, charcoal stripped (Cat.No.: 12676029)	Life Technologies, Paisley, UK
Fetal calf serum (FCS), heat-inactivated (Cat. No.: FBS-HI-11A)	Capricorn Scientific, Ebsdorfergrund, GER
Fetal calf serum (FCS), non- heat-inactivated	Biowest SAS, FR
Gel Loading Dye Purple (6x)	New England Biolabs, Frankfurt am Main, GER
GeneRuler 100bp DNA ladder,	Thermo Scientific, Vilnius, LT
GeneRuler 1kb Plus DNA ladder	Thermo Scientific, Vilnius, LT
Geneticin (G418)	Life Technologies, Paisley, UK
Glutamine, L- (200 mM)	Life Technologies, Paisley, UK
Glycerol (100%)	Sigma-Aldrich, St. Louis, USA
Glycyl-glycine	Sigma-Aldrich, St. Louis, USA
Hydrochloric acid (HCl)	Fisher Scientific, Loughborough, UK
Hydrocortisone 21-hemisuccinate sodium salt	Sigma-Aldrich, St. Louis, USA
Insulin, Recombinant Human	SAFC Biosciences, UK

Isopropanol	Honeywell Riedel-de Haën, Seelze, GER
LB-Medium - Powder according to Lennox	AppliChem, Darmstadt, GER
Lipofectamine RNAiMAX Transfection Reagent	Life Technologies, Paisley, UK
Magnesium chloride hexahydrate (MgCl2·6 H2O)	Merck, Darmstadt, GER
Manganese (II) chloride tetrahydrate (MnCl2·4 H2O)	Carl Roth, Karlsruhe, GER
MEM Non-Essential Amino Acids Solution	Life Technologies, Paisley, UK
MEM-Non-essential amino acids	Life Technologies, Paisley, UK
Methanol	Fisher Scientific, Loughborough, UK
Midori Green	Nippon Genetics Europe, Düren, GER
MLN-4924 (Pevonedistat)	Active Biochem, HK
MOPS	Sigma-Aldrich, St. Louis, USA
Opti-MEM Reduced Serum Medium (Cat.No.:31985)	Life Technologies, Paisley, UK
Penicillin/Streptomycin	Life Technologies, Paisley, UK
Polybrene Infection / Transfection Reagent	Sigma-Aldrich, St. Louis, USA
Polyethylene glycol (PEG) 8000 , BioUltra	Sigma-Aldrich, St. Louis, USA
Potassium acetate (KAc)	Carl Roth, Karlsruhe, GER
Potassium chloride (KCl)	Carl Roth, Karlsruhe, GER
Potassium dihydrogen phosphate (KH2PO4)	Merck, Darmstadt, GER
Potassium hydroxide (KOH)	Carl Roth, Karlsruhe, GER
Precision Plus Protein Dual Color Standards	Bio-Rad Laboratories, GER
Protein A - 10nm gold conjugate	Cell Microscopy Core, NL
Puromycin dihydrochloride	Sigma-Aldrich, St. Louis, USA
RO 04-6790 hydrochloride	Axon Medchem, NE
Saccharose / Sucrose	Carl Roth, Karlsruhe, GER
SB 271046 hydrochloride	Axon Medchem, NE
siRNA Dilution Buffer	Santa Cruz Biotechnology, USA
SirReal 2	Axon Medchem, NE
Sodium chloride (NaCl)	Fisher Scientific, Loughborough, UK
Sodium dodecyl sulfate hydroxide (SDS)	Carl Roth, Karlsruhe, GER
Sodium hydroxide (NaOH)	Sigma-Aldrich, St. Louis, USA
Sodium pyruvate (100 mM)	Life Technologies, Paisley, UK
SYBR Green iTaqTM Universal Supermix	Bio-Rad Laboratories, GER

Tenofovir disoproxil fumarate (TDF)	Sigma-Aldrich, St. Louis, USA
Tetracycline hydrochloride	Sigma-Aldrich, St. Louis, USA
Tetramethylethylenediamine (TEMED)	Sigma-Aldrich Chemie, Steinheim, GER
TransIT-LT1 Transfection Reagent	Mirus Bio, USA
Tris	Carl Roth, Karlsruhe, GER
Triton X-100	AppliChem, Darmstadt, GER
Trypsin-EDTA (0.05%), phenol red	Life Technologies, Paisley, UK
Tween-20	AppliChem, Darmstadt, GER
William's E Medium, no glutamine (Cat.No.:22551)	Life Technologies, Paisley, UK
β-Mercaptoethanol	Sigma-Aldrich, St. Louis, USA

2.1.5 Consumables

Table 2.7. Consumables

Consumable Name	Supplier
4 mL, sterile, open-top thinwall, ultra-clear tube (SW60)	Beckman Coulter GmbH, Krefeld, GER
5mL round bottom plastic tube (ELISA)	Sarstedt, Nümbrecht, GER
Amicon Ultra centrifugal filters, 30k	Merck, Darmstadt, GER
Blunt fill neddle	Becton, Dickinson and Company, New Jersey, USA
Cell culture dish CELLSTAR 6 cm, 10 cm, 15 cm	Greiner Bio-One, Frickenhausen, GER
Cell culture flask T25, T75, T150	Greiner Bio-One, Frickenhausen, GER
Cell culture plate 6, 12, 24, 96 well	Greiner Bio-One, Frickenhausen, GER
Cell scraper	Sarstedt, Nümbrecht, GER
Cell strainer, 40 µm	Greiner Bio-One, Frickenhausen, GER
CellSTACK cell culture chambers (5 stack)	Corning, New York, USA
Costar Aspirating Pipets, Plastic	Corning, New York, USA
Cryo-vials	Greiner Bio-One, Frickenhausen, GER
Disposable overshoe	Diaprax GmbH, Wesel, GER

Extra thick blot paper	Bio-Rad Laboratories GmbH, GER
Face mask	Meditrade, Kiefersfelden, GER
Falcon bacteriological petri dishes, 10 cm	Corning, New York, USA
Falcon cell culture 5-layer multi-flask	Corning, New York, USA
Falcon tube 15 mL, 50 mL	Corning, New York, USA
Gloves Microflex XCEED XC INT	Ansell Healthcare Europe, Brussles, BE
Gloves SHIELDskin Orange Nitril 260	SHIELD Scientific, Bennekom, NE
Hard-Shell 96-Well PCR Plates	Bio-Rad Laboratories GmbH, GER
Low Protein Binding Tube (2mL)	Pierce Biotechnology, *Illinois*, USA
Luer-lok Syringe 1mL	Becton, Dickinson and Company, New Jersey, USA
Non-treated 96-Well Microplates	Greiner Bio-One, Frickenhausen, GER
Nylon membrane	Roche Diagnostics, Mannheim, GER
PCR tubes	Biozym, Hessisch Oldendorf, GER
Plastic cuvets (Cuvettes)	Ratiolab, Dreieich, GER
PVDF membrane for protein blotting	Bio-Rad Laboratories GmbH, GER
Reaction tubes 1.5 mL, 2 mL	Sarstedt, Nümbrecht, GER
Reagent reservoirs	Corning, New York, USA
Scalpel, disposable	PFM Medical, Köln, GER
Sealing sheets PCR plates	Bio-Rad Laboratories GmbH, GER
Sterile Plastic Bottle (500mL)	TPP Techno Plastic Products, Trasadingen, CH
Stripettes 5 mL, 10 mL, 25 mL, 50 mL	Corning, New York, USA
Syringes 5,10,20mL BD DISCARDIT II	Becton, Dickinson and Company, New Jersey, USA
Syringes 50 mL Terumo without needle	Terumo Europe, Leuven, BE
Tips 10, 200 and 1000 µL	Starlab, Hamburg, GER
Vacuum Filtration "rapid"-Filtermax (250 ml)	TPP Techno Plastic Products, Trasadingen, CH
Vacuum Filtration "rapid"-Filtermax (500 ml)	TPP Techno Plastic Products, Trasadingen, CH
Whatman FP30 filters 0.2 µm, 0.45 µm	GE Healthcare UK Limited, Little Chalfont, UK
Whatman paper	GE Healthcare UK Limited, Little Chalfont, UK
White, CELLSTAR 96 well cell culture plate	Greiner Bio-One, Frickenhausen, GER

2.1.6 DNA Oligonucleotides

Table 2.8. DNA Oligonucleotides used for (RT-q)PCR

Name	Sequence 5' → 3'
GAPDH fwd	GAAGGTGAAGGTCGGAGTC
GAPDH rev	GAAGATGGTGATGGGATTTC
HBsAg (HB2.7) fwd	GATTCCTAGGACCCCTTCTC
HBsAg (HB2.7) rev	GGAGGACAAGAGGTTGGTGA
pgRNA specific-fwd	CTCCTCCAGCTTATAGACC
pgRNA specific-rev	GTGAGTGGGCCTACAAA
HBV total RNA-fwd	TCAGCAATGTCAACGACCGA
HBV total RNA-rev	TGCGCAGACCAATTTATGCC

Table 2.9. DNA Oligonucleotides used for cloning

Name	Sequence 5' → 3'
X-(C22T) fwd	GCTGTGCTGCTAACTGGATCC
X-(C22T) rev	CTAGCAGCCATGGAAACG
X-(C259T) fwd	GAACGCCCACTAAATATTGCCC
X-(C259T) rev	ACGGTGGTCTCCATGCGA

Table 2.10. DNA Oligonucleotides used for total HBV DNA qPCR

Name	Sequence 5' → 3'
Total HBV DNA fwd	GTTGCCCGTTTGTCCTCTAATTC
Total HBV DNA rev	GGAGGGATACATAGAGGTTCCTTGA

2.1.7 Plasmids

Table 2.11. Plasmids

All plasmids encode ampicillin resistance genes under prokaryotic promoter.

Plasmid Name	Description	Source/Provider
pLX304-HB2.7	CMV promoter removed lentiviral vector with HBV genotype D subgenomic fragment and blasticidin resistance	Florian Lempp/AG Urban
pLX304-HB2.7(X^-)	pLX304-HB2.7 plasmid with two stop codon insertion into HBx ORF and blasticidin resistance	Firat Nebioglu
pcDNA3.1(+)-mCherry	mCherry red fluorescent protein under CMV promoter -	Minh-Tu Pham
pcDNA3.1(+)-ApoE-3	ApoE3 allele under CMV promoter	Minh-Tu Pham
pcDNA3.1(-)-zeo-HBV1.1	Wildtype HBV genotype D 1.1 overlength genome under CMV promoter and zeocin resistance	Michael Nassal
pSHH2.1	Two copies of HBV genotypeD ligated at EcoRI restriction enzyme cutting sites.	AG Urban
pWPI-neo-FLUC	Lentiviral vector for firefly luciferase expression under EF1alpha promoter	Joschka Willemsen
pMD2.G	2nd generation lentiviral packaging plasmid encoding VSV-G envelope protein	Didier Trono
pCMV-dR8.91	2nd generation lentiviral packaging plasmid encoding Gag, Pol, Rev, and Tat	Didier Trono
pSVSX	S domain of HBV genotypeD under SV40 promoter	Philippe Gripon
pSV12SX	Three HBV envelope proteins and HBx under SV40 promoter	Philippe Gripon

2.1.8 Small interfering RNAs (siRNAs)

Information on siRNAs used during the mini-screen experiment are listed in the appendix section.

Table 2.12. List siRNAs used for validation experiments

siRNA	Catalog Number / Company	Target Sequence
ON-TARGETplus Non-targeting Control siRNA	D-001810-02-05 Dharmacon	
ON-TARGETplus HBsAg Custom Design siRNA	Custom Design Dharmacon	Sense 5' GGUAUGUUGCCCGUUUGUC Antisense 5' GACAAACGGGCAACAUACC
ON-TARGETplus Human NEDD8 siRNA8 siRNA	L-020081-00-0005 Dharmacon	
ON-TARGETplus Human UBE2M siRNA siRNA	L-004348-00-0005 Dharmacon	

2.1.9 Enzymes and reaction buffers

Table 2.13. Enzymes and reaction buffers

Enzymes / Reaction buffers	Supplier
Q5 High-Fidelity DNA Polymerase	New England Biolabs, Frankfurt am Main, GER
5X Q5 High GC Enhancer	New England Biolabs, Frankfurt am Main, GER
5X Q5 Reaction Buffer	New England Biolabs, Frankfurt am Main, GER
Restriction Enzymes (DpnI, XmaI, NheI)	New England Biolabs, Frankfurt am Main, GER
Reaction Buffers (CutSmart)	New England Biolabs, Frankfurt am Main, GER
DNA Polymerase I, Large (Klenow) Fragment	New England Biolabs, Frankfurt am Main, GER
T4 Polynucleotide Kinase	New England Biolabs, Frankfurt am Main, GER
T4 DNA Ligase	New England Biolabs, Frankfurt am Main, GER
T4 DNA Ligase Reaction Buffer	New England Biolabs, Frankfurt am Main, GER

2.1.10 Equipment and Software

Table 2.14. Equipment

Equipment	Supplier
6x Tube magnetic separation rack	New England Biolabs, Frankfurt am Main, GER
Äkta Pure	Cytiva, Little Chalfont, UK (GE Healthcare Life-Sciences)
Äkta Purifier 100	Cytiva, Little Chalfont, UK (GE Healthcare Life-Sciences)
Carbon Coater Leica EM ACE600	Leica Microsystems Wetzlar, GER
Cell culture centrifuge ROTINA 380R	Andreas Hettich, Tuttlingen, GER
Cell culture microscope Primovert	Carl Zeiss, Oberkochen, GER
CO2 cell incubator C200	Labotect, Rosdorf, GER
CO2 cell incubator Thermo Forma 3111 Series II, water jacketed	Thermo Fisher Scientific Waltham, USA
Dot blot chamber, 96 well	Schleicher & Schuell Dassel, GER
Glow discharger	Gala Instrumente Bad Schwalbach, GER
Heat block / shaker Thermomixer C, Thermomixer F1.5	Eppendorf, Hamburg, GER
HiTrap Heparin HP affinity columns (5 and 1 mL)	Cytiva, Little Chalfont, UK (GE Healthcare Life-Sciences)
Intas Advanced Fluorescence Imager	Intas Science Imaging Instruments, Göttingen, GER
Intas Chemocam Imager	Intas Science Imaging Instruments, Göttingen, GER
Laminar flow Safe 2020	Thermo Fisher Scientific Waltham, USA
LI-COR Odyssey CLx	LI-COR Biosciences Bad Homburg vor der Höhe,GER
Light panel LP-400N	Universal Electronics Industries Santa Ana, USA
Luciferase plate reader Mithras² LB 943	Berthold Technologies GmbH & Co. KG, Bad Wildbad, GER

Mini table-top centrifuge 3-1810	Neolab, Heidelberg, GER
Multiskan EX ELISA Reader	Thermo Fisher Scientific Oy Vantaa, FI
NanoDrop NP-1000 Spectrophotometer	PEQLAB Biotechnologie Erlangen, GER
pH and OPR meter HI 2211	Hanna Instruments Vöhringen, GER
Phosphorimager Fuji Typhoon FLA-7000	FUJIFILM Corporation Tokyo, JP
Pipetboy acu 2	Integra Biosciences Biebertal, GER
Pipette 2.5, 10, 20, 200 and 1000 µL Research Plus	Eppendorf, Hamburg, GER
Power Supply Pack Basic	Bio-Rad Laboratories GmbH, GER
Pump for cell culture waste BVC professional	Vacuubrand, Wertheim, GER
Refractometer	Carl Zeiss, Oberkochen, GER
Rotator mit Vortexer	NeoLab, Heidelberg, GER
Rotors SW60-Ti	Beckman Coulter, Krefeld, GER
S3 Cell culture microscope (Nikon Eclipse Ts2-FL)	**Nikon Instruments Europe BV, Amsterdam, NE**
Shaker DRS-12	NeoLab, Heidelberg, GER
Spectrophotometers Ultrospec 3100 pro	Amersham Biosciences, Chalfont St. Giles, UK
Superose 6 column (XK 26/70)	Cytiva, Little Chalfont, UK (GE Healthcare Life-Sciences)
Superose 6 Prep Grade	Cytiva, Little Chalfont, UK (GE Healthcare Life-Sciences)
Superspeed centrifuges Sorvall RC-5C Plus and Lynx 4000	Thermo Fisher Scientific, Waltham, USA
Table-top centrifuge 5424, 5424R, 5810R	Eppendorf, Hamburg, GER
Thermal Cycler T100, C1000 Touch	Bio-Rad Laboratories GmbH, GER
Trans-Blot Turbo transfer system	Bio-Rad Laboratories GmbH, GER
Transmission electron microscope	Jeol, Tokyo, JPN

JEOL JEM-1400	
Tube roller RS-TR05	Phoenix Instrument Garbsen, GER
Ultracentrifuge L7-55	Beckman Coulter, Krefeld, GER
Ultracentrifuge Optima LE-80K	Beckman Coulter, Krefeld, GER
UV crosslinker UV Stratalinker 1800	Stratagene, San Diego, USA
UVP Minidizer Oven	Analytik Jena, Jena, GER
Vortex Genie 2	Scientific Industries, New York, USA
Water bath JB Nova	Grant Instruments, Cambridge, UK
Western blot running chambers Mini Protean Tetra system	Bio-Rad Laboratories GmbH, GER

Table 2.15. Software

Name	Supplier
GraphPad Prism	GraphPad Software, La Jolla, USA
Image J	Wayne Rasband, NIH, USA
Intas Chemostar	Intas Science Imaging, Göttingen, GER
MS Office	
Bio-Rad CFX Manager	Bio-Rad Laboratories, Hercules, California, USA
SnapGene, SnapGene Viewer	GSL Biotech, San Diego, USA
Adobe Illustrator CS 6.0	Adobe Inc., San Jose, California, USA
Image Lab 6.0.1	Bio-Rad Laboratories, Hercules, California, USA
Image Studio Lite 5.2	LI-COR Biosciences Bad Homburg vor der Höhe, GER
UNICORN 7.2	GE Healthcare Bio-Sciences, Uppsala, Schweden
UNICORN 5.11	GE Healthcare Bio-Sciences, Uppsala, Schweden

2.1.11 Kits

Table 2.16. Kits

Name	Supplier
Amersham ECL Prime Western blotting Detection Reagent	GE Healthcare UK Limited, Little Chalfont, UK
Clarity Western ECL Substrate	Bio-Rad Laboratories GmbH, GER
DIG Luminescent Detection Kit for Nucleic Acids	Roche Diagnostics, Mannheim, GER
DIG Wash and Block Buffer Set	Roche Diagnostics, Mannheim, GER
PCR DIG Probe Synthesis Kit	Roche Diagnostics, Mannheim, GER
Pierce Silver Stain Kit	Pierce Biotechnology, Rockford, USA
Nucleobond PC 500	Macherey-Nagel, Düren, GER
NucleoSpin Gel and PCR Cleanup	Macherey-Nagel, Düren, GER
NucleoSpin Plasmid	Macherey-Nagel, Düren, GER
NucleoSpin RNA Plus	Macherey-Nagel, Düren, GER
High-Capacity cDNA Reverse Transcription Kit with RNase Inhibitor	Thermo Scientific, Vilnius, LT
Monarch Total RNA Miniprep Kit	New England Biolabs, Frankfurt am Main, GER

2.1.12 Bacterial Strains and Viruses

Table 2.17. Bacterial Strains

Name	Species
DH5α	Escherichia coli

Table 2.18. Viruses

Virus	Comment
HBV Genotype D	HepAD38 derived
HBV Genotype A	HUH7 derived (from Pascal Mutz-AGB)
HBV Genotype B	HUH7 derived (from Pascal Mutz-AGB)
HBV Genotype D	HUH7 derived (from Pascal Mutz-AGB)
HBV Genotype D	HepAD38 derived (from Florian Lempp-AGU)
HDV Genotype 1	HUH7 derived (from Zhenfeng Zhang-AGU)

HDV Genotype 1	HUH7 derived (from Florian Lempp-AGU)
HDV Genotype 3	HUH7 derived (from Florian Lempp-AGU)

2.2 Methods

2.2.1 Cell Culture

2.2.1.1 Cell culture conditions and maintenance of cell culture

All cell lines were kept at 37ºC at 5%CO_2 in 95% humidity. Unless otherwise stated in the protocol, 293T, HeLa, HUH7, and HepG2 cell lines and their derivatives were maintained in DMEM medium with 10%FCS, 1x non-essential amino acids, 100 U/ml penicillin, 100 µg/ml streptomycin (DMEMcult). HepaRG cell lines were kept in William's E medium supplemented with 10% FCS, 2 mM L-glutamine, 100 U/ml penicillin, 100 µg/ml streptomycin, 50 µM hydrocortisone-hemisuccinate, 5 µg/ml insulin (William's E_{HepaRG}). For HepAD38 cells, DMEM/F-12 medium containing 10% FCS, 100 U/mL penicillin, 100 µg/mL streptomycin,1x MEM-non-essential amino acids, 2 mM L-glutamine,1 mM sodium pyruvate was used. HepAD38 cells harbor 1.1 fold HBV genotype D integrate under inducible tet-off promoter. For suppression of the HBV production, the HepAD38 medium was supplemented with 1ug/mL doxycycline for general maintenance of the cells. Dox-off induction and the protocol for HBV production are described in section 2.2.1.4.

All cell lines cells were maintained by passaging every three or four days and seeding into new sterile dishes/flasks. Briefly, the culture medium was aspirated and the cells were washed with PBS once. After removal of the PBS, the cells were covered with 0.05% trypsin-EDTA solution and incubated at 37°C for three to five minutes. The detached cells were examined under a bright-field microscope and re-suspended with fresh culture media. Depending on the cell line, the cells were split between 1:6 or 1:10 into a new culture.

2.2.1.2 Freezing and thawing cells

Cells were frozen in 10% DMSO containing FCS solution in cryo-vials. Briefly, cells cultured in a 15cm dish were re-suspended in culture medium after detachment from the culture dish as described in 2.2.1.1. To remove the excess medium, the cell suspension was centrifuged down at 400g for 5 minutes. The supernatant was aspirated and the cell pellet was re-suspended in 2mL culture medium. The 2ml concentrated cell suspension was placed on ice and mixed with

ice-cold 2mL 2xFreezing medium (20%DMSO in fetal calf serum). Each cryo-vial contains 1mL of cell suspension-freezing medium solution was immediately frozen at -80ºC for short-term storage. The cryo-vials were transferred to a liquid nitrogen tank for long-term storage. Thawing of the cells was performed by incubating the vials in 37ºC water bath before the cells were re-suspended in 19mL culture medium. The cells were pelleted down to get rid of the DMSO-containing medium and then cultured in 10mL in a 10cm dish.

2.2.1.3 Cell counting

Detached cells were placed on a 40µm cell strainer to obtain single-cell suspension and 10µL of the solution was injected into one side of the cell counting chamber (hemocytometer) for determination of cell number/mL.

2.2.1.4 Long-term culture of HepG2, HepG2-HB2.7, and HepAD38 cells

Long-term cultivation of HepG2, HepG2-HB2.7, and HepAD38 cell lines were performed in DMEM/F12 based HepAD38 medium as described in 2.1.3. The culture of the cells was done on a large-scale; either in 3,180 cm^2 Corning 5-stack cell culture chambers or 875 cm^2 Falcon multi-flask chambers. For seeding and culturing in 875 cm^2 multi-flask chambers the following protocol was followed. The cell lines were grown and expanded in T175cm^2 flasks until getting six confluent T175cm^2 for each cell line. The cells were detached by washing with PBS and adding 3 mL of 0.05% trypsin-EDTA into each flask. The cells in each flask were collected by adding 32mL of fresh medium and then poured through a 40µm cell strainer placed on a 50mL falcon. Total cell suspension from each flask was pooled into a sterile container (210mL) and further diluted by adding fresh medium until 315mL volume reached. From this, 140mL of cell suspension was distributed into each of two multi-flask cell culture containers. For the leftover cells, T25 control flasks were prepared by adding 4mL of cell suspensions and 1mL of fresh medium. The multi-flask and control flasks were kept in doxycycline-containing medium until day14 post-seeding and doxycycline was removed afterward for induction of HBV virus production. The cells were kept in culture for at least 75 days for each purification and the medium was collected/refreshed every 4 or 5 days. Collected cell supernatants were sterile filtered through 0.2µm membranes and analyzed for the presence of HBsAg and HBeAg by ELISA. The collected materials were stored at 4º C for further processing.

2.2.1.5 Lentivirus Production and Transduction

Lentivirus production was done on Hek293T cells seeded on a 10cm dish one day before the transfection of the lentiviral production plasmids. The cells were around 80% confluent before transfection. Briefly, 2.4 µg of pMD2.G and 6.4 µg of pCMV-dR8.91 lentiviral packaging vectors were co-transfected with 6.4 µg of pLX304 or pWPI expression vectors. The plasmids were mixed in sterile water and 62 µL 2M $CaCl_2$ was added to ring the final volume of the mixture to 500uL. The DNA-containing solution was mixed with 500uL 2xHBS (HEPES-buffered saline) and vortexed briefly. The final 1mL mixture was added on top of the cells dropwise, equally distributed over the dish. On the day1 post-transfection, the cell culture medium was refreshed and lentivirus containing supernatants were collected in a falcon starting at day2 post-transfection. Collected supernatants were filtered through 0.45µm Whatman papers for the removal of cell debris. The lentivirus solution was used for transduction of the target cells afterward. For the transduction experiments, the lentivirus-containing mediums were directly applied on target cell culture in presence of polybrene (8µg/mL). The virus was removed on the next of transduction and antibody selection (G418 or blasticidin) was performed for both transduced and non-transduced (negative control) cell lines.

2.2.1.6 DNA Transfection

The overexpression experiments were performed by using Mirus LT-1 DNA transfection reagent on target cell lines. The cells were counted and 7.5 x 10^5 cells were seeded into 6-well plates one day before transfection. The overexpression cassette containing plasmids were incubated in Opti-MEM with Mirus-LT1 reagent for 15-30 minutes and distributed onto the cells. On the 2nd day of transfection, the medium was changed and the experiments were performed on the day4 post transfection. The transfection mixture was prepared according to Table19.

Table 2.19. DNA transfection mix

Reagent	24-well	6-well
Opti-MEM Reduced Serum Medium	50 µl	250 µL
Plasmid DNA Amount	0,5 µg	2,5 µg
Mirus TransIT LT-1	2,5 µl	7,5 µL

2.2.2 Small Interfering RNA (siRNA) Mini-screen

2.2.2.1 Solid-phase reverse transfection in multiwell plates

The library for the siRNA mini-screen was prepared by Advanced Biological Screening Facility (BioQuant) of University of Heidelberg. The Silencer Select siRNAs purchased from Ambion/Thermo Scientific were mixed with OptiMEM/Sucrose solution in presence of Lipofectamine 2000. The mixture was incubated at room temperature for 30 minutes. Gelatin/fibronectin solution was added into the siRNA-Lipofectamine 2000 complex at the end of the incubation period. The solution was mixed with Millipore water for even coating of the wells. The final solution of siRNA complexes was distributed into each well of white cell 96-well cell culture plates and vacuum dried. The plates are stable at room temperature for at least one year. Further details and exact amounts of the reagents can be found in Erfle, H. *et al*. 2008[329]. The plates were seeded with 10,000 HepG2-F-HB2.7 cells in 200µL growth medium. At 48 hours post-seeding, the medium was replaced with 200µL of fresh one, and supernatants and cells were analyzed by homemade HBsAg ELISA and luminometer, respectively at 96 hours post-seeding.

2.2.2.2 siRNA reverse transfection in multi-well plates

Validation experiments were performed by using Dharmacon ON-Target plus siRNAs (Table: 11). The lyophilized siRNAs were solubilized in siRNA resuspension buffer to bring the final siRNA concentration to 20µM. The siRNA stock solution was aliquoted and stored at -80^0 C. Validation experiments were performed in 24-well format multi-well plates. Briefly, the siRNA was added into Opti-MEM reduced serum medium and mixed with Lipofectamine RNAiMax. The siRNA solution was pipetted up and down a few times and then 100µL of the complex was distributed into each well of the plate. The siRNA complex solution was incubated between 20-30 minutes before the addition of 100,000 cells/well in 500µL medium. The final concentration siRNAs were 30nM except HBsAg siRNA which was 60nM. The exact amounts of the reagents for a 24-well format can be found below.

Table 2.20. siRNA transfection mixture

Reagent	24-well format
Opti-MEM Reduced Serum Medium	500 µl
siRNA Stock Solution (20 µM)	4,5 µg
Lipofectamine RNAiMax Transfection Reagent	5 µl

2.2.2.3 Quantification of HBsAg and HBeAg from cell culture medium

Quantifications of HBsAg from 96-well siRNA mini-screen plates were performed by using homemade ELISA kits. The ELISA plates were coated with 100µL HBsAg antibody (10-1324) in coating buffer to a final concentration of 1µg/ml. The plates were sealed and incubated with antibody overnight at room temperature. On the next day, the coating antibody was discarded and the plate was blocked with 200µL of ELISA blocking buffer for 2 hours at 37º C. Following the blocking step, the 50µL samples of interest were added into each well of 96-well plate and incubated for 2 hours at 37ºC. The wells were washed 3 times with 200µL of ELISA washing buffer and 100µL biotinylated HBsAg antibody (10-1323) was applied with a final concentration of 0,5 µg/ml. Excess of biotin-HBsAg antibody was removed by another washing step with four repetitions. At the end of the washing, streptavidin-HRP (1:10,000) in blocking buffer was added into the wells for 1 hour with subsequent washing steps again. As the last step, the wells were incubated with ELISA substrate solution for approximately 5 minutes until sufficient signal was reached. The reaction was stopped by an addition of 50µL of ELISA stop solution. Optical density (OD) 450nm was measured with reference of 620nm by ELISA reader. For culture systems larger than 96-well plate, the samples were submitted to the Analytic Center of University Hospital of Heidelberg, where HBsAg and HBeAg quantification were conducted by ADVIA Centaur XPTM automated chemoluminescence (Siemens, Berlin, GER) and Architect Assay (Abbott, Wiesbaden, GER) systems, respectively.

2.2.2.4 In-cell ELISA

For in-cell ELISA, the cells were lysed with a solution containing 1xTN buffer (20 mM Tris-HCl [pH 7.4], 1% Triton X-100 and protease inhibitor cocktail (Roche)). After freezing and thawing the cells, cell lysates were collected into reaction tubes and rotated at 4°C for 15 minutes. Insoluble material was removed by centrifugation at 400 g for 5 minutes and HBsAg amounts contained in supernatants were quantified by using Architect Assay (Abbott, Wiesbaden, GER) systems as described above.

2.2.2.5 Luciferase Assay

Cells in 96-well format plates were washed with PBS before addition of 25µL of Luciferase lysis buffer per well. The lysis solution was freshly supplemented with DTT with a final concentration of 1mM. The plates were frozen at -80º C until the day of experimentation. For the firefly luminescence measurement, the plates were thawed at room temperature and

luciferase assay buffer containing D-Luciferrin was injected with Mithras² LB 943 luminometer and values were measured. The program for the assay can be found below.

Table 2.21. Luminometer program for firefly luciferase assay

Step	Procedure/Details
Dispense Luciferase Assay buffer + D-Luciferin	4 x 20uL
Shake	2 seconds
Measure	10 seconds
Dispense SDS solution	20uL
Shake	2 seconds

2.2.3 HBV Subviral Particle and Virion Purification

2.2.3.1 Affinity and size-exclusion chromatography

The supernatants of long-term, large-scale cell culture from Section 2.1.4 were applied to HBV particle purification pipeline. Fully automated Äkta liquid chromatography systems (Äkta Purifier 100 and Äkta Pure) were used for 5- or 1-mL HiTrap heparin HP affinity and size exclusion chromatography. For each purification, 450 mL of supernatant were loaded onto H5 heparin column followed by five column volumes of washing with Tris-NaCl pH7.4 buffer. The bound material on the column was eluted by a linear gradient (140mM to 2140mM) of salt solution with ten volumes of the column. The runs were monitored in real-time by measuring absorbance at UV254nm and UV280nm (OD_{254} and OD_{280}). Eluted materials were collected 2.5mL fractions and the three fractions with the highest absorbance were pooled together for Superose 6 (S6) column application (Ø 26 mm, length 600 mm). The samples were loaded into the S6 column with superloop and the virion containing OD_{254} and OD_{280} peak was close to the void volume of the column as described before[260]. The virus peak fractions were subjected to another round of HiTrap heparin HP affinity chromatography in H1 column. Elution of the H1 column was performed again with linear salt concentration and the 0,5mL fractions were collected for equilibrium density gradient centrifugation.

2.2.3.2 Equilibrium density gradient centrifugation

Density gradient for sucrose was created by laying 1 mL of 60% sucrose and 0.5 mL of 45%, 35%, 25%, and 15% sucrose from bottom to top into the ultra-clear polypropylene tubes. The sucrose solutions were prepared by solubilizing (w/w) saccharose powder in 1xTN, pH7.4 buffer which was sterile filtered to avoid any contaminations. The fractions obtained from H1 column elution were pooled, which was approximately 1.5mL from three fractions, and laid on top of the sucrose gradient. Ultracentrifugation of the samples was performed with SW60 rotor, at 164,000 g and 4º C for overnight. On the next day, the sucrose gradients were fractionated from bottom to top of the tubes and around 150µL of the sample was dropped into each 1.5 mL reaction tube. The refractive index of each sucrose fraction was determined and the fractions were further characterized by various methods.

2.2.3.3 HBV Immunoprecipitation

The selected sucrose fractions were diluted in 1xTN buffer and applied to Amicon Ultra 0.5mL centrifugal filter column to get rid of the sucrose. The sucrose-free eluate was brought to 220uL in TN buffer for the immunoprecipitation (IP) experiment. In the meantime, protein-G coupled magnetic beads were incubated with either a-HBsAg antibodies or a-IgG1 isotype controls for 30 minutes at constant rotation. For this process, 10µg antibody / 1,5mg of Dynabeads-ProteinG was used. Uncoupled antibodies were removed by placing the beads on a magnetic rack and washed with 1xTN buffer once. The sucrose-free eluate sample was applied to a-HBsAg or a-IgG1 beads, 100µL per condition. The leftover 20µL was kept as input condition. The beads were incubated with the beads for 3 hours at 4º C on constant rotation. The unbound solution was collected at the end of the incubation and the beads were washed with 1xTN buffer four times, with a transfer of the beads into a fresh reaction tube twice. At the end of the analysis, the beads were resuspended in 100µL of Tris buffer pH8 to eliminate any interference of NaCl in downstream experiments, 30µL out of 100µL was spared for protein gel based analysis. The leftover bead suspension was placed into the magnetic rack for removal of the buffer. The dry beads were stored at -80º C for proteomics experiments. During the IP experiments, only low protein binding reaction tubes were used.

2.2.4 DNA and RNA

2.2.4.1 Site-Directed Mutagenesis by PCR

X deficient versions of pLX304-HB2.7 plasmids were generated by PCR-based site-directed mutagenesis approach. Two stop codons were inserted into amino acid (aa) positions 8 and 86 of X ORF. In the first round of the mutagenesis, the primer pair targeting aa position 8 was used to generate plasmid with a single stop codon, which was followed by the second round of mutagenesis at aa position 86. The PCRs were performed by using Q5 high-fidelity DNA polymerase in T100 thermal cycler. The PCR products were digested with DpnI enzyme for the elimination of the input plasmid. The amplicon was run on agarose gel and extracted from the gel. The product was phosphorylated from the ends by using T4 PNK and circularized by ligation with T4 DNA ligase. The plasmids were transformed into competent bacteria and colonies were culture in mini-culture for plasmid isolation. The plasmids with expected mutations were stored at -20º for future experiments.

Table 2.22. Composition of a standard PCR reaction

Reagent	Volume/Amount
Q5 Reaction buffer (5x)	5 µL
Q5 High GC Enhancer (5x)	5 µL
dNTPs (10mM)	0.5 µL
Template DNA	25 ng (0.5 µL)
Forward Primer (10µM)	1.25 µL
Reverse Primer (10µM)	1.25 µL
Q5 High Fidelity DNA Polymerase	0.25 µL
ddH_2O	11.25 µL

Table 2.23. Standard PCR program

Step	Temperature	Duration	Cycle
Initial Denaturation	98ºC	30 s	1x
Denaturation	98ºC	10 s	
Annealing	64-67ºC	10-20 s	30x
Elongation	72ºC	300 s	
Final elongation	72ºC	120 s	1x
Hold	4ºC	∞	

2.2.4.2 Total HBV DNA quantitative PCR

The HepAD38 cell supernatants were diluted with ddH_2O in a 1:10 ratio and directly applied into quantitative PCR (qPCR) reaction tubes. The absolute number of the HBV total DNA was determined by interpolation of the qPCR Ct values to a standard curve constructed with an HBV genome containing plasmid. The PCR conditions and qPCR reaction components are written below.

Table 2.24. Reaction mixture of HBV DNA qPCR

Reagent	Volume/Amount
2xSYBR green mix	7,5 µL
Forward Primer (100µM)	0,06 µL
Reverse Primer (100µM)	0,06 µL
H_2O	4,5 µL
Template	3 µL

Table 2.25. HBV DNA qPCR program

Step	Temperature	Duration	Cycle
Initial Denaturation	95ºC	180 s	1x
Denaturation	95ºC	10 s	
Annealing	60ºC	30 s	40x
Elongation	65ºC	10 s	

2.2.4.3 DNA Dot Blot

For HBV DNA quantification from HepAD38 cell supernatants and sucrose fractions of equilibrium density centrifugation, a nylon membrane and two Whatman papers were soaked into PBS and placed into a 96-well vacuum chamber for the sample application. Initially, the membrane was washed twice with PBS which was followed by sample and standard plasmid (pcDNA3.1(-)-zeo-HBV1.1) application. The stock plasmid solution contains $1x10^{11}$ copies of linearized HBV genome/50µL solution. This stock was diluted at 1:20 to generate an H1 standard of $5x10^9$ copies of DNA/50µL. The serial dilution of the H1 generated H2-6 standard solutions (H2: $1x10^9$ copies/50µL, H3: $2x10^8$ copies/50µL, H4: $4x10^7$ copies/50µL, H5: $8x10^6$ copies/50µL, H6: $1.6x10^6$ copies/50µL). The membrane was transferred to Soak I buffer for denaturation (90seconds, twice) of the DNA subsequently to Soak II buffer for renaturation (60 seconds, twice). The membrane was dried on a clean Whatman paper before placing into UV-crosslinker UV (Stratalinker 1800). The membrane was auto-crosslinked at 120,000

microjoules/cm^2, two times. Depending on the method of detection, either radioactive or chemiluminescence, two different protocols with the same basic principles were applied on the membrane. Briefly, the membrane was incubated in the pre-hybridization solution for one hour and the probe was hybridized with the HBV DNA on the membrane, overnight with constant rotation in an oven. On the next day, the membrane was washed with buffers and made ready for detection. The radioactively labeled membrane was air-dried and placed on β-radiation-sensitive film in a locked cassette overnight. The signal on the film was acquired with PhosphorImager (Fuji Typhoon FLA-7000). On the other hand, the washed membranes were blocked with the DIG DNA labeling kit buffers and incubated with a-DIG antibody. After washing the membrane with DIG washing buffer and equilibrating it with DIG detection buffer, the membrane was incubated with chemiluminescence substrate CSPD containing DIG detection buffer, and the signal was acquired with Intas Chemocam Imager.

2.2.4.4 RNA Isolation

Cells were washed with PBS at the end of each experiment and lysed with lysis buffer provided by the RNA isolation kit (NucleoSpin RNA Plus or Monarch Total RNA Miniprep Kit). The manufacturer's RNA isolation protocol was followed and the isolated RNA was kept at -20ºC for short-term and -80ºC for long-term storage.

2.2.4.5 Reverse transcription and qPCR

The isolated RNA was reverse transcribed by using the High Capacity cDNA Reverse Transcription kit (Applied Biosystem) in conditions described in Table 26 and Table 27. The synthesized cDNA is diluted with nuclease-free H_2O and used for qPCR reactions.

Table 2.26. Reverse-transcription reaction mixture

Reagents	Volume/Amount
10X RT Buffer	1 µL
RT Random Primers	1 µL
25X dNTP Mix (100mM)	0.4 µL
MultiScribe Reverse Transcriptase (50U/µL)	0.5 µL
RNase Inhibitor	0.5 µL
Nuclease-free H2O	1.6 µL
RNA solution (250ng)	5 µL
Total Volume	10 µL

Table 2.27. Reverse-transcription program

Temperature	Duration
25 ºC	10 minutes
37 ºC	120 minutes
85 ºC	5 minutes
4 ºC	∞

Reactions of qPCR were placed in a thermal cycler (C1000 Touch) and the program written in Table 28 was run. The details on the qPCR reaction mixture can be found in Table 27. For the analysis of the data, ΔΔCt method as described by Livak *et al.* was used, and having GAPDH as a reference, relative expression of the gene of interests calculated[330]. For total HBsAg and pgRNA qPCRs, copy numbers of the mRNAs were calculated using two copies HBV genome containing pSHH2.1 plasmid as a standard. The primers used in qPCR reactions are listed in Table 8.

Table 2.28. Standard RT-qPCR mixture

Reagent	Volume/Amount
2xSYBR green mix	7,5 µL
Forward Primer (100µM)	0.15 µL
Reverse Primer (100µM)	0,15 µL
H_2O	4,2 µL
Template	3 µL

Table 2.29. Standard RT-qPCR program

Step	Temperature	Duration	Cycle
Initial Denaturation	95ºC	180 s	1x
Denaturation	95ºC	10 s	
Annealing/Elongation	60ºC	30 s	40x
Plate Reading			
65 ºC to 95 ºC		0.05 sec / 0.5 ºC	
Plate reading in every 0.5 ºC			

2.2.5 SDS-PAGE & Protein Analysis

2.2.5.1 SDS-Polyacrylamide gel electrophoresis (SDS-PAGE)

In order to analyze the protein content of cells or supernatant purified material, 12% polyacrylamide gels were prepared according to Table 29. The cells in 24-well plate were lysed with 200 µL/well of 1x Laemmli buffer and the sample was collected into 1.5mL plastic reaction tubes for boiling at 95 ºC for 5-10 minutes. Before loading into the well, the samples were pelleted down for 2 minutes at 13,000 g. The gel was run at a constant voltage, 100 V, for approximately 2 hours.

Table 2.30. Standard RT-qPCR program

The indicated amount are for casting 2x mini 1.5 mm gels

Gel Type	Composition
Stacking Gel	3.875 mL ddH2O, 0.625 mL stacking gel buffer, 0.5 mL acrylamide solution (40%), 15 µL TEMED, 15 µL APS
Resolving Gel	6.75 mL ddH2O, 3.75 mL resolving gel buffer, 4.5 mL acrylamide solution (40%), 30 µL TEMED, 30 µL APS

2.2.5.2 Coomassie Staining of SDS-PAGE

For coomassie staining, the gel was briefly rinsed with ddH_2O in a 15-cm dish and fixed with Coomassie gel fixation solution for 1 hour. The fixed gel was stained with coomassie stain overnight while gently shaking at room temperature. On the next day, the stain was removed and destained briefly with coomassie gel destain solution. The gel was transferred to ddH_2O containing 15 cm dish and destained for additional 1-2 hours until the background blue color disappear. The gel was scanned with LI-COR Odyssey CLx.

2.2.5.3 Silver Stain of SDS-PAGE

To detect the proteins in high sensitivity, silver staining of the gels was performed by using the Pierce silver stain kit. The gels were fixed as stated in the protocol of the kit, stained, and developed shortly until enough signal was acquired. The gel images were acquired by placing the gels on a white lightbox in Intas Chemocam system.

2.2.5.4 Western Blot

At the end of the SDS-PAGE run, the gel was transferred into a semi-dry transfer buffer for 5 minutes and in the meantime, PVDF membrane was activated with pure methanol. The proteins on the gel were transferred using a semi-dry blotting chamber for 1 hour at 25V. The membrane was blocked with WB blocking buffer for 1 hour and incubated with primary antibodies overnight at 4 ºC on a rotating wheel. The membrane was washed 3x for 15 minutes before the addition of secondary antibodies for 1 hour. After application of another round of washing, the membrane was incubated with Clarity Western ECL Substrate for ones incubated with secondary-HRP antibodies. The images were acquired by Intas Chemocam system. For the fluorescence-labeled antibodies, the membranes were placed into LI-COR Odyssey CLx or Intas Advanced Fluorescence Imager during the image acquisition.

2.2.5.5 Signal Quantification

The bands on the gels were quantified by using Image Lab 6.0.1 or Image Studio Lite 5.2 software. Intensities of the protein of interest were entered into Microsoft Excel and GraphPad for finding the best-fitting curve and performing statistical calculations.

2.2.6 Competent Bacteria Stock

2.2.6.1 DH5α Competent Bacteria Generation

Glycerol stock of DH5α bacteria was touched with a sterile stick and used for spreading on agar plate without antibiotics. The plate was incubated at 37ºC overnight and on the next day, a colony was selected for culturing in 50mL of LB medium overnight. The 50mL bacteria culture was used for inoculation of 4 x 600mL LB medium containing Erlenmeyer flasks. Each of the Erlenmeyer flasks received 5mL of the bacteria and was kept at 37ºC under constant rotation for 3-4 hours. Bacteria growth over time was determined by measuring optical density (OD) at the wavelength of 600nm in a spectrophotometer (Spectrophotometers Ultrospec 3100 pro). When the OD_{600} values reached 0.5-0.7, the bacteria culture was transferred on ice and kept at a temperature between 0-4ºC until the end of the experiment. The bacteria-LB suspension in each flask was transferred to pre-cooled centrifugation buckets and pelleted down at 4ºC for 10 minutes at 1729g (Sorvall RC-5C). The pelleted bacteria were suspended in 80mL of TfBI buffer per bucket and incubated in the buffer for 10 minutes. The solutions were combined and centrifuged back with the same parameters in two buckets. The bacteria pellet was solubilized again using the TfBII buffer of 75 mL per bucket. A total of 150mL bacteria stock was aliquoted

into 1.5mL reaction tubes and snap-frozen in liquid nitrogen. The tubes were stored at -80ºC. The stock quality was assessed by comparing plasmid transformation efficiency on old and new bacteria stocks.

2.2.6.2 Bacterial Transformation

For amplification of the plasmid of interest, 50µL of DH5α bacteria was thawed on ice and incubated with purified plasmid or DNA ligation mix. The plasmid-bacteria tube was kept on ice for 30 minutes before heat-shock treatment for 2 minutes at 42ºC. The tube was transferred back on the ice for 5 minutes. For phenotypic expression of the antibiotic resistance gene, 950uL of LB was added into the tube and incubated at 37ºC at constant rotation in a heat block. As a final step, 50-100µL of bacteria solution was added into ampicillin containing agar plate and spread. The plates were cultured overnight at 37º.

2.2.7 Electron Microscopy

Purified HBV particles in sucrose fractions were subjected to negative staining and immuno-gold labeling. The sucrose in the sample was removed by using Amicon Ultra (30k) centrifugal filter units by diluting and washing the material in 1xTN buffer. For infectious HBV virion containing materials were fixed with 2% PFA for 4 hours at 4ºC.

2.2.7.1 Negative Staining

Sucrose-free HBV particles were applied on carbon & pioloform coated 300-mesh copper grids which were cleaned in a glow discharger. Different dilutions of the sample in 1xTN buffer were prepared and one drop –appx. 7µL of the sample- was incubated on the grid for 5 minutes. In the meantime, 3% uranyl-acetate (UA) solution was spun down to pellet any precipitates present in the tube. The sample was removed by touching one side of the grid to a Whatman paper and briefly touched to a droplet of 3% UA solution followed by incubation on another 3% UA droplet for 2 minutes. The dye was removed by Whatman paper again and the grid was dried at room temperature before imaging with JEOL JEM-1400.

2.2.7.2 Immuno-gold Labeling of the HBV Particles

Quality of the HBV particle samples was assessed with negative staining before starting the immuno-gold staining protocol. The protocol for grids preparation and sample application was

described in 2.2.7.1. The grids were washed with H_2O and blocked for 20 minutes in blocking buffer (0.8% BSA, 0.1% fish skin gelatin, 50 mM glycine in PBS). Primary antibodies were incubated for 20 minutes in a blocking buffer and this was followed by washing the grids with PBS three times. The antibodies used in immuno-gold labeling are listed in Table 1. If necessary, a bridging antibody was used before incubation of the grids with Protein A- 10nm gold conjugate in blocking buffer for 20 minutes. The grids were washed again with PBS and fixed with 1% glutaraldehyde in PBS for 5 minutes. After a final wash of the grids with H_2O three times, the negative staining protocol was performed.

3 Results

To identify host factors having a role in HBV biology, we have performed experiments focused on discrete steps of the HBV life-cycle by application of diverse techniques. In the first part of the results section, HBsAg secretion modulators were studied and the results are currently in preparation for publication. In the second part, host factors association in/on the HBV particles were studied from highly pure materials.

3.1 HBV Subviral Particles and Host factors

3.1.1 Establishment of HBV subviral particles secreting hepatoma cell

In order to perform an siRNA mini-screen for the identification of HBsAg secretion modulators, we established a simple system by using HB2.7 construct which can express all HBV envelope proteins and HBV X proteins from its endogenous promoters. The construct contains 2.7kb of the full 3.2kb HBV genotypeD and the expression of HBV capsid and polymerase was abolished by removing the N-terminus of their ORFs[331] (Figure 3.1.1A). By introducing this construct into cell lines, the expression and secretion of SVPs can be studied under the natural HBV promotor uncoupled from laborious and time-intensive infection experiments. As the first step of cell line generation, we transduced hepatoma cell lines namely; HepG2, HUH7 Low Passage (LP), and HUH7 High Passage (HP) with a very low amount of lentivirus bearing firefly luciferase transgene to provide a surrogate marker for cell viability. The cell lines having G418 resistance were further passaged and used for the second transduction with lentivirus at different concentrations carrying HB2.7(X+) subgenomic HBV sequence. The overexpression of HBV envelope proteins leads to the secretion of HBsAg into the cell culture supernatant spontaneously. From the supernatants of the generated cell lines, we measured HBsAg levels by ELISA. The secretion amount was very low for the HUH7HP and HUH7LP cell lines thus they were omitted from further analysis (Figure 3.1.1B). The HBsAg secretion values of transduced HepG2 cells were higher than both HUH7 based cells independent of the lentivirus

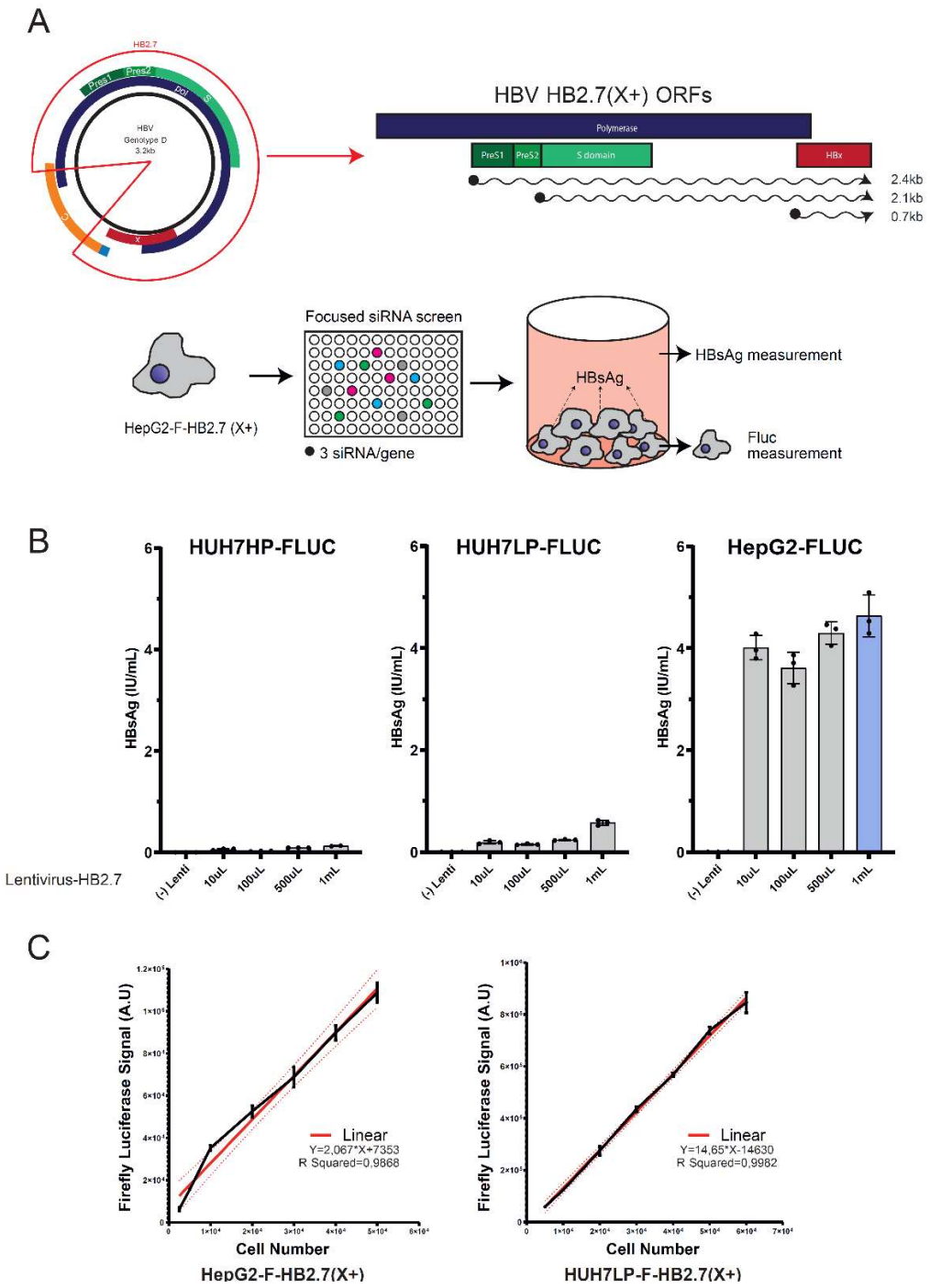

Figure 3.1.1. **Overview of and generation cell lines for the siRNA mini-screen for identification of HBsAg secretion regulators (Ambion)**

(A) Overview of the HB2.7(X+) construct derived from HBV genotypeD and siRNA mini-screen plan. **(B)** HepG2-FLUC, HUH7LP-FLUC, and HUH7HP-FLUC cells were transduced with different amounts of HB2.7 lentiviruses. The cells were selected by blasticidin resistance and HBsAg secretion levels were determined 24 hours post-medium change. The condition in blue color was used for further analysis **(C)** HepG2-F-HB2.7 and HUH7LP-F-HB2.7 cells were seeded into 96 well-plates and lysed for firefly luciferase (FLUC) measurement after 8 hours. Linearity of FLUC signal versus cell number was determined. The figure data is used in Qu, B. & Nebioglu, F. *et al*[420].

titer used for the transduction experiment. The condition with the highest HBsAg secretion was picked for HepG2 cells and used in the siRNA mini-screen analysis. Thereafter, the selected cell line was named HepG2-F-HB2.7. Moreover, we tested the linearity of the firefly signal versus cell number seeded into 96-well plates. After washing and lysing the cells 8 hours post-seeding, we observed that the firefly luciferase signal was linearly increasing with cell number thus, it was displayed as a surrogate marker for cell viability in our siRNA mini-screen (Figure 3.1.1C).

3.1.2 siRNA mini-screen for identification of HBV subviral particles secretion modulators

In the aim of identification HBsAg secretion modulators, siRNA mini-screen of 64 genes was performed by using 3 independent siRNAs/gene which were seeded into 96-well plate randomly. The custom-made library of the screened 64 genes was mostly derived from the study of Simon. J. C. *et al*. 2012, in which regulators of the early secretory pathway was identified by using a temperature-sensitive variant of the spike glycoprotein of vesicular stomatitis virus, TSO45G, in HeLa cells[332]. The cell supernatant of HepG2-F-HB2.7(X+) cells was analyzed at 96 hours post-transfection by HBsAg ELISA and intracellular firefly luciferase signal was determined by luminometer measurements. The HBsAg ELISA results were normalized to NTsiRNA values and an HBsAg Z-score was calculated for each siRNA to identify the potential HBsAg regulators among 192 siRNAs. The screen results revealed that 4 out of 64 genes fulfilled the hit selection criteria of HBsAg Z-score <-1 and with at least two independent siRNAs ($n \geq 3$) (Figure 3.1.2A). These genes were namely Nedd8, Ube2m, Htr6, and Sirt2. It is noteworthy to mention that Nedd8 and Ube2m are components of the neddylation post-translational modification pathway. Firefly luciferase measurement of the identified siRNAs did not cause any significant cytotoxic effect, rather the opposite was observed for Nedd8 siRNAs leading to an increase in the measured luminometer values relative to the siRNAs pool (Z-score>0) (Figure 3.1.2B).

In the screen, we focused on dependency factors of HBsAg secretion and omitted the genes potentially restricting the HBsAg secretion; upon siRNA targeting of which leading an increase in the supernatant HBsAg values. We performed the validation experiments of the identified four genes in two alternative ways. For the HTR6 and SIRT2 proteins that are druggable, we determined the inhibitory effect of small molecule inhibitors of each using two different drugs. Our results on HepG2-HB2.7(X+) cells did not show any inhibitory effect of the drugs on

HBsAg secretion after 4 days and 6 days of treatment but rather an increase in HBsAg secretion observed with Htr6 inhibitor SB271046. The increase of the subviral particle secretion is dose-

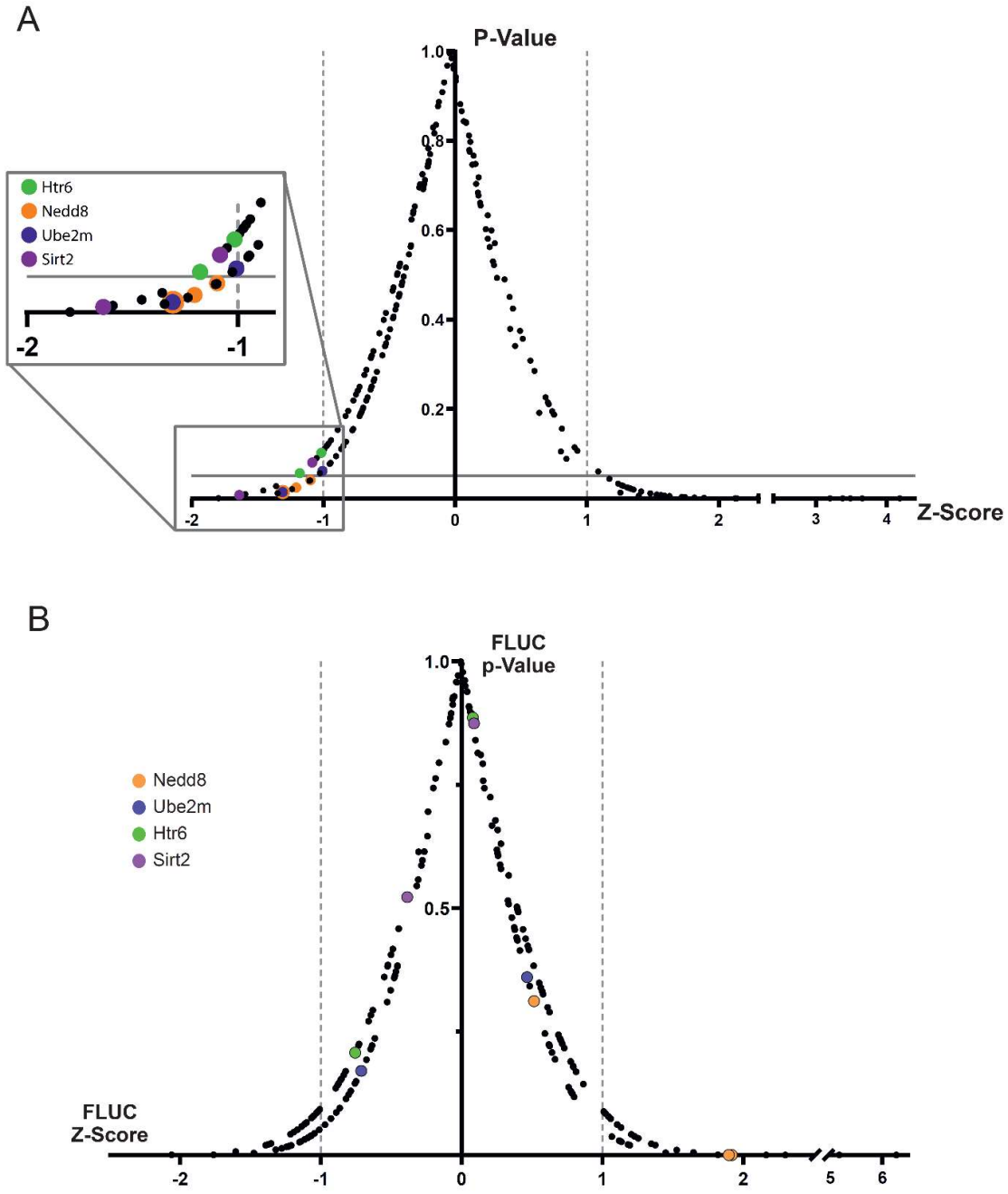

Figure 3.1.2. **Focused siRNA mini-screen identifies neddylation pathway genes involved in HBsAg secretion**

(A) The screen results from HepG2-F-HB2.7 showing mean Z-score and p-values of HBsAg relative to NT siRNA from n≥3 experiments. The genes targeted by ≥2 independent siRNAs with Z-score ≤-1 were selected for further investigation

(B) The Z-score and p-values of each siRNA's firefly luciferase signal were calculated after normalization to NT siRNA.

The figure data is used in Qu, B. & Nebioglu, F. *et al*[420]

dependent and more pronounced with the duration of the treatment (Figure 7.1A and 7.1B). Since this data is contradictory to the mini-screen results, possibly due to the off-target effect of the siRNAs, we focused our attention on neddylation pathway genes, Nedd8 and Ube2m. With the application of different sets of siRNAs from another supplier (Dharmacon), we set up another knock-down experiment on HepG2 and a physiologically more relevant cell line called HepaRG, both carrying HB2.7(X+) subgenomic HBV integrants. Examination of the supernatant of the HepG2 cells at day4 and day6 post siRNA transfection (p.t.) revealed a

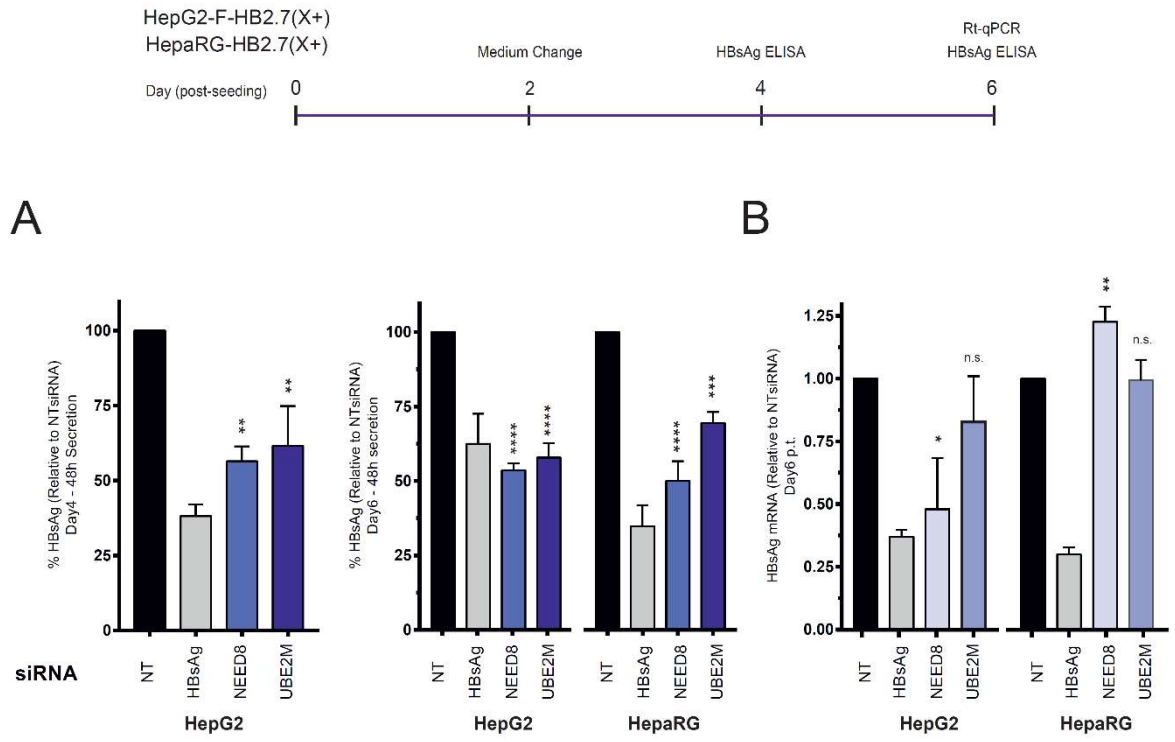

Figure 3.1.3. **Validation of siRNA mini-screen hits with Dharmacon siRNAs**

Neddylation pathway genes were validated by different sets of siRNAs (Dharmacon) on HepG2-F-HB2.7 and HepaRG-HB2.7 cells. **(A)** Secreted HBsAg and **(B)** intracellular HBsAg mRNA levels were demonstrated after normalization to NT siRNA. Data represent the mean±SD of triplicate. n.s. not significant, *P<0.05, **P<0.01, ***P<0.001, ****P<0.0001 compared with NTsiRNA control (one-way ANOVA)

The figure data is used in Qu, B. & Nebioglu, F. *et al*[420]

statistically significant reduction in HBsAg levels, comparable to the siRNA targeting S domain of the HBV envelope (Figure 3.1.3A). This decline was accompanied by a reduction in the HBsAg transcripts for siNedd8 condition at day6 p.t., while siUbe2m did not result in any significant decline of the HBsAg transcripts (Figure 3.1.3B). Intriguingly, we could also observe substantial inhibition of HBsAg secretion in non-differentiated HepaRG-HB2.7(X+) cells in the absence of a reduction in the HBsAg transcript levels (Figure 3.1.3B). The results

suggest a complex interplay between HBsAg and neddylation pathway which can modulate the secretion of the HBV SVPs in various means depending on the cell line in use.

3.1.3 MLN4924, small-molecule inhibitor of neddylation pathway inhibits HBsAg from subgenomic HBV integrates

To confirm the siRNA results with a different approach, we used MLN4924, a small-molecule inhibitor of the neddylation pathway targeting the NAE1 E1 enzyme. The drug treatment was sustained on HepaRG-HB2.7(X+) for 6 days and dose-dependent cytotoxicity was determined by WST-1 assay (Figure 7.2A, B). The MLN4924 drug was very well tolerable by the cells at 200nM and below, a mild decrease of the viability was observed at 1μM concentration. The secretion of HBsAg was impaired upon MLN4924 employment at day4 and day6 post drug treatment without significant change in the HBsAg transcript levels in concordance with our siRNA knockdown results (Figure 3.1.4A and 3.1.4D). Intracellular levels of the small HBV envelope proteins were determined by quantification of band intensities of the p24 and glycosylated p27 from western blot images. Both forms of the HBV small envelope proteins were curtailed by MLN4924 treatment (Figure 3.1.4B and 3.1.4C, left panel). We further confirmed the intracellular decrease of the HBV envelopes by MLN4924 by applying in-cell ELISA on HepaRG-HB2.7(X+) (Figure 3.1.4C, right panel).

To assess the reversibility of the MLN4924 treatment on HepaRG-HB2.7(X+), we cultured the cells in a drug-free medium and examined the HBsAg secretion for 7 days at the end of the MLN4924 treatment. Interestingly, HBsAg levels rebounded back to the DMSO control levels for ≤200nM in 2 days while the rebound of the 1 μM concentration occurred in 4 days. As expected, the secretion stayed at low levels for the cytotoxic concentration of 5μM MLN4924 even after 7 days post drug removal (Figure 7.3).

Recent reports on HBV revealed the hijacking of NEDD8-Cullin4A-DDB1 ubiquitin ligases by HBx protein for counteraction of the Smc5/6 restriction factors[129,130]. To investigate the role of HBx protein in MLN4924 mediated HBsAg secretion inhibition, we generated a HepaRG-HB2.7(X-) cell line by insertion of two stop codons into the ORF of HBx. Using the new HBx(-) cell line, we observed that secretion and intracellular levels of HBsAg were diminished by MLN4924 treatment to the same extent compared to parental HepaRG-HB2.7(X+) cell line, without any reduction in HBsAg transcripts (Figure 3.1.4A, 3.1.4B and 3.1.4D). This data

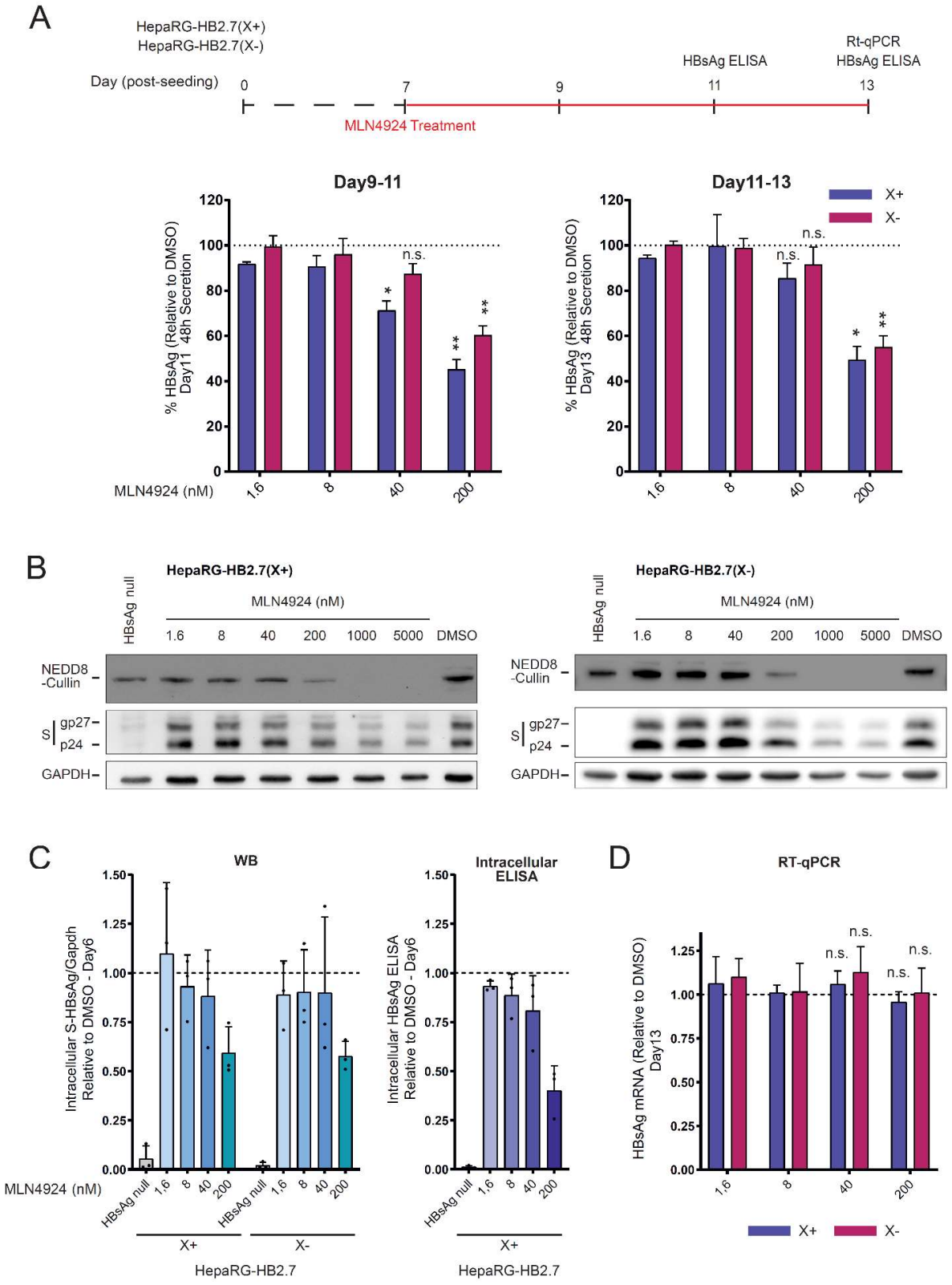

Figure 3.1.4. **Impact of neddylation pathway inhibitor MLN4924 on HBsAg integrates**

Figure legends, see page 72

indicates an HBx independent and post-transcriptionally modulatory role of neddylation pathway on the secretion of HBsAg from HBV integrates.

3.1.4 Dual effect of MLN4924 on cccDNA transcription and expression from HBV genomes

It has been reported that HBV exploits CUL4a ubiquitin ligase by using HBx as a DDB1 and CUL4 associated factor (DCAF) for ubiquitination and subsequent degradation of the Smc5/6, a well-known restriction factor of cccDNA[129,130]. The inhibition of the NEDD8 conjugation pathway by MLN4924 treatment impairs the HBx protein dependent release/degradation of the SMC5/6 restriction by causing inactivation of CUL4 E3 ubiquitin ligase complex and leads to the suppression of cccDNA dependent transcription[313]. To distinguish the roles of MLN4924 on integrated HBV sequence and cccDNA dependent transcription, we benefited from the HepAD38 cell line system[333]. The cell line bears a 1.1 fold overlength HBV genome under tet-off inducible promoter, remained suppressed in the presence of tetracycline or doxycycline antibiotics while the endogenous HBV promoters are still transcriptionally active. Upon doxycycline removal, pgRNA overexpression is induced for the production of progeny HBV and establishment of cccDNA in the cells (Figure 3.1.5A)[333]. This process can be monitored by measuring HBeAg in the medium, the expression of which relies on cccDNA[334]. Moreover, it has been shown that the nucleoside analog (NA); lamivudine can efficiently inhibit the production of HBV from HepAD38 by preventing HBV reverse transcription in the induced state[333]. In our hands, we observed the antiviral potential of MLN4924 on both HBV integrates and cccDNA by keeping cells in (+/-)DOX states for over 40 days of culture (Figure 3.1.5A).

Figure 3.1.4. Impact of neddylation pathway inhibitor MLN4924 on HBsAg integrates **(see page 71)**

Confluent HepaRG-HB2.7-X(+) and -X(-) cells were cultured for 7 days and treated with MLN4924 for 6 days. **(A)** The supernatants were collected from the HepaRG-HB2.7(X+/-) cells at Day11 and Day13 post seeding for HBsAg measurement. Data represent mean±SD of triplicate. **(B)** Intracellular HBV S envelope and Nedd8-Cullin proteins from HepaRG-HB2.7(X+) and HepaRG-HB2.7(X-) cells were detected by western blot. **(C)** Quantification of western blot images and intracellular ELISA at day13 p.s. **(D)** Rt-qPCR of HBsAg mRNA of MLN4924 treated cells at Day13 p.s.

Representative results of three independent experiments are shown for western blot images. Data represent the mean±SD of triplicate. n.s. not significant, *P<0.05, **P<0.01, ***P<0.001, ****P<0.0001 compared with NT siRNA control (one-way ANOVA)

The figure data is used in Qu, B. & Nebioglu, F. *et al*[420]

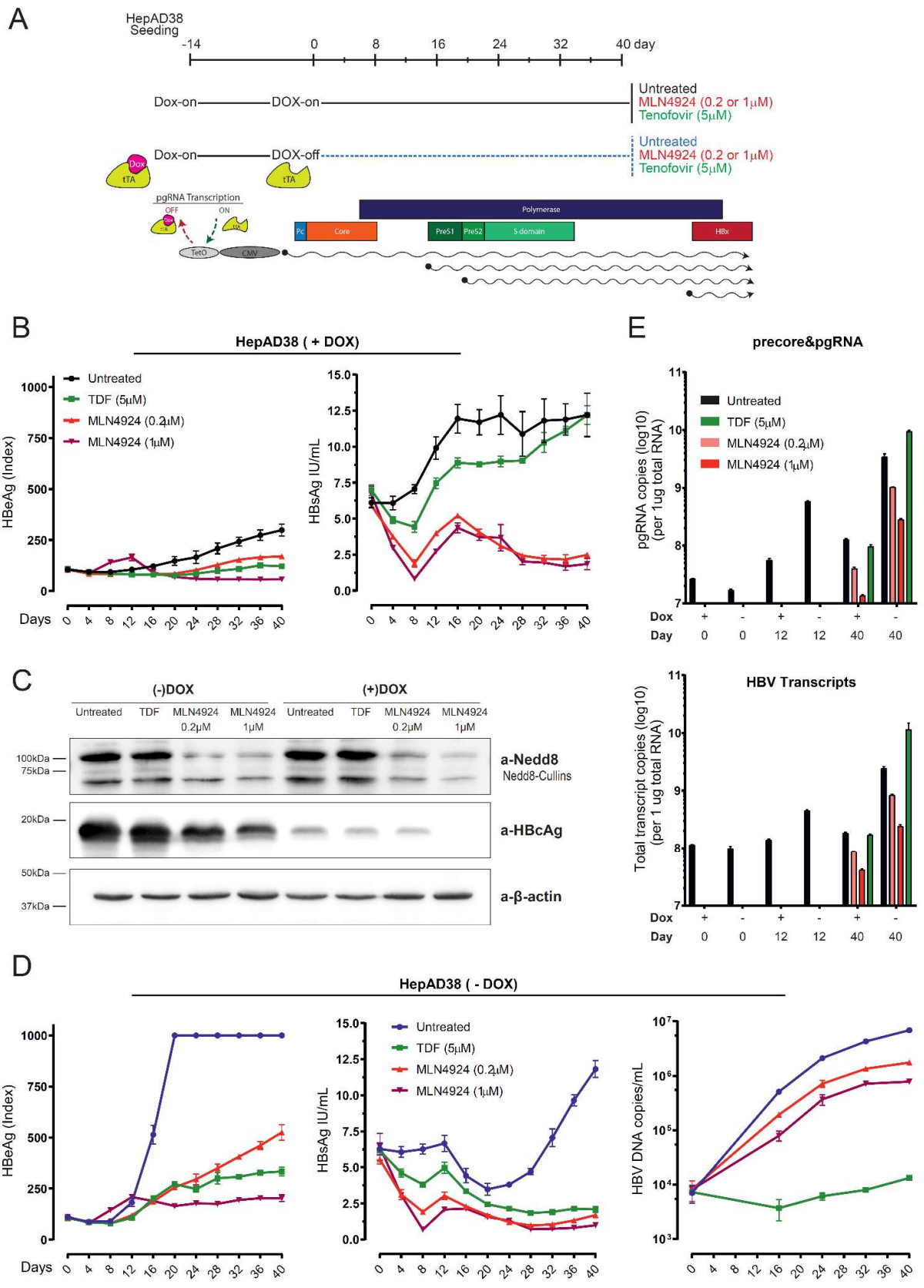

Figure 3.1.5. **MLN4924 shows a dual effect against HBV in HepAD38 model**

Figure legend, see page 74

Tenofovir disoproxil fumarate (TDF), served as NA inhibitor control throughout the study. The MLN4924 drug could inhibit the cccDNA dependent transcription in (-)DOX state and lead to a low level of HBsAg in the collected culture medium (Figure 3.1.5E and 3.1.5D). The inhibitory effect of low (200nM) and high (1μM) concentrations of MLN4924 treatments were comparable to the TDF control group. Furthermore, for the 200nM MLN4924 and TDF conditions, HBeAg levels increased slightly in the period of treatment while TDF posed better suppression over 200nM MLN4924 (Figure 3.1.5D). The amount of HBV DNA in the supernatant was determined by DNA dot blot and qPCR analysis at the indicated time points. The results showed that TDF was very effective in the inhibition of HBV DNA, appx.1000 fold decrease relative to untreated condition, while both MLN4924 treatments were causing around 10-fold decrease (Figure 3.1.5D and Figure 7.5). On the other hand, quantification of pgRNA and total HBV RNA demonstrated dose-dependent inhibition of HBV transcription in MLN4924 treated cells but a slight increase in TDF conditions (Figure 3.1.5E). This pattern was independent of the presence or absence of doxycycline, hence MLN4924 could inhibit transcription from both integrate and cccDNA in HepAD38 cells. Our analysis in HBV repressed state (+DOX) revealed unaffected HBsAg secretion in TDF conditions since the integrated HBV sequences were the main contributor of HBsAg expression (Figure 3.1.5B). Whereas, MLN4924 could inhibit the HBsAg secretion effectively showing a dual effect of MLN4924 on both cccDNA and HBV integrate derived HBsAg secretion. HBeAg amounts were in equal range for TDF and MLN4924 doses in HBV repressed condition. We could confirm the induction of HBV production by immuno-blotting HBcAg at the end of the culture

Figure 3.1.5. **MLN4924 shows a dual effect against HBV in HepAD38 model (see page 73)** **(A)** Overview of the HepAD38 experiment. HepAD38 cells were seeded and maintained in the presence of doxycycline (+DOX) for 14 days. MLN4924 (0.2 and 1 μM) and Tenofovir (5 μM) treatments started in both +DOX and -DOX conditions for 40 days. **(B)** In +DOX condition, HBsAg and HBeAg levels were shown until day 40 **(C)** For both -/+ DOX conditions, cells on day40 post-treatment were lysed. The levels of neddylated-Cullin proteins and HBcAg were measured. **(D)** HBsAg, HBeAg, and total DNA from the supernatants were shown in -DOX condition for 40 days (**E**) Levels of intracellular pgRNA/preCoreRNA and total transcripts on day 40 in both -/+ DOX conditions were depicted. Only the untreated group was examined on day0 and day12. The result for each panel is representative of two independent experiments. HBV DNA and RNA quantifications were performed by Dr.Yi Ni and Dr. Bingqian Qu, respectively.

with a dose-dependent inhibitory action of MLN4924 in concordance with HBV total RNA data (Figure 3.1.5C and Figure 3.1.5E).

3.2 Proteomics Analysis of HBV Particles

3.2.1 Detection of Ubiquitin and Nedd8 in Heparin Purified HBV Stocks

To understand and explain the mechanism behind the MLN4924 mediated HBsAg inhibition, we investigated whether the HBV envelope proteins are directly modified by ubiquitin or Nedd8 proteins. Therefore, we performed western blot analysis on heparin column purified stocks of HBV and HBV pseudotyped HDV (both supernatants were from transiently transfected HUH7 cell supernatants) using ubiquitin and Nedd8 antibodies. To our surprise, we could observe a significant amount of ubiquitin and Nedd8 only from HBV stocks. The intensity of the HBV envelope proteins was not correlating with any of the modifiers (Figure 3.2.1 A).

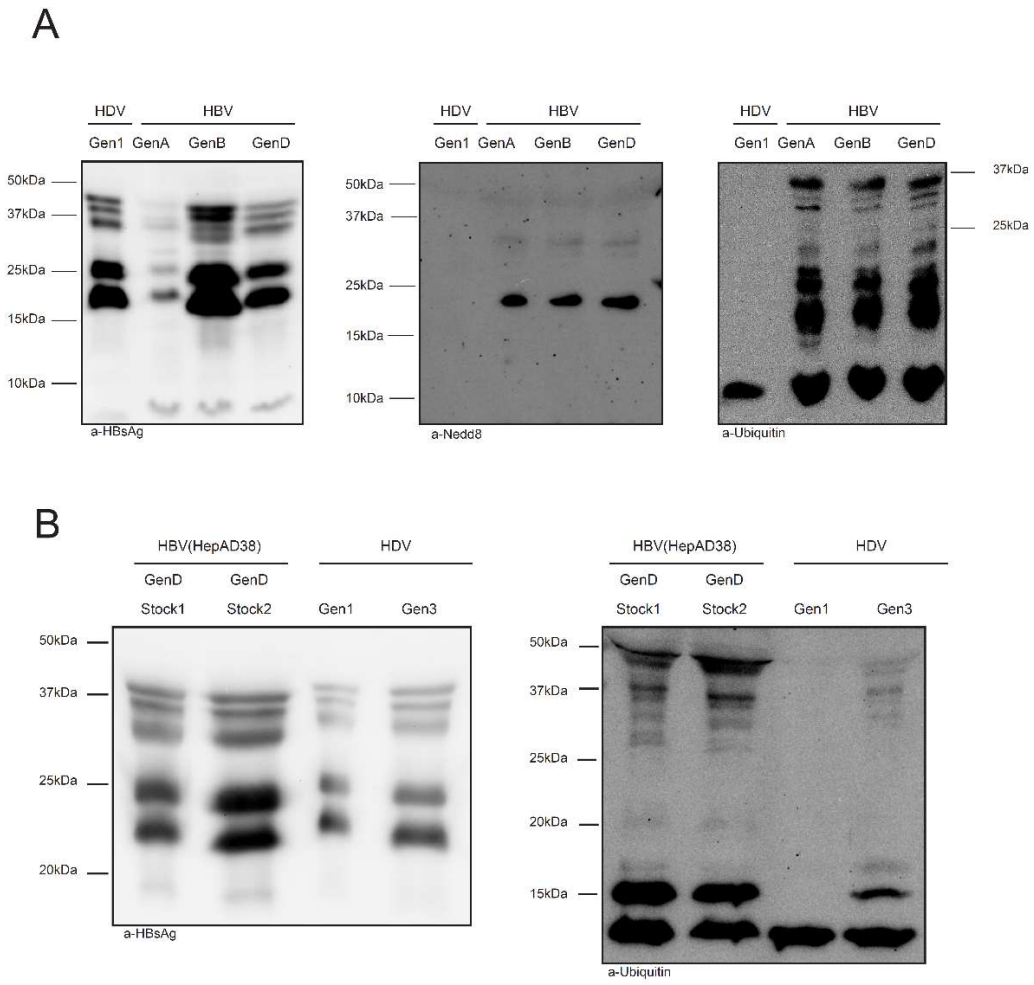

Figure 3.2.1. **Ubiquitin and Nedd8 modifications in HBV and HDV stocks**

Figure legend, see page 76

Of note, the NEDD8 and ubiquitin presence in HBV stocks was confirmed for three different genotypes.

To further examine the source of the ubiquitin and the relevance of our observation to the HBV particles, we repeated the same experiment using different HBV stocks purified from HepAD38 cells (GenD) and HDV virus stocks derived from HUH7 cells. To rule out genotypic effects, a second HDV genotype (Gen3) was analyzed. All of the viral stock preparations were generated by Dr.Florian Lempp with the application of the same purification protocol. Once more, we could detect abundant ubiquitin presence in HBV stocks and confirmed the absence of ubiquitin in HDV genotype 1. Interestingly, HDV genotype 3 showed a low amount of ubiquitin in the virus stock (Figure 3.2.1 B).

3.2.2 Long-term culture of HBV particle secreting cell lines & Purification of HBV Particles

To verify the presence of ubiquitin and to identify host-factors associated with HBV particles by mass spectroscopy, we prepared ultra-pure HBV particles based on a sophisticated purification pipeline[260]. In this setup, we benefited from HepG2 derived cell lines namely HepG2-HB2.7 and HepAD38 that were described in the results sections 3.1.1 and 3.1.4, respectively. In order to obtain enough material with high purity, we seeded our cells into large cell culture factories and kept the culture long-term, over 2 months. Since the culture media of the cells contains plenty of proteins contributing to background signal in highly sensitive proteomics experiments, we employed culture of HepG2 parental cell line in addition to only SVP secreting HepG2-HB2.7 and HBV replicating HepAD38 cells (Figure 3.2.1A). By continuous sampling and monitoring HBsAg and HBeAg secretion into the culture media, we could infer the time-points with high HBV titer and prove the lack of cross-contamination

Figure 3.2.1. **Ubiquitin and Nedd8 modifications in HBV and HDV stocks (see page 75)**
(A) HBV and HDV stocks were generated by transfecting HUH7 cells with viral genomes and followed by heparin column purification. The virus stocks were supplemented with FCS before long-term storage at -80 ^{0}C. The ubiquitin, Nedd8 and HBsAg amounts were examined by protein gel. HDV stock was taken from Dr.Zhenfeng Zhang and HBV stocks were from Dr. Pascal Mutz **(B)** Western blot analysis of ubiquitin and HBsAg levels in HBV stocks prepared by heparin column purification of HepAD38 supernatants. HDV stocks were generated from HUH7 based cells. All of the virus stocks were supplemented with FCS before storage at -80 ^{0}C. The virus stocks were provided by Dr.Florian Lempp

between cell lines in the course of collection. Interestingly, the secretion dynamics of HBV parameters were highly reproducible between two batches of culture gathered from different times. In HepAD38 cells, we always observed early induction of HBeAg around

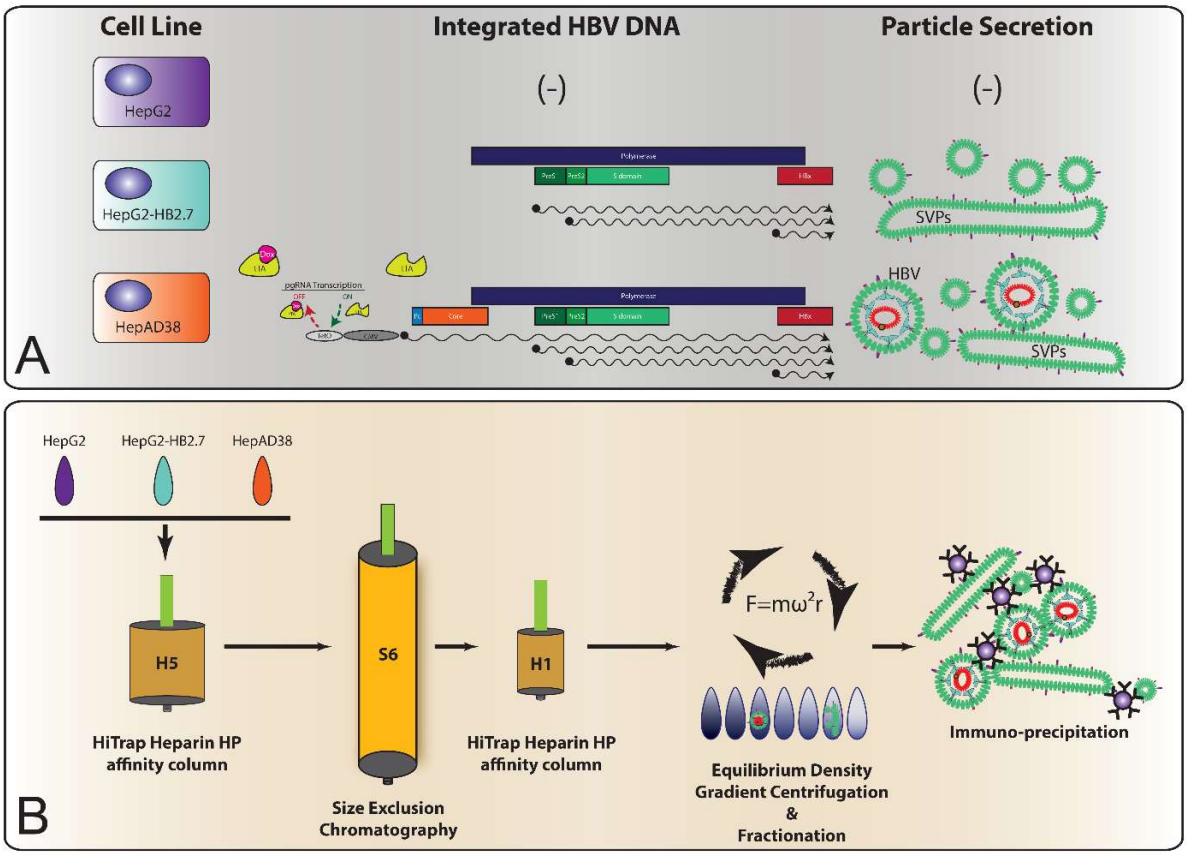

Figure 3.2.2. **Overview of the HBV Particle Purification**

(A) Purification of the HBV particles were performed using HepG2-HB2.7 and HepAD38 cell lines. The cell lines contains integrated HBV sequences having capacity to express HBV proteins on HepG2 background. **(B)** Purification pipeline of the particles obtained from HepG2-HB2.7 and HepAD38 supernatants

Day10 which was followed by HBsAg around Day20 post doxycycline removal (Figure 3.2.2A). The numbers of HBsAg reached peak values after day50 post-induction. This ordered and punctual dynamics of the HBV parameters is most likely due to the establishment and start of the transcription from cccDNA in the nucleus. Indeed, cccDNA deficient HepG2-HB2.7 cells demonstrated a subtle increase of the HBsAg over time (3.2.2B). To keep the conditions the same between the cell lines, we supplemented tetracycline to the non-inducible HepG2 and HepG2-HB2.7 cells. As expected, ELISA measurements from HepG2 control cells did not detect any HBsAg or HBeAg in the collected supernatants (data not shown).

HBV envelope proteins have an intrinsic capacity to bind heparan sulfate proteoglycans on the surface of primary human hepatocytes by electrostatic interaction of antigenic loop region[76]. Taking advantage of this weak interaction, we applied our supernatants into automated heparin

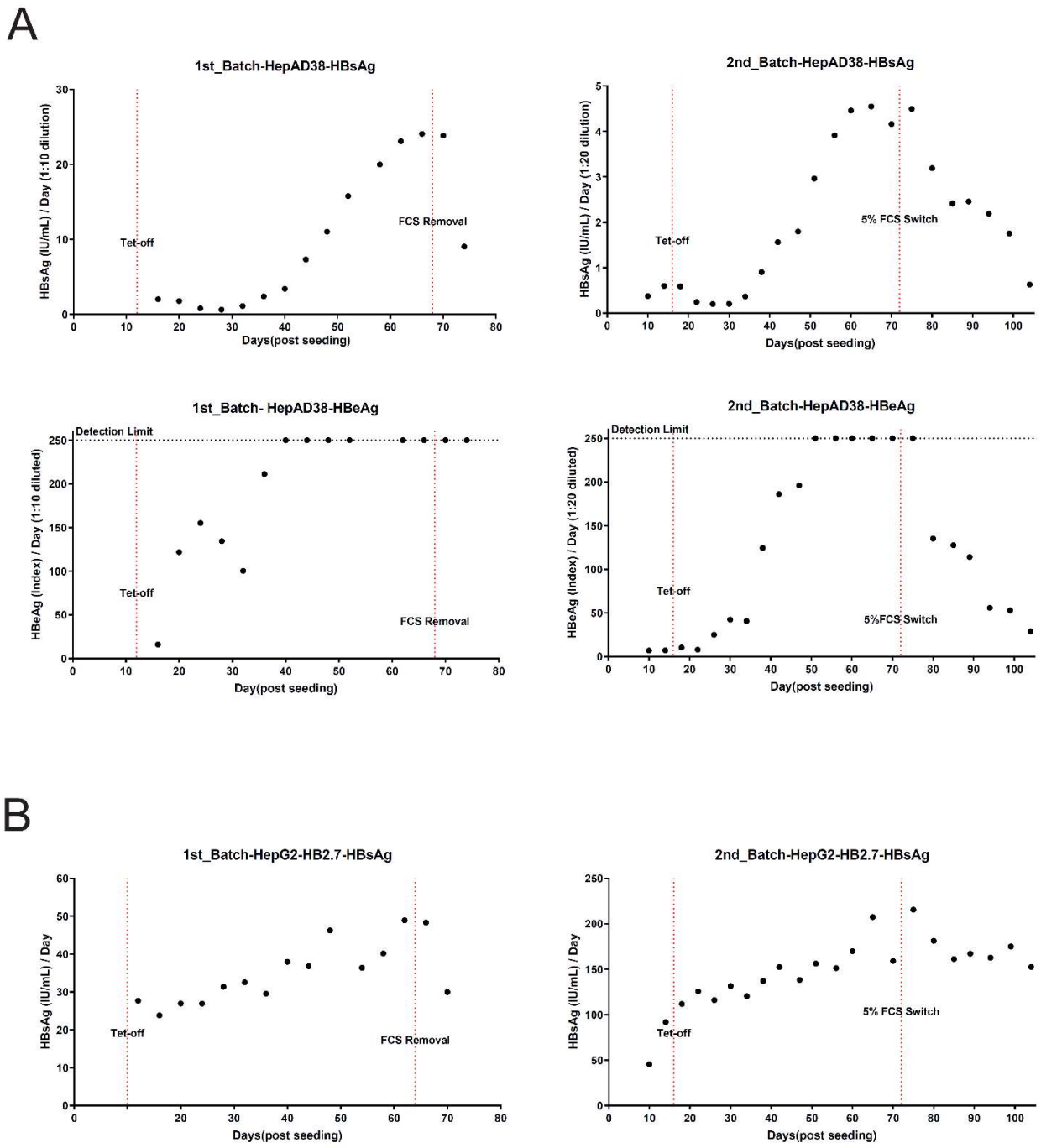

Figure 3.2.3. **Secretion dynamics of the HBV particles from HepG2-HB2.7, and HepAD38 cells** **(A)** HBsAg and HBeAg ELISA values over 2 month of HepAD38 culture **(B)** Long-term culture of HepG2-HB2.7 and HBsAg ELISA values. The effect of complete removal or decrease in FCS on the HBV parameter is shown for the both cell lines.

affinity chromatography (HAC) and subsequent Superose 6 size exclusion chromatography (SEC). The characterization of the collected materials from heparin affinity chromatography and Superose 6 size exclusion chromatography (SEC) were described and published[260].

Briefly, the heparin column (H5) was eluted with a linear NaCl gradient -in the range of 340mM NaCl- and the particle containing fractions were subsequently used in Superose 6 size exclusion chromatography (Figure3.2.1B). The elution profiles of supernatants were nearly identical independent of the applied supernatant type. It is known that heparin interacts with plenty of proteins such as chemokines, growth factors, and lipid-binding proteins[335]. Hence, the HepG2 elution profile showed a background protein binding to the column, detected as UV signal, which is probably due to the fetal calf serum and/or HepG2 secreted factors. Further isolation of the purified HBV particles was done by SEC and the peak absorbance eluted in the void volume of the column was collected. In like manner, absorbance profiles of the SEC were quite comparable between the supernatants. The separation in SEC led to a dilution of the desired material thus, we ran another round of HAC on a small scale (H1) for the concentration of the particles before the final ultracentrifugation step (Figure 3.2.2).

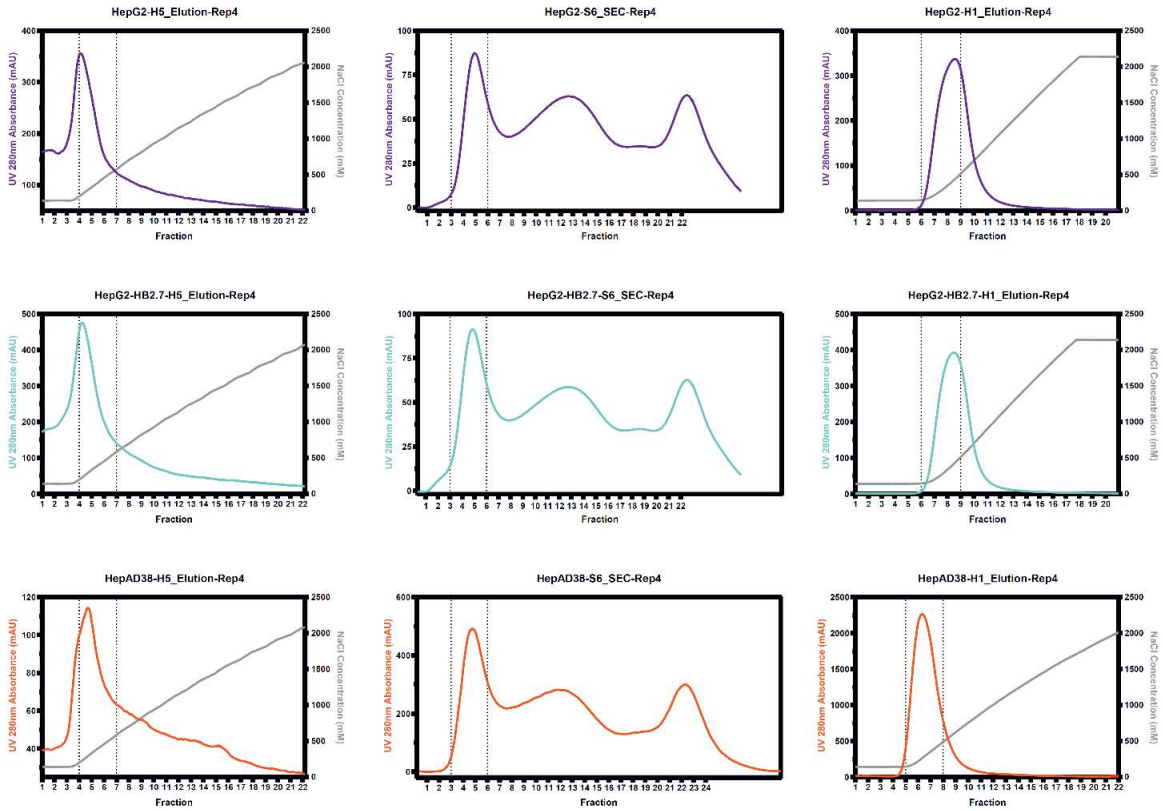

Figure 3.2.4. **Purification of the HBV particles by affinity column and size exclusion chromatography**

HepG2 (purple), HepG2-HB2.7 (turquoise), and HepAD38 (red) cell supernatants were applied to H5 heparin HP affinity column, superpose 6 size exclusion column, and H1 heparin HP affinity column sequentially. The eluates of the H1 column were collected for equilibrium density gradient centrifugation.

Representative results from repetition 4 are shown.

3.2.3 Biochemical Characterization of Purified HBV Particles

To improve the purity of HBV particles after column chromatography, we executed sucrose density gradient ultracentrifugation to separate naked capsids, HBV virions, and SVPs according to their buoyant densities. The sucrose fractions in the range of 1.25 to 1.05 g/cm^3

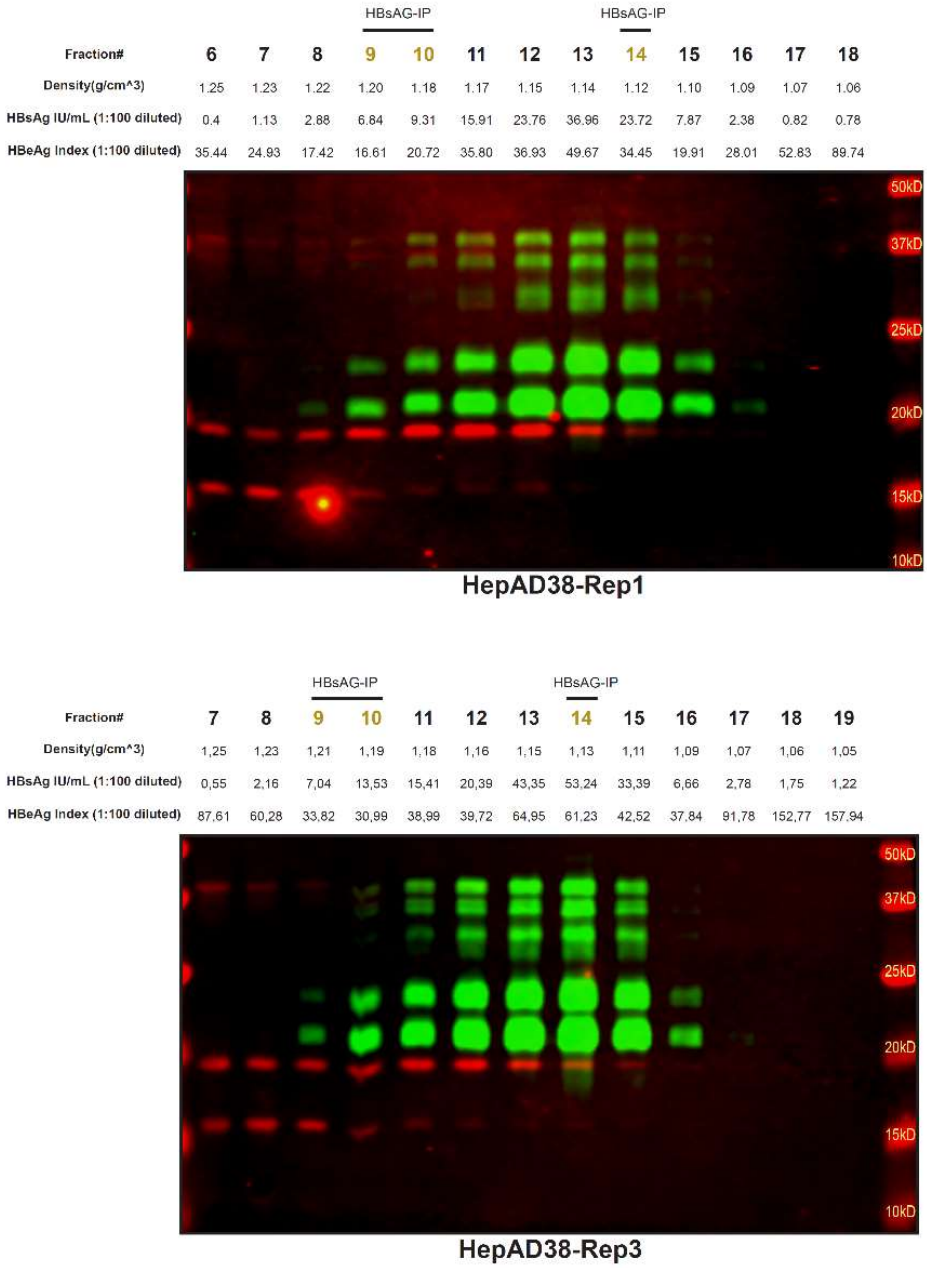

Figure 3.2.5. **Density distribution of HBV core and envelope proteins**
Sucrose fractions of equilibrium density gradients were examined by dual fluorescence western blot for HBV envelope (green) and HBV core proteins (red). HBsAg and HBeAg ELISA values and sucrose density of each fraction is shown above the pictures. The yellow colored fractions were used for HBsAg immunoprecipitation experiments

were analyzed with ELISA, DNA dot blot, and SDS-PAGE for investigation of the total protein content as well as HBV proteins. The densities of SVPs are known to be lower than HBV virion while nucleocapsids or naked capsids are denser than HBV virions.

We could substantiate this notion by western blot and DNA dot blot analysis of the fractions. The fractions around 1.19 g/cm^3 buoyant densities demonstrated HBV core and envelope signal with a significant amount of HBV DNA (Figure7.7A and Figure 7.7B). On a different batch of virus purification, we could demonstrate the same pattern of HBV proteins distribution by dual-fluorescence western blot (Figure3.2.5). The naked capsids without any envelope proteins were dominant in high-density fractions, near 1.25g/cm^3, with only core signal detection. Intriguingly, the core band around 19kDa was accompanied by another band detected just above 15 kDa which was quite prominent in this high-density fractions of all investigated HepAD38 purifications of both batches. The intensity of the approximately 17kDa lower band disappeared gradually towards the lower density fractions. Conversely, the 19kDa core signal reached the apex value close to 1.17g/cm^3, at which a significant amount of HBV envelope protein was detected as well (Figure3.2.5). This data suggests the presence of the small band of core mainly in the naked capsid fractions. The envelope proteins bands were contributed by both SVPs and HBV virion and distributed over the gradient between 1.20 to 1.10 g/cm^3. As expected, HBV envelope proteins showed near 1/1 ratio for the unglycosylated (p24, p39) and glycosylated (gp27, gp42) forms of small and large proteins, respectively. In addition to that, M envelope proteins were detected between S and L envelope proteins as at least in the 2 different isoforms. As previously documented, L:S ratio differs between HBV particles, the virions having the higher ratio compared to SVPs. Among the SVPs, the ratio of L:S differs as well, filamentous SVPs having a higher L:S ratio[223]. Gross morphology of our SVPs fractions in negative stain transmission electron microscopy revealed clear enrichment of the filamentous subviral particles over spherical ones (Figure 3.2.13 and Figure 7.10), presumably due to the elimination of the spherical SVPs in the SEC step. This data is in line with western blot analysis of the sucrose fraction showing a significant amount of large envelope proteins from both HBV and SVP enriched fractions. To ascertain HBsAg amounts quantitatively in the sucrose gradient, ELISA measurement of the diluted sucrose fractions was performed. The peak values of HBsAg resided around 1.12 g/cm^3 for HepG2-HB2.7 derived subviral particles (Figure 3.2.6A) whereas the peak of SVPs from HepAD38 (Figure 3.2.6B) was located in slightly higher sucrose density, approximately at 1.13 g/cm^3. Furthermore, a minor HBsAg peak was present in the high-density range, being much more prominent in HepAD38, likely due to HBV virions. Second, we examined the presence of HBeAg in the purified material by applying the diluted sucrose

fractions to quantitative HBeAg ELISA. Interestingly, we observed a distinct pattern of HBeAg presence over the gradient, showing 3 peaks with clear separation in terms of density. A high degree of sequence similarity between HBeAg and HBcAg often leads to antibody cross reactivity[336] that was recently proven in our lab by using E.coli derived HBc149 capsids (Eva Maria Stork - data not shown). Therefore, the naked capsids detected in western blot were probably the target of the HBeAg ELISA antibodies. Surprisingly, the peak of HBeAg detected at the very low end of the sucrose gradient, 1.06 g/cm^3, was not overlapping with any HBcAg signal in western blot results (Figure 3.2.5 and Figure 3.2.6B), indicating HBeAg or anti-HBeAg cross-reacting HBcAg peptides at low densities. Once more, we could prove that purifications from HepG2 control cell derived supernatants were devoid of any HBV protein by HBeAg and HBsAg ELISA, excluding the possibility of cross-contamination during the column chromatography experiments (data not shown).

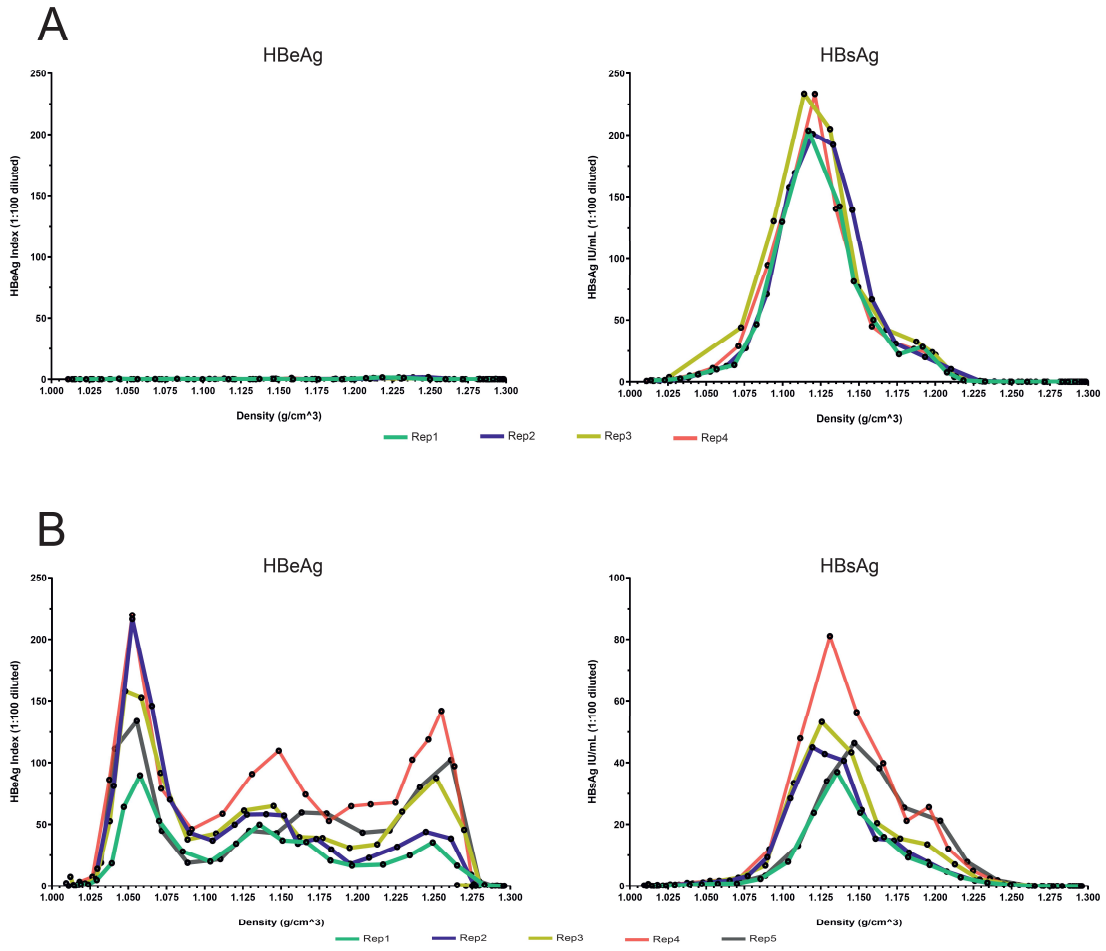

Figure 3.2.6. **HBsAg and HBeAg distribution over sucrose density gradient of HepG2-HB2.7 and HepAD38 purifications**

The eluates of the H1 heparin HP affinity column were separated by equilibrium centrifugation and HBsAg and HBeAg ELISA experiments were performed on the sucrose density gradient fractions of **(A)** HepG2-HB2.7 and **(B)** HepAD38 cells.

To investigate whether HBx protein, which is essential for initiation and maintenance of infection in HBV infected cells, can be packaged into the particles we applied our purified/concentrated virus into western blot analysis using our homemade polyclonal (#644) and recently developed and validated monoclonal mouse and rabbit antibodies against HBx proteins[337]. We showed that all tested antibodies could detect as low as 100pg of recombinant HBx protein (X45/46, kindly provided by Prof.Stephan Urban) (Figure 7.8B), displaying comparable sensitivity. Unfortunately, investigation of HBV containing sucrose fractions by using these three antibodies demonstrated plenty of unspecific bands in western blotting. The bands were found particularly in the 1.20-1.26 g/cm^3 density range spanning low and high molecular weight spectrum. Once more, we could detect the positive control recombinant HBx protein with great sensitivity even as low as 2pg with rabbit monoclonal-HBx antibody (Figure 7.9). The immunoblot investigations of HBx protein in the HBV sucrose fractions were inconclusive and required further experimentations by other methods.

3.2.4 Immuno-precipitation enhances the purity of the HBV particle stocks

Our ultimate aim of high sensitive particle analysis by liquid chromatography tandem mass spectroscopy (LC-MS/MS) requires a purification with minimal background contamination. Inspection of the general protein content of the sucrose fractions with silver stain revealed loads of bands at different densities. The background bands were independent of the cell line of interest whereas we could observe a very thick HBV envelope protein banding pattern as shown above with western blot (Figure 3.2.7). Moreover, HepAD38 cells displayed an additional distinct band just below the p24 envelope protein; the size of the band was in good concordance with the HBcAg band size of western blotting. For optimization of LC-MS/MS protocol, some of the selected sucrose fractions were processed and analyzed. Our preliminary results showed as many as 4000 proteins (data not provided) per fraction. This number of contaminants was unanticipated, prohibiting a reliable and statistically significant HBV proteome analysis. Thus, we incorporated α-HBsAg immuno-precipitation (IP) as an additional step into the purification pipeline of HBV particles. To differentiate the SVP's and virion particle's proteome, we exploited the difference in their buoyant densities. Hence, the sucrose densities around 1.20 g/cm^3 were marked as virion enriched while 1.13 g/cm^3 were SVP enriched fractions (Figure 3.2.5). We could see a clear improvement in the purity of the material by immuno-precipitation of the samples with α-HBsAg antibody coupled magnetic beads (Figure 3.2.8A and Figure 3.2.8B). The silver staining revealed the same protein banding in α-HBsAg IP from HepG2

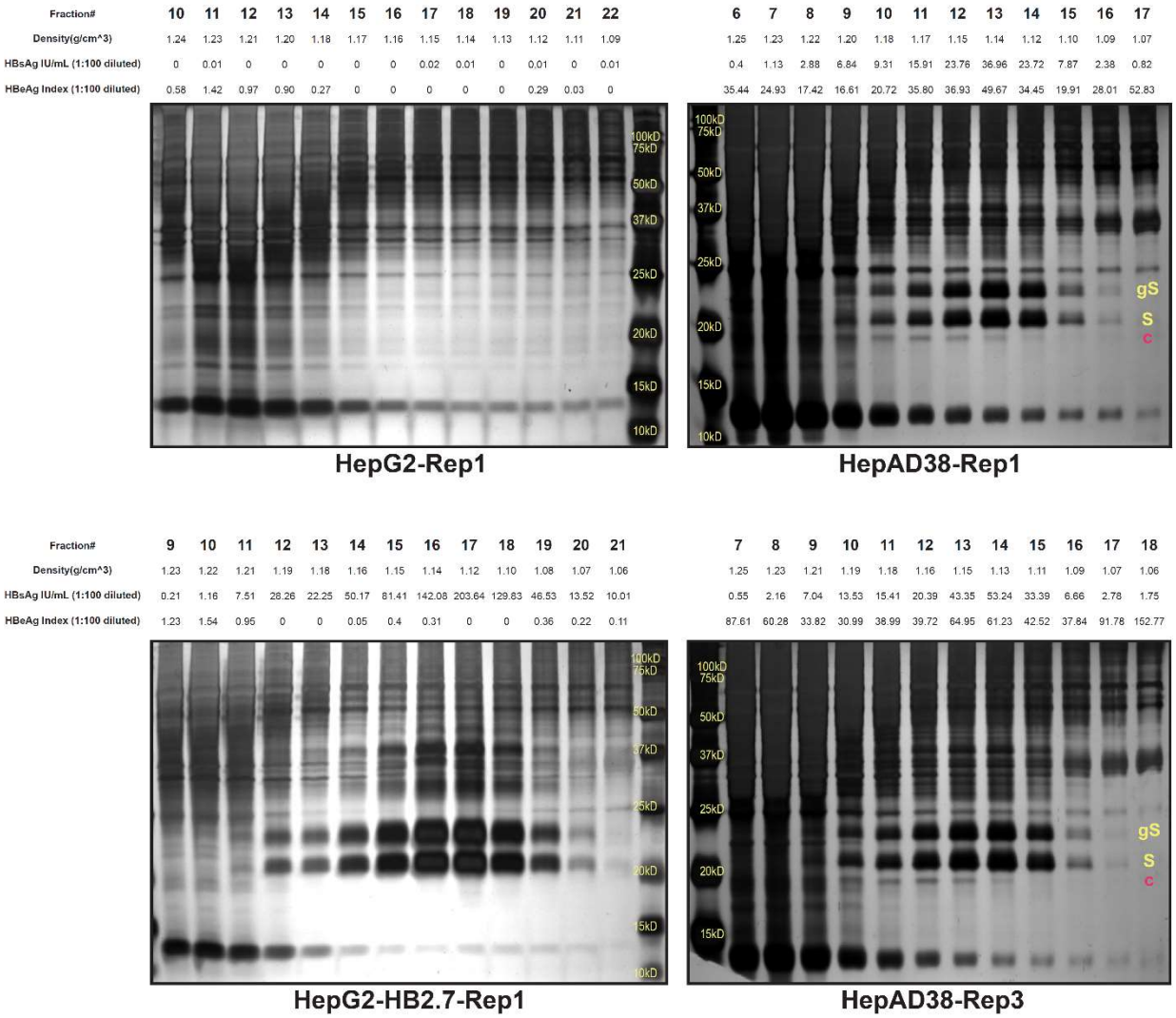

Figure 3.2.7. **Examination of sucrose gradient fractions of HepG2, HepG2-HB2.7, and HepAD38 for total protein content**

Sucrose fractions of equilibrium density gradients were examined by silver gel staining for the determination of protein abundance in each sample. The bands corresponding to the size of viral proteins are labeled on the gel. HBsAg and HBeAg ELISA values and sucrose density of each fraction are shown above the pictures.

gS: glycosylated HBV small envelope protein, S: HBV small envelope protein and c: HBV core protein

condition and in α-HBsAg beads only condition which demonstrates an absence of any unspecific interaction with the beads. The distinct banding pattern in the control conditions could be attributed to HBsAg antibodies co-eluted during the harsh treatment with Laemmli buffer at 95°C; 25kDa and 50kDa were IgG light and heavy chain, respectively. In HepG2-HB2.7 fractions, the IP was very efficient: we could collect most of the HBsAg proteins on the beads in addition to efficient elimination of the protein background in the input. Moreover, our

IgG1 isotype controls did not show any affinity against HBV envelopes. Our previous experiments demonstrated that the virion enriched fractions (density: 1.18-1.20 g/cm^3) had a lower concentration of HBsAg compared to the SVP enriched fractions (density: 1.12-1.13 g/cm^3) (Figure 3.2.6A and Figure 3.2.6B). Hence, we combined two fractions of HepAD38 virion for the IP experiment and analyzed the eluate again with silver staining. Similarly to the HepG2-HB2.7 results, we conclude that the IP step could successfully remove the contaminants from HBV virions and collect the HBV envelope proteins only in α-HBsAg but not in a-IgG1 isotype control condition (Figure 3.2.8B).

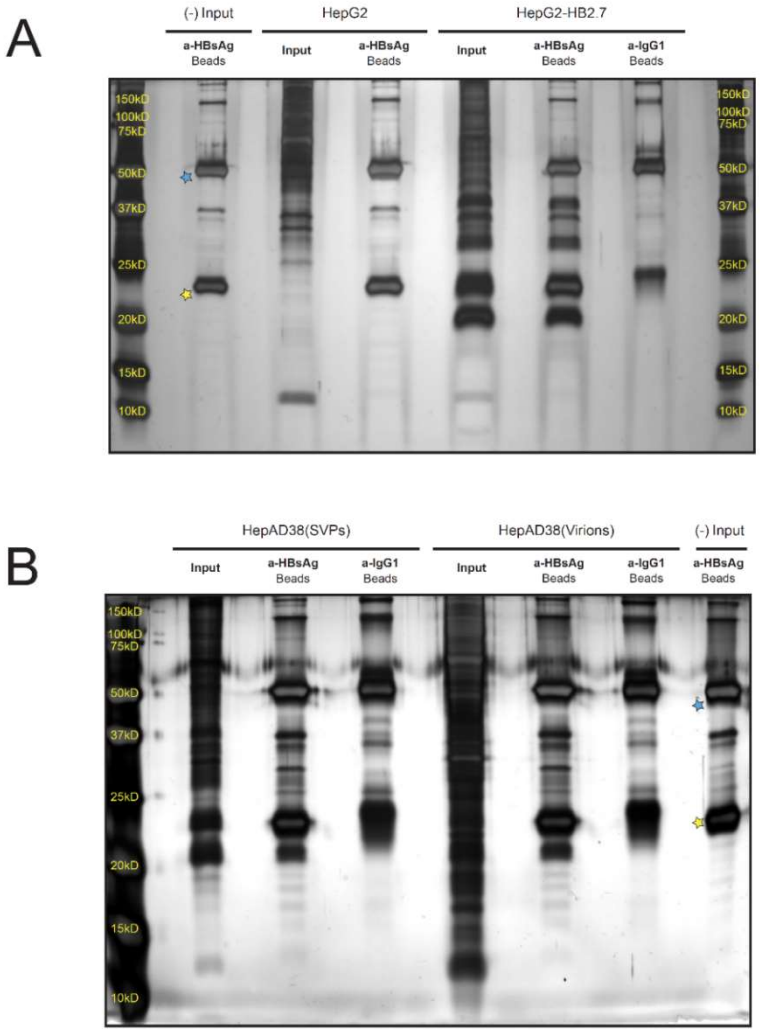

Figure 3.2.8. **Investigation of the protein content of the fractions after HBV surface antigen immuno-precipitation**

(A) HepG2 and HepG2-HB2.7 purified sucrose fractions were used for HBsAg and IgG1 immuno-precipitation and background banding associated with antibody-containing beads were indicated (Lane1). **(B)** SVP or HBV enriched fractions of HepAD38 purifications were applied for HBsAg and IgG1 immunoprecipitation. Visible clearance of the background proteins is observed with immunoprecipitation.

The stars show immunoglobulin light (yellow) and heavy (blue) chains.

Preservation of the HBV particle integrity is essential for a proper particle proteome analysis until the ultimate step, LC-MS/MS analysis, is reached. To confirm the intactness of HBV virions, we examined the existence of HBcAg which is located under the envelope layer of the virion at the end of the IP protocol. The western blotting verified that a decent amount of HBcAg is present after immuno-precipitation against HBsAg (Figure 3.2.9A). Of note, the quantity of the core was significantly less than the input core; the small 17kDa band was almost completely diminished in the a-HBsAg eluates. This indicates that most of the HBcAg signal of the input was mainly contributed by the non-enveloped sources, like naked capsids. Quantification of the HBcAg bands from all replicates showed an intriguing trend as well; a great reduction in the ratio of 17kDa/19kDa HBcAg isoforms upon HBsAg immunoprecipitation (Figure 3.2.9C). Moreover, the HBcAg blots were re-probed with a-HBsAg for showing the levels of HBV envelope proteins. As expected, we could observe the HBV envelopes from different isoforms in HepAD38 virion fractions (Figure 3.2.9A). The IP reaction was very efficient in HepG2-HB2.7 cells, hence, we could collect almost all of the HBsAg at the end of the experiments (Figure 3.2.9B). In conclusion, we could prove the HBV virion's intactness in an indirect way by targeting interior HBcAg protein. Since HBV SVPs consist of just the envelope proteins, we could not apply this strategy for SVPs.

Another way of studying HBV particle intactness is the direct visualization in negative staining transmission electron microscopy. In this strategy, the SVPs of HepAD38 cells were eluted from a-HBsAg-ProteinG complex by using a low pH glycine buffer, which was followed by pH neutralization of the collected material. As expected, the low pH caused elution of the antibodies together with the HBsAg SVPs that were clearly visible in our silver gel analysis. The elution step was very efficient. The analysis of the eluted beads showed a minute amount of HBsAg leftover. Moreover, there was not any background protein binding to the IgG1 control beads (Figure 3.2.10A). Unfortunately, the ultrastructural analysis of the SVPs revealed aggregation of the particle which appeared as large islands on the examined grids. This phenomenon was previously described in experiments conducted on DHBV large envelope proteins[338]. Despite that, a closer look into the aggregates presented distinct structures of the filamentous SVPs, especially at the edge of the bulky aggregates, as evidence of the intactness of the particles (Figure 3.2.10B). All in all, we could prove that the HBV virions and SVPs were able to endure numerous steps of the purification and immunoprecipitation protocol by maintaining their structural stability; hence, keeping the entrapped/incorporated host factors associated with the particles.

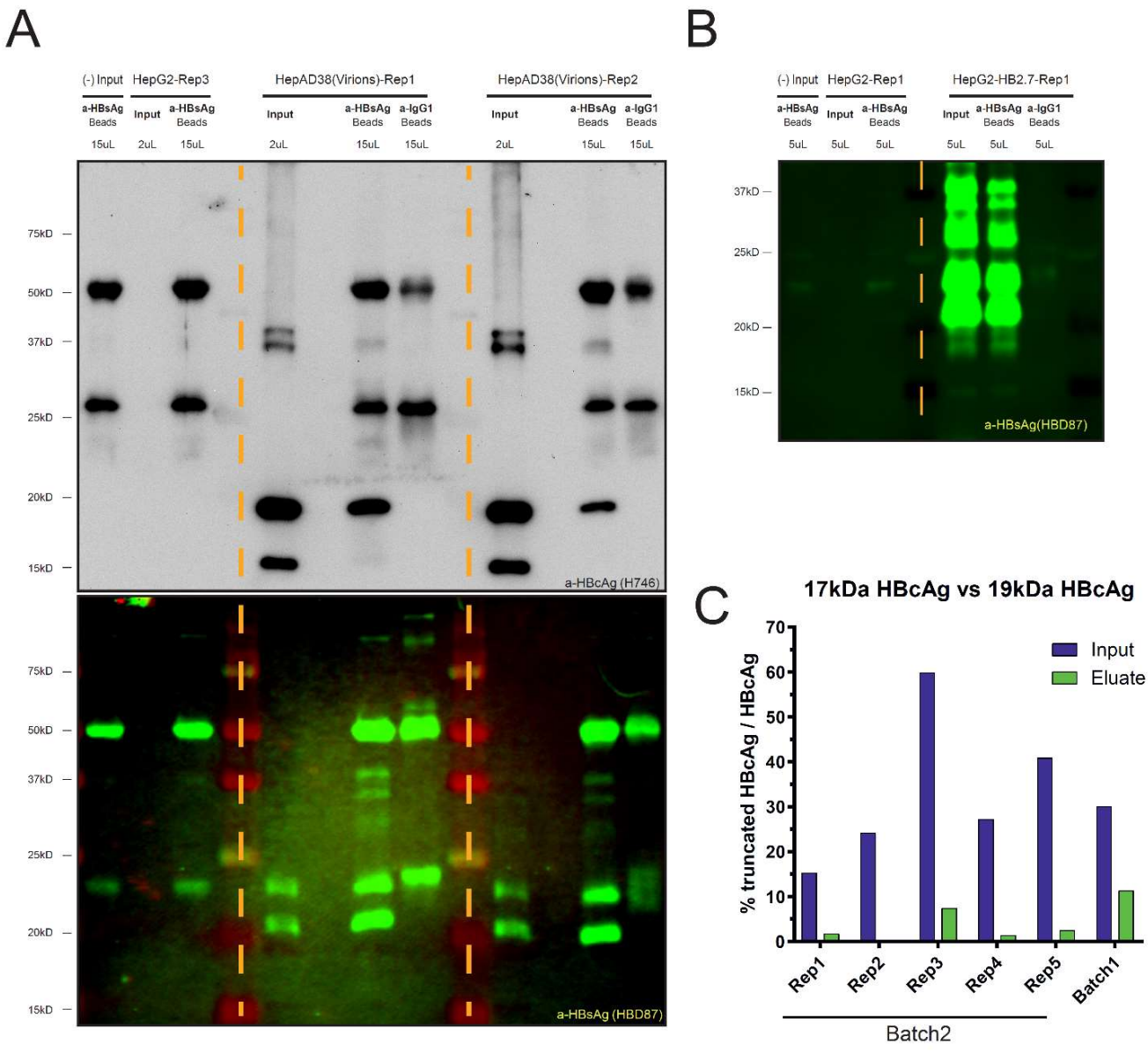

Figure 3.2.9. **Determination of HBV virion integrity upon HBsAg immuno-precipitation**

(A) In order to determine the integrity of the HBV particles during the HBsAg immunoprecipitation, HBcAg western blotting was performed on HepAD38 samples. Re-probing of the blot with anti-HBsAg was performed (anti-human800). The sample from HepG2 purification was used as a negative control.

(B) HepG2-HB2.7 cells derived SVPs were shown to be successfully enriched after incubation with anti-HBsAg beads.

(C) Truncated HBcAg signal was quantified from both input and anti-HBsAg captured samples and the percentage of the truncated/full HBcAg signal was calculated for each IP replicate.

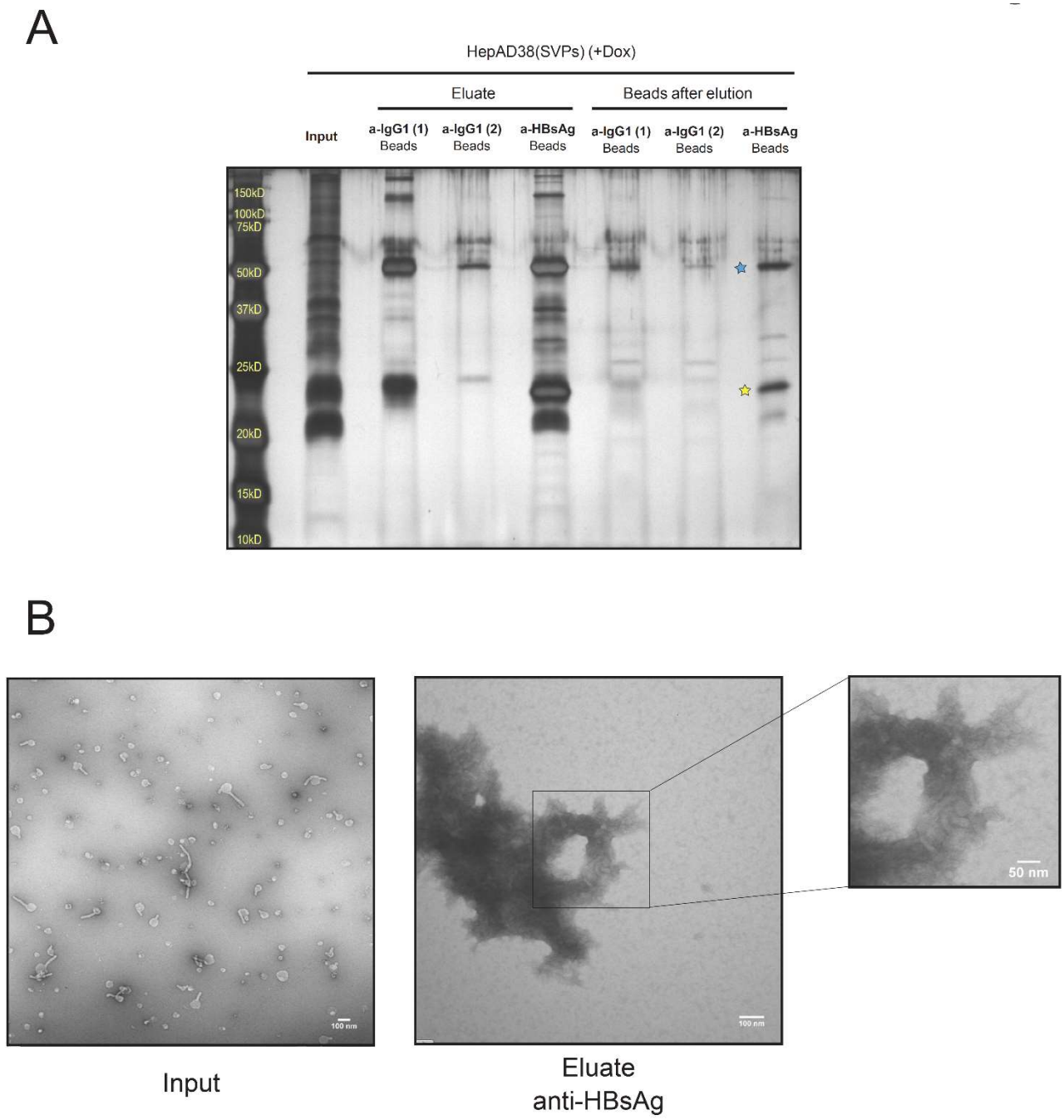

Figure 3.2.10. **Determination of SVPs integrity upon HBsAg immuno-precipitation**

(A) SVPs in sucrose fractions of HepAD38 (+) were applied to a-HBsAg and a-IgG1-beads and eluted with glycine buffer, pH2.5, twice and neutralized to pH 7. The eluates and the beads were applied to SDS-PAGE and stained with silver stain.

(B) The input and a-HBsAg eluates were stained with 3% uranyl-acetate for negative staining transmission electron microscopy. The SVP cluster in the box is enlarged in ImageJ and shown on the right.

3.2.5 LC-MS/MS Results - Detection and mapping HBV Peptides

The HBV particles on beads were directly processed for LC-MS/MS analysis without any elution steps. We examined seven different conditions with at least four repetitions. Identified viral proteins and host proteins were listed (Figure 3.2.11A and Figure 3.2.12). As anticipated, the HBV virion stocks revealed peptides of HBV polymerase, core, and envelope proteins, however, HBx and the HBeAg specific peptides were not identified. Moreover, HepG2-HB2.7 purified SVPs showed a very strong signal for the HBV envelope protein while the virion-associated proteins such as polymerase and core were absent as expected. Since HBV encodes three different envelope proteins sharing the same C-terminal S domain and with additional PreS2 and PreS1 domains, we mapped the envelope peptides on the HBV genome and indicated each peptide's corresponding domain (Figure3.2.11A, B). Interestingly, certain peptides' intensities fluctuated depending on the analyzed group; the peptides were either absent or in a scarce amount in one condition while present and abundant in another condition. This can be illustrated by peptide4 of the HBV envelope protein (PreS1 39-46aa), which was detected in higher amounts in the HepAD38 SVP fraction compared to the viral fraction of HepAD38 or the SVP fraction of HepG2-HB2.7 cells. On the other hand, SVPs of HepG2-HB2.7 exhibited very intense signal from PreS2 specific peptide8. The peptides of the S domain were concentrated on the major hydrophilic region, the so-called a-determinant, of the protein. We could detect three peptides covering the a-determinant. They were mapped to the amino acid positions 123-169 of the S domain. Exclusive to the HepG2-HB2.7 group, we could identify a peptide which is spanning PreS2-S junction of the envelope protein, encompassing the first 24aa of the S domain. The PreS2 region of SVPs from HepG2-HB2.7 cells harbored the only post translational modification among the identified peptides, as S40 phosphorylation. We could not detect any ubiquitination or other ubiquitin-like modifications on the viral proteins.
Some of the HBV core and polymerase peptides were found exclusively in the viral fractions. The core peptides were covering the whole ORF of HBcAg except the C-terminal end, between aa151-183, of the protein. For the polymerase protein, we could identify TP and spacer domains peptides. The only peptide which was detected from all replicates of the HepAD38, even in HepAD38 SVP fractions, was polymerase peptide4 that was mapped to the spacer region.
To sum up, the analyzed conditions/groups were very well clustered without any cross-contamination.

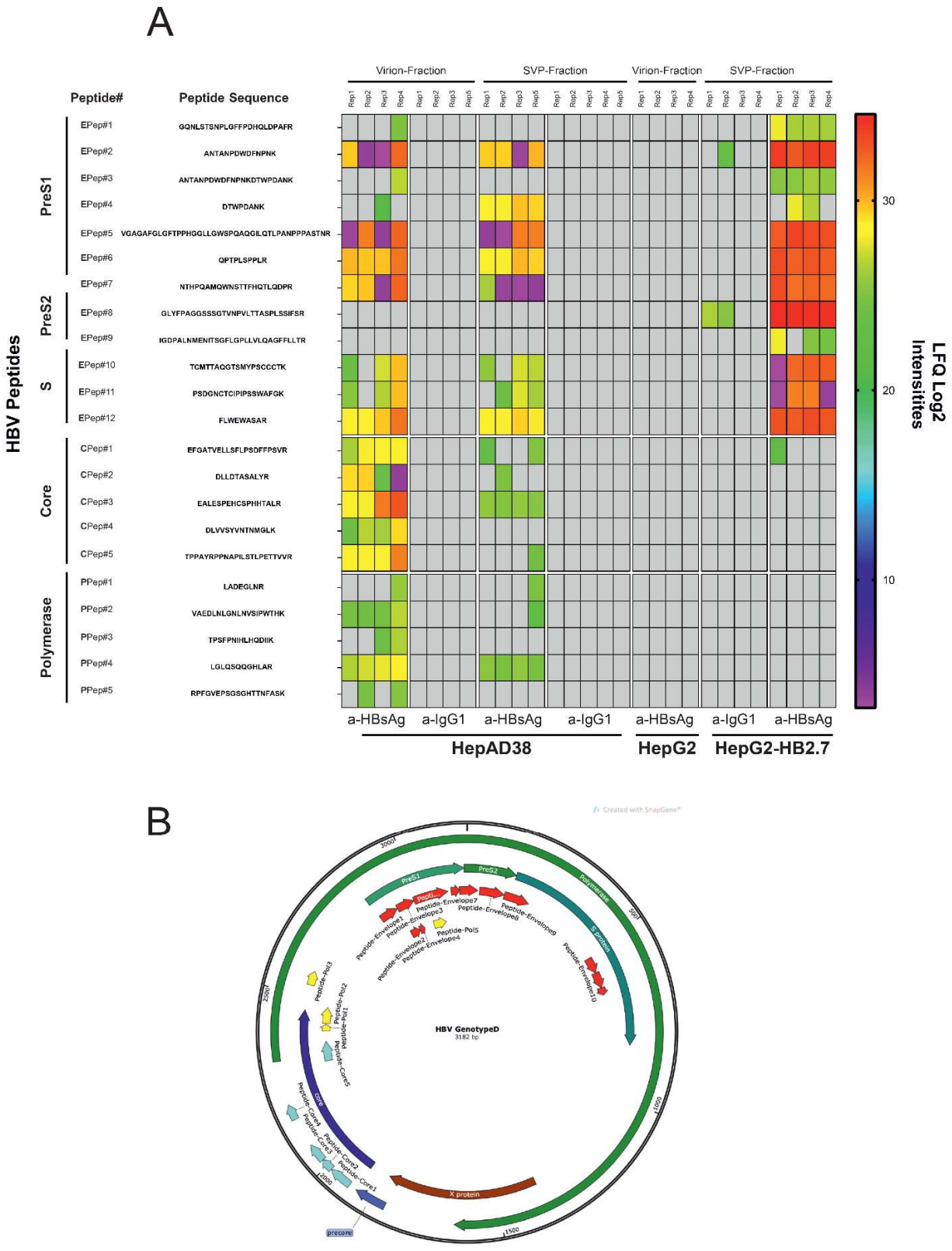

Figure 3.2.11. **Detection of HBV proteins by mass spectroscopy**

(A) Viral peptides identified from AP-LC-MS/MS analysis of the samples were illustrated and categorized according to the matching viral proteins.

(B) The map of HBV genotype D is shown with an overlay of the peptides detected from mass spectroscopy.

3.2.6 Discovery of novel host-factors associated with HBV particles

To determine the host factors associated with the HBV particles, the identified peptides were filtered and the potential contaminants such as keratin proteins were excluded from the list. The results revealed 166 candidate proteins in total from all conditions containing HBV particles (Figure 3.2.12). The majority of these host factors appeared in the HepG2-HB2.7 derived SVPs while only about half the proteins were manifested in HepAD38 particles. As mentioned earlier, the quantity of the HBV envelopes was much higher in SVPs of HepG2-HB2.7 compared to HepAD38 virion and SVPs. We observed strong enrichment of some of the proteins like RAN, APOE, and CYB5A in all types of particles from both cell lines with complete absence in HepG2 control condition. A slight unspecific binding to IgG1 beads was detected for APOE protein, however, the ApoE intensities were around 16 to 64-fold higher in the a-HBsAg beads compared to a-IgG1 control. In general, our negative HepG2 control group was relatively clean, only a few proteins were found as a background binder. In the proteome of SVPs of HepAD38 and HepG2-HB2.7, we could also identify other members of the apolipoprotein family such as APOA1, APOA2, APOC1, and APOC3. In addition to that, APOB APOF and APOL2 were exclusively present in HepG2-HB2.7 SVPs. Chaperone proteins of different families were among the enriched proteins identified in our dataset. We detected PPIA, HSPA8, HSPB1, DNAJB12, CANX, HSP90AB1, DNAJB2, and HSPA1B from all conditions; several of the factors were previously shown to be important regulators of HBV biology. All of the chaperone factors, except HSP90AB1, were found in SVPs independent of the cell line source.

The most interesting proteins of the analysis were SBSN, CASP14, CWF19L2, and HNRNPC since they could be identified mainly in HepAD38 virion fractions with a lack of signal from HepG2-HB2.7 SVPs. Although showing some background signal in the IgG1 and HepG2 controls, the following proteins HSP90AB1 and LMO7 were detected specifically in the HepAD38 virion fractions as well. For some virus-specific host factor, the intensity score for the protein decreases in the SVP fraction of HepAD38 compared to the virion fraction, further supporting the notion of virus specificity (Figure 3.2.12).

To corroborate our findings from the proteomic analysis, we selected around 55 proteins from the list (labeled in red). Currently, these proteins are being examined in the context of HBV morphogenesis and egress.

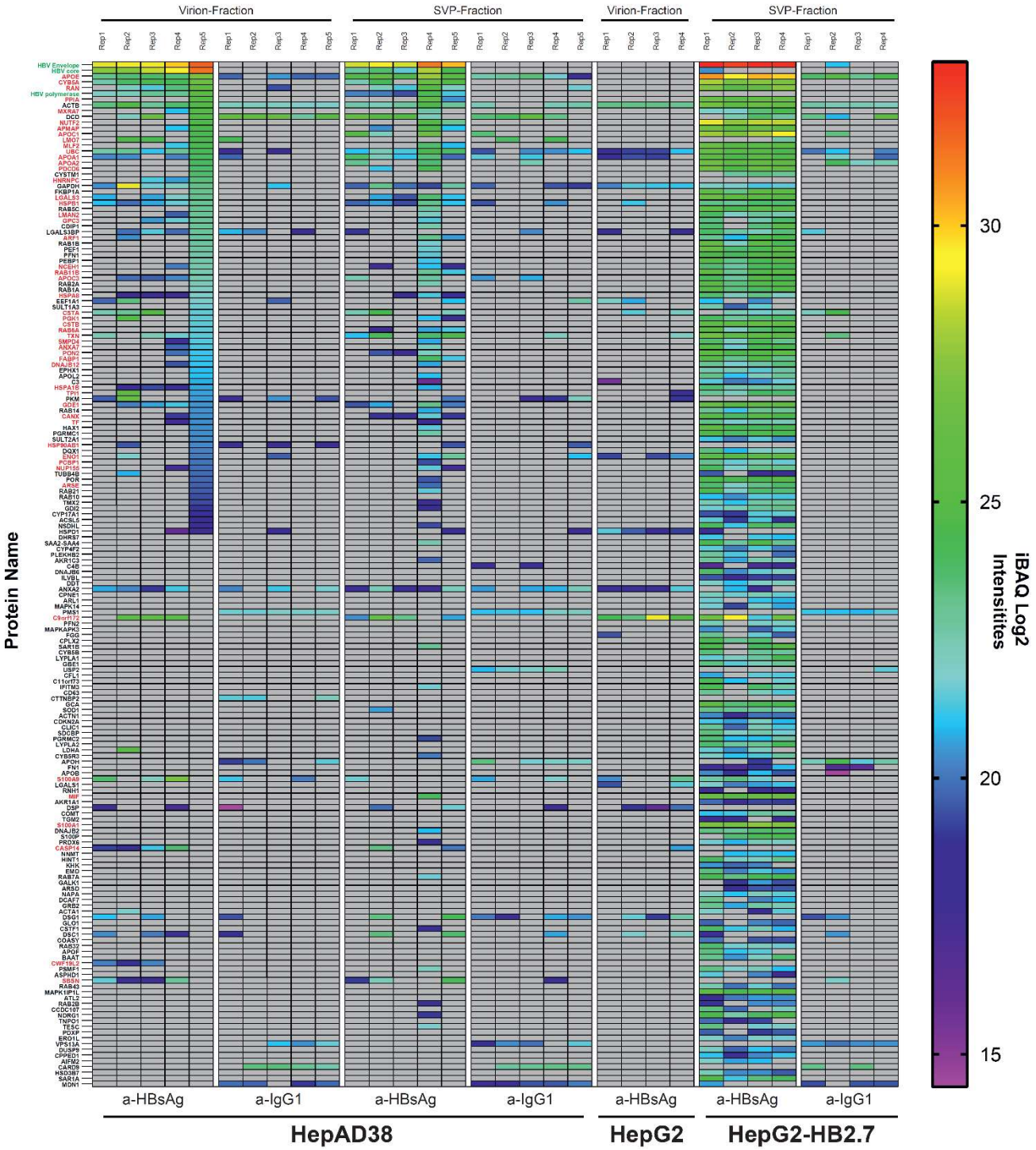

Figure 3.2.12. **The comparative proteome of HBV SVPs and Virion**

The affinity-purified particles were investigated for their total proteome by LC-MS/MS (n≥4). Each column represents the proteome of a different pull-down sample. The color of the box represents the score of the protein on a logarithmic scale (Log_2).

3.2.6 Immuno-gold labeling of the ApoE at the surface of Dane Particles and filamentous SVPs

The association of ApoE on HBV virions was reported previously in PEG-precipitated virus stocks and its depletion on the producer cells was shown to be detrimental for virus production[339]. In concordance with this study, we found a significant amount of ApoE in both

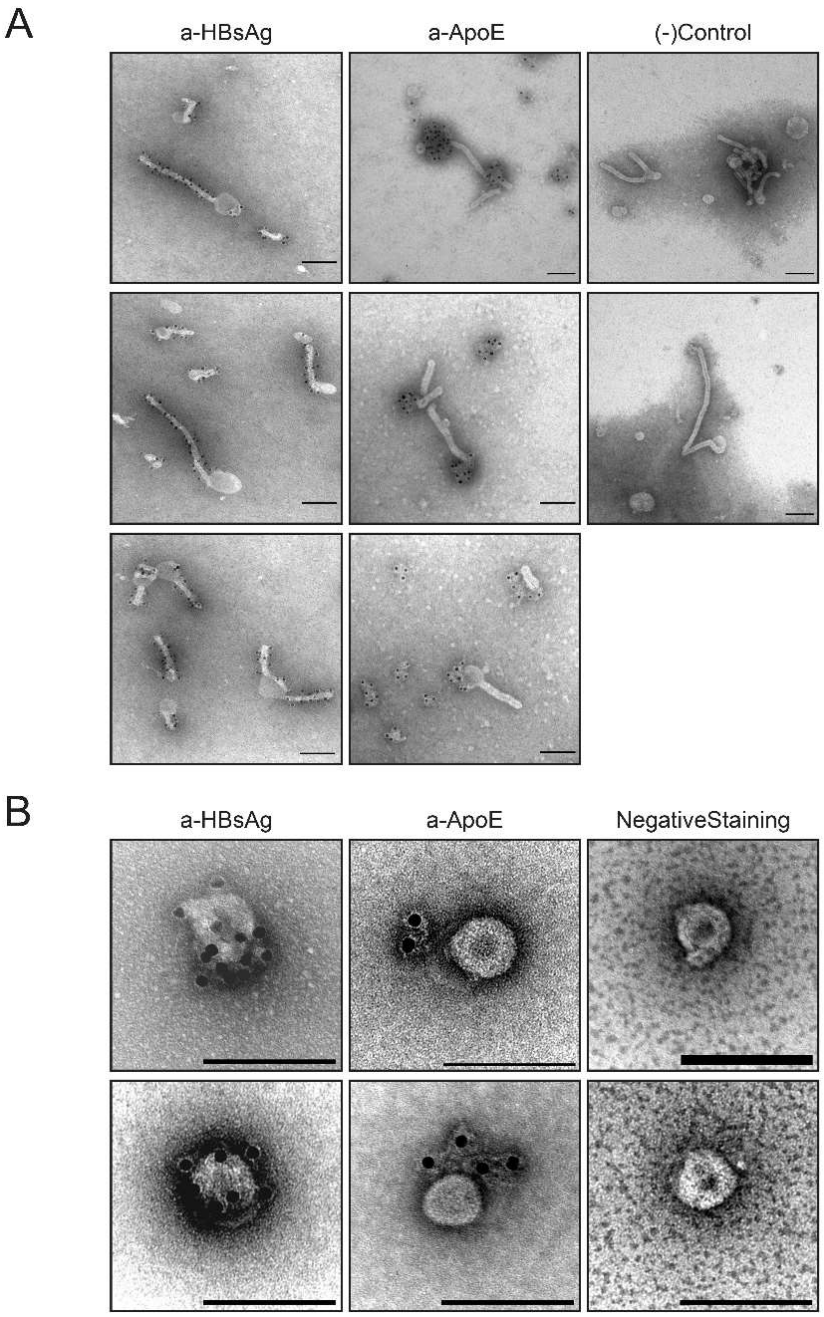

Figure 3.2.13. **Association of ApoE protein with HBV particles**
Sucrose fractions of HepG2-HB2.7 and HepAD38 cell purifications were probed with anti-HBsAg and anti-ApoE antibodies and negatively stained. **A)** HBV subviral particles from HepG2-HB2.7 were shown. **B)** HBV virions from HepAD38 cells were shown.
Scale bar: 100nm The images were taken by Minh-Tu Pham and Uta Haselmann.

virions and SVPs at the end of our stringent particle purification pipeline. We decided to validate the ApoE presence on the particles by immuno-gold labeling of the SVPs derived from HepG2-HB2.7 and virions from HepAD38 sucrose fractions, respectively (Figure3.2.13A and Figure3.2.13B). The particles were targeted by α-HBsAg antibodies (HBC34) as a positive control of the immuno-gold protocol, the same antibody used in the IP experiments of the HBV particles.

The a-HBsAg antibody, recognizing a-determinant, nicely decorated the filaments thoroughly except the round, head part. Moreover, negative staining of the filaments revealed a slightly different color of the head part compared to the filament part, likely due to the dissimilarity between their compositions. In contrast to HBsAg, we could detect exclusive localization of ApoE at the round end of the filaments usually in clusters. The ApoE was rarely detected on the trunk part of the filament. Moreover, we could see some clusters of ApoE-gold labeling

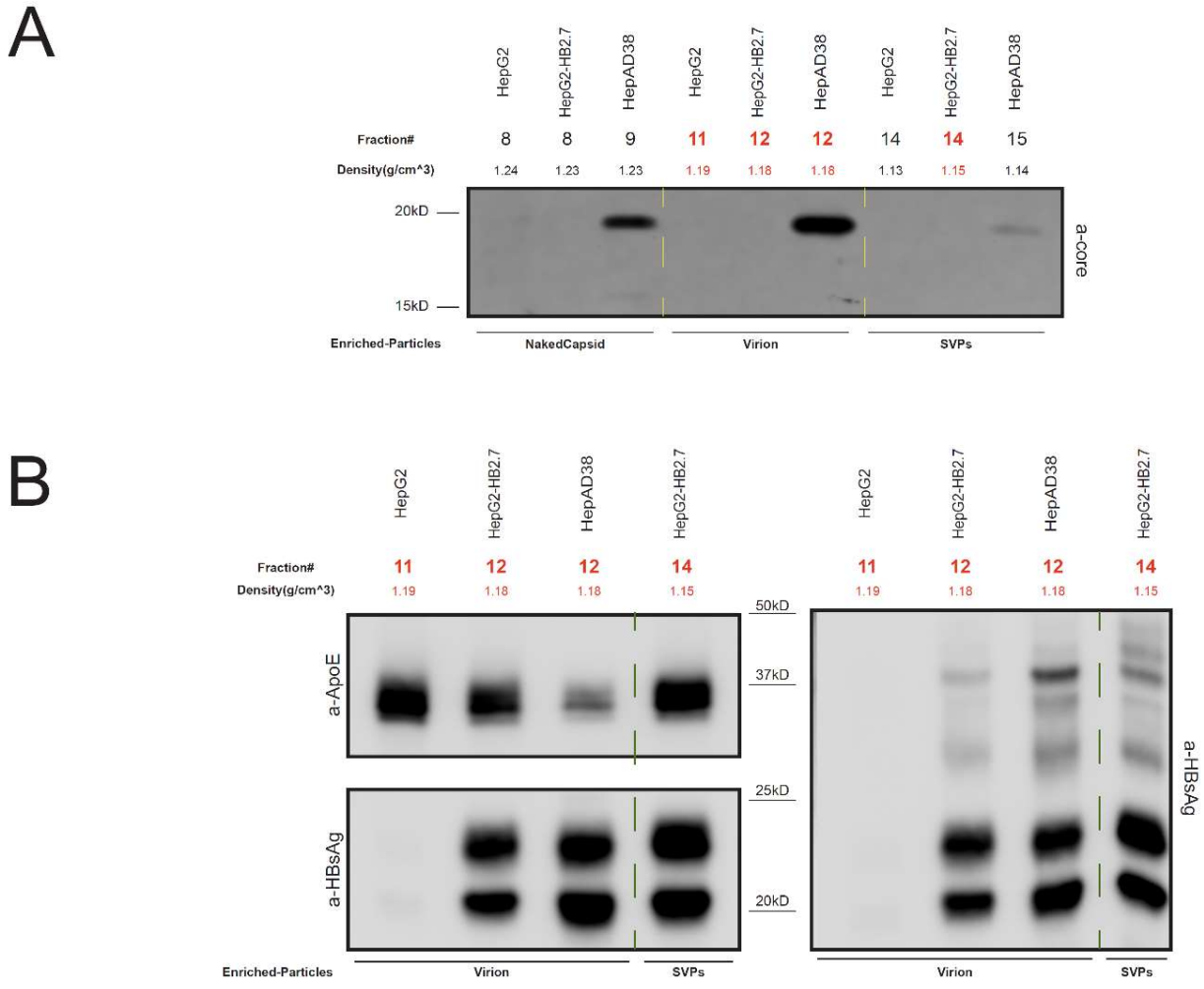

Figure 3.2.14. **ApoE is a heparin binding protein**

Figure legends, see page 95

independent to the HBV particles which can be attributed as a sign of ApoE background in the used sucrose fractions (Figure 3.2.13A). By using the same experimental setup with SVP immuno-gold labeling, the association of the ApoE was demonstrated on HBV virions as well (Figure3.2.13B). To prove the presence of ApoE in our sucrose fractions and explain the free ApoE-gold particle clusters, we performed western blot on HepG2, HepG2-HB2.7 and HepAD38 derived samples. The applied samples showed HBcAg signal in only HepAD38 derived virion samples (Figure 3.2.14A) as expected and a decent amount of HBsAg in both HepG2-HB2.7 and HepAD38 sucrose fractions (Figure 3.2.14B). The ApoE signal was detected for all of the conditions independent of the HBsAg status. Therefore, this confirms the ApoE existence and co-purification into our sucrose fractions from all three cell lines.

Due to the striking localization pattern of the ApoE on the particles and the significant association even after the IP experiment, we decided to address the role of ApoE in the context of HBsAg secretion. For this, we benefited from apolipoprotein deficient cell lines namely HeLa and 293T, besides ApoE expressing HUH7 cells. The cell lines were co-transfected with HBV envelope protein overexpression constructs under SV40 promoter together with either ApoE or mCherry plasmids (Figure 3.2.15A). The results illustrated that overexpression of small envelope protein alone from SV40-S plasmids resulted in a reasonable HBsAg secretion from all three cell lines used. Co-transfection of ApoE overexpressing plasmid caused a 2x fold increase of the HBsAg secretion only in HeLa cells. On the contrary, HBV large envelope protein expression from SV40-L plasmids yielded in very low HBsAg in the analyzed supernatants, approximately 40-80 fold less than SV40-S transfected conditions. These low values of the HBsAg increased upon ApoE overexpression for all of the cell lines but the phenotype was more dramatic in 293T and HeLa cells with 4.5 and 5-fold increases, respectively (Figure 3.2.14B). The data suggest a potential role of the ApoE in the secretion of HBsAg especially in the context of L protein.

Figure 3.2.14. **ApoE is a heparin-binding protein** **(see page 94)**

The sucrose density gradient fractions were examined for the presence of ApoE

(A) Purified fractions of HepG2, HepG2-HB2.7 and HepAD38 cells were compared side-by-side with matching densities for the presence of HBcAg.

(B) The fractions labeled in red color were further studied for the presence of ApoE and HBsAg. The samples were loaded twice; the left part showing ApoE and small HBV envelope protein, the right showing isoforms of HBV envelope proteins.

The loaded samples were from batch1 purifications.

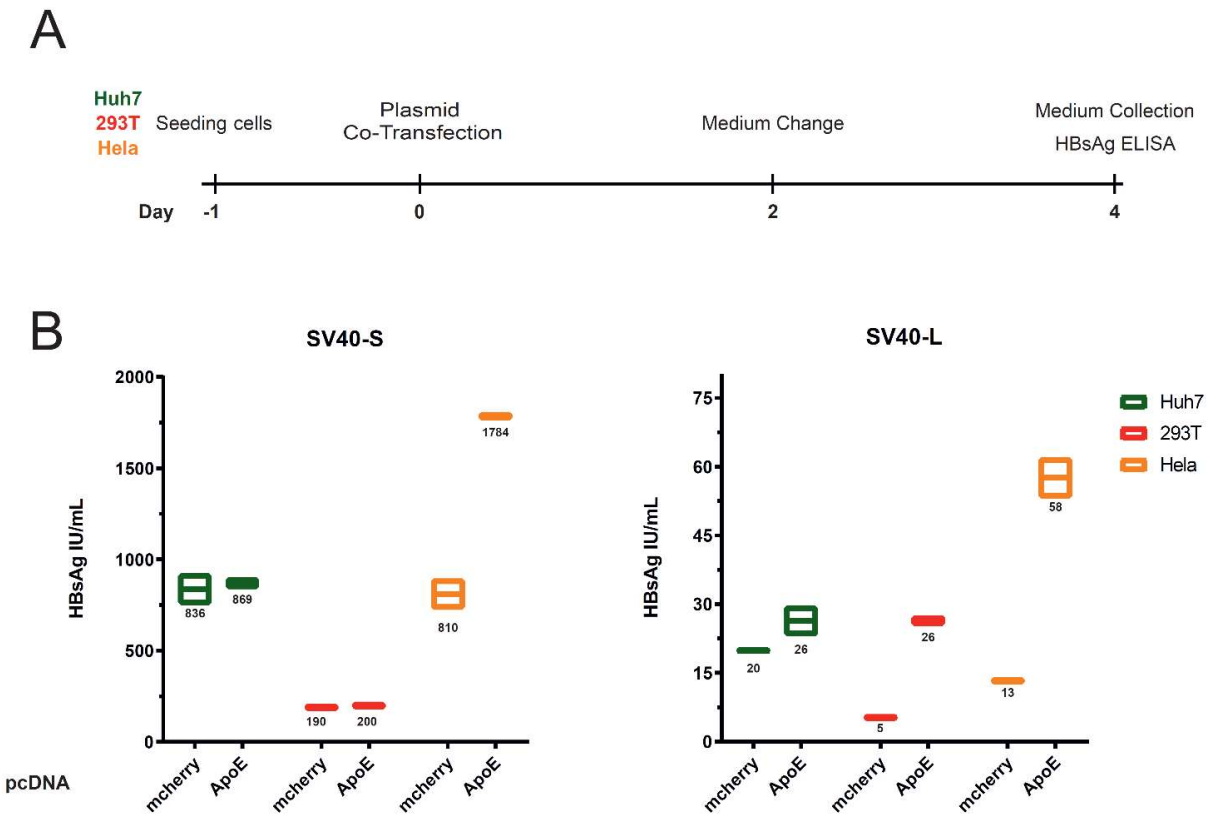

Figure 3.2.15. **ApoE overexpression increases HBsAg secretion**

The role of ApoE in HBsAg secretion was examined in HUH7, 293T, and HeLa cells.

(A) The timeline of the experiment showing transfection and supernatant collection days post-seeding.

(B) The secretion of HBsAg was examined with ELISA by overexpressing small or large HBV envelope proteins in the presence or absence of ApoE.

4 Discussion

4.1 Host factors and SVPs Secretion from Integrates

The integration of the genome is a common by-product reaction observed in many hepadnaviral infections which is not essential for the generation of progeny virus but might be important for the establishment of the persistence and chronicity[46,340-343]. Integrated linear HBV sequence lacks the regulatory elements next to core protein ORF, hence infectious virion formation is impaired[344]. It can contribute to the circulating HBsAg in the infected patients and help envelopment of HDV during the assembly. Importantly, the level of the HBsAg in the blood is postulated to be an immune-modulator itself by suppression of innate immune cells and exhaustion of T cells[328,345,346]. To better understand the host factors involved in the HBsAg secretion in integrate context, we have established cell lines carrying a partial HBV genome (HB2.7) as described earlier[331]. It has been known that HUH7 and HepG2 hepatocarcinoma cell lines differ each other significantly at genomic, proteomic levels and ultimately phenotypic levels which can be exemplified by the permissiveness for HCV: only in HUH7 but not in HepG2 cells can be infected[347-350]. HBsAg secretion amount was significantly lower in HUH7 derived cells among the three HCC cell lines transduced with HB2.7 lentiviral construct and were therefore excluded from further analysis. The release path of the HBsAg follows the constitutive secretory pathway starting at the perinuclear region and then continues to ERGIC and Golgi apparatus where the N-glycosylation modification takes place. The research on the early secretory pathway has identified plenty of host factors responsible for proper trafficking of the cargo protein[332]. We gathered a small set of genes from the literature and studied the role of these proteins on the HBsAg secretion subject.

As an astonishing outcome of the mini-screen, the neddylation pathway components Nedd8 and Ube2m genes were among the highest-ranked genes for HBsAg inhibition upon siRNA knockdown. NEDD8 has the highest sequence homology to ubiquitin with 59% compared to other ubiquitin-like proteins[316]. It is covalently conjugated to the proteins analogous to the ubiquitin conjugation pathway; NEDD8 E1 activating enzyme (NAE) catalyzes the transfer of NEDD8 to E2 conjugating enzymes which are UBE2M and UBE2F in metazoans. The final step, NEDD8 ligation reaction on the substrate is performed by E3 ligases. The best-characterized substrates for the NEDD8 E3 ligases are cullin-ring ubiquitin ligases (CRLs) that are responsible for 20% of the proteasome-associated ubiquitination process[351]. This expands

the complexity and consequences of Nedd8 modulation dramatically due to the cascade of reactions dependent on ubiquitination.

The validation experiments revealed a divergence between HepaRG and HepG2 cells in terms of HBsAg transcripts levels following siRNA knockdown of neddylation components, suggesting that the mechanism behind the HBsAg secretion inhibition might differ between the cell lines. Depletion of Nedd8 transcripts led to a reduction of the measured HBsAg transcripts in HepG2-F-HB2.7(X+) whereas, the transcripts were not affected in HepaRG-HB2.7(X+) cells. It is highly likely that the binding of host transcription factors on the HBV enhancer or promoter regions was impaired in HepG2 due to a decrease in the expression of HNF1a, C/EBP, and HNF4a proteins as reported by Xie, M *et al.* recently[314], thus reflected as HBsAg mRNA decrease. On the other hand, the distinct mechanism for the post-transcriptional inhibition of HBsAg in HepaRGs is not clear, indicating a novel/alternative mode of inhibition of HBsAg secretion after knock-down of Nedd8 pathway. A similar mode of inhibition might be posed by MLN4924 treatment. Finding the exact mechanism is a challenging task due to the aforementioned complexity and hundreds of potential substrates of the neddylation pathway in addition to CRLs[352,353].

As the hit selection criteria were fulfilled by the Sirt2 and Htr6 genes as well, small-molecule inhibitors against each gene product were used for validation and this revealed non-significant changes in HBsAg secretion in HepG2-HB2.7 cells. Sirt2 is a member of the sirtuin histone deacetylase family which uses NAD+ as a cofactor for the removal of acetyl functional groups from lysine residues[354]. Sirt2 localizes to the cytoplasm, leading to deacetylation of tubulin and thereby decreasing stability of microtubules[354]. Sirt2 expression was found to be correlating with HBV replication *in vitro* together with increased deacetylation of tubulin[355]. Moreover, a potent Sirt2 inhibitor AGK2, also used in our study, was shown to decrease the replication of HBV *in vitro* and *in vivo*[355]. One particular difference between the literature and our data is the source of the transcripts for HBsAg. Our results do not indicate any antiviral effect of AGK2 and SirReal2 small molecule inhibitors in various concentrations and duration of treatment. It is highly probable that the Sirt2 and Htr6 genes were identified as hits due to off-target effects of siRNAs.

Inhibition of the neddylation pathway by NAE1 targeting drug MLN4924 (pevonedistat) upregulates the host restriction factors and controls the genome replication of various RNA and DNA viruses[356,357]. Sekiba *et al*. demonstrated that Smc5/6 complex is restored in MLN4924 treated HBV infected hepatocytes thereby epigenetically silencing the transcription from cccDNA[313]. In non-treated cells, HBV degrades Smc5/6 in an HBx dependent process in which

HBx hijacks CRL4-DDB1-ROC1 ubiquitin E3 ligase to counteract Smc5/6. The same research group identified nitazoxanide as an antiviral agent preventing DDB1-HBx interaction thus leading to the inhibition of HBV transcription in the same way with neddylation inhibitor MLN4924[315]. Furthermore, neddylation of HBV X protein by HDM2 E3 ligase is known to increase the stability of the protein, making NEDD8 modification a crucial regulator for X protein stability[358]. In our experiments on HepaRG-HB2.7 cells, we could demonstrate the potency of the MLN4924 drug in a different context by studying integrated HBV genome in the presence or absence of functional X ORFs. A recent study on HBV and the neddylation pathway indicated an X-independent phenotype supporting our findings; overexpression of sentrin-specific protease 8 (SENP8), which is a deneddylase for removing the conjugated Nedd8 modifications, suppresses the HBV replication in the absence of X protein[359].

MLN4924 drug on many cell lines, including HepG2 and HUH7, triggers autophagy as a survival signal besides inducing cell death via apoptosis and/or senescence[360]. In this study, the experiments on HepaRG based cell lines were performed on a confluent cell layer at day7 post-seeding to minimalize the variation due to the input cell number and to eliminate the effect MLN4924 induced senescence on the HBsAg phenotype. Periodic examination of the cells under a microscope and WST-1 biochemical assay confirmed the inhibition of HBsAg in a non-toxic range. Interestingly, the rebound of the HBsAg secretion arises as quickly as 2 days to 4 days post- MLN4924 removal at 200nM and 1µM MLN4924 concentration, respectively (Figure 7.3). On the other hand, the 5µM MLN4924 could not rebound to the DMSO condition level even at 6 days after off-treatment due to the toxicity. Our observation indicates that the inhibition is transient and the activity of the MLN4924 has to be sustained for the suppression of HBsAg secretion. Although controversy is present on the role of the autophagy pathway in HBV biology, MLN4924 triggered autophagosomal degradation might provide a plausible explanation for the mechanism beneath the inhibition. Rab7 and Snap29 dependent autophagosome and lysosome fusion has been reported to mediate the degradation of HBV particles[361-363]. Therefore, the examination of the autophagy machinery regulation and interplay with the neddylation pathway is necessary. Our preliminary result indicates an increase in the secretion of HBsAg from Atg5, Atg14L and Atg16L1 knock-out cell lines in HepaRG-HB2.7 background (data not shown). Moreover, a recent proteomic analysis for the identification of neddylated proteins revealed that proteins related to ribosome biogenesis and mRNA transport are the target of neddylation pathway[352]. The role of the MLN4924 on the translation efficacy of HBsAg transcripts is waiting to be examined, particularly in HepaRG based cell lines.

Our long-term experiment on HepAD38 illustrated the dual antiviral activity of neddylation inhibition on both cccDNA and integrated HBV sequences. The lack of effect for TDF treatment on HBsAg secretion was expected in doxycycline suppressed HepAD38 cells because the SVPs expressed from the endogenous promoters of integrated HBV genome were the only source of HBsAg. In line with our observations from knockdown experiments on HepG2-F-HB2.7 cells, MLN4924 treatment lowered the HBsAg secretion in the repressed (+DOX) state along with a decrease in HBV transcripts. Nucleoside analogs prevent the generation of rcDNA from pgRNAs and subsequent re-shuttling of the rcDNA containing nucleocapsids into the nucleus. Although the cccDNA quantification is missing in our experimental setup, the significant inhibition of HBeAg and HBsAg in the presence of TDF can be a surrogate for the accumulation of cccDNA in the nucleus in induced and non-treated cells.

Historically, the HBeAg is used as a marker for HBV DNA replication. Our results showed a discrepancy between HBV DNA and HBeAg levels from induced-HepAD38 cells under MLN4924 treatment. The decrease in the HBeAg was not reflected to the same extent in the released HBV DNA while TDF could suppress the replication effectively in parallel to HBeAg measurement. The incomplete HBV suppression by MLN4924 conditions is probably due to the technical limitation of the HepAD38 system, which overexpresses pgRNA under CMV promoter, thereby providing sufficient components for rcDNA synthesis and virion morphogenesis. Nevertheless, the formed cccDNA are probably inactivated by Smc5/6 complex mediated transcriptional silencing which prevents HBeAg expression. Taken together, combination therapy of NUCs and MLN4924 can provide a complete anti-HBV activity by targeting both the viral replication and the antigen secretion independent of the source of the transcription.

Neddylation deregulation is common in various chronic liver diseases which makes understanding/aiming the components of the pathway a promising approach for amelioration of HBV infection, liver fibrosis, non-alcoholic fatty liver disease (NAFLD), and HCC[364]. In bile acid ligation and carbon tetrachloride animal models, neddylation inhibitor was reported to decrease liver injury and inflammatory markers leading to better liver phenotype[365]. MLN4924 drug is currently in clinical trials at phase I/II/III for treatment of solid tumors and hematological malignancies (*clinicaltrials.gov*). The early clinical trial results of MLN4924 showed a reasonable safety profile though E1 activating enzyme subunit, Uba3, mutation was reported to cause drug resistance[364,366,367].

All in all, neddylation pathway inhibition might provide a novel anti-HBV strategy by the lowering circulating HBsAg levels and ultimately reactivating the exhausted immune system

components in CHB patients. It can be instrumental especially in HBV positive HCC setting and can be applied as mono- or combination therapy with currently approved therapeutics.

4.2 Proteomic Analysis of HBV Particles

Host factors exploited by HBV during its lifecycle are potential drug targets to treat chronic HBV patients. Therefore, there have been several reports investigating the whole proteome and transcriptome-wide analysis of HBV replicating cells to gain a better understanding of HBV biology[326,327]. In conjunction with the findings from our mini-screen, we scrutinized the presence of post-translational modifications, namely ubiquitin and NEDD8 in the heparin purified HBV stocks. Previously, Liu *et al.* showed neddylation of HBV X protein in Nedd8 overexpression setup[358] thus, ubiquitin or Nedd8 modifications on the other HBV viral proteins or associated proteins were not clear. The source of the striking ubiquitin banding pattern and Nedd8 in HBV stocks is not clear yet, though one should take the information carefully considering both HBV and HDV stocks were stabilized by FCS from different sources (Figure3.2.1A). Recent proteomic approach on HBV replicating hepatocarcinoma cell lines indicated significant differences in the content of released exosomes upon HBV replication[368,369]. Based on this, secretion of ubiquitin or ubiquitin modified proteins might be enhanced and enriched in the HBV viral stocks that were partially purified by heparin affinity column chromatography. The ubiquitin presence was *per se* an intriguing observation since the incorporation of ubiquitin has been described in the proteome of various virus families such as poxviridae, retroviridae, orthomyxoviridae, rhabdoviridae, paramyxoviridae, and arenaviridae[370-376]. Asymmetric reconstitution of the Cryo-EM images from pgRNA containing nucleocapsids showed an electron-dense region in the interior of the capsid structure. Of this electron dense feature, in addition to the pgRNA and a donut-shaped HBV polymerase protein, some host factors were speculated to be entrapped[377].

To substantiate our observation and identify host factors associated with HBV, we have applied a multi-step purification pipeline to HBV particles. Due to the slow nature of the HBV producing HepAD38 cell line, the culture duration was extended over 2 months. HBeAg value was used as a surrogate marker of HBV replication and cccDNA amount in the cells as suggested previously[334]. The kinetics of HBeAg and HBsAg had the same pattern of secretion in both culture batches; the early HBeAg rise was followed by an HBsAg increase in about one to two weeks. A plausible explanation for that is the re-shuttling of rcDNA into the nucleus

where the cccDNA pool accumulates and serves as a template for viral transcription. Hence, the HBsAg transcripts of cccDNA might cause the late HBsAg soaring. The relatively flat pattern of HBsAg secretion from HB2.7 cells supports this notion.

Even after isopycnic density gradient centrifuge, an ample amount of non-HBV proteins were visible on silver gel analysis of the collected fractions, which was not expected considering the steps of purifications the samples went through. Indeed, our pilot proteomic experiments proved that thousands of proteins were collectively identified in HBV or SVPs containing sucrose fractions (data not shown). Moreover, our first attempt to determine the HBV particle lipidome from sucrose fractions was not successful, showing lipid background likely contributed by the FCS presence. Despite this, we could see an enrichment of the phosphatidylcholine which is previously identified as the main lipid component of SVPs[228,229]. In addition, dihexosylceramide (Hex2Cer) was significantly higher in HepAD38 virus fractions compared to the controls, which needs more experimentation on a purer material to validate (Figure 7.11). Our final particle purification setup with HBsAg immunoprecipitation step proved to be highly successful and specific which was verified by EM images and biochemical methods. Interestingly, the HBV core antigen analysis of HepAD38 samples has shown double bands; one at the expected core size, just below 20kDa, while the other was just above 15kDa marker. This unknown small HBcAg band was getting more prominent towards the high-density range of the sucrose gradient in all our experiments. In concordance with our observation, the low molecular weight band appeared in the western blot analysis of purified nucleocapsid from HepDES19 cells as well (unpublished results of Eva Maria Stork)[378]. Moreover, immune-precipitation of the fractions with an HBV envelope specific antibody showed exclusion of the small HBcAg from the enveloped particles. The findings have strong similarities to the observations made by Hong, X. and his colleagues who characterized biochemical and biophysical properties of HBV precore/core particles[193]. In their study, the proteolytic processing of precore peptide generated a single HBeAg band in HBV genotypeD condition and in parallel to our observation, the HBeAg/precore proteins were detected in denser sucrose fractions than the viral particles after sedimentation. Furthermore, the precore/e antigens were found to be not incorporated into the capsid structure under physiological conditions[193]. The source of these HBsAg-less, high density HBV core related antigen (HBcrAg) in our sucrose fractions is not known yet. The first step of our purification, heparin column affinity chromatography takes advantage of low-affinity binding between HBV envelope proteins with the heparan sulfate proteoglycans[74,76]. Binding affinity of naked HBV capsid and HBcAg dimers towards the heparin matrix is waiting for examination. The highly sulfated nature of

heparin allows capturing of positively charged biomolecules. Thus, the non phosphorylated arginine rich C-terminus of core proteins could provide the positive charge necessary for the binding in its monomeric or dimeric forms. In the same line, heparin and heparan sulfate proteoglycans dependent interference of HBV capsids binding has been demonstrated on the surface of THP-1 macrophages and truncation of CTD inhibited the capsid attachment to cell surface[379]. Another explanation for the appearance of high-density HBcrAg might be a complete/partial destruction of a subset of virion particles during the purification process exposing nucleocapsids to extracellular enzymes. It has been speculated that HBV genome maturation can lead to structural changes in the capsid structures such as exposure of NLS signal in CTD for the establishment of infection in the nucleus[108]. Likewise, disruption of the envelope layer of HBV virion by purification conditions like high salt or shear stress can lead to the unveiling of HBcAg CTD and cause digestion by the surrounding proteases. Supporting this notion, LC-MS/MS results displayed no peptide corresponding to the precore region of the HBV but only core peptides. A more detailed characterization of the band is currently in progress.

Previously, it has been shown that the HBx protein is not incorporated into the HBV particles while its transcripts are identified in the virus preparations generated via PEG-precipitation[131,380]. Recently, highly sensitive HBx antibodies were used for microscopic examination of HBx in infected PHHs. The HBx could be identified in PHHs earliest at 24 hours post infection[337]. In line with the literature, we could not detect any HBx peptides in any HBV particles purified from HepAD38 and HepG2-HB2.7 cell lines. The secretion and transfer of the HBx could be still taking place in a paracrine manner via exosomes as described previously[381]. Since the proteomic profiling of the exosome was out of the scope of the current study, we could not confirm that data.

Identification and preservation of ubiquitin and phosphorylation modifications in the sample require special sample preparation conditions like the addition of inhibitors for deubiquitylases or phosphatases and subsequent enrichment for modified peptides. Lacking any of these optimizations in our sample preparation pipeline impaired proper analysis of these modifications on the host factors and viral proteome. Essentially, the only post-translational modification detected on the viral peptides, phosphorylation of S40 of PreS2, is intriguing due to the previous report on phosphorylation dependent trans-activator function of truncated middle and large envelope proteins[382,383]. As a consequence of mislocalization of truncated M envelope protein or due to cytoplasmic positioning of L PreS1 domain, PreS2 sequences are exposed to the cytosolic milieu that renders protein kinase C phosphorylation of S27/28 on

PreS2 segment[382,383]. Furthermore, phosphorylation of duck hepatitis B virus large envelope protein is studied by several research groups previously and shown to be dispensable for the infectivity of the virus[384,385]. To our knowledge, our study is the first one reporting phosphorylation of HBV envelope proteins of the secreted particles. The impact of the S40 PreS2 phosphorylation on the morphogenesis and on the fitness of HBV is not studied yet.

Our proteomic analysis revealed around 150 host proteins in/on the subviral and virion particles following subtraction of the background proteins associated with control cell purifications and IgG1 immuno-precipitations. Only a few host factors were unique for the virions while around 50 of them were detected in both HepAD38 and HepG2-HB2.7 derived HBV particles. The remaining factors could be identified only in SVPs of HepG2-HB2.7 cells possibly due to the availability of a greater amount of HBsAg as LC-MS/MS input material.

A considerably significant portion of HBV-associated host factors have been already discovered in other proteome studies based on evolutionary diverse yet, all enveloped virus families. Considering the application of different culturing and purification setups for the each type of virus, the similarities between the studies are probably due to the exploitation of common egress pathways by the viruses rather than common contaminants. To illustrate, ubiquitin, cyclophilin A and annexin proteins have been identified in the structures of HIV, vaccinia virus, and Influenza A (IAV)[370,375,376]. Of note, we detected calcium-binding protein family S100 proteins particularly in SVPs, which can form a functional complex with annexin protein family members interacting with phospholipid membranes. There are reports available that the gaps on the plasma membrane are repaired by the concerted action of the actin cytoskeleton, annexins, and ESCRT-III complex[386-388]. We detected ACTB, ANXA7, ANXA2, S100P, S100A1, S100A9, and PDCD6 (ALG-2) proteins in our samples. This is suggesting that activities of the membrane repair complex components might facilitate viral budding process on MVBs in the light of evidences on the role of ESCRT-II and ESCRT-III components during the HBV virion egress [253,254,256,389]. On the other hand, abundant cytosolic proteins can end up in the particles due to accidental entrapment of the protein at the virus morphogenesis site. Cyclophilin A, GAPDH, enolase 1, actin, tubulin, and pyruvate kinase are the potential candidates for this fortuitous association though several of them were studied and demonstrated as crucial factors for HBV lifecyle[390-392].

Transmission electron microscopy analysis of the cholesterol-depleted HBV virions by methyl-*β*-cyclodextrin treatment showed shrinkage of the virion diameter besides loss of infectivity whereas, the replenishment of cholesterol reverses the condition back to the normal morphology and infectivity[393]. Supporting the role of the cholesterol in HBV morphogenesis, Dorobantu *et*

al. lowered the total cholesterol amount in HepG2.2.15 cells by brief incubation of the cells with lipid depleted serum and measured the secretion of SVPs and virion in the supernatant[394]. Inhibition was specific on virions without any decrease in the levels of SVPs. The authors postulated that the derangement on L topology ascribed to cholesterol depletion impaired the interaction of PreS1 with capsid during the envelopment process[394]. More evidence on the role of cholesterol during the HBV morphogenesis comes from a comparative proteomics analysis of lipid rafts derived from HepG2 and HBV replicating HepG2.2.15 cells[395]. Lipid rafts are rigid, stable, and detergent-resistant microdomains on lipid membranes that are enriched with cholesterol and sphingomyelin. Some of the lipid raft proteins were identified to be altered in quantity (> 2 fold) in HBV replicating cells compared to control and interestingly a small subset of them are also detected in our proteomics analysis such as ENO1, CLIC1, MIF, and GAPDH. The number of raft-associated proteins in our list is probably much higher. For instance, HSPB1 protein is known to reside in cholesterol-rich lipid raft domains of extracellular vesicles collected from HepG2 cells[396]. Additionally, HSP90, HSC70, HSP60, and HSP40 heat shock protein has been found as the components of lipid rafts in rat brain[397].

To our knowledge, there is not any cholesterol recognition/interaction amino acid consensus sequence (CRAC) present on the HBV transmembrane domains of envelope proteins. The interconnection between the host factors identified in both lipid rafts and HBV particles and their importance for HBV virion morphogenesis is vague and demands further investigation. Lipid transfer in the body is mediated by the actions of apolipoproteins present on lipoproteins, which have amphipathic properties conferring interaction with lipids and aqueous environment of the body. Lipoproteins can be categorized according to their buoyant densities and different combination of apolipoproteins are associated regarding the type of the lipoprotein. Efficient propagation of HCV in hepatocytes depends on the interaction of very low-density lipoproteins with the viral particles carrying a wide spectrum of apolipoproteins on the surface of HCV particles[398]. Recently, some similarities are reported in the HBV context, ApoE seems to perform a multifaceted role in HBV life-cycle ranging from entry to egress[339]. It has been shown to reside on the surface of HBV particles by biochemical analysis. Interestingly, the entry of HBV can be blocked by the ApoE neutralizing antibodies[339]. In addition to that, interference of the ApoE expression by shRNA knockdown leads to a decrease in secreted HBV. In another study, tail vein injection of HBV into ApoE -/- animals resulted in less rcDNA in the liver and more HBV in the serum compared to wild type Bl6 mice suggesting a connection between lipoprotein uptake pathway and HBV internalization into hepatocytes *in vivo*[399]. In this study, we could also identify plenty of ApoE on the HBV virions and SVPs particles and validated the

existence of ApoE on the particles by visualization under a transmission electron microscope. The distribution of ApoE proteins were strikingly concentrated at the head of the filamentous SVPs where the immune-gold labeling of HBsAg antigen showed negative results. In contrast to HBsAg-rich trunk part of the filaments, the head part displayed low contrast in negative staining, which might be due to compositional differences between these regions.

Important for reverse cholesterol transfer pathway, ATP-binding cassette A1 (Abca1) protein can mediate cholesterol homeostasis by loading the lipids mainly onto ApoA-I and also on ApoE in central nervous system. As a result of cholesterol efflux across the plasma membrane, high-density lipoproteins are generated at the expense of intracellular cholesterol[400]. In our siRNA mini-screen experiments on HepG2-HB2.7 cells, we have observed a significant upregulation of SVP particle secretion by siRNA knockdown of Abca1 gene expression. In the light of HBV particle proteome results and taking the published works on cholesterol and HBV virion secretion axis into consideration, the induction of intracellular accumulation of cholesterol by Abca1 depletion might lead to a favorable condition for filamentous SVP secretion by causing accumulation of cholesterol and/or ApoE on the particles. In a remarkably similar manner, HIV Nef protein has been shown to inhibit Abca1 function in the infected cells, generating increasing HIV production by inducing lipid raft formation[400-402]. The envelopment process of HBV nucleocapsids and our EM findings illustrating ApoE at the head part of the filamentous SVPs might be mechanistically connected entities in the viral life-cycle. Supporting this notion, cobra-shaped particles have been observed from human serum derived HBV particles for a long time and these virion-filament like structures might be a snapshot of an intermediate phase of HBV morphogenesis[403,404].

It is worth mentioning that ApoE protein contains heparan sulfate proteoglycans binding domains thus it could be enriched in our heparin column chromatography containing purification pipeline independent of HBsAg particles[405,406]. We could prove the ApoE enrichment by biochemical analysis of the sucrose gradient fractions from HepG2 parental cell line (Figure 3.2.14B). In spite of this background binding, mass spectroscopy results indicated a significant association between ApoE and the HBsAg particle even following anti-HBsAg immune-precipitation and we could image a striking accumulation of the ApoE-gold particles on the globular head of SVP filaments, which are suggesting a specific interaction between ApoE and HBsAg. Questions regarding the site of this interaction, intracellularly or extracellularly, and how the ApoE and the particles find each other are waiting for further investigation. Our attempts to study ApoE expression in HBsAg secretion context revealed that complementation of ApoE into apolipoprotein deficient cell lines, 293T and HeLa, facilitated

the secretion of only L containing HBsAg about 5-fold. It has been well characterized that L protein accumulates in ER due to the retention signal on PreS1 explaining why we measured low HBsAg concentrations in the supernatant from the transfected cells[407]. Moreover, we could also demonstrate that the secretion of only S containing HBsAg could be augmented by ApoE in HeLa cell line but not in HUH7 or 293T cells. Altogether, upregulation of HBsAg secretion only in ApoE deficient but not in ApoE expressing HUH7 cells giving us a hint for the intracellular role of ApoE for HBV particle egress. Considering the potential artifact related to SV40 promoter-driven overexpression of HBsAg, recapitulation of the results using HBsAg expressing constructs under the authentic HBV promoters is essential

One of the main aims of our study was to identify host factors exclusively associated with HBV virions. Through careful examination of the mass spectroscopy results, we could identify a small number of such exclusive host factors. These proteins are named CWF19L2, CASP14, SBSN, and HNRNPC. In addition to that, two more host factors, LMO7 and HSP90AB1, were identified frequently in the virions though accompanied by a low/moderate background in IgG1 control conditions of HepAD38. Identification of HSP90AB1 is not a surprise to us since the functions of host chaperones have been of interest of HBV researchers for decades and experiments on DHBV provided numerous evidence for the HSP90 complex's role on HBV polymerase-epsilon interaction and reorganization of replication initiation complex[190,191]. HSP90 chaperone complex formation requires activities of additional HSP70 and HSP40 chaperones which were reported to be not incorporated into the HBV particles, unlike HSP90[190]. Apart from this, HSP90 and HSP70 chaperoning activities have been demonstrated to facilitate HBV capsid formation as well[408,409].

Besides HSP90, we could detect a significant number of heat shock and chaperones proteins such as well-known cytosolic anchorage determinant HSC70 protein, DNAJB12, DNAJB6, DNAJB2, HSPA1B (HSP70), HSPB1, and CANX, predominantly in SVP samples. Highlighting the drug discovery potential of our hit list, DNAJB12 serves as a remarkable example which was reported as the target of NAP-based HBsAg secretion inhibitor drug, REP-2139 recently (AASLD The Liver Meeting 2020, LP42). Moreover, in an independent study HSPB1 was found as the most upregulated protein in HepG2.2.15 cells relative to HepG2 in quantitative proteomics using isobaric tagging (iTRAQ) which was validated in HBV positive patients' samples[410].

To our knowledge, available information on our virion exclusive host factors is very limited in the HBV context. HNRNPC was found out to be an HBc interacting protein in a recent study along with Cyclophilin A, DNAJB6, ubiquitin, and MLF2, which were identified mainly with

the SVP particles[411]. Furthermore, an indirect connection of CASP14 and SBSN proteins with HBV replication/release was reported by examination of exosome proteome gathered from HBV or HBx plasmid transfected HUH7 cells[368]. Zhao and colleagues showed that CASP14 and SBSN were significantly lowered in the exosomes of HBx and HBV expressing cells[368]. Relating to this, all the exosomes were negatively selected by anti-HBsAg before SILAC quantification of the total protein content. The negative correlation between the common host factors in exosomes of HBV replicating cells and our proteome results can be extended to CSTA, GPC3, APOA1, APOC3, and S100A9 proteins[368]. By hijacking exocytic release machinery and recruiting the common aforementioned factors explicitly to the HBV budding site, HBV particles might be depleting the factors from other exocytosed cargos. Interestingly, the current knowledge and function of CASP14 and SBSN proteins are very poorly defined, the studies depicted the function of these genes generally in skin development[412,413]. An emerging link between CASP14 and SBNS expression and tumorigenesis is getting stronger in recent years albeit their role in viral infections and normal physiology of hepatocytes is waiting for further analysis. Interestingly, regulatory T (Treg) cell induction in spleen has been reported to be impaired after oral nickel administration to SBSN (-/-) mice[414]. It is likely that SBSN has a role on Tregs development. Thus, examination of the SBSN serum levels in different stages of CHB, especially in the immune-tolerant phase, could be a valuable marker in clinics. Furthermore, in an interactome study for HBV L envelope protein in hTERT-immortalized hepatic progenitor cell line NeHepLxHT, Wu, Y.H. *et al.* could demonstrate that some of our hit factors such as SBSN, CSTA, HSPB1, HSC70 and HSP70, PKM and S100A9 as an interaction partner of L envelope protein[392]. This finding is contradicting with our observations. Although the filamentous SVP contains a significant amount of L protein in its structure, we could detect SBSN only in the proteome of HBV virion.

CFW19L2 is a part of intron lariat spliceosome (ILS) machinery bearing positive charge on its surface allowing it to bind RNA duplex between U2 small nuclear RNA (snRNA) & branch point sequence of lariat structure[415]. Spliceosomes are arguably the most complex RNPs in the cells performing maturation of the pre-mRNAs sequentially. Considering the reported splice variants of HBV RNAs, postulating a role of CWF19L2 in HBV splicing is probably the most direct and simple one. However, due to the absence of any other spliceosome complex components in the HBV virion proteome list, it could be very well possible that CWF19L2 is recruited by the virion for an alternative function such as regulation of replication.

It has been shown that N6-methyladenosine modifications on mRNAs cause structural alteration on mRNAs and facilitating HNRNPC binding[416]. Recent reports have shown that the

N6-methyladenosine epigenetic modifications on epsilon stem-loop structure of HBV transcripts are crucial for the stability of HBV transcripts and reverse transcription of pgRNA[172,417]. Whether the HBV replication depends on the intra-capsid HNRNPC activities is among the pending questions.

With the data in our hands, it is hard to predict any interaction or synergism between the six identified HBV-specific host factors in any cellular process involved in the viral lifecycle. In a comprehensive yeast-two hybrid protein-protein interaction study for vaccinia virus proteins with human cDNAs, it is reported that a small vaccinia protein named uncharacterized protein G6 can interact with 19 human proteins including SBSN, LMO7, and CWF19L2[418]. This astonishing coincidence might reflect a reliance on the same set of factors for a certain biological process by both HBV and vaccinia virus. The vaccinia G6R is a conserved protein in poxviruses and belongs to NLPC/P60 protein family. It is located between envelope and capsid structure and shown to be important as a virulence factor *in vivo* but not important for the virus replication *in vitro*[419]. Therefore, the roles of SBSN, LMO7 and CWF19L2 in animal models or patients have to be examined in parallel to the *in vitro* experiments to avoid misinterpretation of the results due to limitations of traditional cell culture systems.

All in all, in this study we could successfully obtain proteomes derived from highly pure HBV virions and SVP. The results highlight many novel host factors previously not documented to be associated with HBV and confirm a significant number of proteins described in the HBV literature.

4.3 Conclusion and perspectives

With this study, we could determine hitherto unidentified role of neddylation pathway components in the HBsAg secreting process from HBV subgenomic integrant. The small molecule drug, MLN4924, targeting the neddylation pathway, which is currently in clinical trials for various cancer therapies, could inhibit HBsAg effectively in a non-toxic range. In an inducible cell culture setup, we could demonstrate the dual inhibitory effect of neddylation pathway perturbation on both the cccDNA dependent RNA transcription and on the HBsAg secretion from the integrants. The mechanism of how the NEDD8 protein contributes to the HBsAg secretion is not clear yet. Further studies pinpointing downstream components of the neddylation pathway are necessary to reveal the genes specifically hijacked by HBV during the HBsAg morphogenesis/secretion. Well-tolerable properties and capability to alleviate the HBV

antigens from both cccDNA and integrated HBV sequences make MLN4924 a promising candidate as HBV antiviral.

In the second part of the study, we could successfully generate very pure viral stocks to determine the protein composition of filamentous SVPs and HBV virions by a very sensitive LC-MS/MS method. To our knowledge, this is the first study in the literature studying the HBV particle proteome. Besides identification of all HBV structural proteins, numerous host factors were detected in the HBV particles. Our results indicated many novel host factors associated with the HBV particles in addition to some proteins already described in HBV biology like APOE, HSC70, and HSP90. Again for the first time in the literature, we could visualize APOE on the HBV virion and SVPs which indicated a distinct distribution of ApoE molecules on filamentous SVPs. Role of the APOE during the HBV morphogenesis and its contribution to the entry of the virion waiting to be addressed. Taking the heparin-binding properties of APOE into account, detailed examinations of ApoE's role; i) in the context of L topology switch and ii) at the attachment to the hepatocytes surface proteoglycans would further deepen our understanding of HBV entry. Of note, fluorescent labeling of ApoE or any other HBV-associated host proteins might be used as a tool to track the HBV during entry or egress pathways.

Future experiments for the validation of the proteome list involve siRNAs knockdown and the characterization of the secreted HBV particles in terms of infectivity and biochemical/biophysical properties. Investigations on patient samples and PHH will be helpful to prove the clinical significance of our results coming from the cell culture system.

All in all, by application of two different strategies, we could identify a significant number of host proteins/pathways which might serve as a resource to uncover new anti-HBV drugs. By displaying trace amount background, the success of the purification process can pave the way towards long-waiting research topics such as HBV lipidome.

5 References

1 Stanaway, J. D. *et al.* The global burden of viral hepatitis from 1990 to 2013: findings from the Global Burden of Disease Study 2013. *Lancet* **388**, 1081-1088, doi:10.1016/S0140-6736(16)30579-7 (2016).

2 Thomas, D. L. Global Elimination of Chronic Hepatitis. *N Engl J Med* **380**, 2041-2050, doi:10.1056/NEJMra1810477 (2019).

3 Foreman, K. J. *et al.* Forecasting life expectancy, years of life lost, and all-cause and cause-specific mortality for 250 causes of death: reference and alternative scenarios for 2016-40 for 195 countries and territories. *Lancet* **392**, 2052-2090, doi:10.1016/S0140-6736(18)31694-5 (2018).

4 Organization, W. *Global Hepatitis Report, 2017*. (2017).

5 Lemon, S. M., Ott, J. J., Van Damme, P. & Shouval, D. Type A viral hepatitis: A summary and update on the molecular virology, epidemiology, pathogenesis and prevention. *J Hepatol*, doi:10.1016/j.jhep.2017.08.034 (2017).

6 WHO position paper on hepatitis A vaccines - June 2012. *Wkly Epidemiol Rec* **87**, 261-276 (2012).

7 Jacobsen, K. H. & Wiersma, S. T. Hepatitis A virus seroprevalence by age and world region, 1990 and 2005. *Vaccine* **28**, 6653-6657, doi:10.1016/j.vaccine.2010.08.037 (2010).

8 Klevens, R. M. *et al.* Seroprevalence of hepatitis A virus antibodies in the U.S.: results from the National Health and Nutrition Examination Survey. *Public Health Rep* **126**, 522-532, doi:10.1177/003335491112600408 (2011).

9 Klevens, R. M., Denniston, M. M., Jiles-Chapman, R. B. & Murphy, T. V. Decreasing immunity to hepatitis A virus infection among US adults: Findings from the National Health and Nutrition Examination Survey (NHANES), 1999-2012. *Vaccine* **33**, 6192-6198, doi:10.1016/j.vaccine.2015.10.009 (2015).

10 Xu, Z. Y. & Wang, X. Y. Live attenuated hepatitis A vaccines developed in China. *Hum Vaccin Immunother* **10**, 659-666, doi:10.4161/hv.27124 (2014).

11 Sattar, S. A., Jason, T., Bidawid, S. & Farber, J. Foodborne spread of hepatitis A: Recent studies on virus survival, transfer and inactivation. *Can J Infect Dis* **11**, 159-163, doi:10.1155/2000/805156 (2000).

12 Perez-Gracia, M. T., Suay-Garcia, B. & Mateos-Lindemann, M. L. Hepatitis E and pregnancy: current state. *Rev Med Virol* **27**, e1929, doi:10.1002/rmv.1929 (2017).

13 Colson, P. *et al.* Pig liver sausage as a source of hepatitis E virus transmission to humans. *J Infect Dis* **202**, 825-834, doi:10.1086/655898 (2010).

14 King, N. J., Hewitt, J. & Perchec-Merien, A. M. Hiding in Plain Sight? It's Time to Investigate Other Possible Transmission Routes for Hepatitis E Virus (HEV) in Developed Countries. *Food Environ Virol* **10**, 225-252, doi:10.1007/s12560-018-9342-8 (2018).

15 Pavio, N., Merbah, T. & Thebault, A. Frequent hepatitis E virus contamination in food containing raw pork liver, France. *Emerg Infect Dis* **20**, 1925-1927, doi:10.3201/eid2011.140891 (2014).

16 Szabo, K. *et al.* Detection of hepatitis E virus RNA in raw sausages and liver sausages from retail in Germany using an optimized method. *Int J Food Microbiol* **215**, 149-156, doi:10.1016/j.ijfoodmicro.2015.09.013 (2015).

17 Kamar, N. *et al.* Factors associated with chronic hepatitis in patients with hepatitis E virus infection who have received solid organ transplants. *Gastroenterology* **140**, 1481-1489, doi:10.1053/j.gastro.2011.02.050 (2011).

18 Kamar, N. *et al.* Hepatitis E virus and chronic hepatitis in organ-transplant recipients. *N Engl J Med* **358**, 811-817, doi:10.1056/NEJMoa0706992 (2008).

19 Wu, X., Chen, P., Lin, H., Hao, X. & Liang, Z. Hepatitis E virus: Current epidemiology and vaccine. *Hum Vaccin Immunother* **12**, 2603-2610, doi:10.1080/21645515.2016.1184806 (2016).
20 Gower, E., Estes, C., Blach, S., Razavi-Shearer, K. & Razavi, H. Global epidemiology and genotype distribution of the hepatitis C virus infection. *J Hepatol* **61**, S45-57, doi:10.1016/j.jhep.2014.07.027 (2014).
21 Jafri, S. M. & Gordon, S. C. Epidemiology of Hepatitis C. *Clin Liver Dis (Hoboken)* **12**, 140-142, doi:10.1002/cld.783 (2018).
22 Saab, S., Le, L., Saggi, S., Sundaram, V. & Tong, M. J. Toward the elimination of hepatitis C in the United States. *Hepatology* **67**, 2449-2459, doi:10.1002/hep.29685 (2018).
23 Martinello, M., Hajarizadeh, B., Grebely, J., Dore, G. J. & Matthews, G. V. Management of acute HCV infection in the era of direct-acting antiviral therapy. *Nat Rev Gastroenterol Hepatol* **15**, 412-424, doi:10.1038/s41575-018-0026-5 (2018).
24 Schweitzer, A., Horn, J., Mikolajczyk, R. T., Krause, G. & Ott, J. J. Estimations of worldwide prevalence of chronic hepatitis B virus infection: a systematic review of data published between 1965 and 2013. *Lancet* **386**, 1546-1555, doi:10.1016/S0140-6736(15)61412-X (2015).
25 Ginzberg, D., Wong, R. J. & Gish, R. Global HBV burden: guesstimates and facts. *Hepatol Int* **12**, 315-329, doi:10.1007/s12072-018-9884-8 (2018).
26 Hyun Kim, B. & Ray Kim, W. Epidemiology of Hepatitis B Virus Infection in the United States. *Clin Liver Dis (Hoboken)* **12**, 1-4, doi:10.1002/cld.732 (2018).
27 Viral Hepatitis Surveillance–United States. *CDC* (2016-2018).
28 Hauri, A. M., Armstrong, G. L. & Hutin, Y. J. The global burden of disease attributable to contaminated injections given in health care settings. *Int J STD AIDS* **15**, 7-16, doi:10.1258/095646204322637182 (2004).
29 Trepo, C., Chan, H. L. & Lok, A. Hepatitis B virus infection. *Lancet* **384**, 2053-2063, doi:10.1016/S0140-6736(14)60220-8 (2014).
30 Shiffman, M. L. Management of acute hepatitis B. *Clin Liver Dis* **14**, 75-91; viii-ix, doi:10.1016/j.cld.2009.11.013 (2010).
31 Nayagam, S. *et al.* Requirements for global elimination of hepatitis B: a modelling study. *Lancet Infect Dis* **16**, 1399-1408, doi:10.1016/S1473-3099(16)30204-3 (2016).
32 European Association for the Study of the Liver. Electronic address, e. e. e. & European Association for the Study of the, L. EASL 2017 Clinical Practice Guidelines on the management of hepatitis B virus infection. *J Hepatol* **67**, 370-398, doi:10.1016/j.jhep.2017.03.021 (2017).
33 Hughes, S. A., Wedemeyer, H. & Harrison, P. M. Hepatitis delta virus. *Lancet* **378**, 73-85, doi:10.1016/S0140-6736(10)61931-9 (2011).
34 Botelho-Souza, L. F., Vasconcelos, M. P. A., Dos Santos, A. O., Salcedo, J. M. V. & Vieira, D. S. Hepatitis delta: virological and clinical aspects. *Virol J* **14**, 177, doi:10.1186/s12985-017-0845-y (2017).
35 Stockdale, A. J. *et al.* The global prevalence of hepatitis D virus infection: Systematic review and meta-analysis. *J Hepatol* **73**, 523-532, doi:10.1016/j.jhep.2020.04.008 (2020).
36 Lempp, F. A., Ni, Y. & Urban, S. Hepatitis delta virus: insights into a peculiar pathogen and novel treatment options. *Nat Rev Gastroenterol Hepatol* **13**, 580-589, doi:10.1038/nrgastro.2016.126 (2016).
37 Fattovich, G. *et al.* Influence of hepatitis delta virus infection on morbidity and mortality in compensated cirrhosis type B. The European Concerted Action on Viral Hepatitis (Eurohep). *Gut* **46**, 420-426, doi:10.1136/gut.46.3.420 (2000).
38 Chen, H. Y. *et al.* Prevalence and burden of hepatitis D virus infection in the global population: a systematic review and meta-analysis. *Gut* **68**, 512-521, doi:10.1136/gutjnl-2018-316601 (2019).
39 Zhang, Z. & Urban, S. New insights into HDV persistence: The role of interferon response and implications for upcoming novel therapies. *J Hepatol* **74**, 686-699, doi:10.1016/j.jhep.2020.11.032 (2021).
40 Sinn, D. H. *et al.* Current status and strategies for viral hepatitis control in Korea. *Clin Mol Hepatol* **23**, 189-195, doi:10.3350/cmh.2017.0033 (2017).

41 McMahon, B. J. *et al.* Acute hepatitis B virus infection: relation of age to the clinical expression of disease and subsequent development of the carrier state. *J Infect Dis* **151**, 599-603, doi:10.1093/infdis/151.4.599 (1985).
42 Ostapowicz, G. *et al.* Results of a prospective study of acute liver failure at 17 tertiary care centers in the United States. *Ann Intern Med* **137**, 947-954, doi:10.7326/0003-4819-137-12-200212170-00007 (2002).
43 Burns, G. S. & Thompson, A. J. Viral hepatitis B: clinical and epidemiological characteristics. *Cold Spring Harb Perspect Med* **4**, a024935, doi:10.1101/cshperspect.a024935 (2014).
44 Hui, C. K. *et al.* Natural history and disease progression in Chinese chronic hepatitis B patients in immune-tolerant phase. *Hepatology* **46**, 395-401, doi:10.1002/hep.21724 (2007).
45 Attar, B. M. CON: All Patients With Immune-Tolerated Hepatitis B Virus Do Not Need to Be Treated. *Clin Liver Dis (Hoboken)* **15**, 25-30, doi:10.1002/cld.893 (2020).
46 Mason, W. S. *et al.* HBV DNA Integration and Clonal Hepatocyte Expansion in Chronic Hepatitis B Patients Considered Immune Tolerant. *Gastroenterology* **151**, 986-998 e984, doi:10.1053/j.gastro.2016.07.012 (2016).
47 Maruyama, T., Iino, S., Koike, K., Yasuda, K. & Milich, D. R. Serology of acute exacerbation in chronic hepatitis B virus infection. *Gastroenterology* **105**, 1141-1151, doi:10.1016/0016-5085(93)90960-k (1993).
48 Chan, H. L. *et al.* A longitudinal study on the natural history of serum hepatitis B surface antigen changes in chronic hepatitis B. *Hepatology* **52**, 1232-1241, doi:10.1002/hep.23803 (2010).
49 Lok, A. S., Lai, C. L., Wu, P. C., Leung, E. K. & Lam, T. S. Spontaneous hepatitis B e antigen to antibody seroconversion and reversion in Chinese patients with chronic hepatitis B virus infection. *Gastroenterology* **92**, 1839-1843, doi:10.1016/0016-5085(87)90613-5 (1987).
50 Fattovich, G. *et al.* Long-term outcome of chronic hepatitis B in Caucasian patients: mortality after 25 years. *Gut* **57**, 84-90, doi:10.1136/gut.2007.128496 (2008).
51 Cornberg, M. *et al.* The role of quantitative hepatitis B surface antigen revisited. *J Hepatol* **66**, 398-411, doi:10.1016/j.jhep.2016.08.009 (2017).
52 Simonetti, J. *et al.* Clearance of hepatitis B surface antigen and risk of hepatocellular carcinoma in a cohort chronically infected with hepatitis B virus. *Hepatology* **51**, 1531-1537, doi:10.1002/hep.23464 (2010).
53 Chu, C. M. & Liaw, Y. F. Predictive factors for reactivation of hepatitis B following hepatitis B e antigen seroconversion in chronic hepatitis B. *Gastroenterology* **133**, 1458-1465, doi:10.1053/j.gastro.2007.08.039 (2007).
54 Raimondo, G. *et al.* Update of the statements on biology and clinical impact of occult hepatitis B virus infection. *J Hepatol* **71**, 397-408, doi:10.1016/j.jhep.2019.03.034 (2019).
55 Pollicino, T. *et al.* Molecular and functional analysis of occult hepatitis B virus isolates from patients with hepatocellular carcinoma. *Hepatology* **45**, 277-285, doi:10.1002/hep.21529 (2007).
56 Miller, R. H., Kaneko, S., Chung, C. T., Girones, R. & Purcell, R. H. Compact organization of the hepatitis B virus genome. *Hepatology* **9**, 322-327, doi:10.1002/hep.1840090226 (1989).
57 Beck, J. & Nassal, M. Hepatitis B virus replication. *World J Gastroenterol* **13**, 48-64, doi:10.3748/wjg.v13.i1.48 (2007).
58 Tu, T., Budzinska, M. A., Shackel, N. A. & Urban, S. HBV DNA Integration: Molecular Mechanisms and Clinical Implications. *Viruses* **9**, doi:10.3390/v9040075 (2017).
59 Hu, J. & Seeger, C. Hepadnavirus Genome Replication and Persistence. *Cold Spring Harb Perspect Med* **5**, a021386, doi:10.1101/cshperspect.a021386 (2015).
60 Tsukuda, S. & Watashi, K. Hepatitis B virus biology and life cycle. *Antiviral Res* **182**, 104925, doi:10.1016/j.antiviral.2020.104925 (2020).
61 Long, Q. *et al.* The role of host DNA ligases in hepadnavirus covalently closed circular DNA formation. *PLoS Pathog* **13**, e1006784, doi:10.1371/journal.ppat.1006784 (2017).

62 Qi, Y. *et al.* DNA Polymerase kappa Is a Key Cellular Factor for the Formation of Covalently Closed Circular DNA of Hepatitis B Virus. *PLoS Pathog* **12**, e1005893, doi:10.1371/journal.ppat.1005893 (2016).
63 Tang, L., Sheraz, M., McGrane, M., Chang, J. & Guo, J. T. DNA Polymerase alpha is essential for intracellular amplification of hepatitis B virus covalently closed circular DNA. *PLoS Pathog* **15**, e1007742, doi:10.1371/journal.ppat.1007742 (2019).
64 Kramvis, A. Genotypes and genetic variability of hepatitis B virus. *Intervirology* **57**, 141-150, doi:10.1159/000360947 (2014).
65 Revill, P. A. *et al.* The evolution and clinical impact of hepatitis B virus genome diversity. *Nat Rev Gastroenterol Hepatol* **17**, 618-634, doi:10.1038/s41575-020-0296-6 (2020).
66 Quasdorff, M. & Protzer, U. Control of hepatitis B virus at the level of transcription. *J Viral Hepat* **17**, 527-536, doi:10.1111/j.1365-2893.2010.01315.x (2010).
67 Rall, L. B., Standring, D. N., Laub, O. & Rutter, W. J. Transcription of hepatitis B virus by RNA polymerase II. *Mol Cell Biol* **3**, 1766-1773, doi:10.1128/mcb.3.10.1766-1773.1983 (1983).
68 Stadelmayer, B. *et al.* Full-length 5'RACE identifies all major HBV transcripts in HBV-infected hepatocytes and patient serum. *J Hepatol* **73**, 40-51, doi:10.1016/j.jhep.2020.01.028 (2020).
69 Lim, C. S. *et al.* Quantitative analysis of the splice variants expressed by the major hepatitis B virus genotypes. *Microb Genom* **7**, doi:10.1099/mgen.0.000492 (2021).
70 Soussan, P. *et al.* The expression of hepatitis B spliced protein (HBSP) encoded by a spliced hepatitis B virus RNA is associated with viral replication and liver fibrosis. *J Hepatol* **38**, 343-348, doi:10.1016/s0168-8278(02)00422-1 (2003).
71 Chen, W. N., Chen, J. Y., Lin, W. S., Lin, J. Y. & Lin, X. Hepatitis B doubly spliced protein, generated by a 2.2 kb doubly spliced hepatitis B virus RNA, is a pleiotropic activator protein mediating its effects via activator protein-1- and CCAAT/enhancer-binding protein-binding sites. *J Gen Virol* **91**, 2592-2600, doi:10.1099/vir.0.022517-0 (2010).
72 Huang, H. L. *et al.* Identification and characterization of a structural protein of hepatitis B virus: a polymerase and surface fusion protein encoded by a spliced RNA. *Virology* **275**, 398-410, doi:10.1006/viro.2000.0478 (2000).
73 Leistner, C. M., Gruen-Bernhard, S. & Glebe, D. Role of glycosaminoglycans for binding and infection of hepatitis B virus. *Cell Microbiol* **10**, 122-133, doi:10.1111/j.1462-5822.2007.01023.x (2008).
74 Schulze, A., Gripon, P. & Urban, S. Hepatitis B virus infection initiates with a large surface protein-dependent binding to heparan sulfate proteoglycans. *Hepatology* **46**, 1759-1768, doi:10.1002/hep.21896 (2007).
75 Simon Davis, D. A. & Parish, C. R. Heparan sulfate: a ubiquitous glycosaminoglycan with multiple roles in immunity. *Front Immunol* **4**, 470, doi:10.3389/fimmu.2013.00470 (2013).
76 Sureau, C. & Salisse, J. A conformational heparan sulfate binding site essential to infectivity overlaps with the conserved hepatitis B virus a-determinant. *Hepatology* **57**, 985-994, doi:10.1002/hep.26125 (2013).
77 Verrier, E. R. *et al.* A targeted functional RNA interference screen uncovers glypican 5 as an entry factor for hepatitis B and D viruses. *Hepatology* **63**, 35-48, doi:10.1002/hep.28013 (2016).
78 Yan, H. *et al.* Sodium taurocholate cotransporting polypeptide is a functional receptor for human hepatitis B and D virus. *Elife* **1**, e00049, doi:10.7554/eLife.00049 (2012).
79 Ni, Y. *et al.* Hepatitis B and D viruses exploit sodium taurocholate co-transporting polypeptide for species-specific entry into hepatocytes. *Gastroenterology* **146**, 1070-1083, doi:10.1053/j.gastro.2013.12.024 (2014).
80 Xia, Y. *et al.* Human stem cell-derived hepatocytes as a model for hepatitis B virus infection, spreading and virus-host interactions. *J Hepatol* **66**, 494-503, doi:10.1016/j.jhep.2016.10.009 (2017).
81 Alrefai, W. A. & Gill, R. K. Bile acid transporters: structure, function, regulation and pathophysiological implications. *Pharm Res* **24**, 1803-1823, doi:10.1007/s11095-007-9289-1 (2007).

82 Hu, Q. *et al.* E-cadherin Plays a Role in Hepatitis B Virus Entry Through Affecting Glycosylated Sodium-Taurocholate Cotransporting Polypeptide Distribution. *Front Cell Infect Microbiol* **10**, 74, doi:10.3389/fcimb.2020.00074 (2020).
83 Schulze, A., Mills, K., Weiss, T. S. & Urban, S. Hepatocyte polarization is essential for the productive entry of the hepatitis B virus. *Hepatology* **55**, 373-383, doi:10.1002/hep.24707 (2012).
84 Iwamoto, M. *et al.* Epidermal growth factor receptor is a host-entry cofactor triggering hepatitis B virus internalization. *Proc Natl Acad Sci U S A* **116**, 8487-8492, doi:10.1073/pnas.1811064116 (2019).
85 Herrscher, C., Roingeard, P. & Blanchard, E. Hepatitis B Virus Entry into Cells. *Cells* **9**, doi:10.3390/cells9061486 (2020).
86 Macovei, A. *et al.* Hepatitis B virus requires intact caveolin-1 function for productive infection in HepaRG cells. *J Virol* **84**, 243-253, doi:10.1128/JVI.01207-09 (2010).
87 Chakraborty, A. *et al.* Synchronised infection identifies early rate-limiting steps in the hepatitis B virus life cycle. *Cell Microbiol* **22**, e13250, doi:10.1111/cmi.13250 (2020).
88 Herrscher, C. *et al.* Hepatitis B virus entry into HepG2-NTCP cells requires clathrin-mediated endocytosis. *Cell Microbiol* **22**, e13205, doi:10.1111/cmi.13205 (2020).
89 Huang, H. C., Chen, C. C., Chang, W. C., Tao, M. H. & Huang, C. Entry of hepatitis B virus into immortalized human primary hepatocytes by clathrin-dependent endocytosis. *J Virol* **86**, 9443-9453, doi:10.1128/JVI.00873-12 (2012).
90 Iwamoto, M. *et al.* The machinery for endocytosis of epidermal growth factor receptor coordinates the transport of incoming hepatitis B virus to the endosomal network. *J Biol Chem* **295**, 800-807, doi:10.1074/jbc.AC119.010366 (2020).
91 Sweitzer, S. M. & Hinshaw, J. E. Dynamin undergoes a GTP-dependent conformational change causing vesiculation. *Cell* **93**, 1021-1029, doi:10.1016/s0092-8674(00)81207-6 (1998).
92 Macovei, A., Petrareanu, C., Lazar, C., Florian, P. & Branza-Nichita, N. Regulation of hepatitis B virus infection by Rab5, Rab7, and the endolysosomal compartment. *J Virol* **87**, 6415-6427, doi:10.1128/JVI.00393-13 (2013).
93 Yoshimori, T., Yamamoto, A., Moriyama, Y., Futai, M. & Tashiro, Y. Bafilomycin A1, a specific inhibitor of vacuolar-type H(+)-ATPase, inhibits acidification and protein degradation in lysosomes of cultured cells. *J Biol Chem* **266**, 17707-17712 (1991).
94 Chojnacki, J., Anderson, D. A. & Grgacic, E. V. A hydrophobic domain in the large envelope protein is essential for fusion of duck hepatitis B virus at the late endosome. *J Virol* **79**, 14945-14955, doi:10.1128/JVI.79.23.14945-14955.2005 (2005).
95 Watashi, K. *et al.* Cyclosporin A and its analogs inhibit hepatitis B virus entry into cultured hepatocytes through targeting a membrane transporter, sodium taurocholate cotransporting polypeptide (NTCP). *Hepatology* **59**, 1726-1737, doi:10.1002/hep.26982 (2014).
96 White, J. M. & Whittaker, G. R. Fusion of Enveloped Viruses in Endosomes. *Traffic* **17**, 593-614, doi:10.1111/tra.12389 (2016).
97 Funk, A., Mhamdi, M., Hohenberg, H., Will, H. & Sirma, H. pH-independent entry and sequential endosomal sorting are major determinants of hepadnaviral infection in primary hepatocytes. *Hepatology* **44**, 685-693, doi:10.1002/hep.21297 (2006).
98 Rigg, R. J. & Schaller, H. Duck hepatitis B virus infection of hepatocytes is not dependent on low pH. *J Virol* **66**, 2829-2836, doi:10.1128/JVI.66.5.2829-2836.1992 (1992).
99 Rodriguez-Crespo, I., Gomez-Gutierrez, J., Nieto, M., Peterson, D. L. & Gavilanes, F. Prediction of a putative fusion peptide in the S protein of hepatitis B virus. *J Gen Virol* **75 (Pt 3)**, 637-639, doi:10.1099/0022-1317-75-3-637 (1994).
100 Delgado, C. L. *et al.* Study of the putative fusion regions of the preS domain of hepatitis B virus. *Biochim Biophys Acta* **1848**, 895-906, doi:10.1016/j.bbamem.2014.12.020 (2015).
101 Somiya, M. *et al.* Intracellular trafficking of bio-nanocapsule-liposome complex: Identification of fusogenic activity in the pre-S1 region of hepatitis B virus surface antigen L protein. *J Control Release* **212**, 10-18, doi:10.1016/j.jconrel.2015.06.012 (2015).

102 Scott, C. C. & Gruenberg, J. Ion flux and the function of endosomes and lysosomes: pH is just the start: the flux of ions across endosomal membranes influences endosome function not only through regulation of the luminal pH. *Bioessays* **33**, 103-110, doi:10.1002/bies.201000108 (2011).
103 Gallucci, L. & Kann, M. Nuclear Import of Hepatitis B Virus Capsids and Genome. *Viruses* **9**, doi:10.3390/v9010021 (2017).
104 Osseman, Q. *et al.* The chaperone dynein LL1 mediates cytoplasmic transport of empty and mature hepatitis B virus capsids. *J Hepatol* **68**, 441-448, doi:10.1016/j.jhep.2017.10.032 (2018).
105 Rabe, B., Glebe, D. & Kann, M. Lipid-mediated introduction of hepatitis B virus capsids into nonsusceptible cells allows highly efficient replication and facilitates the study of early infection events. *J Virol* **80**, 5465-5473, doi:10.1128/JVI.02303-05 (2006).
106 Kann, M., Sodeik, B., Vlachou, A., Gerlich, W. H. & Helenius, A. Phosphorylation-dependent binding of hepatitis B virus core particles to the nuclear pore complex. *J Cell Biol* **145**, 45-55, doi:10.1083/jcb.145.1.45 (1999).
107 Chen, C. *et al.* Importin beta Can Bind Hepatitis B Virus Core Protein and Empty Core-Like Particles and Induce Structural Changes. *PLoS Pathog* **12**, e1005802, doi:10.1371/journal.ppat.1005802 (2016).
108 Rabe, B., Vlachou, A., Pante, N., Helenius, A. & Kann, M. Nuclear import of hepatitis B virus capsids and release of the viral genome. *Proc Natl Acad Sci U S A* **100**, 9849-9854, doi:10.1073/pnas.1730940100 (2003).
109 Selzer, L., Kant, R., Wang, J. C., Bothner, B. & Zlotnick, A. Hepatitis B Virus Core Protein Phosphorylation Sites Affect Capsid Stability and Transient Exposure of the C-terminal Domain. *J Biol Chem* **290**, 28584-28593, doi:10.1074/jbc.M115.678441 (2015).
110 Schmitz, A. *et al.* Nucleoporin 153 arrests the nuclear import of hepatitis B virus capsids in the nuclear basket. *PLoS Pathog* **6**, e1000741, doi:10.1371/journal.ppat.1000741 (2010).
111 Kock, J. & Schlicht, H. J. Analysis of the earliest steps of hepadnavirus replication: genome repair after infectious entry into hepatocytes does not depend on viral polymerase activity. *J Virol* **67**, 4867-4874, doi:10.1128/JVI.67.8.4867-4874.1993 (1993).
112 Moraleda, G. *et al.* Lack of effect of antiviral therapy in nondividing hepatocyte cultures on the closed circular DNA of woodchuck hepatitis virus. *J Virol* **71**, 9392-9399, doi:10.1128/JVI.71.12.9392-9399.1997 (1997).
113 Cui, X. *et al.* Does Tyrosyl DNA Phosphodiesterase-2 Play a Role in Hepatitis B Virus Genome Repair? *PLoS One* **10**, e0128401, doi:10.1371/journal.pone.0128401 (2015).
114 Koniger, C. *et al.* Involvement of the host DNA-repair enzyme TDP2 in formation of the covalently closed circular DNA persistence reservoir of hepatitis B viruses. *Proc Natl Acad Sci U S A* **111**, E4244-4253, doi:10.1073/pnas.1409986111 (2014).
115 Kitamura, K. *et al.* Flap endonuclease 1 is involved in cccDNA formation in the hepatitis B virus. *PLoS Pathog* **14**, e1007124, doi:10.1371/journal.ppat.1007124 (2018).
116 Sheraz, M., Cheng, J., Tang, L., Chang, J. & Guo, J. T. Cellular DNA Topoisomerases Are Required for the Synthesis of Hepatitis B Virus Covalently Closed Circular DNA. *J Virol* **93**, doi:10.1128/JVI.02230-18 (2019).
117 Wei, L. & Ploss, A. Hepatitis B virus cccDNA is formed through distinct repair processes of each strand. *Nat Commun* **12**, 1591, doi:10.1038/s41467-021-21850-9 (2021).
118 Bock, C. T., Schranz, P., Schroder, C. H. & Zentgraf, H. Hepatitis B virus genome is organized into nucleosomes in the nucleus of the infected cell. *Virus Genes* **8**, 215-229, doi:10.1007/BF01703079 (1994).
119 Bock, C. T. *et al.* Structural organization of the hepatitis B virus minichromosome. *J Mol Biol* **307**, 183-196, doi:10.1006/jmbi.2000.4481 (2001).
120 Chu, C. M., Yeh, C. T., Chien, R. N., Sheen, I. S. & Liaw, Y. F. The degrees of hepatocyte nuclear but not cytoplasmic expression of hepatitis B core antigen reflect the level of viral replication in chronic hepatitis B virus infection. *J Clin Microbiol* **35**, 102-105, doi:10.1128/jcm.35.1.102-105.1997 (1997).

121 Liu, C. J. *et al.* Hepatitis B virus basal core promoter mutation and DNA load correlate with expression of hepatitis B core antigen in patients with chronic hepatitis B. *J Infect Dis* **199**, 742-749, doi:10.1086/596655 (2009).
122 Tropberger, P. *et al.* Mapping of histone modifications in episomal HBV cccDNA uncovers an unusual chromatin organization amenable to epigenetic manipulation. *Proc Natl Acad Sci U S A* **112**, E5715-5724, doi:10.1073/pnas.1518090112 (2015).
123 Pollicino, T. *et al.* Hepatitis B virus replication is regulated by the acetylation status of hepatitis B virus cccDNA-bound H3 and H4 histones. *Gastroenterology* **130**, 823-837, doi:10.1053/j.gastro.2006.01.001 (2006).
124 Belloni, L. *et al.* Nuclear HBx binds the HBV minichromosome and modifies the epigenetic regulation of cccDNA function. *Proc Natl Acad Sci U S A* **106**, 19975-19979, doi:10.1073/pnas.0908365106 (2009).
125 Belloni, L. *et al.* IFN-alpha inhibits HBV transcription and replication in cell culture and in humanized mice by targeting the epigenetic regulation of the nuclear cccDNA minichromosome. *J Clin Invest* **122**, 529-537, doi:10.1172/JCI58847 (2012).
126 Zhang, W. *et al.* PRMT5 restricts hepatitis B virus replication through epigenetic repression of covalently closed circular DNA transcription and interference with pregenomic RNA encapsidation. *Hepatology* **66**, 398-415, doi:10.1002/hep.29133 (2017).
127 Benhenda, S. *et al.* Methyltransferase PRMT1 is a binding partner of HBx and a negative regulator of hepatitis B virus transcription. *J Virol* **87**, 4360-4371, doi:10.1128/JVI.02574-12 (2013).
128 Riviere, L. *et al.* HBx relieves chromatin-mediated transcriptional repression of hepatitis B viral cccDNA involving SETDB1 histone methyltransferase. *J Hepatol* **63**, 1093-1102, doi:10.1016/j.jhep.2015.06.023 (2015).
129 Decorsiere, A. *et al.* Hepatitis B virus X protein identifies the Smc5/6 complex as a host restriction factor. *Nature* **531**, 386-389, doi:10.1038/nature17170 (2016).
130 Murphy, C. M. *et al.* Hepatitis B Virus X Protein Promotes Degradation of SMC5/6 to Enhance HBV Replication. *Cell Rep* **16**, 2846-2854, doi:10.1016/j.celrep.2016.08.026 (2016).
131 Niu, C. *et al.* The Smc5/6 Complex Restricts HBV when Localized to ND10 without Inducing an Innate Immune Response and Is Counteracted by the HBV X Protein Shortly after Infection. *PLoS One* **12**, e0169648, doi:10.1371/journal.pone.0169648 (2017).
132 Greenberg, M. V. C. & Bourc'his, D. The diverse roles of DNA methylation in mammalian development and disease. *Nat Rev Mol Cell Biol* **20**, 590-607, doi:10.1038/s41580-019-0159-6 (2019).
133 Vivekanandan, P., Thomas, D. & Torbenson, M. Hepatitis B viral DNA is methylated in liver tissues. *J Viral Hepat* **15**, 103-107, doi:10.1111/j.1365-2893.2007.00905.x (2008).
134 Zhang, Y. *et al.* Comparative analysis of CpG islands among HBV genotypes. *PLoS One* **8**, e56711, doi:10.1371/journal.pone.0056711 (2013).
135 Zhang, Y. *et al.* Transcription of hepatitis B virus covalently closed circular DNA is regulated by CpG methylation during chronic infection. *PLoS One* **9**, e110442, doi:10.1371/journal.pone.0110442 (2014).
136 Vivekanandan, P., Daniel, H. D., Kannangai, R., Martinez-Murillo, F. & Torbenson, M. Hepatitis B virus replication induces methylation of both host and viral DNA. *J Virol* **84**, 4321-4329, doi:10.1128/JVI.02280-09 (2010).
137 Dandri, M. Epigenetic modulation in chronic hepatitis B virus infection. *Semin Immunopathol* **42**, 173-185, doi:10.1007/s00281-020-00780-6 (2020).
138 Okamoto, Y. *et al.* Hepatitis virus infection affects DNA methylation in mice with humanized livers. *Gastroenterology* **146**, 562-572, doi:10.1053/j.gastro.2013.10.056 (2014).
139 Turton, K. L., Meier-Stephenson, V., Badmalia, M. D., Coffin, C. S. & Patel, T. R. Host Transcription Factors in Hepatitis B Virus RNA Synthesis. *Viruses* **12**, doi:10.3390/v12020160 (2020).

140 Li, J., Xu, Z., Zheng, Y., Johnson, D. L. & Ou, J. H. Regulation of hepatocyte nuclear factor 1 activity by wild-type and mutant hepatitis B virus X proteins. *J Virol* **76**, 5875-5881, doi:10.1128/jvi.76.12.5875-5881.2002 (2002).
141 Zheng, Y., Li, J. & Ou, J. H. Regulation of hepatitis B virus core promoter by transcription factors HNF1 and HNF4 and the viral X protein. *J Virol* **78**, 6908-6914, doi:10.1128/JVI.78.13.6908-6914.2004 (2004).
142 Chen, M., Hieng, S., Qian, X., Costa, R. & Ou, J. H. Regulation of hepatitis B virus ENI enhancer activity by hepatocyte-enriched transcription factor HNF3. *Virology* **205**, 127-132, doi:10.1006/viro.1994.1627 (1994).
143 Li, M., Xie, Y., Wu, X., Kong, Y. & Wang, Y. HNF3 binds and activates the second enhancer, ENII, of hepatitis B virus. *Virology* **214**, 371-378, doi:10.1006/viro.1995.0046 (1995).
144 Raney, A. K., Zhang, P. & McLachlan, A. Regulation of transcription from the hepatitis B virus large surface antigen promoter by hepatocyte nuclear factor 3. *J Virol* **69**, 3265-3272, doi:10.1128/JVI.69.6.3265-3272.1995 (1995).
145 He, F. *et al.* Inhibition of hepatitis B Virus replication by hepatocyte nuclear factor 4-alpha specific short hairpin RNA. *Liver Int* **32**, 742-751, doi:10.1111/j.1478-3231.2011.02748.x (2012).
146 Long, Y. *et al.* The correlation of hepatocyte nuclear factor 4 alpha and 3 beta with hepatitis B virus replication in the liver of chronic hepatitis B patients. *J Viral Hepat* **16**, 537-546, doi:10.1111/j.1365-2893.2009.01089.x (2009).
147 Mouzannar, K. *et al.* Farnesoid X receptor-alpha is a proviral host factor for hepatitis B virus that is inhibited by ligands in vitro and in vivo. *FASEB J* **33**, 2472-2483, doi:10.1096/fj.201801181R (2019).
148 Ramiere, C. *et al.* Transactivation of the hepatitis B virus core promoter by the nuclear receptor FXRalpha. *J Virol* **82**, 10832-10840, doi:10.1128/JVI.00883-08 (2008).
149 Curtil, C. *et al.* The metabolic sensors FXRalpha, PGC-1alpha, and SIRT1 cooperatively regulate hepatitis B virus transcription. *FASEB J* **28**, 1454-1463, doi:10.1096/fj.13-236372 (2014).
150 Huan, B., Kosovsky, M. J. & Siddiqui, A. Retinoid X receptor alpha transactivates the hepatitis B virus enhancer 1 element by forming a heterodimeric complex with the peroxisome proliferator-activated receptor. *J Virol* **69**, 547-551, doi:10.1128/JVI.69.1.547-551.1995 (1995).
151 Tang, H., Raney, A. K. & McLachlan, A. Replication of the wild type and a natural hepatitis B virus nucleocapsid promoter variant is differentially regulated by nuclear hormone receptors in cell culture. *J Virol* **75**, 8937-8948, doi:10.1128/JVI.75.19.8937-8948.2001 (2001).
152 Garcia, A. D., Ostapchuk, P. & Hearing, P. Functional interaction of nuclear factors EF-C, HNF-4, and RXR alpha with hepatitis B virus enhancer I. *J Virol* **67**, 3940-3950, doi:10.1128/JVI.67.7.3940-3950.1993 (1993).
153 Song, M. *et al.* Silencing Retinoid X Receptor Alpha Expression Enhances Early-Stage Hepatitis B Virus Infection In Cell Cultures. *J Virol* **92**, doi:10.1128/JVI.01771-17 (2018).
154 Dubuquoy, L., Louvet, A., Hollebecque, A., Mathurin, P. & Dharancy, S. Peroxisome proliferator-activated receptors in HBV-related infection. *PPAR Res* **2009**, 145124, doi:10.1155/2009/145124 (2009).
155 Raney, A. K., Kline, E. F., Tang, H. & McLachlan, A. Transcription and replication of a natural hepatitis B virus nucleocapsid promoter variant is regulated in vivo by peroxisome proliferators. *Virology* **289**, 239-251, doi:10.1006/viro.2001.1169 (2001).
156 Lu, C. C. & Yen, T. S. Activation of the hepatitis B virus S promoter by transcription factor NF-Y via a CCAAT element. *Virology* **225**, 387-394, doi:10.1006/viro.1996.0613 (1996).
157 Lin, Y. C., Hsu, E. C. & Ting, L. P. Repression of hepatitis B viral gene expression by transcription factor nuclear factor-kappaB. *Cell Microbiol* **11**, 645-660, doi:10.1111/j.1462-5822.2008.01280.x (2009).
158 Li, J. & Ou, J. H. Differential regulation of hepatitis B virus gene expression by the Sp1 transcription factor. *J Virol* **75**, 8400-8406, doi:10.1128/jvi.75.18.8400-8406.2001 (2001).
159 He, Q. *et al.* ZEB2 inhibits HBV transcription and replication by targeting its core promoter. *Oncotarget* **7**, 16003-16011, doi:10.18632/oncotarget.7435 (2016).

160 Lee, H., Kim, H. T. & Yun, Y. Liver-specific enhancer II is the target for the p53-mediated inhibition of hepatitis B viral gene expression. *J Biol Chem* **273**, 19786-19791, doi:10.1074/jbc.273.31.19786 (1998).
161 Ori, A. *et al.* p53 binds and represses the HBV enhancer: an adjacent enhancer element can reverse the transcription effect of p53. *EMBO J* **17**, 544-553, doi:10.1093/emboj/17.2.544 (1998).
162 Lopez-Cabrera, M., Letovsky, J., Hu, K. Q. & Siddiqui, A. Multiple liver-specific factors bind to the hepatitis B virus core/pregenomic promoter: trans-activation and repression by CCAAT/enhancer binding protein. *Proc Natl Acad Sci U S A* **87**, 5069-5073, doi:10.1073/pnas.87.13.5069 (1990).
163 Choi, B. H., Park, G. T. & Rho, H. M. Interaction of hepatitis B viral X protein and CCAAT/ enhancer-binding protein alpha synergistically activates the hepatitis B viral enhancer II/pregenomic promoter. *J Biol Chem* **274**, 2858-2865, doi:10.1074/jbc.274.5.2858 (1999).
164 Yu, X. & Mertz, J. E. Distinct modes of regulation of transcription of hepatitis B virus by the nuclear receptors HNF4alpha and COUP-TF1. *J Virol* **77**, 2489-2499, doi:10.1128/jvi.77.4.2489-2499.2003 (2003).
165 Kim, B. K., Lim, S. O. & Park, Y. G. Requirement of the cyclic adenosine monophosphate response element-binding protein for hepatitis B virus replication. *Hepatology* **48**, 361-373, doi:10.1002/hep.22359 (2008).
166 Bogomolski-Yahalom, V., Klein, A., Greenblat, I., Haviv, Y. & Tur-Kaspa, R. The TATA-less promoter of hepatitis B virus S gene contains a TBP binding site and an active initiator. *Virus Res* **49**, 1-7, doi:10.1016/s0168-1702(96)01429-3 (1997).
167 Lauer, U., Weiss, L., Lipp, M., Hofschneider, P. H. & Kekule, A. S. The hepatitis B virus preS2/St transactivator utilizes AP-1 and other transcription factors for transactivation. *Hepatology* **19**, 23-31 (1994).
168 Kim, H. S., Ryu, C. J. & Hong, H. J. Hepatitis B virus preS1 functions as a transcriptional activation domain. *J Gen Virol* **78 (Pt 5)**, 1083-1086, doi:10.1099/0022-1317-78-5-1083 (1997).
169 Yang, Y. *et al.* Targeting blockage of STAT3 inhibits hepatitis B virus-related hepatocellular carcinoma. *Cancer Biol Ther* **17**, 449-456, doi:10.1080/15384047.2016.1156257 (2016).
170 Nakanishi-Matsui, M., Hayashi, Y., Kitamura, Y. & Koike, K. Integrated hepatitis B virus DNA preserves the binding sequence of transcription factor Yin and Yang 1 at the virus-cell junction. *J Virol* **74**, 5562-5568, doi:10.1128/jvi.74.12.5562-5568.2000 (2000).
171 Radziwill, G., Tucker, W. & Schaller, H. Mutational analysis of the hepatitis B virus P gene product: domain structure and RNase H activity. *J Virol* **64**, 613-620, doi:10.1128/JVI.64.2.613-620.1990 (1990).
172 Imam, H. *et al.* N6-methyladenosine modification of hepatitis B virus RNA differentially regulates the viral life cycle. *Proc Natl Acad Sci U S A* **115**, 8829-8834, doi:10.1073/pnas.1808319115 (2018).
173 Beck, J., Seitz, S., Lauber, C. & Nassal, M. Conservation of the HBV RNA element epsilon in nackednaviruses reveals ancient origin of protein-primed reverse transcription. *Proc Natl Acad Sci U S A* **118**, doi:10.1073/pnas.2022373118 (2021).
174 Jones, S. A., Boregowda, R., Spratt, T. E. & Hu, J. In vitro epsilon RNA-dependent protein priming activity of human hepatitis B virus polymerase. *J Virol* **86**, 5134-5150, doi:10.1128/JVI.07137-11 (2012).
175 Bartenschlager, R. & Schaller, H. Hepadnaviral assembly is initiated by polymerase binding to the encapsidation signal in the viral RNA genome. *EMBO J* **11**, 3413-3420 (1992).
176 Bartenschlager, R., Junker-Niepmann, M. & Schaller, H. The P gene product of hepatitis B virus is required as a structural component for genomic RNA encapsidation. *J Virol* **64**, 5324-5332, doi:10.1128/JVI.64.11.5324-5332.1990 (1990).
177 Jeong, J. K., Yoon, G. S. & Ryu, W. S. Evidence that the 5'-end cap structure is essential for encapsidation of hepatitis B virus pregenomic RNA. *J Virol* **74**, 5502-5508, doi:10.1128/jvi.74.12.5502-5508.2000 (2000).

178 Junker-Niepmann, M., Bartenschlager, R. & Schaller, H. A short cis-acting sequence is required for hepatitis B virus pregenome encapsidation and sufficient for packaging of foreign RNA. *EMBO J* **9**, 3389-3396 (1990).
179 Wang, G. H. & Seeger, C. The reverse transcriptase of hepatitis B virus acts as a protein primer for viral DNA synthesis. *Cell* **71**, 663-670, doi:10.1016/0092-8674(92)90599-8 (1992).
180 Zoulim, F. & Seeger, C. Reverse transcription in hepatitis B viruses is primed by a tyrosine residue of the polymerase. *J Virol* **68**, 6-13, doi:10.1128/JVI.68.1.6-13.1994 (1994).
181 Lanford, R. E., Notvall, L., Lee, H. & Beames, B. Transcomplementation of nucleotide priming and reverse transcription between independently expressed TP and RT domains of the hepatitis B virus reverse transcriptase. *J Virol* **71**, 2996-3004, doi:10.1128/JVI.71.4.2996-3004.1997 (1997).
182 Nassal, M. & Rieger, A. A bulged region of the hepatitis B virus RNA encapsidation signal contains the replication origin for discontinuous first-strand DNA synthesis. *J Virol* **70**, 2764-2773, doi:10.1128/JVI.70.5.2764-2773.1996 (1996).
183 Chen, Y. & Marion, P. L. Amino acids essential for RNase H activity of hepadnaviruses are also required for efficient elongation of minus-strand viral DNA. *J Virol* **70**, 6151-6156, doi:10.1128/JVI.70.9.6151-6156.1996 (1996).
184 Will, H. *et al.* Replication strategy of human hepatitis B virus. *J Virol* **61**, 904-911, doi:10.1128/JVI.61.3.904-911.1987 (1987).
185 Yu, M. & Summers, J. A domain of the hepadnavirus capsid protein is specifically required for DNA maturation and virus assembly. *J Virol* **65**, 2511-2517, doi:10.1128/JVI.65.5.2511-2517.1991 (1991).
186 Basagoudanavar, S. H., Perlman, D. H. & Hu, J. Regulation of hepadnavirus reverse transcription by dynamic nucleocapsid phosphorylation. *J Virol* **81**, 1641-1649, doi:10.1128/JVI.01671-06 (2007).
187 Kaplan, P. M., Greenman, R. L., Gerin, J. L., Purcell, R. H. & Robinson, W. S. DNA polymerase associated with human hepatitis B antigen. *J Virol* **12**, 995-1005, doi:10.1128/JVI.12.5.995-1005.1973 (1973).
188 Summers, J., O'Connell, A. & Millman, I. Genome of hepatitis B virus: restriction enzyme cleavage and structure of DNA extracted from Dane particles. *Proc Natl Acad Sci U S A* **72**, 4597-4601, doi:10.1073/pnas.72.11.4597 (1975).
189 Hu, J. & Seeger, C. Hsp90 is required for the activity of a hepatitis B virus reverse transcriptase. *Proc Natl Acad Sci U S A* **93**, 1060-1064, doi:10.1073/pnas.93.3.1060 (1996).
190 Hu, J., Toft, D. O. & Seeger, C. Hepadnavirus assembly and reverse transcription require a multi-component chaperone complex which is incorporated into nucleocapsids. *EMBO J* **16**, 59-68, doi:10.1093/emboj/16.1.59 (1997).
191 Stahl, M., Retzlaff, M., Nassal, M. & Beck, J. Chaperone activation of the hepadnaviral reverse transcriptase for template RNA binding is established by the Hsp70 and stimulated by the Hsp90 system. *Nucleic Acids Res* **35**, 6124-6136, doi:10.1093/nar/gkm628 (2007).
192 Wang, X., Qian, X., Guo, H. C. & Hu, J. Heat shock protein 90-independent activation of truncated hepadnavirus reverse transcriptase. *J Virol* **77**, 4471-4480, doi:10.1128/jvi.77.8.4471-4480.2003 (2003).
193 Hong, X. *et al.* Characterization of Hepatitis B Precore/Core-Related Antigens. *J Virol* **95**, doi:10.1128/JVI.01695-20 (2021).
194 Possehl, C. *et al.* Absence of free core antigen in anti-HBc negative viremic hepatitis B carriers. *Arch Virol Suppl* **4**, 39-41, doi:10.1007/978-3-7091-5633-9_8 (1992).
195 Summers, J., Smith, P. M., Huang, M. J. & Yu, M. S. Morphogenetic and regulatory effects of mutations in the envelope proteins of an avian hepadnavirus. *J Virol* **65**, 1310-1317, doi:10.1128/JVI.65.3.1310-1317.1991 (1991).
196 Zhang, Y. Y. *et al.* Single-cell analysis of covalently closed circular DNA copy numbers in a hepadnavirus-infected liver. *Proc Natl Acad Sci U S A* **100**, 12372-12377, doi:10.1073/pnas.2033898100 (2003).

197 Lentz, T. B. & Loeb, D. D. Roles of the envelope proteins in the amplification of covalently closed circular DNA and completion of synthesis of the plus-strand DNA in hepatitis B virus. *J Virol* **85**, 11916-11927, doi:10.1128/JVI.05373-11 (2011).
198 Ling, R. & Harrison, T. J. Production of hepatitis B virus covalently closed circular DNA in transfected cells is independent of surface antigen synthesis. *J Gen Virol* **78 (Pt 6)**, 1463-1467, doi:10.1099/0022-1317-78-6-1463 (1997).
199 Gerelsaikhan, T., Tavis, J. E. & Bruss, V. Hepatitis B virus nucleocapsid envelopment does not occur without genomic DNA synthesis. *J Virol* **70**, 4269-4274, doi:10.1128/JVI.70.7.4269-4274.1996 (1996).
200 Ning, X. *et al.* Secretion of genome-free hepatitis B virus--single strand blocking model for virion morphogenesis of para-retrovirus. *PLoS Pathog* **7**, e1002255, doi:10.1371/journal.ppat.1002255 (2011).
201 Hu, J. & Liu, K. Complete and Incomplete Hepatitis B Virus Particles: Formation, Function, and Application. *Viruses* **9**, doi:10.3390/v9030056 (2017).
202 Seitz, S., Habjanic, J., Schutz, A. K. & Bartenschlager, R. The Hepatitis B Virus Envelope Proteins: Molecular Gymnastics Throughout the Viral Life Cycle. *Annu Rev Virol* **7**, 263-288, doi:10.1146/annurev-virology-092818-015508 (2020).
203 Ponsel, D. & Bruss, V. Mapping of amino acid side chains on the surface of hepatitis B virus capsids required for envelopment and virion formation. *J Virol* **77**, 416-422, doi:10.1128/jvi.77.1.416-422.2003 (2003).
204 Roseman, A. M., Berriman, J. A., Wynne, S. A., Butler, P. J. & Crowther, R. A. A structural model for maturation of the hepatitis B virus core. *Proc Natl Acad Sci U S A* **102**, 15821-15826, doi:10.1073/pnas.0504874102 (2005).
205 Bruss, V. & Ganem, D. The role of envelope proteins in hepatitis B virus assembly. *Proc Natl Acad Sci U S A* **88**, 1059-1063, doi:10.1073/pnas.88.3.1059 (1991).
206 Eble, B. E., MacRae, D. R., Lingappa, V. R. & Ganem, D. Multiple topogenic sequences determine the transmembrane orientation of the hepatitis B surface antigen. *Mol Cell Biol* **7**, 3591-3601, doi:10.1128/mcb.7.10.3591-3601.1987 (1987).
207 Ostapchuk, P., Hearing, P. & Ganem, D. A dramatic shift in the transmembrane topology of a viral envelope glycoprotein accompanies hepatitis B viral morphogenesis. *EMBO J* **13**, 1048-1057 (1994).
208 Bruss, V., Lu, X., Thomssen, R. & Gerlich, W. H. Post-translational alterations in transmembrane topology of the hepatitis B virus large envelope protein. *EMBO J* **13**, 2273-2279 (1994).
209 Prange, R. & Streeck, R. E. Novel transmembrane topology of the hepatitis B virus envelope proteins. *EMBO J* **14**, 247-256 (1995).
210 Bruss, V. A short linear sequence in the pre-S domain of the large hepatitis B virus envelope protein required for virion formation. *J Virol* **71**, 9350-9357, doi:10.1128/JVI.71.12.9350-9357.1997 (1997).
211 Pastor, F. *et al.* Direct interaction between the hepatitis B virus core and envelope proteins analyzed in a cellular context. *Sci Rep* **9**, 16178, doi:10.1038/s41598-019-52824-z (2019).
212 Loffler-Mary, H., Werr, M. & Prange, R. Sequence-specific repression of cotranslational translocation of the hepatitis B virus envelope proteins coincides with binding of heat shock protein Hsc70. *Virology* **235**, 144-152, doi:10.1006/viro.1997.8689 (1997).
213 Prange, R., Werr, M. & Loffler-Mary, H. Chaperones involved in hepatitis B virus morphogenesis. *Biol Chem* **380**, 305-314, doi:10.1515/BC.1999.042 (1999).
214 Lambert, C. & Prange, R. Chaperone action in the posttranslational topological reorientation of the hepatitis B virus large envelope protein: Implications for translocational regulation. *Proc Natl Acad Sci U S A* **100**, 5199-5204, doi:10.1073/pnas.0930813100 (2003).
215 Loffler-Mary, H., Dumortier, J., Klentsch-Zimmer, C. & Prange, R. Hepatitis B virus assembly is sensitive to changes in the cytosolic S loop of the envelope proteins. *Virology* **270**, 358-367, doi:10.1006/viro.2000.0268 (2000).

216 Le Seyec, J., Chouteau, P., Cannie, I., Guguen-Guillouzo, C. & Gripon, P. Infection process of the hepatitis B virus depends on the presence of a defined sequence in the pre-S1 domain. *J Virol* **73**, 2052-2057, doi:10.1128/JVI.73.3.2052-2057.1999 (1999).
217 Gripon, P., Le Seyec, J., Rumin, S. & Guguen-Guillouzo, C. Myristylation of the hepatitis B virus large surface protein is essential for viral infectivity. *Virology* **213**, 292-299, doi:10.1006/viro.1995.0002 (1995).
218 Bruss, V., Hagelstein, J., Gerhardt, E. & Galle, P. R. Myristylation of the large surface protein is required for hepatitis B virus in vitro infectivity. *Virology* **218**, 396-399, doi:10.1006/viro.1996.0209 (1996).
219 Schulze, A., Schieck, A., Ni, Y., Mier, W. & Urban, S. Fine mapping of pre-S sequence requirements for hepatitis B virus large envelope protein-mediated receptor interaction. *J Virol* **84**, 1989-2000, doi:10.1128/JVI.01902-09 (2010).
220 Drexler, J. F. *et al.* Bats carry pathogenic hepadnaviruses antigenically related to hepatitis B virus and capable of infecting human hepatocytes. *Proc Natl Acad Sci U S A* **110**, 16151-16156, doi:10.1073/pnas.1308049110 (2013).
221 Bruss, V. Hepatitis B virus morphogenesis. *World J Gastroenterol* **13**, 65-73, doi:10.3748/wjg.v13.i1.65 (2007).
222 Seeger, C. & Mason, W. S. Hepatitis B virus biology. *Microbiol Mol Biol Rev* **64**, 51-68, doi:10.1128/MMBR.64.1.51-68.2000 (2000).
223 Heermann, K. H. *et al.* Large surface proteins of hepatitis B virus containing the pre-s sequence. *J Virol* **52**, 396-402, doi:10.1128/JVI.52.2.396-402.1984 (1984).
224 McAleer, W. J. *et al.* Human hepatitis B vaccine from recombinant yeast. *Nature* **307**, 178-180, doi:10.1038/307178a0 (1984).
225 Gilbert, R. J. *et al.* Hepatitis B small surface antigen particles are octahedral. *Proc Natl Acad Sci U S A* **102**, 14783-14788, doi:10.1073/pnas.0505062102 (2005).
226 Gavilanes, F., Gonzalez-Ros, J. M. & Peterson, D. L. Structure of hepatitis B surface antigen. Characterization of the lipid components and their association with the viral proteins. *J Biol Chem* **257**, 7770-7777 (1982).
227 Cao, J. *et al.* Cryo-EM structure of native spherical subviral particles isolated from HBV carriers. *Virus Res* **259**, 90-96, doi:10.1016/j.virusres.2018.10.015 (2019).
228 Satoh, O., Umeda, M., Imai, H., Tunoo, H. & Inoue, K. Lipid composition of hepatitis B virus surface antigen particles and the particle-producing human hepatoma cell lines. *J Lipid Res* **31**, 1293-1300 (1990).
229 Satoh, O. *et al.* Membrane structure of the hepatitis B virus surface antigen particle. *J Biochem* **127**, 543-550, doi:10.1093/oxfordjournals.jbchem.a022639 (2000).
230 Wounderlich, G. & Bruss, V. Characterization of early hepatitis B virus surface protein oligomers. *Arch Virol* **141**, 1191-1205, doi:10.1007/BF01718824 (1996).
231 Huovila, A. P., Eder, A. M. & Fuller, S. D. Hepatitis B surface antigen assembles in a post-ER, pre-Golgi compartment. *J Cell Biol* **118**, 1305-1320, doi:10.1083/jcb.118.6.1305 (1992).
232 Zeyen, L., Doring, T., Stieler, J. T. & Prange, R. Hepatitis B subviral envelope particles use the COPII machinery for intracellular transport via selective exploitation of Sec24A and Sec23B. *Cell Microbiol* **22**, e13181, doi:10.1111/cmi.13181 (2020).
233 Yang, S. *et al.* A putative amphipathic alpha helix in hepatitis B virus small envelope protein plays a critical role in the morphogenesis of subviral particles. *J Virol*, doi:10.1128/JVI.02399-20 (2021).
234 Patient, R. *et al.* Hepatitis B virus subviral envelope particle morphogenesis and intracellular trafficking. *J Virol* **81**, 3842-3851, doi:10.1128/JVI.02741-06 (2007).
235 Patient, R., Hourioux, C. & Roingeard, P. Morphogenesis of hepatitis B virus and its subviral envelope particles. *Cell Microbiol* **11**, 1561-1570, doi:10.1111/j.1462-5822.2009.01363.x (2009).
236 Peterson, D. L. Isolation and characterization of the major protein and glycoprotein of hepatitis B surface antigen. *J Biol Chem* **256**, 6975-6983 (1981).

237 Peterson, D. L., Nath, N. & Gavilanes, F. Structure of hepatitis B surface antigen. Correlation of subtype with amino acid sequence and location of the carbohydrate moiety. *J Biol Chem* **257**, 10414-10420 (1982).
238 Mangold, C. M., Unckell, F., Werr, M. & Streeck, R. E. Analysis of intermolecular disulfide bonds and free sulfhydryl groups in hepatitis B surface antigen particles. *Arch Virol* **142**, 2257-2267, doi:10.1007/s007050050240 (1997).
239 Stibbe, W. & Gerlich, W. H. Structural relationships between minor and major proteins of hepatitis B surface antigen. *J Virol* **46**, 626-628, doi:10.1128/JVI.46.2.626-628.1983 (1983).
240 Schmitt, S. *et al.* Structure of pre-S2 N- and O-linked glycans in surface proteins from different genotypes of hepatitis B virus. *J Gen Virol* **85**, 2045-2053, doi:10.1099/vir.0.79932-0 (2004).
241 Ito, K. *et al.* Impairment of hepatitis B virus virion secretion by single-amino-acid substitutions in the small envelope protein and rescue by a novel glycosylation site. *J Virol* **84**, 12850-12861, doi:10.1128/JVI.01499-10 (2010).
242 Julithe, R., Abou-Jaoude, G. & Sureau, C. Modification of the hepatitis B virus envelope protein glycosylation pattern interferes with secretion of viral particles, infectivity, and susceptibility to neutralizing antibodies. *J Virol* **88**, 9049-9059, doi:10.1128/JVI.01161-14 (2014).
243 Block, T. M. *et al.* Secretion of human hepatitis B virus is inhibited by the imino sugar N-butyldeoxynojirimycin. *Proc Natl Acad Sci U S A* **91**, 2235-2239, doi:10.1073/pnas.91.6.2235 (1994).
244 Mehta, A., Lu, X., Block, T. M., Blumberg, B. S. & Dwek, R. A. Hepatitis B virus (HBV) envelope glycoproteins vary drastically in their sensitivity to glycan processing: evidence that alteration of a single N-linked glycosylation site can regulate HBV secretion. *Proc Natl Acad Sci U S A* **94**, 1822-1827, doi:10.1073/pnas.94.5.1822 (1997).
245 Werr, M. & Prange, R. Role for calnexin and N-linked glycosylation in the assembly and secretion of hepatitis B virus middle envelope protein particles. *J Virol* **72**, 778-782, doi:10.1128/JVI.72.1.778-782.1998 (1998).
246 Patzer, E. J., Nakamura, G. R. & Yaffe, A. Intracellular transport and secretion of hepatitis B surface antigen in mammalian cells. *J Virol* **51**, 346-353, doi:10.1128/JVI.51.2.346-353.1984 (1984).
247 Patzer, E. J., Nakamura, G. R., Simonsen, C. C., Levinson, A. D. & Brands, R. Intracellular assembly and packaging of hepatitis B surface antigen particles occur in the endoplasmic reticulum. *J Virol* **58**, 884-892, doi:10.1128/JVI.58.3.884-892.1986 (1986).
248 Stanley, P. Golgi glycosylation. *Cold Spring Harb Perspect Biol* **3**, doi:10.1101/cshperspect.a005199 (2011).
249 Wagatsuma, T. *et al.* Highly Sensitive Glycan Profiling of Hepatitis B Viral Particles and a Simple Method for Dane Particle Enrichment. *Anal Chem* **90**, 10196-10203, doi:10.1021/acs.analchem.8b01030 (2018).
250 Salpini, R. *et al.* A Hyper-Glycosylation of HBV Surface Antigen Correlates with HBsAg-Negativity at Immunosuppression-Driven HBV Reactivation in Vivo and Hinders HBsAg Recognition in Vitro. *Viruses* **12**, doi:10.3390/v12020251 (2020).
251 Hartmann-Stuhler, C. & Prange, R. Hepatitis B virus large envelope protein interacts with gamma2-adaptin, a clathrin adaptor-related protein. *J Virol* **75**, 5343-5351, doi:10.1128/JVI.75.11.5343-5351.2001 (2001).
252 Rost, M. *et al.* Gamma-adaptin, a novel ubiquitin-interacting adaptor, and Nedd4 ubiquitin ligase control hepatitis B virus maturation. *J Biol Chem* **281**, 29297-29308, doi:10.1074/jbc.M603517200 (2006).
253 Lambert, C., Doring, T. & Prange, R. Hepatitis B virus maturation is sensitive to functional inhibition of ESCRT-III, Vps4, and gamma 2-adaptin. *J Virol* **81**, 9050-9060, doi:10.1128/JVI.00479-07 (2007).
254 Watanabe, T. *et al.* Involvement of host cellular multivesicular body functions in hepatitis B virus budding. *Proc Natl Acad Sci U S A* **104**, 10205-10210, doi:10.1073/pnas.0704000104 (2007).

255 Hoffmann, J. *et al.* Identification of alpha-taxilin as an essential factor for the life cycle of hepatitis B virus. *J Hepatol* **59**, 934-941, doi:10.1016/j.jhep.2013.06.020 (2013).
256 Stieler, J. T. & Prange, R. Involvement of ESCRT-II in hepatitis B virus morphogenesis. *PLoS One* **9**, e91279, doi:10.1371/journal.pone.0091279 (2014).
257 Jiang, B., Himmelsbach, K., Ren, H., Boller, K. & Hildt, E. Subviral Hepatitis B Virus Filaments, like Infectious Viral Particles, Are Released via Multivesicular Bodies. *J Virol* **90**, 3330-3341, doi:10.1128/JVI.03109-15 (2015).
258 Blondot, M. L., Bruss, V. & Kann, M. Intracellular transport and egress of hepatitis B virus. *J Hepatol* **64**, S49-S59, doi:10.1016/j.jhep.2016.02.008 (2016).
259 Seitz, S., Urban, S., Antoni, C. & Bottcher, B. Cryo-electron microscopy of hepatitis B virions reveals variability in envelope capsid interactions. *EMBO J* **26**, 4160-4167, doi:10.1038/sj.emboj.7601841 (2007).
260 Seitz, S. *et al.* A Slow Maturation Process Renders Hepatitis B Virus Infectious. *Cell Host Microbe* **20**, 25-35, doi:10.1016/j.chom.2016.05.013 (2016).
261 Sadler, A. J. & Williams, B. R. Interferon-inducible antiviral effectors. *Nat Rev Immunol* **8**, 559-568, doi:10.1038/nri2314 (2008).
262 Gill, U. S. & Kennedy, P. T. F. The impact of currently licensed therapies on viral and immune responses in chronic hepatitis B: Considerations for future novel therapeutics. *J Viral Hepat* **26**, 4-15, doi:10.1111/jvh.13040 (2019).
263 Craxi, A. & Cooksley, W. G. Pegylated interferons for chronic hepatitis B. *Antiviral Res* **60**, 87-89, doi:10.1016/j.antiviral.2003.08.015 (2003).
264 Woo, A. S. J., Kwok, R. & Ahmed, T. Alpha-interferon treatment in hepatitis B. *Ann Transl Med* **5**, 159, doi:10.21037/atm.2017.03.69 (2017).
265 Suk-Fong Lok, A. Hepatitis B Treatment: What We Know Now and What Remains to Be Researched. *Hepatol Commun* **3**, 8-19, doi:10.1002/hep4.1281 (2019).
266 Terrault, N. A. *et al.* Update on prevention, diagnosis, and treatment of chronic hepatitis B: AASLD 2018 hepatitis B guidance. *Hepatology* **67**, 1560-1599, doi:10.1002/hep.29800 (2018).
267 Yapali, S., Talaat, N. & Lok, A. S. Management of hepatitis B: our practice and how it relates to the guidelines. *Clin Gastroenterol Hepatol* **12**, 16-26, doi:10.1016/j.cgh.2013.04.036 (2014).
268 Erhardt, A. *et al.* Response to interferon alfa is hepatitis B virus genotype dependent: genotype A is more sensitive to interferon than genotype D. *Gut* **54**, 1009-1013, doi:10.1136/gut.2004.060327 (2005).
269 Wai, C. T., Chu, C. J., Hussain, M. & Lok, A. S. HBV genotype B is associated with better response to interferon therapy in HBeAg(+) chronic hepatitis than genotype C. *Hepatology* **36**, 1425-1430, doi:10.1053/jhep.2002.37139 (2002).
270 Lin, C. L. & Kao, J. H. Hepatitis B viral factors and treatment responses in chronic hepatitis B. *J Formos Med Assoc* **112**, 302-311, doi:10.1016/j.jfma.2013.02.001 (2013).
271 Xia, Y. *et al.* Secreted Interferon-Inducible Factors Restrict Hepatitis B and C Virus Entry In Vitro. *J Immunol Res* **2017**, 4828936, doi:10.1155/2017/4828936 (2017).
272 Allweiss, L. *et al.* Therapeutic shutdown of HBV transcripts promotes reappearance of the SMC5/6 complex and silencing of the viral genome in vivo. *Gut*, doi:10.1136/gutjnl-2020-322571 (2021).
273 Lucifora, J. *et al.* Specific and nonhepatotoxic degradation of nuclear hepatitis B virus cccDNA. *Science* **343**, 1221-1228, doi:10.1126/science.1243462 (2014).
274 Xu, F., Song, H., Li, N. & Tan, G. HBsAg blocks TYPE I IFN induced up-regulation of A3G through inhibition of STAT3. *Biochem Biophys Res Commun* **473**, 219-223, doi:10.1016/j.bbrc.2016.03.082 (2016).
275 Liu, Y. *et al.* Interferon-inducible ribonuclease ISG20 inhibits hepatitis B virus replication through directly binding to the epsilon stem-loop structure of viral RNA. *PLoS Pathog* **13**, e1006296, doi:10.1371/journal.ppat.1006296 (2017).
276 Wang, Y. X. *et al.* Interferon-inducible MX2 is a host restriction factor of hepatitis B virus replication. *J Hepatol* **72**, 865-876, doi:10.1016/j.jhep.2019.12.009 (2020).

277 Gao, B., Duan, Z., Xu, W. & Xiong, S. Tripartite motif-containing 22 inhibits the activity of hepatitis B virus core promoter, which is dependent on nuclear-located RING domain. *Hepatology* **50**, 424-433, doi:10.1002/hep.23011 (2009).
278 Tan, G. *et al.* Type I IFN augments IL-27-dependent TRIM25 expression to inhibit HBV replication. *Cell Mol Immunol* **15**, 272-281, doi:10.1038/cmi.2016.67 (2018).
279 Tan, G. *et al.* Type-I-IFN-Stimulated Gene TRIM5gamma Inhibits HBV Replication by Promoting HBx Degradation. *Cell Rep* **29**, 3551-3563 e3553, doi:10.1016/j.celrep.2019.11.041 (2019).
280 Tan, G., Song, H., Xu, F. & Cheng, G. When Hepatitis B Virus Meets Interferons. *Front Microbiol* **9**, 1611, doi:10.3389/fmicb.2018.01611 (2018).
281 Tan, A. T. *et al.* Reduction of HBV replication prolongs the early immunological response to IFNalpha therapy. *J Hepatol* **60**, 54-61, doi:10.1016/j.jhep.2013.08.020 (2014).
282 Micco, L. *et al.* Differential boosting of innate and adaptive antiviral responses during pegylated-interferon-alpha therapy of chronic hepatitis B. *J Hepatol* **58**, 225-233, doi:10.1016/j.jhep.2012.09.029 (2013).
283 Gill, U. S. *et al.* Interferon Alpha Induces Sustained Changes in NK Cell Responsiveness to Hepatitis B Viral Load Suppression In Vivo. *PLoS Pathog* **12**, e1005788, doi:10.1371/journal.ppat.1005788 (2016).
284 Shen, X. *et al.* NKp30(+) NK cells are associated with HBV control during pegylated-interferon-alpha-2b therapy of chronic hepatitis B. *Sci Rep* **6**, 38778, doi:10.1038/srep38778 (2016).
285 Fletcher, S. P. *et al.* Intrahepatic Transcriptional Signature Associated with Response to Interferon-alpha Treatment in the Woodchuck Model of Chronic Hepatitis B. *PLoS Pathog* **11**, e1005103, doi:10.1371/journal.ppat.1005103 (2015).
286 Penna, A. *et al.* Peginterferon-alpha does not improve early peripheral blood HBV-specific T-cell responses in HBeAg-negative chronic hepatitis. *J Hepatol* **56**, 1239-1246, doi:10.1016/j.jhep.2011.12.032 (2012).
287 Crouse, J. *et al.* Type I interferons protect T cells against NK cell attack mediated by the activating receptor NCR1. *Immunity* **40**, 961-973, doi:10.1016/j.immuni.2014.05.003 (2014).
288 Xu, H. C. *et al.* Type I interferon protects antiviral CD8+ T cells from NK cell cytotoxicity. *Immunity* **40**, 949-960, doi:10.1016/j.immuni.2014.05.004 (2014).
289 Marcellin P, G. E., Flisiak R, Trinh HN, Petersen J, Gurel S, Kaita KD, Kotzev IA, Tsai N, Flaherty JF, Schall REA, Kitrinos KM, Subramanian M, McHutchison JG, George J, Janssen HL, Buti M. in *65th Annual Meeting of the American Association for the Study of Liver Diseases: The Liver Meeting 2014* Vol. 60 (Hepatology, Boston, MA United States, 2014).
290 Okada, M., Enomoto, M., Kawada, N. & Nguyen, M. H. Effects of antiviral therapy in patients with chronic hepatitis B and cirrhosis. *Expert Rev Gastroenterol Hepatol* **11**, 1095-1104, doi:10.1080/17474124.2017.1361822 (2017).
291 Nguyen, M. H., Wong, G., Gane, E., Kao, J. H. & Dusheiko, G. Hepatitis B Virus: Advances in Prevention, Diagnosis, and Therapy. *Clin Microbiol Rev* **33**, doi:10.1128/CMR.00046-19 (2020).
292 Marcellin, P. *et al.* Regression of cirrhosis during treatment with tenofovir disoproxil fumarate for chronic hepatitis B: a 5-year open-label follow-up study. *Lancet* **381**, 468-475, doi:10.1016/S0140-6736(12)61425-1 (2013).
293 Papatheodoridis, G. V. *et al.* The risk of hepatocellular carcinoma decreases after the first 5 years of entecavir or tenofovir in Caucasians with chronic hepatitis B. *Hepatology* **66**, 1444-1453, doi:10.1002/hep.29320 (2017).
294 Levrero, M., Subic, M., Villeret, F. & Zoulim, F. Perspectives and limitations for nucleo(t)side analogs in future HBV therapies. *Curr Opin Virol* **30**, 80-89, doi:10.1016/j.coviro.2018.04.006 (2018).
295 Wedemeyer, H. *et al.* GS-13-Final results of a multicenter, open-label phase 2 clinical trial (MYR203) to assess safety and efficacy of myrcludex B in cwith PEG-interferon Alpha 2a in patients with chronic HBV/HDV co-infection. *Journal of Hepatology* **70**, e81, doi:10.1016/S0618-8278(19)30141-0 (2019).

296 Kang, C. & Syed, Y. Y. Bulevirtide: First Approval. *Drugs* **80**, 1601-1605, doi:10.1007/s40265-020-01400-1 (2020).
297 Nkongolo, S. *et al.* Cyclosporin A inhibits hepatitis B and hepatitis D virus entry by cyclophilin-independent interference with the NTCP receptor. *J Hepatol* **60**, 723-731, doi:10.1016/j.jhep.2013.11.022 (2014).
298 Tu, T. & Urban, S. Virus entry and its inhibition to prevent and treat hepatitis B and hepatitis D virus infections. *Curr Opin Virol* **30**, 68-79, doi:10.1016/j.coviro.2018.04.004 (2018).
299 Stray, S. J. *et al.* A heteroaryldihydropyrimidine activates and can misdirect hepatitis B virus capsid assembly. *Proc Natl Acad Sci U S A* **102**, 8138-8143, doi:10.1073/pnas.0409732102 (2005).
300 Katen, S. P., Chirapu, S. R., Finn, M. G. & Zlotnick, A. Trapping of hepatitis B virus capsid assembly intermediates by phenylpropenamide assembly accelerators. *ACS Chem Biol* **5**, 1125-1136, doi:10.1021/cb100275b (2010).
301 Cole, A. G. Modulators of HBV capsid assembly as an approach to treating hepatitis B virus infection. *Curr Opin Pharmacol* **30**, 131-137, doi:10.1016/j.coph.2016.08.004 (2016).
302 Lee, H. W., Lee, J. S. & Ahn, S. H. Hepatitis B Virus Cure: Targets and Future Therapies. *Int J Mol Sci* **22**, doi:10.3390/ijms22010213 (2020).
303 Berke, J. M. *et al.* Capsid Assembly Modulators Have a Dual Mechanism of Action in Primary Human Hepatocytes Infected with Hepatitis B Virus. *Antimicrob Agents Chemother* **61**, doi:10.1128/AAC.00560-17 (2017).
304 Zoulim, F. *et al.* JNJ-56136379, an HBV Capsid Assembly Modulator, Is Well-Tolerated and Has Antiviral Activity in a Phase 1 Study of Patients With Chronic Infection. *Gastroenterology* **159**, 521-533 e529, doi:10.1053/j.gastro.2020.04.036 (2020).
305 Yuen, R. M. F. in *The Science of HBV Cure, 2019* (2019).
306 Yuen, M. F. *et al.* Antiviral Activity, Safety, and Pharmacokinetics of Capsid Assembly Modulator NVR 3-778 in Patients with Chronic HBV Infection. *Gastroenterology* **156**, 1392-1403 e1397, doi:10.1053/j.gastro.2018.12.023 (2019).
307 Fanning, G. C., Zoulim, F., Hou, J. & Bertoletti, A. Therapeutic strategies for hepatitis B virus infection: towards a cure. *Nat Rev Drug Discov* **18**, 827-844, doi:10.1038/s41573-019-0037-0 (2019).
308 Burdette, D. *et al.* PS-150-Evidence for the presence of infectious virus in the serum from chronic hepatitis B patients suppressed on nucleos (t)ide therapy with detectable but not quantifiable HBV DNA. *Journal of Hepatology* **70**, e95, doi:10.1016/S0618-8278(19)30168-9 (2019).
309 Ma, X. *et al.* LBO-06-Interim safety and efficacy results of the ABI-H0731 phase 2a program exploring the combination of ABI-H0731 with Nuc therapy in treatment-naive and treatment-suppressed chronic hepatitis B patients. *Journal of Hepatology* **70**, e130, doi:10.1016/S0618-8278(19)30230-0 (2019).
310 Chen, J. *et al.* An efficient antiviral strategy for targeting hepatitis B virus genome using transcription activator-like effector nucleases. *Mol Ther* **22**, 303-311, doi:10.1038/mt.2013.212 (2014).
311 Seeger, C. & Sohn, J. A. Complete Spectrum of CRISPR/Cas9-induced Mutations on HBV cccDNA. *Mol Ther* **24**, 1258-1266, doi:10.1038/mt.2016.94 (2016).
312 Seeger, C. Control of viral transcripts as a concept for future HBV therapies. *Curr Opin Virol* **30**, 18-23, doi:10.1016/j.coviro.2018.01.009 (2018).
313 Sekiba, K. *et al.* Pevonedistat, a Neuronal Precursor Cell-Expressed Developmentally Down-Regulated Protein 8-Activating Enzyme Inhibitor, Is a Potent Inhibitor of Hepatitis B Virus. *Hepatology* **69**, 1903-1915, doi:10.1002/hep.30491 (2019).
314 Xie, M. *et al.* Neddylation inhibitor MLN4924 has anti-HBV activity via modulating the ERK-HNF1alpha-C/EBPalpha-HNF4alpha axis. *J Cell Mol Med* **25**, 840-854, doi:10.1111/jcmm.16137 (2021).

315 Sekiba, K. *et al.* Inhibition of HBV Transcription From cccDNA With Nitazoxanide by Targeting the HBx-DDB1 Interaction. *Cell Mol Gastroenterol Hepatol* **7**, 297-312, doi:10.1016/j.jcmgh.2018.10.010 (2019).
316 Enchev, R. I., Schulman, B. A. & Peter, M. Protein neddylation: beyond cullin-RING ligases. *Nat Rev Mol Cell Biol* **16**, 30-44, doi:10.1038/nrm3919 (2015).
317 Wooddell, C. I. *et al.* RNAi-based treatment of chronically infected patients and chimpanzees reveals that integrated hepatitis B virus DNA is a source of HBsAg. *Sci Transl Med* **9**, doi:10.1126/scitranslmed.aan0241 (2017).
318 Wooddell, C. I. *et al.* Hepatocyte-targeted RNAi therapeutics for the treatment of chronic hepatitis B virus infection. *Mol Ther* **21**, 973-985, doi:10.1038/mt.2013.31 (2013).
319 Yuen, M.-F. *et al.* PS-080-Short term RNA interference therapy in chronic hepatitis B using JNJ-3989 brings majority of patients to HBsAg < 100 IU/ml threshold. *Journal of Hepatology* **70**, e51-e52, doi:10.1016/S0618-8278(19)30092-1 (2019).
320 Billioud, G. *et al.* In vivo reduction of hepatitis B virus antigenemia and viremia by antisense oligonucleotides. *J Hepatol* **64**, 781-789, doi:10.1016/j.jhep.2015.11.032 (2016).
321 Han, K. *et al.* A Randomized, Double-Blind, Placebo-Controlled, First-Time-in-Human Study to Assess the Safety, Tolerability, and Pharmacokinetics of Single and Multiple Ascending Doses of GSK3389404 in Healthy Subjects. *Clin Pharmacol Drug Dev* **8**, 790-801, doi:10.1002/cpdd.670 (2019).
322 Mueller, H. *et al.* A novel orally available small molecule that inhibits hepatitis B virus expression. *J Hepatol* **68**, 412-420, doi:10.1016/j.jhep.2017.10.014 (2018).
323 Mueller, H. *et al.* PAPD5/7 Are Host Factors That Are Required for Hepatitis B Virus RNA Stabilization. *Hepatology* **69**, 1398-1411, doi:10.1002/hep.30329 (2019).
324 Vaillant, A. Nucleic acid polymers: Broad spectrum antiviral activity, antiviral mechanisms and optimization for the treatment of hepatitis B and hepatitis D infection. *Antiviral Res* **133**, 32-40, doi:10.1016/j.antiviral.2016.07.004 (2016).
325 Bazinet, M. *et al.* Safety and Efficacy of 48 Weeks REP 2139 or REP 2165, Tenofovir Disoproxil, and Pegylated Interferon Alfa-2a in Patients With Chronic HBV Infection Naive to Nucleos(t)ide Therapy. *Gastroenterology* **158**, 2180-2194, doi:10.1053/j.gastro.2020.02.058 (2020).
326 Lamontagne, J., Mell, J. C. & Bouchard, M. J. Transcriptome-Wide Analysis of Hepatitis B Virus-Mediated Changes to Normal Hepatocyte Gene Expression. *PLoS Pathog* **12**, e1005438, doi:10.1371/journal.ppat.1005438 (2016).
327 Yuan, S. *et al.* Global analysis of HBV-mediated host proteome and ubiquitylome change in HepG2.2.15 human hepatoblastoma cell line. *Cell Biosci* **11**, 75, doi:10.1186/s13578-021-00588-3 (2021).
328 Kim, J. H. *et al.* Circulating serum HBsAg level is a biomarker for HBV-specific T and B cell responses in chronic hepatitis B patients. *Sci Rep* **10**, 1835, doi:10.1038/s41598-020-58870-2 (2020).
329 Erfle, H. *et al.* Work flow for multiplexing siRNA assays by solid-phase reverse transfection in multiwell plates. *J Biomol Screen* **13**, 575-580, doi:10.1177/1087057108320133 (2008).
330 Livak, K. J. & Schmittgen, T. D. Analysis of relative gene expression data using real-time quantitative PCR and the 2(-Delta Delta C(T)) Method. *Methods* **25**, 402-408, doi:10.1006/meth.2001.1262 (2001).
331 Lempp, F. A. *et al.* Recapitulation of HDV infection in a fully permissive hepatoma cell line allows efficient drug evaluation. *Nat Commun* **10**, 2265, doi:10.1038/s41467-019-10211-2 (2019).
332 Simpson, J. C. *et al.* Genome-wide RNAi screening identifies human proteins with a regulatory function in the early secretory pathway. *Nat Cell Biol* **14**, 764-774, doi:10.1038/ncb2510 (2012).
333 Ladner, S. K. *et al.* Inducible expression of human hepatitis B virus (HBV) in stably transfected hepatoblastoma cells: a novel system for screening potential inhibitors of HBV replication. *Antimicrob Agents Chemother* **41**, 1715-1720, doi:10.1128/AAC.41.8.1715 (1997).

334 Zhou, T. *et al.* Hepatitis B virus e antigen production is dependent upon covalently closed circular (ccc) DNA in HepAD38 cell cultures and may serve as a cccDNA surrogate in antiviral screening assays. *Antiviral Res* **72**, 116-124, doi:10.1016/j.antiviral.2006.05.006 (2006).
335 Bolten, S. N., Rinas, U. & Scheper, T. Heparin: role in protein purification and substitution with animal-component free material. *Appl Microbiol Biotechnol* **102**, 8647-8660, doi:10.1007/s00253-018-9263-3 (2018).
336 Watts, N. R. *et al.* Molecular basis for the high degree of antigenic cross-reactivity between hepatitis B virus capsids (HBcAg) and dimeric capsid-related protein (HBeAg): insights into the enigmatic nature of the e-antigen. *J Mol Biol* **398**, 530-541, doi:10.1016/j.jmb.2010.03.026 (2010).
337 Kornyeyev, D. *et al.* Spatiotemporal Analysis of Hepatitis B Virus X Protein in Primary Human Hepatocytes. *J Virol* **93**, doi:10.1128/JVI.00248-19 (2019).
338 Grgacic, E. V. & Schaller, H. A metastable form of the large envelope protein of duck hepatitis B virus: low-pH release results in a transition to a hydrophobic, potentially fusogenic conformation. *J Virol* **74**, 5116-5122, doi:10.1128/jvi.74.11.5116-5122.2000 (2000).
339 Qiao, L. & Luo, G. G. Human apolipoprotein E promotes hepatitis B virus infection and production. *PLoS Pathog* **15**, e1007874, doi:10.1371/journal.ppat.1007874 (2019).
340 Mason, W. S., Liu, C., Aldrich, C. E., Litwin, S. & Yeh, M. M. Clonal expansion of normal-appearing human hepatocytes during chronic hepatitis B virus infection. *J Virol* **84**, 8308-8315, doi:10.1128/JVI.00833-10 (2010).
341 Yang, W. & Summers, J. Integration of hepadnavirus DNA in infected liver: evidence for a linear precursor. *J Virol* **73**, 9710-9717, doi:10.1128/JVI.73.12.9710-9717.1999 (1999).
342 Gong, S. S., Jensen, A. D., Chang, C. J. & Rogler, C. E. Double-stranded linear duck hepatitis B virus (DHBV) stably integrates at a higher frequency than wild-type DHBV in LMH chicken hepatoma cells. *J Virol* **73**, 1492-1502, doi:10.1128/JVI.73.2.1492-1502.1999 (1999).
343 Mason, W. S. *et al.* Detection of clonally expanded hepatocytes in chimpanzees with chronic hepatitis B virus infection. *J Virol* **83**, 8396-8408, doi:10.1128/JVI.00700-09 (2009).
344 Tu, T., Budzinska, M. A., Vondran, F. W. R., Shackel, N. A. & Urban, S. Hepatitis B Virus DNA Integration Occurs Early in the Viral Life Cycle in an In Vitro Infection Model via Sodium Taurocholate Cotransporting Polypeptide-Dependent Uptake of Enveloped Virus Particles. *J Virol* **92**, doi:10.1128/JVI.02007-17 (2018).
345 Kondo, Y., Ninomiya, M., Kakazu, E., Kimura, O. & Shimosegawa, T. Hepatitis B surface antigen could contribute to the immunopathogenesis of hepatitis B virus infection. *ISRN Gastroenterol* **2013**, 935295, doi:10.1155/2013/935295 (2013).
346 Zhu, D. *et al.* Clearing Persistent Extracellular Antigen of Hepatitis B Virus: An Immunomodulatory Strategy To Reverse Tolerance for an Effective Therapeutic Vaccination. *J Immunol* **196**, 3079-3087, doi:10.4049/jimmunol.1502061 (2016).
347 Shi, J., Wang, X., Lyu, L., Jiang, H. & Zhu, H. J. Comparison of protein expression between human livers and the hepatic cell lines HepG2, Hep3B, and Huh7 using SWATH and MRM-HR proteomics: Focusing on drug-metabolizing enzymes. *Drug Metab Pharmacokinet* **33**, 133-140, doi:10.1016/j.dmpk.2018.03.003 (2018).
348 Bressac, B. *et al.* Abnormal structure and expression of p53 gene in human hepatocellular carcinoma. *Proc Natl Acad Sci U S A* **87**, 1973-1977, doi:10.1073/pnas.87.5.1973 (1990).
349 Kasai, F., Hirayama, N., Ozawa, M., Satoh, M. & Kohara, A. HuH-7 reference genome profile: complex karyotype composed of massive loss of heterozygosity. *Hum Cell* **31**, 261-267, doi:10.1007/s13577-018-0212-3 (2018).
350 Zhou, B. *et al.* Haplotype-resolved and integrated genome analysis of the cancer cell line HepG2. *Nucleic Acids Res* **47**, 3846-3861, doi:10.1093/nar/gkz169 (2019).
351 Soucy, T. A. *et al.* An inhibitor of NEDD8-activating enzyme as a new approach to treat cancer. *Nature* **458**, 732-736, doi:10.1038/nature07884 (2009).
352 Lobato-Gil, S. *et al.* Proteome-wide identification of NEDD8 modification sites reveals distinct proteomes for canonical and atypical NEDDylation. *Cell Rep* **34**, 108635, doi:10.1016/j.celrep.2020.108635 (2021).

353 Vogl, A. M. *et al.* Global site-specific neddylation profiling reveals that NEDDylated cofilin regulates actin dynamics. *Nat Struct Mol Biol* **27**, 210-220, doi:10.1038/s41594-019-0370-3 (2020).
354 North, B. J., Marshall, B. L., Borra, M. T., Denu, J. M. & Verdin, E. The human Sir2 ortholog, SIRT2, is an NAD+-dependent tubulin deacetylase. *Mol Cell* **11**, 437-444, doi:10.1016/s1097-2765(03)00038-8 (2003).
355 Piracha, Z. Z. *et al.* Sirtuin 2 Isoform 1 Enhances Hepatitis B Virus RNA Transcription and DNA Synthesis through the AKT/GSK-3beta/beta-Catenin Signaling Pathway. *J Virol* **92**, doi:10.1128/JVI.00955-18 (2018).
356 Le-Trilling, V. T. *et al.* Broad and potent antiviral activity of the NAE inhibitor MLN4924. *Sci Rep* **6**, 19977, doi:10.1038/srep19977 (2016).
357 Han, K. & Zhang, J. Roles of neddylation against viral infections. *Cell Mol Immunol* **15**, 292-294, doi:10.1038/cmi.2017.100 (2018).
358 Liu, N. *et al.* HDM2 Promotes NEDDylation of Hepatitis B Virus HBx To Enhance Its Stability and Function. *J Virol* **91**, doi:10.1128/JVI.00340-17 (2017).
359 Chen, D. V. *et al.* Deneddylation by SENP8 restricts hepatitis B virus propagation. *Microbiol Immunol* **65**, 125-135, doi:10.1111/1348-0421.12874 (2021).
360 Luo, Z. *et al.* The Nedd8-activating enzyme inhibitor MLN4924 induces autophagy and apoptosis to suppress liver cancer cell growth. *Cancer Res* **72**, 3360-3371, doi:10.1158/0008-5472.CAN-12-0388 (2012).
361 Lin, Y. *et al.* Hepatitis B virus is degraded by autophagosome-lysosome fusion mediated by Rab7 and related components. *Protein Cell* **10**, 60-66, doi:10.1007/s13238-018-0555-2 (2019).
362 Lin, Y. *et al.* Synaptosomal-associated protein 29 is required for the autophagic degradation of hepatitis B virus. *FASEB J* **33**, 6023-6034, doi:10.1096/fj.201801995RR (2019).
363 Lin, Y., Zhao, Z., Huang, A. & Lu, M. Interplay between Cellular Autophagy and Hepatitis B Virus Replication: A Systematic Review. *Cells* **9**, doi:10.3390/cells9092101 (2020).
364 Yao, J., Liang, X., Liu, Y. & Zheng, M. Neddylation: A Versatile Pathway Takes on Chronic Liver Diseases. *Front Med (Lausanne)* **7**, 586881, doi:10.3389/fmed.2020.586881 (2020).
365 Zubiete-Franco, I. *et al.* Deregulated neddylation in liver fibrosis. *Hepatology* **65**, 694-709, doi:10.1002/hep.28933 (2017).
366 Milhollen, M. A. *et al.* Treatment-emergent mutations in NAEbeta confer resistance to the NEDD8-activating enzyme inhibitor MLN4924. *Cancer Cell* **21**, 388-401, doi:10.1016/j.ccr.2012.02.009 (2012).
367 Xu, G. W. *et al.* Mutations in UBA3 confer resistance to the NEDD8-activating enzyme inhibitor MLN4924 in human leukemic cells. *PLoS One* **9**, e93530, doi:10.1371/journal.pone.0093530 (2014).
368 Zhao, X. *et al.* Quantitative proteomic analysis of exosome protein content changes induced by hepatitis B virus in Huh-7 cells using SILAC labeling and LC-MS/MS. *J Proteome Res* **13**, 5391-5402, doi:10.1021/pr5008703 (2014).
369 Jia, X. *et al.* Label-free Proteomic Analysis of Exosomes Derived from Inducible Hepatitis B Virus-Replicating HepAD38 Cell Line. *Mol Cell Proteomics* **16**, S144-S160, doi:10.1074/mcp.M116.063503 (2017).
370 Shaw, M. L., Stone, K. L., Colangelo, C. M., Gulcicek, E. E. & Palese, P. Cellular proteins in influenza virus particles. *PLoS Pathog* **4**, e1000085, doi:10.1371/journal.ppat.1000085 (2008).
371 Radhakrishnan, A. *et al.* Protein analysis of purified respiratory syncytial virus particles reveals an important role for heat shock protein 90 in virus particle assembly. *Mol Cell Proteomics* **9**, 1829-1848, doi:10.1074/mcp.M110.001651 (2010).
372 Ziegler, C. M. *et al.* A Proteomics Survey of Junin Virus Interactions with Human Proteins Reveals Host Factors Required for Arenavirus Replication. *J Virol* **92**, doi:10.1128/JVI.01565-17 (2018).

373 Linde, M. E. *et al.* The conserved set of host proteins incorporated into HIV-1 virions suggests a common egress pathway in multiple cell types. *J Proteome Res* **12**, 2045-2054, doi:10.1021/pr300918r (2013).
374 Zhang, Y. *et al.* Proteomic Profiling of Purified Rabies Virus Particles. *Virol Sin* **35**, 143-155, doi:10.1007/s12250-019-00157-6 (2020).
375 Chung, C. S. *et al.* Vaccinia virus proteome: identification of proteins in vaccinia virus intracellular mature virion particles. *J Virol* **80**, 2127-2140, doi:10.1128/JVI.80.5.2127-2140.2006 (2006).
376 Chertova, E. *et al.* Proteomic and biochemical analysis of purified human immunodeficiency virus type 1 produced from infected monocyte-derived macrophages. *J Virol* **80**, 9039-9052, doi:10.1128/JVI.01013-06 (2006).
377 Wang, J. C., Nickens, D. G., Lentz, T. B., Loeb, D. D. & Zlotnick, A. Encapsidated hepatitis B virus reverse transcriptase is poised on an ordered RNA lattice. *Proc Natl Acad Sci U S A* **111**, 11329-11334, doi:10.1073/pnas.1321424111 (2014).
378 Stork, E. M. *Generation and Characterization of Authentic Hepatitis B Virus Nucleocapsidsto Study their Ultrastructure and their Interaction with Envelope Peptides* Master of Science thesis, Ruprecht-Karls-University Heidelberg, (2020).
379 Cooper, A., Tal, G., Lider, O. & Shaul, Y. Cytokine induction by the hepatitis B virus capsid in macrophages is facilitated by membrane heparan sulfate and involves TLR2. *J Immunol* **175**, 3165-3176, doi:10.4049/jimmunol.175.5.3165 (2005).
380 Lucifora, J. *et al.* Hepatitis B virus X protein is essential to initiate and maintain virus replication after infection. *J Hepatol* **55**, 996-1003, doi:10.1016/j.jhep.2011.02.015 (2011).
381 Kapoor, N. R. *et al.* The HBx gene of hepatitis B virus can influence hepatic microenvironment via exosomes by transferring its mRNA and protein. *Virus Res* **240**, 166-174, doi:10.1016/j.virusres.2017.08.009 (2017).
382 Hildt, E., Munz, B., Saher, G., Reifenberg, K. & Hofschneider, P. H. The PreS2 activator MHBs(t) of hepatitis B virus activates c-raf-1/Erk2 signaling in transgenic mice. *EMBO J* **21**, 525-535, doi:10.1093/emboj/21.4.525 (2002).
383 Kekule, A. S. *et al.* The preS2/S region of integrated hepatitis B virus DNA encodes a transcriptional transactivator. *Nature* **343**, 457-461, doi:10.1038/343457a0 (1990).
384 Grgacic, E. V., Lin, B., Gazina, E. V., Snooks, M. J. & Anderson, D. A. Normal phosphorylation of duck hepatitis B virus L protein is dispensable for infectivity. *J Gen Virol* **79 (Pt 11)**, 2743-2751, doi:10.1099/0022-1317-79-11-2743 (1998).
385 Rothmann, K. *et al.* Host cell-virus cross talk: phosphorylation of a hepatitis B virus envelope protein mediates intracellular signaling. *J Virol* **72**, 10138-10147, doi:10.1128/JVI.72.12.10138-10147.1998 (1998).
386 Sonder, S. L. *et al.* Annexin A7 is required for ESCRT III-mediated plasma membrane repair. *Sci Rep* **9**, 6726, doi:10.1038/s41598-019-43143-4 (2019).
387 Jaiswal, J. K. *et al.* S100A11 is required for efficient plasma membrane repair and survival of invasive cancer cells. *Nat Commun* **5**, 3795, doi:10.1038/ncomms4795 (2014).
388 Hager, S. C. & Nylandsted, J. Annexins: players of single cell wound healing and regeneration. *Commun Integr Biol* **12**, 162-165, doi:10.1080/19420889.2019.1676139 (2019).
389 Bardens, A., Doring, T., Stieler, J. & Prange, R. Alix regulates egress of hepatitis B virus naked capsid particles in an ESCRT-independent manner. *Cell Microbiol* **13**, 602-619, doi:10.1111/j.1462-5822.2010.01557.x (2011).
390 Phillips, S. *et al.* Alisporivir inhibition of hepatocyte cyclophilins reduces HBV replication and hepatitis B surface antigen production. *Gastroenterology* **148**, 403-414 e407, doi:10.1053/j.gastro.2014.10.004 (2015).
391 Xiang-Chun, D. *et al.* Alpha-enolase regulates hepatitis B virus replication through suppression of the interferon signalling pathway. *J Viral Hepat* **25**, 289-295, doi:10.1111/jvh.12813 (2018).
392 Wu, Y. H. *et al.* Aerobic glycolysis supports hepatitis B virus protein synthesis through interaction between viral surface antigen and pyruvate kinase isoform M2. *PLoS Pathog* **17**, e1008866, doi:10.1371/journal.ppat.1008866 (2021).

393 Bremer, C. M., Bung, C., Kott, N., Hardt, M. & Glebe, D. Hepatitis B virus infection is dependent on cholesterol in the viral envelope. *Cell Microbiol* **11**, 249-260, doi:10.1111/j.1462-5822.2008.01250.x (2009).
394 Dorobantu, C. *et al.* Cholesterol depletion of hepatoma cells impairs hepatitis B virus envelopment by altering the topology of the large envelope protein. *J Virol* **85**, 13373-13383, doi:10.1128/JVI.05423-11 (2011).
395 Xie, N. *et al.* Comprehensive proteomic analysis of host cell lipid rafts modified by HBV infection. *J Proteomics* **75**, 725-739, doi:10.1016/j.jprot.2011.09.011 (2012).
396 De Maio, A. *et al.* The small heat shock proteins, HSPB1 and HSPB5, interact differently with lipid membranes. *Cell Stress Chaperones* **24**, 947-956, doi:10.1007/s12192-019-01021-y (2019).
397 Chen, S., Bawa, D., Besshoh, S., Gurd, J. W. & Brown, I. R. Association of heat shock proteins and neuronal membrane components with lipid rafts from the rat brain. *J Neurosci Res* **81**, 522-529, doi:10.1002/jnr.20575 (2005).
398 Hueging, K. *et al.* Several Human Liver Cell Expressed Apolipoproteins Complement HCV Virus Production with Varying Efficacy Conferring Differential Specific Infectivity to Released Viruses. *PLoS One* **10**, e0134529, doi:10.1371/journal.pone.0134529 (2015).
399 Esser, K. *et al.* Lipase inhibitor orlistat prevents hepatitis B virus infection by targeting an early step in the virus life cycle. *Antiviral Res* **151**, 4-7, doi:10.1016/j.antiviral.2018.01.001 (2018).
400 Jacobo-Albavera, L., Dominguez-Perez, M., Medina-Leyte, D. J., Gonzalez-Garrido, A. & Villarreal-Molina, T. The Role of the ATP-Binding Cassette A1 (ABCA1) in Human Disease. *Int J Mol Sci* **22**, doi:10.3390/ijms22041593 (2021).
401 Mujawar, Z. *et al.* Human immunodeficiency virus impairs reverse cholesterol transport from macrophages. *PLoS Biol* **4**, e365, doi:10.1371/journal.pbio.0040365 (2006).
402 Jennelle, L. *et al.* HIV-1 protein Nef inhibits activity of ATP-binding cassette transporter A1 by targeting endoplasmic reticulum chaperone calnexin. *J Biol Chem* **289**, 28870-28884, doi:10.1074/jbc.M114.583591 (2014).
403 Dane, D. S., Cameron, C. H. & Briggs, M. Virus-like particles in serum of patients with Australia-antigen-associated hepatitis. *Lancet* **1**, 695-698, doi:10.1016/s0140-6736(70)90926-8 (1970).
404 Kaito, M. *et al.* The ultrastructural morphology of native hepatitis B virus. *Med Mol Morphol* **39**, 136-145, doi:10.1007/s00795-006-0330-y (2006).
405 Fu, Y. *et al.* Apolipoprotein E lipoprotein particles inhibit amyloid-beta uptake through cell surface heparan sulphate proteoglycan. *Mol Neurodegener* **11**, 37, doi:10.1186/s13024-016-0099-y (2016).
406 Libeu, C. P. *et al.* New insights into the heparan sulfate proteoglycan-binding activity of apolipoprotein E. *J Biol Chem* **276**, 39138-39144, doi:10.1074/jbc.M104746200 (2001).
407 Bruss, V. & Vieluf, K. Functions of the internal pre-S domain of the large surface protein in hepatitis B virus particle morphogenesis. *J Virol* **69**, 6652-6657, doi:10.1128/JVI.69.11.6652-6657.1995 (1995).
408 Shim, H. Y., Quan, X., Yi, Y. S. & Jung, G. Heat shock protein 90 facilitates formation of the HBV capsid via interacting with the HBV core protein dimers. *Virology* **410**, 161-169, doi:10.1016/j.virol.2010.11.005 (2011).
409 Seo, H. W., Seo, J. P. & Jung, G. Heat shock protein 70 and heat shock protein 90 synergistically increase hepatitis B viral capsid assembly. *Biochem Biophys Res Commun* **503**, 2892-2898, doi:10.1016/j.bbrc.2018.08.065 (2018).
410 Tong, S. W. *et al.* HSPB1 is an intracellular antiviral factor against hepatitis B virus. *J Cell Biochem* **114**, 162-173, doi:10.1002/jcb.24313 (2013).
411 Chabrolles, H. *et al.* Hepatitis B virus Core protein nuclear interactome identifies SRSF10 as a host RNA-binding protein restricting HBV RNA production. *PLoS Pathog* **16**, e1008593, doi:10.1371/journal.ppat.1008593 (2020).
412 Pribyl, M., Hodny, Z. & Kubikova, I. Suprabasin-A Review. *Genes (Basel)* **12**, doi:10.3390/genes12010108 (2021).

413 Markiewicz, A., Sigorski, D., Markiewicz, M., Owczarczyk-Saczonek, A. & Placek, W. Caspase-14-From Biomolecular Basics to Clinical Approach. A Review of Available Data. *Int J Mol Sci* **22**, doi:10.3390/ijms22115575 (2021).

414 Nakazawa, S. *et al.* Suprabasin-null mice retain skin barrier function and show high contact hypersensitivity to nickel upon oral nickel loading. *Sci Rep* **10**, 14559, doi:10.1038/s41598-020-71536-3 (2020).

415 Zhang, X. *et al.* Structures of the human spliceosomes before and after release of the ligated exon. *Cell Res* **29**, 274-285, doi:10.1038/s41422-019-0143-x (2019).

416 Liu, N. *et al.* N(6)-methyladenosine-dependent RNA structural switches regulate RNA-protein interactions. *Nature* **518**, 560-564, doi:10.1038/nature14234 (2015).

417 Kim, G. W. & Siddiqui, A. Hepatitis B virus X protein recruits methyltransferases to affect cotranscriptional N6-methyladenosine modification of viral/host RNAs. *Proc Natl Acad Sci U S A* **118**, doi:10.1073/pnas.2019455118 (2021).

418 Zhang, L. *et al.* Analysis of vaccinia virus-host protein-protein interactions: validations of yeast two-hybrid screenings. *J Proteome Res* **8**, 4311-4318, doi:10.1021/pr900491n (2009).

419 Senkevich, T. G., Wyatt, L. S., Weisberg, A. S., Koonin, E. V. & Moss, B. A conserved poxvirus NlpC/P60 superfamily protein contributes to vaccinia virus virulence in mice but not to replication in cell culture. *Virology* **374**, 506-514, doi:10.1016/j.virol.2008.01.009 (2008).

420 Bingqian Qu, F. N., Mila M. Leuthold, Yi Ni, Pascal Mutz, Jürgen Beneke, Holger Erfle, Florian W.R. Vondran, Ralf Bartenschlager, Stephan Urban. Dual role of neddylation for transcription of hepatitis B virus RNAs from cccDNA and secretion of viral surface antigen. Manuscript submitted for publication.

6 Presentations and Publications

6.1 Oral Presentation

Firat Nebioglu, Bingqian Qu, Mila M. Leuthold[1], Yi Ni, Pascal Mutz, Jürgen Beneke[5], Holger Erfle, Stephan Urban, Ralf Bartenschlager

Identification of Host Cell Factors involved in HBsAg Secretion
17th Schauinsland Joint Retreat; Freiburg, Germany (2018)

6.2 Publications

Bingqian Qu[#], **Firat Nebioglu**[#], Mila M. Leuthold, Yi Ni, Pascal Mutz, Jürgen Beneke, Holger Erfle, Florian W.R. Vondran, Ralf Bartenschlager, Stephan Urban
#These authors contributed equally to the work

Dual role of neddylation for transcription of hepatitis B virus RNAs from cccDNA and secretion of viral surface antigen (submitted to JHEP Reports)

Daniela Stadler, Martin Kächele, Julia Hess, Alisha N. Jones, Christian Urban, Jessica Schneider, Yuchen Xia, Andreas Oswald, **Firat Nebioglu**, Romina Bester, Felix Lasitschka, Marc Ringelhan, Chunkyu Ko, Wen-Min Chou, Maarten van de Klundert, Jochen M. Wettengel, Peter Schirmacher, Mathias Heikenwalder, Sabrina Schreiner, Andreas Pichlmair, Ralf Bartenschlager, Michael Sattler, Kristian Unger, Ulrike Protzer

Interferon-induced degradation of the persistent hepatitis B virus cccDNA form depends on ISG20 EMBO Rep. 2021 Jun 4;22(6):e49568. doi: 10.15252/embr.201949568

7 Appendix

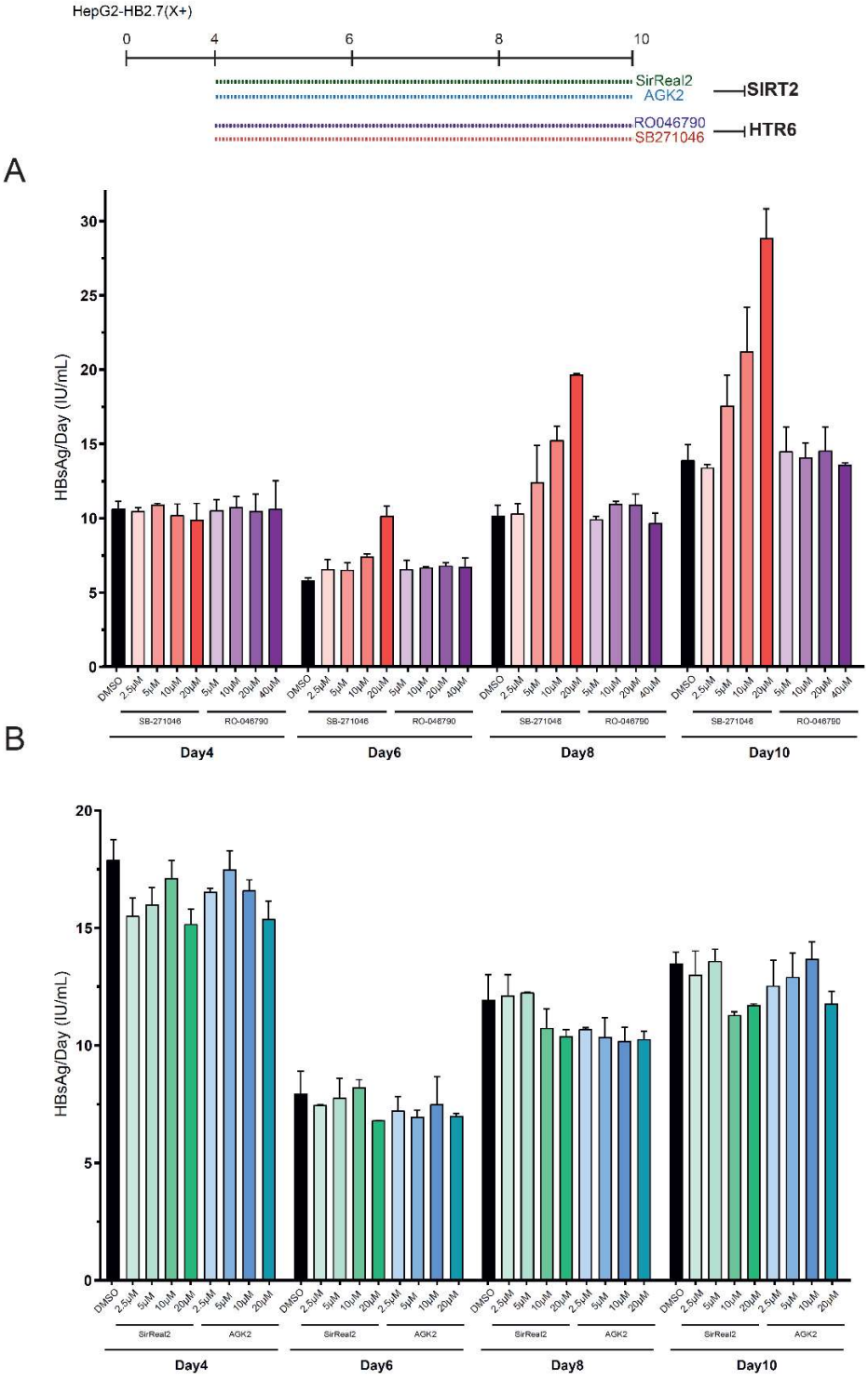

Figure 7.1. **Effect of small molecule antagonist of HTR6 and SIRT2 on HBsAg secretion**
HepG2-HB2.7 (X+) cells were treated with **A)** HTR6 inhibitors (RO046790 and SB271046) or **B)** SIRT2 inhibitors (SirReal2 and AGK2) starting at day4 post-seeding for 6 days. Collected supernatants from the depicted time-points used for HBsAg ELISA
The figure data is used in Qu, B. & Nebioglu, F. *et al*[420]

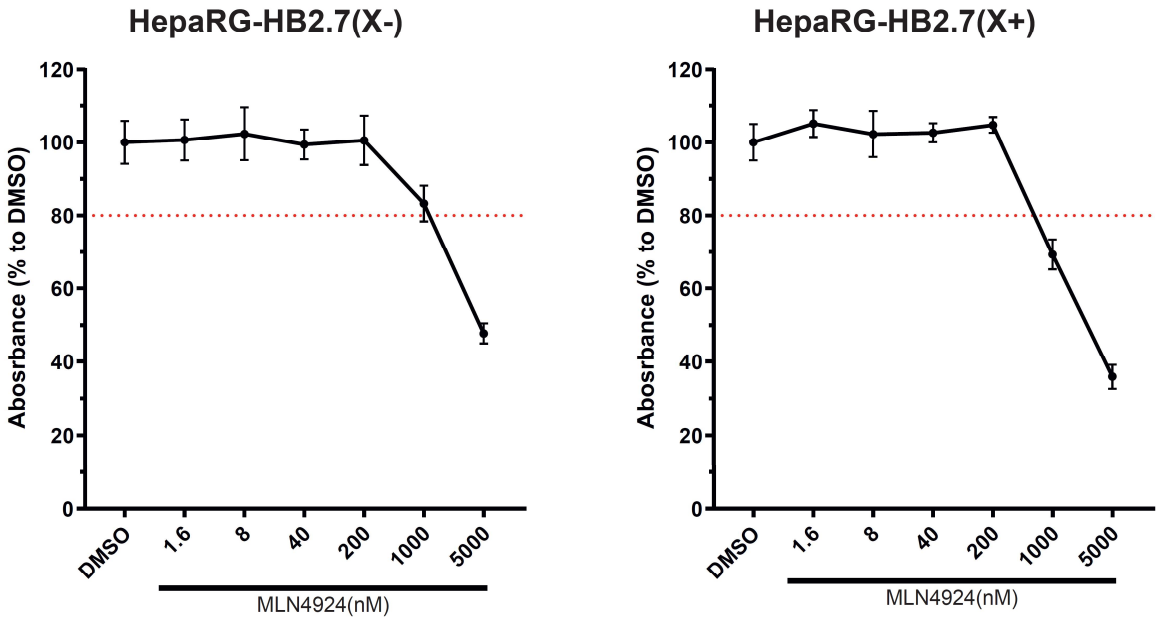

Figure 7.2. **Tolerance of HepaRG-HB2.7(X+/-) cells to MLN4924 treatment**

HepaRG-HB2.7 (-/+) cell lines were seeded and cultured one week before MLN4924 treatment. WST-1 assays were performed on both HepaRG-HB2.7(X-/+) cell lines at day6 post MLN4924 treatment. The concentrations below 80% were regarded as toxic.

The figure data is used in Qu, B. & Nebioglu, F. *et al*[420]

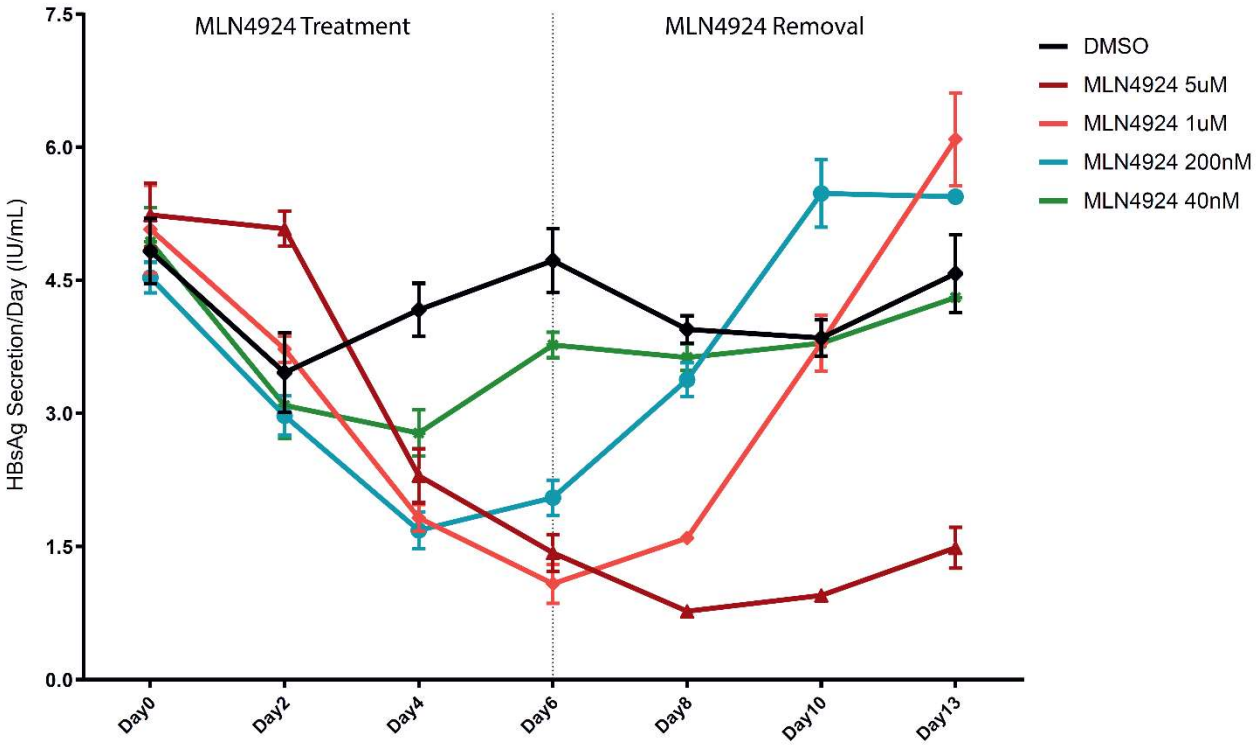

Figure 7.3. **Rebound of the HBsAg secretion upon MLN4924 removal**

HepaRG-HB2.7(X+) cells were treated with different concentrations of MLN4924 for 6 days. Removal of the MLN4924 drug leads rebound of the HBsAg values in 2 and 4 days post drug removal for 200nM and 1000nM concentrations.

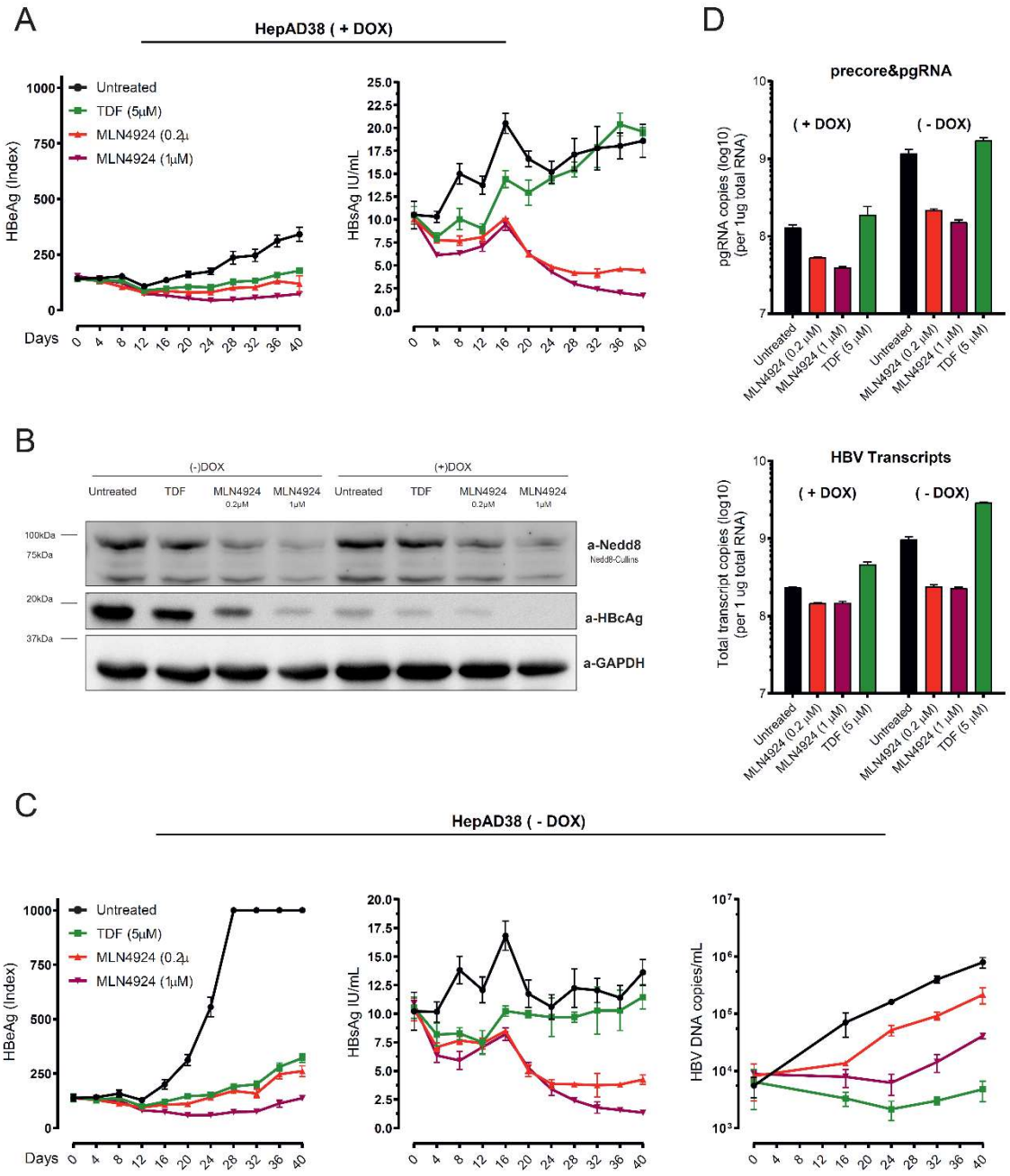

Figure 7.4. **MLN4924 shows a dual effect against HBV in HepAD38 model (Rep2)**

HepAD38 cells were seeded and maintained in the presence of doxycycline (+DOX) for 14 days (day -14 to 0). MLN4924 (0.2 and 1 μM) and Tenofovir (5 μM) treatments started in both +DOX and -DOX conditions for 40 days. In every four days, the culture medium was collected **(A)** In +DOX condition (pgRNA expression is repressed), HBsAg and HBeAg levels were shown until day40 **(B)** For both -/+ DOX conditions, cells on day40 post treatment were lysed. The levels of neddylated Cullin proteins and HBcAg were measured. **(C)** HBsAg, HBeAg, and total DNA from the supernatant were shown in -DOX condition for 40 days (**D**) Levels of intracellular pgRNA/preCoreRNA and total transcripts on day40 in both -/+ DOX conditions were depicted. The indicated results are from the second repetition.

HBV DNA and RNA quantifications were performed by Dr.Yi Ni and Dr. Bingqian Qu, respectively.

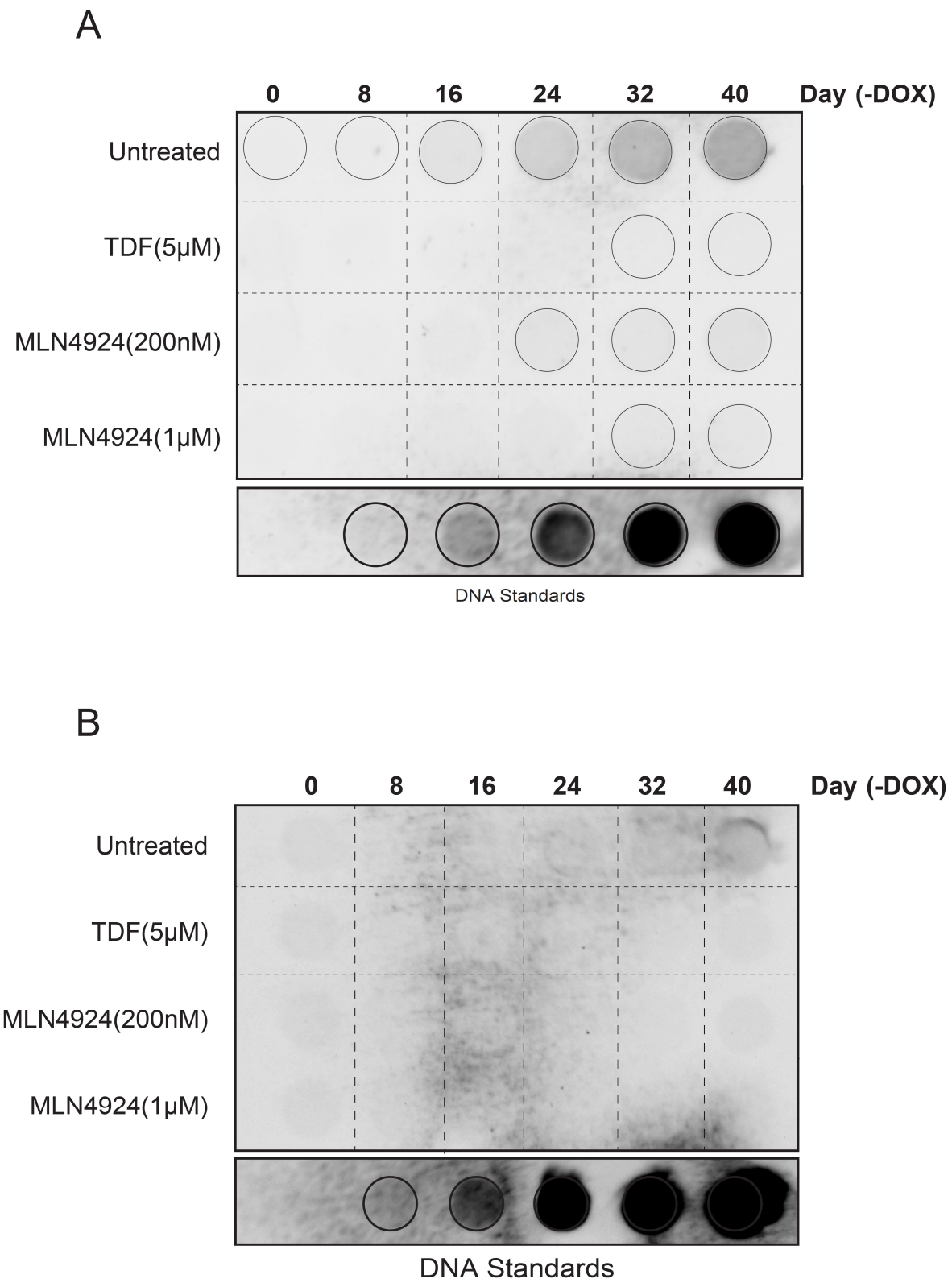

Figure 7.5. **DNA dot blot analysis of the MLN4924 treated HepAD38 cell supernatants**
HepAD38 cells supernatants were applied to DNA dot blot from untreated, TDF and MLN4924 treated conditions. 1:5 serially diluted DNA standards were added aside. Results from **A)** repetition1 and **B)** repetition2 are shown. DNA Copies: $1{,}6x10^6$, $8x10^6$, $4x10^7$, $2x10^8$, $1x10^9$, $5x10^9$

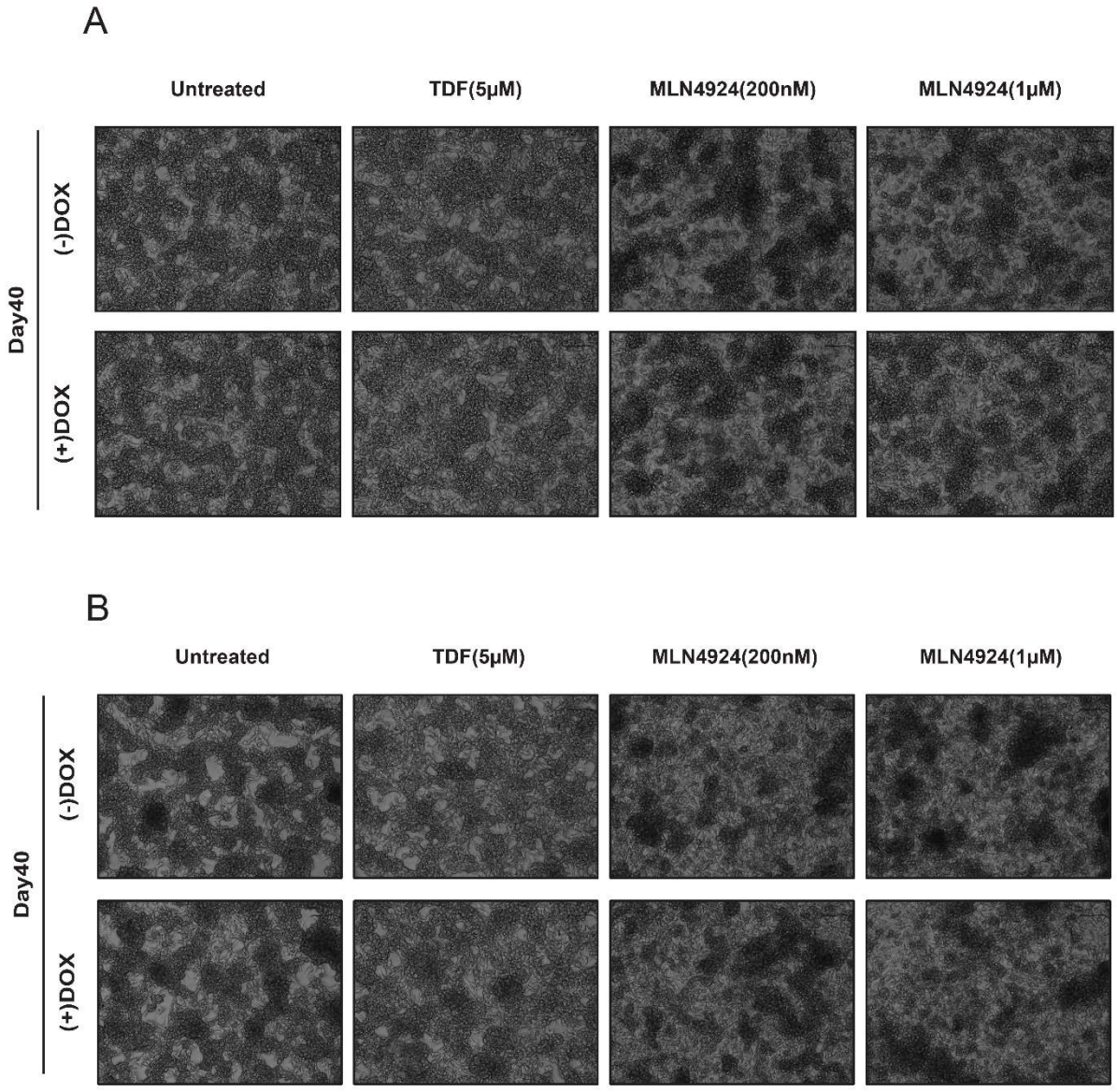

Figure 7.6. **Microscopic examination of HepAD38 cell under long-term MLN4924 treatment**
Confluency of the HepAD38 cells was examined at day40 post drug treatment for (-)DOX and(+)DOX conditions.
Representative images from **(A)** repetition1 and **(B)** repetition2 were depicted.

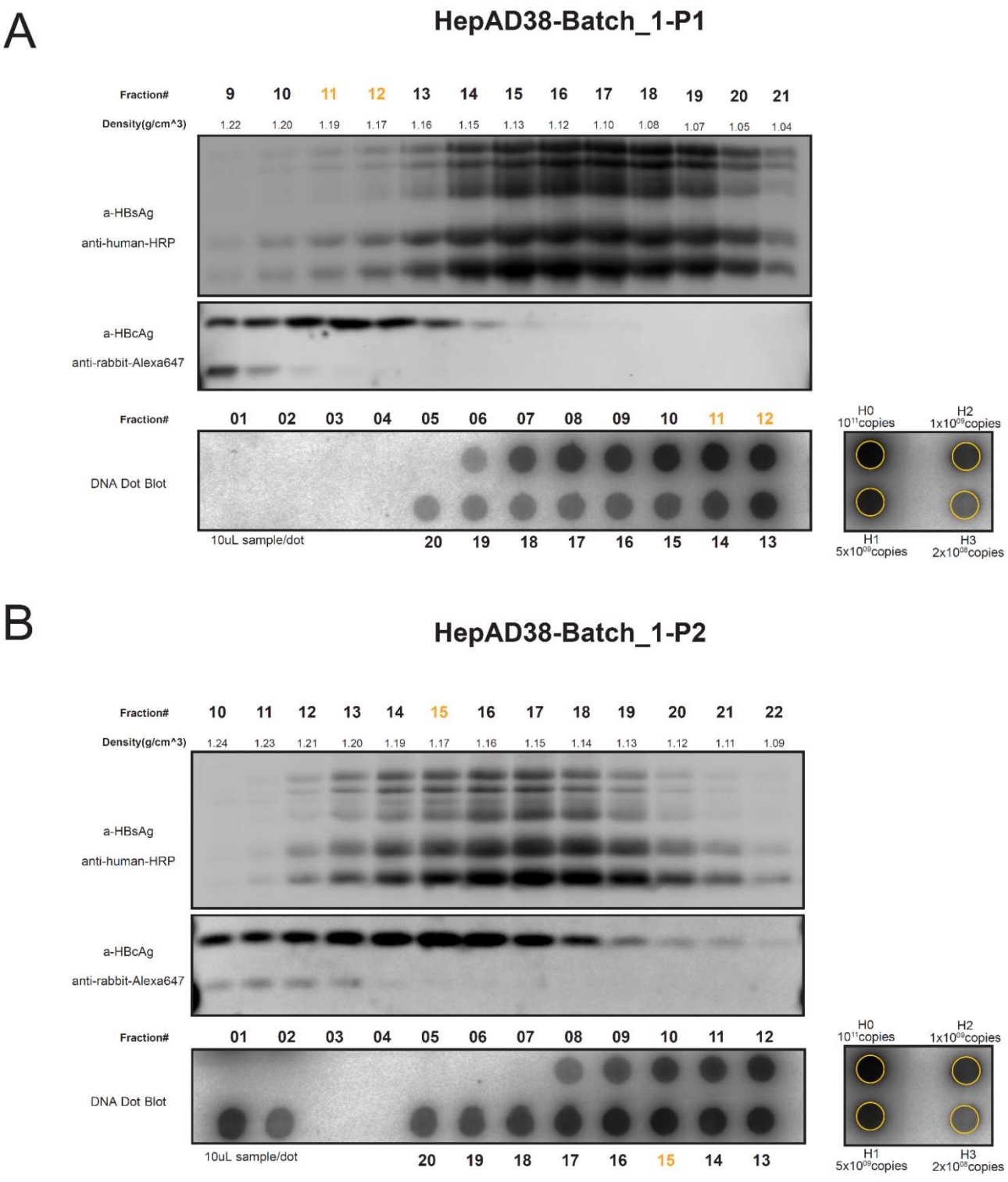

Figure 7.7. **Characterization of purified HepAD38 supernatants for HBV parameters**

HBV sucrose fractions from two independent HBV purifications of batch1 were characterized for HBsAg, HBcAg, and DNA dot blot. The purification **A)** number 1 (P1) and **B)** number 2 (P2) are shown. The DNA dot blot experiment was performed together with Dr.Stephan Seitz.

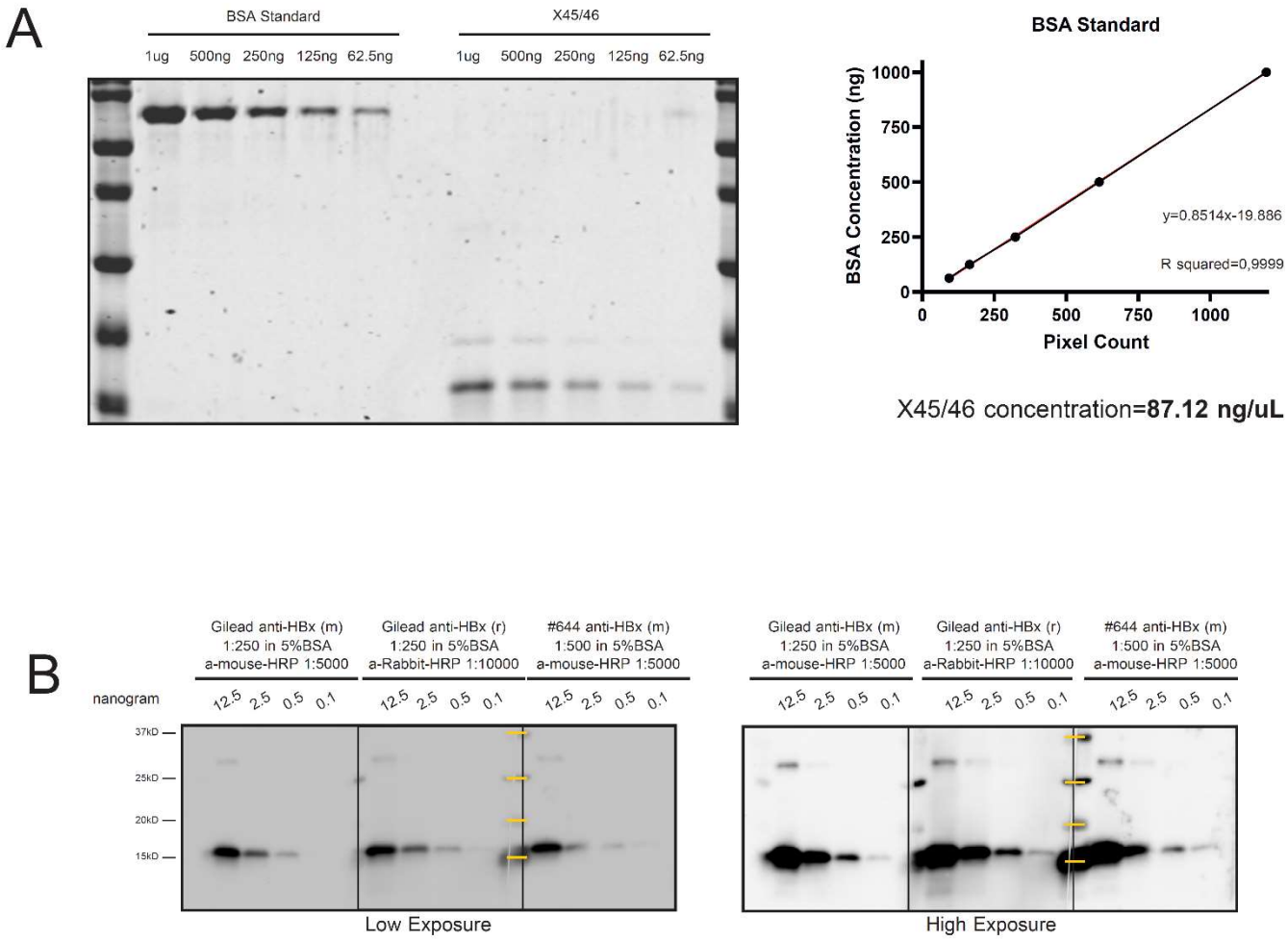

Figure 7.8. **HBx antibodies' Sensitivity Determination**

A) Concentration of recombinant X proteins stock (X45/46) was calculated by quantification of signal intensities of BSA standard and X45/46 from coomassie gel. X recombinant protein (X45/46) was provided by AG Urban.

B) Using recombinant HBx protein, Gilead and homemade HBx specific antibodies were tested for sensitivity comparison.

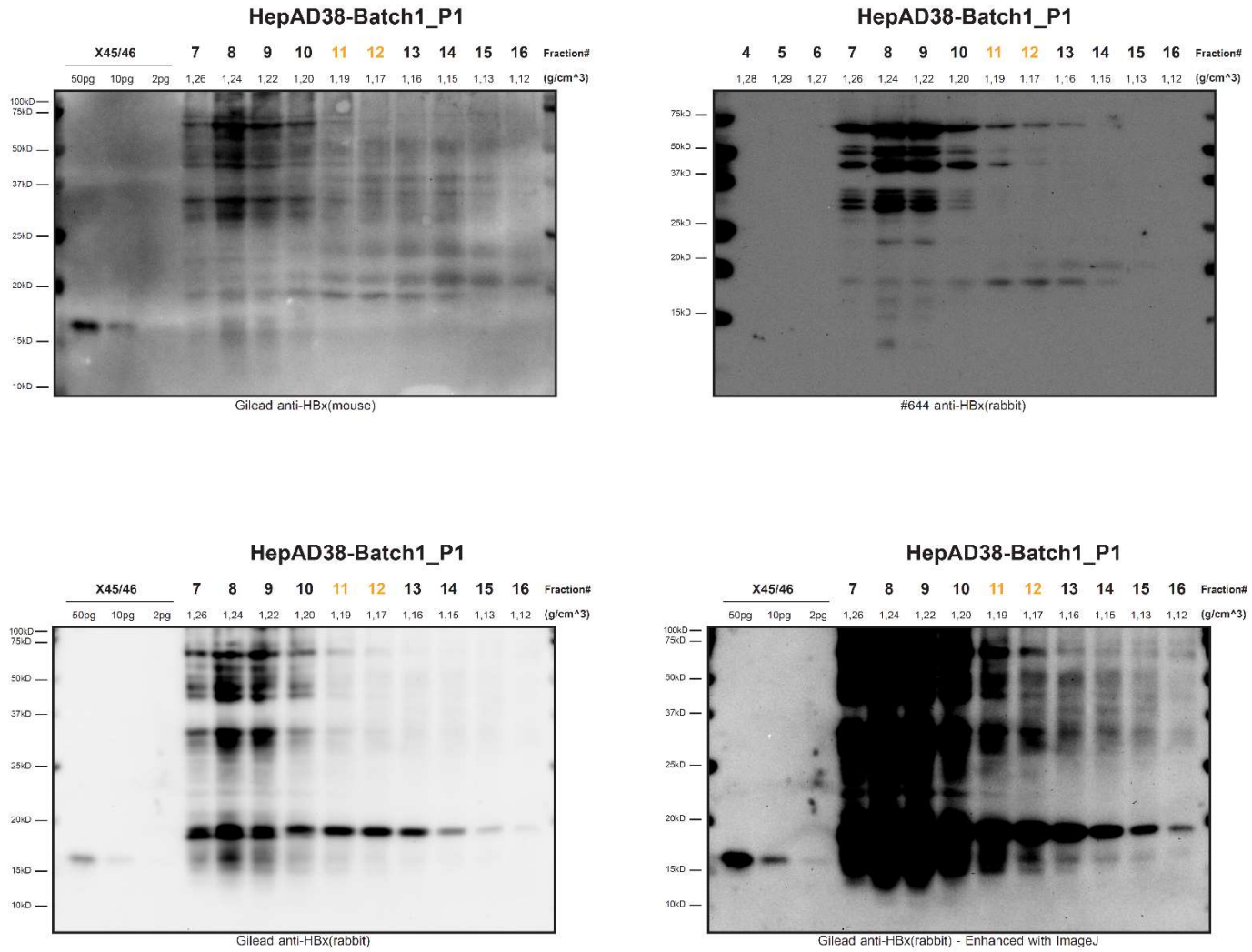

Figure 7.9. **Western blotting of HepAD38 sucrose fraction for detection of HBx protein**
Different HBx antibodies, namely Gilead anti-HBx (mouse and rabbit) and homemade #644 (rabbit) were used to detect HBx protein in the sucrose fractions of HepAD38 purifications.

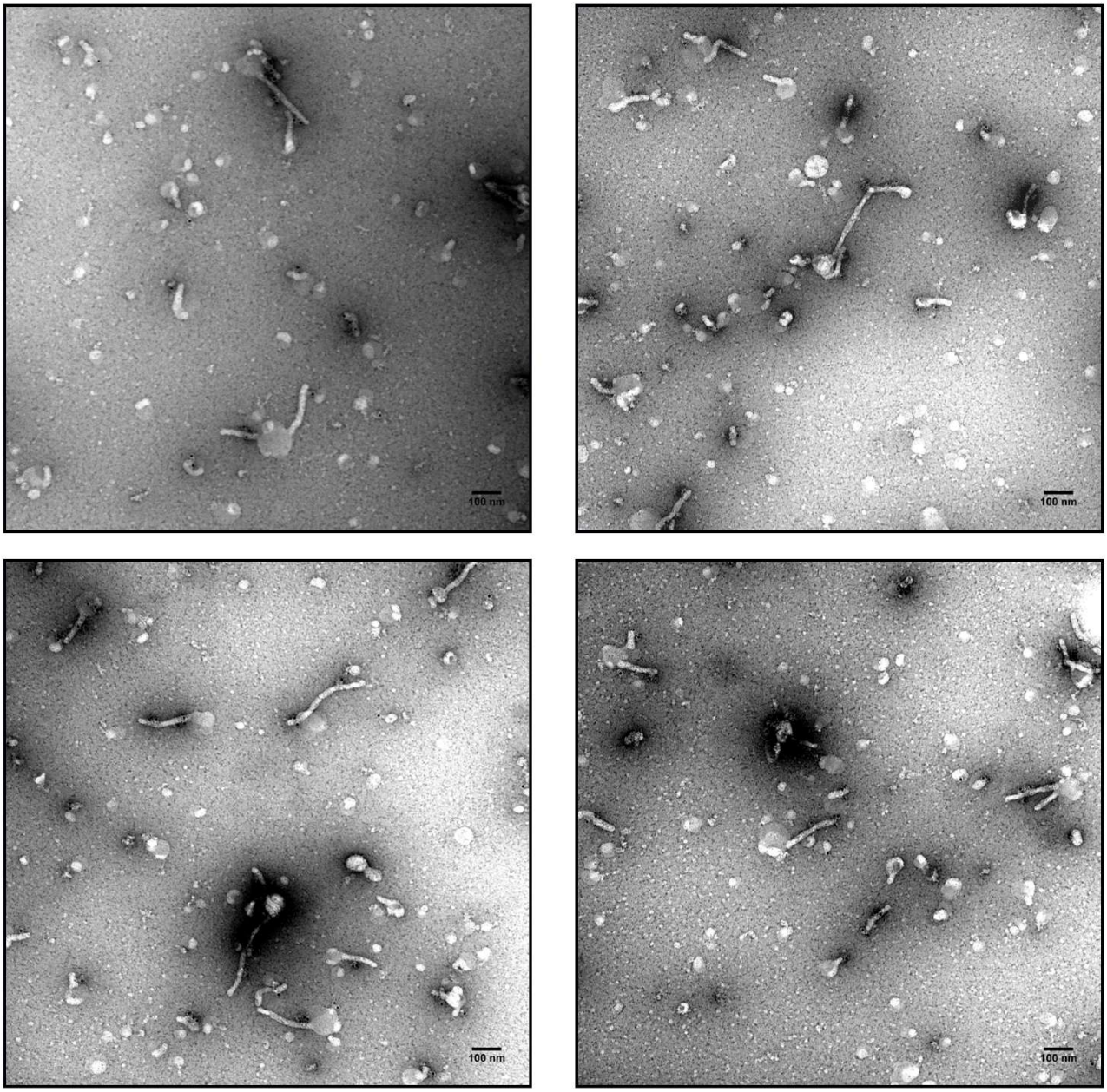

Figure 7.10. **Immuno-gold labeling of the SVP filaments with L specific antibodies**

SVPs particles purified from HepG2-HB2.7 cells were immuno-gold labeled with PreS1 specific antibodies (AP-1) and examined for the localization of L proteins.

The experiment was performed together with Uta Haselmann.

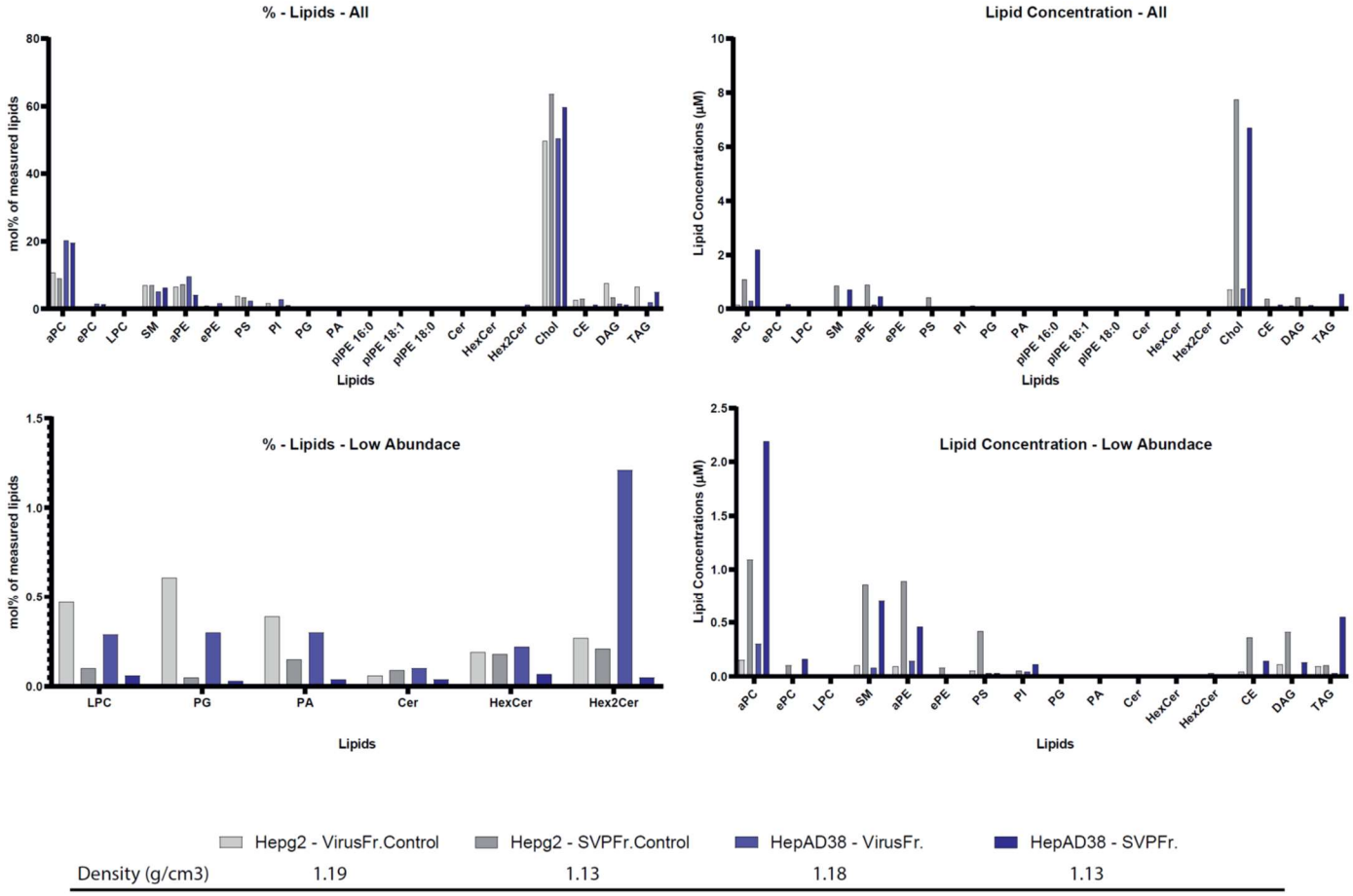

Figure 7.11. **Preliminary lipidome results of HepG2 and HepAD38 sucrose fractions**

Sucrose fractions of the indicated densities were submitted for lipidome analysis for HepG2 and HepAD38 cells. The samples were directly applied to methanol following sucrose removal. The high-density and low-density fractions were used to separate virions from SVPs.

Table 7.1. List of siRNA used in the HBsAg mini-screen

Gene Name	Gene Name / Identifier	siRNA#	siRNA Catalog Number	Company
USP1	**ubiquitin specific peptidase 1**	siRNA#1	s14723	Silencer Select Ambion
Ensemble	ENSG00000162607	siRNA#2	s14724	Silencer Select Ambion
Entrez ID	7398	siRNA#3	s14725	Silencer Select Ambion
USP12	**ubiquitin specific peptidase 12**	siRNA#1	s47595	Silencer Select Ambion
Ensemble	ENSG00000152484	siRNA#2	s47596	Silencer Select Ambion
Entrez ID	219333	siRNA#3	s47597	Silencer Select Ambion
USP19	**ubiquitin specific peptidase 19**	siRNA#1	s21339	Silencer Select Ambion
Ensemble	ENSG00000172046	siRNA#2	s21340	Silencer Select Ambion
Entrez ID	10869	siRNA#3	s21341	Silencer Select Ambion
USP30	**ubiquitin specific peptidase 30**	siRNA#1	s39399	Silencer Select Ambion
Ensemble	ENSG00000135093	siRNA#2	s39400	Silencer Select Ambion
Entrez ID	84749	siRNA#3	s39401	Silencer Select Ambion
USP34	**Ubiquitin Specific Peptidase 34**	siRNA#1	s18779	Silencer Select Ambion
Ensemble	ENSG00000115464	siRNA#2	s18780	Silencer Select Ambion
Entrez ID	9736	siRNA#3	s18781	Silencer Select Ambion
USP35	**ubiquitin specific peptidase 35**	siRNA#1	s33304	Silencer Select Ambion
Ensemble	ENSG00000118369	siRNA#2	s33305	Silencer Select Ambion
Entrez ID	57558	siRNA#3	s33306	Silencer Select Ambion
OTUD7A	**OTU Deubiquitinase 7A**	siRNA#1	s46284	Silencer Select Ambion
Ensemble	ENSG00000169918	siRNA#2	s46285	Silencer Select Ambion
Entrez ID	161725	siRNA#3	s46286	Silencer Select Ambion
UBE2Q2	**Ubiquitin Conjugating Enzyme E2 Q2**	siRNA#1	s41043	Silencer Select Ambion
Ensemble	ENSG00000140367	siRNA#2	s41044	Silencer Select Ambion
Entrez ID	92912	siRNA#3	s41045	Silencer Select Ambion
UBE2T	**Ubiquitin Conjugating Enzyme E2 T**	siRNA#1	s26459	Silencer Select Ambion

Ensemble	ENSG00000077152	siRNA#2	s26460	Silencer Select Ambion
Entrez ID	29089	siRNA#3	s26461	Silencer Select Ambion
UBXN1	**UBX domain-containing protein 1**	siRNA#1	s27291	Silencer Select Ambion
Ensemble	ENSG00000162191	siRNA#2	s27292	Silencer Select Ambion
Entrez ID	51035	siRNA#3	s27293	Silencer Select Ambion
UBE2V2	**Ubiquitin Conjugating Enzyme E2 V2**	siRNA#1	s14601	Silencer Select Ambion
Ensemble	ENSG00000169139	siRNA#2	s14602	Silencer Select Ambion
Entrez ID	7336	siRNA#3	s14603	Silencer Select Ambion
UBE2E1	**Ubiquitin Conjugating Enzyme E2 E1**	siRNA#1	s560	Silencer Select Ambion
Ensemble	ENSG00000170142	siRNA#2	s561	Silencer Select Ambion
Entrez ID	7324	siRNA#3	s562	Silencer Select Ambion
UBE2D3	**Ubiquitin Conjugating Enzyme E2 D3**	siRNA#1	s14577	Silencer Select Ambion
Ensemble	ENSG00000109332	siRNA#2	s14578	Silencer Select Ambion
Entrez ID	7323	siRNA#3	s14579	Silencer Select Ambion
UBE2D2	**Ubiquitin Conjugating Enzyme E2 D2**	siRNA#1	s14574	Silencer Select Ambion
Ensemble	ENSG00000131508	siRNA#2	s14575	Silencer Select Ambion
Entrez ID	7322	siRNA#3	s14576	Silencer Select Ambion
RNF11	**Ring Finger Protein 11**	siRNA#1	s25670	Silencer Select Ambion
Ensemble	ENSG00000123091	siRNA#2	s25671	Silencer Select Ambion
Entrez ID	26994	siRNA#3	s25672	Silencer Select Ambion
NEDD4	**Neural Precursor Cell Expressed, Developmentally Down-Regulated 4**	siRNA#1	s9415	Silencer Select Ambion
Ensemble	ENSG00000069869	siRNA#2	s9416	Silencer Select Ambion
Entrez ID	4734	siRNA#3	s9417	Silencer Select Ambion
DST	**Dystonin**	siRNA#1	s2065	Silencer Select Ambion
Ensemble	ENSG00000151914	siRNA#2	s2066	Silencer Select Ambion
Entrez ID	667	siRNA#3	s2067	Silencer Select Ambion
ARRDC1	**Arrestin Domain Containing 1**	siRNA#1	s41001	Silencer Select Ambion
Ensemble	ENSG00000197070	siRNA#2	s41002	Silencer Select Ambion
Entrez ID	92714	siRNA#3	s41003	Silencer Select Ambion

WBP2	**WW Domain Binding Protein 2**	siRNA#1	s24092	Silencer Select Ambion
Ensemble	ENSG00000132471	siRNA#2	s24093	Silencer Select Ambion
Entrez ID	23558	siRNA#3	s24094	Silencer Select Ambion
STAM2	**Signal transducing adaptor molecule (SH3 domain and ITAM motif)**	siRNA#1	s20030	Silencer Select Ambion
Ensemble	ENSG00000115145	siRNA#2	s20031	Silencer Select Ambion
Entrez ID	10254	siRNA#3	s20032	Silencer Select Ambion
TNKS	**Tankyrase**	siRNA#1	s16480	Silencer Select Ambion
Ensemble	ENSG00000173273	siRNA#2	s16481	Silencer Select Ambion
Entrez ID	8658	siRNA#3	s16482	Silencer Select Ambion
DCAF12	**DDB1 And CUL4 Associated Factor 12**	siRNA#1	s24626	Silencer Select Ambion
Ensemble	ENSG00000198876	siRNA#2	s24627	Silencer Select Ambion
Entrez ID	25853	siRNA#3	s24628	Silencer Select Ambion
DCUN1D1	**Defective In Cullin Neddylation 1 Domain Containing 1**	siRNA#1	s28890	Silencer Select Ambion
Ensemble	ENSG00000043093	siRNA#2	s28891	Silencer Select Ambion
Entrez ID	54165	siRNA#3	s28892	Silencer Select Ambion
DCUN1D2	**Defective In Cullin Neddylation 1 Domain Containing 2**	siRNA#1	s30441	Silencer Select Ambion
Ensemble	ENSG00000150401	siRNA#2	s30442	Silencer Select Ambion
Entrez ID	55208	siRNA#3	s30443	Silencer Select Ambion
DCUN1D3	**Defective In Cullin Neddylation 1 Domain Containing 3**	siRNA#1	s42682	Silencer Select Ambion
Ensemble	ENSG00000188215	siRNA#2	s42683	Silencer Select Ambion
Entrez ID	123879	siRNA#3	s42684	Silencer Select Ambion
DCUN1D4	**Defective In Cullin Neddylation 1 Domain Containing 4**	siRNA#1	s23127	Silencer Select Ambion
Ensemble	ENSG00000109184	siRNA#2	s23128	Silencer Select Ambion
Entrez ID	23142	siRNA#3	s23129	Silencer Select Ambion
DCUN1D5	**Defective In Cullin Neddylation 1 Domain Containing 5**	siRNA#1	s38745	Silencer Select Ambion
Ensemble	ENSG00000137692	siRNA#2	s38746	Silencer Select Ambion
Entrez ID	84259	siRNA#3	s38747	Silencer Select Ambion

NEDD8	**Neural Precursor Cell Expressed, Developmentally Down-Regulated 8**	siRNA#1	s9424	Silencer Select Ambion
Ensemble	ENSG00000129559	siRNA#2	s9425	Silencer Select Ambion
Entrez ID	4738	siRNA#3	s9426	Silencer Select Ambion
UBE2M	**Ubiquitin Conjugating Enzyme E2 M**	siRNA#1	s17229	Silencer Select Ambion
Ensemble	ENSG00000130725	siRNA#2	s17230	Silencer Select Ambion
Entrez ID	9040	siRNA#3	s17231	Silencer Select Ambion
UBE2F	**Ubiquitin Conjugating Enzyme E2 F**	siRNA#1	s44387	Silencer Select Ambion
Ensemble	ENSG00000184182	siRNA#2	s44388	Silencer Select Ambion
Entrez ID	140739	siRNA#3	s44389	Silencer Select Ambion
NAE1	**NEDD8 Activating Enzyme E1 Subunit 1**	siRNA#1	s16975	Silencer Select Ambion
Ensemble	ENSG00000159593	siRNA#2	s16976	Silencer Select Ambion
Entrez ID	8883	siRNA#3	s16977	Silencer Select Ambion
CAND1	**Cullin Associated And Neddylation Dissociated 1**	siRNA#1	s31616	Silencer Select Ambion
Ensemble	ENSG00000111530	siRNA#2	s31617	Silencer Select Ambion
Entrez ID	55832	siRNA#3	s31618	Silencer Select Ambion
ABAT	**4-aminobutyrate aminotransferase**	siRNA#1	s843	Silencer Select Ambion
Ensemble	ENSG00000183044	siRNA#2	s844	Silencer Select Ambion
Entrez ID	18	siRNA#3	s845	Silencer Select Ambion
ABCA1	**ATP-binding cassette, sub-family A (ABC1), member 1**	siRNA#1	s846	Silencer Select Ambion
Ensemble	ENSG00000165029	siRNA#2	s847	Silencer Select Ambion
Entrez ID	19	siRNA#3	s848	Silencer Select Ambion
AR	**Androgen receptor**	siRNA#1	s1538	Silencer Select Ambion
Ensemble	ENSG00000169083	siRNA#2	s1539	Silencer Select Ambion
Entrez ID	367	siRNA#3	s1540	Silencer Select Ambion
ATP6V1B2	**ATPase, H+ transporting, lysosomal V1 subunit B2**	siRNA#1	s1797	Silencer Select Ambion
Ensemble	ENSG00000147416	siRNA#2	s1798	Silencer Select Ambion
Entrez ID	526	siRNA#3	s1799	Silencer Select Ambion
BCR	**Breakpoint cluster region**	siRNA#1	s1949	Silencer Select Ambion

Ensemble	ENSG00000186716	siRNA#2	s1948	Silencer Select Ambion
Entrez ID	613	siRNA#3	s1947	Silencer Select Ambion
ITPR2	**Inositol 1,4,5-triphosphate receptor, type 2**	siRNA#1	s7636	Silencer Select Ambion
Ensemble	ENSG00000123104	siRNA#2	s7635	Silencer Select Ambion
Entrez ID	3709	siRNA#3	s7634	Silencer Select Ambion
CACNA1A	**Calcium channel, voltage-dependent, P/Q type, alpha 1A subunit**	siRNA#1	s2278	Silencer Select Ambion
Ensemble	ENSG00000141837	siRNA#2	s2277	Silencer Select Ambion
Entrez ID	773	siRNA#3	s2279	Silencer Select Ambion
CYSLTR1	**Cysteinyl leukotriene receptor 1**	siRNA#1	s21220	Silencer Select Ambion
Ensemble	ENSG00000173198	siRNA#2	s21219	Silencer Select Ambion
Entrez ID	10800	siRNA#3	s21221	Silencer Select Ambion
GLRA1	**Glycine receptor, alpha 1**	siRNA#1	s5831	Silencer Select Ambion
Ensemble	ENSG00000145888	siRNA#2	s5829	Silencer Select Ambion
Entrez ID	2741	siRNA#3	s5830	Silencer Select Ambion
GLRB	**Glycine receptor, beta**	siRNA#1	s5835	Silencer Select Ambion
Ensemble	ENSG00000109738	siRNA#2	s5836	Silencer Select Ambion
Entrez ID	2743	siRNA#3	s5837	Silencer Select Ambion
GPT	**Glutamic-pyruvate transaminase (alanine aminotransferase)**	siRNA#1	s6101	Silencer Select Ambion
Ensemble	ENSG00000167701	siRNA#2	s6102	Silencer Select Ambion
Entrez ID	2875	siRNA#3	s6103	Silencer Select Ambion
GRIK2	**Glutamate receptor, ionotropic, kainate 2**	siRNA#1	s6155	Silencer Select Ambion
Ensemble	ENSG00000164418	siRNA#2	s6156	Silencer Select Ambion
Entrez ID	2898	siRNA#3	s6157	Silencer Select Ambion
GRIN2B	**Glutamate ionotropic receptor NMDA type subunit 2B**	siRNA#1	s6173	Silencer Select Ambion
Ensemble	ENSG00000273079	siRNA#2	s6174	Silencer Select Ambion
Entrez ID	2904	siRNA#3	s6175	Silencer Select Ambion
ITGAV	**Integrin, alpha V (vitronectin receptor, alpha polypeptide, antigen CD51)**	siRNA#1	s7568	Silencer Select Ambion

Ensemble	ENSG00000138448	siRNA#2	s7569	Silencer Select Ambion
Entrez ID	3685	siRNA#3	s7570	Silencer Select Ambion
HTR6	**5-hydroxytryptamine (serotonin) receptor 6**	siRNA#1	s7059	Silencer Select Ambion
Ensemble	ENSG00000158748	siRNA#2	s7060	Silencer Select Ambion
Entrez ID	3362	siRNA#3	s7061	Silencer Select Ambion
IGF1R	**Insulin-like growth factor 1 receptor**	siRNA#1	s7211	Silencer Select Ambion
Ensemble	ENSG00000140443	siRNA#2	s7212	Silencer Select Ambion
Entrez ID	3480	siRNA#3	s223918	Silencer Select Ambion
HSD17B1	**Hydroxysteroid (17-beta) dehydrogenase 1**	siRNA#1	s6938	Silencer Select Ambion
Ensemble	ENSG00000108786	siRNA#2	s6939	Silencer Select Ambion
Entrez ID	3292	siRNA#3	s6940	Silencer Select Ambion
KCNMB2	**Potassium large conductance calcium-activated channel, subfamily M, beta member 2**	siRNA#1	s19997	Silencer Select Ambion
Ensemble	ENSG00000197584	siRNA#2	s19998	Silencer Select Ambion
Entrez ID	10242	siRNA#3	s19999	Silencer Select Ambion
KCNN4	**Potassium intermediate/small conductance calcium-activated channel, subfamily N, member 4**	siRNA#1	s7801	Silencer Select Ambion
Ensemble	ENSG00000104783	siRNA#2	s7802	Silencer Select Ambion
Entrez ID	3783	siRNA#3	s7803	Silencer Select Ambion
MAPK12	**Mitogen-activated protein kinase 12**	siRNA#1	s12467	Silencer Select Ambion
Ensemble	ENSG00000188130	siRNA#2	s12468	Silencer Select Ambion
Entrez ID	6300	siRNA#3	s12469	Silencer Select Ambion
MMP14	**Matrix metallopeptidase 14 (membrane-inserted)**	siRNA#1	s8877	Silencer Select Ambion
Ensemble	ENSG00000157227	siRNA#2	s8878	Silencer Select Ambion
Entrez ID	4323	siRNA#3	s8879	Silencer Select Ambion
OXTR	**Oxytocin receptor**	siRNA#1	s9946	Silencer Select Ambion
Ensemble	ENSG00000180914	siRNA#2	s9947	Silencer Select Ambion
Entrez ID	5021	siRNA#3	s9948	Silencer Select Ambion

PDGFA	**Platelet-derived growth factor alpha polypeptide**	siRNA#1	s10228	Silencer Select Ambion
Ensemble	ENSG00000197461	siRNA#2	s10229	Silencer Select Ambion
Entrez ID	5154	siRNA#3	s10230	Silencer Select Ambion
PROC	**Protein C (inactivator of coagulation factors Va and VIIIa)**	siRNA#1	s11215	Silencer Select Ambion
Ensemble	ENSG00000115718	siRNA#2	s11216	Silencer Select Ambion
Entrez ID	5624	siRNA#3	s11217	Silencer Select Ambion
SIRT2	**Sirtuin 2**	siRNA#1	s22706	Silencer Select Ambion
Ensemble	ENSG00000068903	siRNA#2	s22707	Silencer Select Ambion
Entrez ID	22933	siRNA#3	s22708	Silencer Select Ambion
CNR2	**Cannabinoid receptor 2 (macrophage)**	siRNA#1	s3263	Silencer Select Ambion
Ensemble	ENSG00000188822	siRNA#2	s3264	Silencer Select Ambion
Entrez ID	1269	siRNA#3	s3265	Silencer Select Ambion
RXRA	**Retinoid X receptor, alpha**	siRNA#1	s12384	Silencer Select Ambion
Ensemble	ENSG00000186350	siRNA#2	s12385	Silencer Select Ambion
Entrez ID	6256	siRNA#3	s12386	Silencer Select Ambion
MADD	**MAP-kinase activating death domain**	siRNA#1	s16313	Silencer Select Ambion
Ensemble	ENSG00000110514	siRNA#2	s16314	Silencer Select Ambion
Entrez ID	8567	siRNA#3	s16315	Silencer Select Ambion
NMRAL1	**NmrA-like family domain containing 1**	siRNA#1	s33004	Silencer Select Ambion
Ensemble	ENSG00000153406	siRNA#2	s33005	Silencer Select Ambion
Entrez ID	57407	siRNA#3	s33006	Silencer Select Ambion
CYTH2	**Pleckstrin homology, Sec7 and coiled-coil domains 2 (cytohesin-2)**	siRNA#1	s17718	Silencer Select Ambion
Ensemble	ENSG00000105443	siRNA#2	s17719	Silencer Select Ambion
Entrez ID	9266	siRNA#3	s17720	Silencer Select Ambion
ENOX2	**Ecto-NOX disulfide-thiol exchanger 2**	siRNA#1	s20571	Silencer Select Ambion
Ensemble	ENSG00000165675	siRNA#2	s20572	Silencer Select Ambion
Entrez ID	10495	siRNA#3	s20573	Silencer Select Ambion
GPR35	**G protein-coupled receptor 35**	siRNA#1	s6063	Silencer Select Ambion

Ensemble	ENSG00000178623	siRNA#2	s6064	Silencer Select Ambion
Entrez ID	2859	siRNA#3	s6065	Silencer Select Ambion
NTsiRNA	**Non-Targeting siRNA**	UGGUUUACAUGUCGACUAATT		Silencer Select Ambion
		UUAGUCGACAUGUAAACCATT		

Table 7.2. HBsAg mini-screen results

			% HBsAg ELISA Values (Normalized to NTsiRNA)						HBsAG Average of All SiRNAs	HBsAG St.Dev of All siRNAs	% Firefly Luciferase Signal (Normalized to NTsiRNA)						FLUC Average of All SiRNAs	FLUC St.Dev of All siRNAs
									145,37	67,72							170,11	63,24
siRNA ID	Entrez Gene ID	Gene_siRNA#	Rep1	Rep2	Rep3	Rep4	Average	St.Dev	Z-Score	p-Value	Rep1	Rep2	Rep3	Rep4	Average	St.Dev	Z-Score	p-Value
s39399	84749	USP30_1	22,55	32,55	19,24	20,53	23,72	5,23	-1,80	0,00	102,62	107,09	88,58	93,42	97,93	8,44	-1,14	0,03
s22706	22933	SIRT2_1	24,34	21,51	57,52		34,46	20,02	-1,64	0,01	178,06	191,76	157,12		175,64	17,44	0,09	0,87
s3264	1269	CNR2_2	33,62	39,64	39,22		37,49	3,36	-1,59	0,01	135,32	115,61	139,61		130,18	12,80	-0,63	0,29
s1947	613	BCR_3	55,88	40,53	43,86		46,76	8,07	-1,46	0,02	120,92	96,53	99,30		105,58	13,35	-1,02	0,09
s7802	3783	KCNN4_2	63,95	47,36	48,74		53,35	9,21	-1,36	0,03	229,30	201,76	226,27		219,11	15,10	0,77	0,19
s25672	26994	RNF11_3	43,69	64,65	44,85	63,45	54,16	9,91	-1,35	0,01	125,74	156,71	147,37	129,42	139,81	14,70	-0,48	0,36
s17231	9040	UBE2M_3	65,05	59,44	64,29	38,14	56,73	10,95	-1,31	0,01	119,98	130,71	140,52	109,00	125,05	13,60	-0,71	0,17
s9425	4738	NEDD8_2	46,00	60,79	62,69	57,46	56,74	6,47	-1,31	0,01	243,73	266,09	347,48	303,17	290,12	45,43	1,90	0,00
s14723	7398	USP1_1	45,74	71,31	65,07	64,18	61,58	9,54	-1,24	0,02	154,37	151,07	169,02	185,58	165,01	15,78	-0,08	0,89
s9426	4738	NEDD8_3	51,42	64,91	63,49	75,17	63,75	8,42	-1,21	0,02	256,90	290,41	305,45	313,17	291,48	24,91	1,92	0,00
s7059	3362	HTR6_1	60,31	87,33	48,85		65,50	19,76	-1,18	0,06	126,73	125,82	114,26		122,27	6,95	-0,76	0,21
s23129	23142	DCUN1D4_3	97,77	81,23	65,09	37,77	70,46	22,13	-1,11	0,04	104,93	121,76	88,05	74,30	97,26	20,59	-1,15	0,03
s26459	29089	UBE2T_1	48,96	84,50	71,87	77,88	70,80	13,38	-1,10	0,04	101,60	97,52	103,95	121,41	106,12	10,54	-1,01	0,05
s9424	4738	NEDD8_1	48,15	81,47	74,08	80,31	71,00	13,49	-1,10	0,04	193,12	208,77	211,05	197,75	202,67	8,62	0,51	0,31
s22707	22933	SIRT2_2	74,60	70,82	70,39		71,94	2,32	-1,08	0,08	152,49	154,82	129,62		145,64	13,92	-0,39	0,52
s5829	2741	GLRA1_2	70,36	93,87	54,59		72,94	19,77	-1,07	0,08	128,80	112,71	99,10		113,54	14,86	-0,89	0,14
s6065	2859	GPR35_3	61,73	104,78	55,99		74,17	26,67	-1,05	0,09	81,10	84,05	84,51		83,22	1,85	-1,37	0,02
s42683	123879	DCUN1D3_2	76,81	105,04	64,13	57,46	75,86	18,22	-1,03	0,06	203,83	217,30	197,03	184,45	200,65	13,70	0,48	0,34
s7060	3362	HTR6_2	99,50	56,53	73,68		76,57	21,63	-1,02	0,10	206,81	162,36	156,15		175,11	27,63	0,08	0,89
s17230	9040	UBE2M_2	72,57	89,80	60,94	85,12	77,11	11,26	-1,01	0,06	197,38	208,32	177,44	214,91	199,51	16,40	0,46	0,36
s44388	140739	UBE2F_2	95,43	74,34	68,61	73,60	78,00	10,30	-0,99	0,06	176,28	195,85	198,45	205,31	193,97	12,45	0,38	0,46
s8878	4323	MMP14_2	104,54	65,69	64,29		78,17	22,84	-0,99	0,11	213,95	198,16	188,88		200,33	12,68	0,48	0,42

Non-Targeting siRNA		Plate4-NT#2	85,24	79,27	73,66		79,39	5,79	-0,97	0,12	92,08	91,22	100,76		94,69	5,28	-1,19	0,05
s17720	9266	**CYTH2_3**	75,66	65,06	97,95		79,56	16,79	-0,97	0,12	209,24	225,00	206,56		213,60	9,96	0,69	0,24
s6156	2898	**GRIK2_2**	82,44	75,94	82,65		80,35	3,82	-0,96	0,12	123,17	96,70	94,79		104,89	15,86	-1,03	0,09
s33304	57558	**USP35_1**	98,69	82,10	71,34	71,35	80,87	11,19	-0,95	0,08	201,47	222,41	227,99	227,69	219,89	12,54	0,79	0,12
s20032	10254	**STAM2_3**	93,55	79,59	77,63	73,79	81,14	7,46	-0,95	0,08	102,43	95,17	84,51	75,06	89,29	12,01	-1,28	0,01
s28890	54165	**DCUN1D1_1**	80,65	84,47	90,61	69,51	81,31	7,68	-0,95	0,08	182,79	188,93	214,12	194,14	194,99	13,57	0,39	0,44
Non-Targeting siRNA		Plate3-NT#6	81,34	87,84	75,49		81,56	6,18	-0,94	0,13	101,90	101,82	97,59		100,44	2,47	-1,10	0,07
s14602	7336	**UBE2V2_2**	64,77	93,95	85,78	92,06	84,14	11,58	-0,90	0,09	162,09	185,70	146,61	192,56	171,74	21,24	0,03	0,95
s2279	773	**CACNA1A_3**	62,52	90,13	102,31		84,99	20,39	-0,89	0,15	307,94	307,16	305,75		306,95	1,11	2,16	0,00
Non-Targeting siRNA		Plate2-NT#4	86,05	85,95	87,12	88,15	86,82	0,90	-0,86	0,11	90,55	90,63	95,33	93,55	92,51	2,34	-1,23	0,02
Non-Targeting siRNA		Plate1-NT#2	71,81	97,50	95,06	86,88	87,81	10,04	-0,85	0,12	101,04	103,71	97,16	102,26	101,04	2,81	-1,09	0,04
Non-Targeting siRNA		Plate3-NT#4	96,69	94,00	76,40		89,03	11,02	-0,83	0,18	113,00	105,08	99,17		105,75	6,94	-1,02	0,09
Non-Targeting siRNA		Plate1-NT#4	97,79	88,15	86,82	83,88	89,16	5,22	-0,83	0,13	104,92	99,95	104,01	89,18	99,52	7,22	-1,12	0,03
s21340	10869	**USP19_2**	108,25	83,36	71,87	93,65	89,28	13,39	-0,83	0,13	102,77	123,26	112,42	116,64	113,77	8,58	-0,89	0,09
Non-Targeting siRNA		Plate4-NT#4	90,98	109,47	70,83		90,43	19,33	-0,81	0,20	96,82	103,93	94,12		98,29	5,07	-1,14	0,06
s7803	3783	**KCNN4_3**	83,05	105,02	83,25		90,44	12,63	-0,81	0,20	257,37	246,62	244,44		249,48	6,92	1,25	0,03
Non-Targeting siRNA		Plate2-NT#5	94,65	107,42	85,97	82,30	92,58	9,67	-0,78	0,15	86,59	88,63	106,34	84,16	91,43	10,11	-1,24	0,02
s27292	51035	**UBXN1_2**	97,50	82,79	83,06	108,51	92,96	10,77	-0,77	0,16	217,48	245,83	233,20	253,78	237,57	15,85	1,07	0,04
Non-Targeting siRNA		Plate3-NT#5	71,82	109,21	98,07		93,03	19,20	-0,77	0,22	102,40	103,66	105,36		103,80	1,49	-1,05	0,08
Non-Targeting siRNA		Plate4-NT#5	81,77	98,54	103,05		94,45	11,21	-0,75	0,23	94,70	106,53	97,89		99,71	6,12	-1,11	0,06
s12385	6256	**RXRA_2**	103,76	98,08	84,13		95,32	10,10	-0,74	0,24	173,08	182,09	143,03		166,07	20,45	-0,06	0,92
Non-Targeting siRNA		Plate3-NT#2	93,54	90,64	101,81		95,33	5,79	-0,74	0,24	85,43	94,41	99,75		93,20	7,23	-1,22	0,04
s6103	2875	**GPT_3**	98,79	101,24	88,57		96,20	6,72	-0,73	0,25	180,14	154,37	168,72		167,74	12,91	-0,04	0,96
Non-Targeting siRNA		Plate2-NT#6	100,70	102,78	84,16	97,21	96,21	7,24	-0,73	0,18	101,61	93,22	88,94	90,49	93,56	5,65	-1,21	0,02
s26461	29089	**UBE2T_3**	124,29	86,56	84,61	91,68	96,78	16,09	-0,72	0,19	432,40	620,22	557,03	657,46	566,78	98,71	6,27	0,00
Non-Targeting siRNA		Plate1-NT#3	77,98	97,15	105,63	106,59	96,84	11,49	-0,72	0,19	98,80	105,51	101,35	104,80	102,62	3,12	-1,07	0,04
s38747	84259	**DCUN1D5_3**	98,54	84,01	105,47	99,94	96,99	7,93	-0,71	0,19	134,38	138,26	125,99	125,85	131,12	6,21	-0,62	0,24
Non-Targeting siRNA		Plate2-NT#2	92,44	88,45	109,35	98,68	97,23	7,89	-0,71	0,19	94,08	107,97	100,77	106,48	102,33	6,31	-1,07	0,04
s41003	92714	**ARRDC1_3**	83,78	91,94	94,13	121,45	97,82	14,17	-0,70	0,20	173,33	184,22	191,68	231,11	195,09	25,17	0,39	0,44
s33306	57558	**USP35_3**	104,66	102,49	82,15	103,07	98,09	9,24	-0,70	0,20	142,28	141,48	156,14	162,57	150,62	10,43	-0,31	0,56
s2066	667	**DST_2**	108,77	88,00	108,64	87,14	98,14	10,57	-0,70	0,20	212,65	226,13	209,43	234,50	220,68	11,71	0,80	0,12
s7569	3685	**ITGAV_2**	112,80	99,25	84,06		98,70	14,38	-0,69	0,28	215,37	187,43	193,80		198,87	14,64	0,45	0,44
s47597	219333	**USP12_3**	82,10	106,51	113,18	96,96	99,69	11,67	-0,67	0,22	176,56	200,30	169,28	203,23	187,35	16,96	0,27	0,59
s16482	8658	**TNKS_3**	95,12	108,10	108,29	87,34	99,71	8,92	-0,67	0,22	205,86	208,67	225,01	208,61	212,04	8,75	0,66	0,19

Non-Targeting siRNA		Plate4-NT#3	116,90	85,22	97,07		99,73	16,01	-0,67	0,29	95,78	96,62	102,43		98,28	3,62	-1,14	0,06
s25670	26994	**RNF11_1**	94,52	91,22	117,93	97,68	100,34	10,41	-0,66	0,23	84,90	76,55	95,81	89,16	86,60	8,07	-1,32	0,01
Non-Targeting siRNA		Plate1-NT#6	122,76	101,90	88,77	94,11	101,89	12,93	-0,64	0,24	93,18	91,95	92,25	89,28	91,66	1,67	-1,24	0,02
s7570	3685	**ITGAV_3**	107,25	87,08	111,75		102,03	13,14	-0,64	0,31	113,39	134,83	98,96		115,72	18,05	-0,86	0,15
s2067	667	**DST_3**	112,83	100,77	116,20	79,51	102,33	14,37	-0,64	0,25	201,85	246,26	213,50	211,04	218,16	19,39	0,76	0,14
s19999	10242	**KCNMB2_3**	84,69	112,55	110,19		102,48	15,45	-0,63	0,32	217,91	210,94	191,17		206,67	13,87	0,58	0,33
s42684	123879	**DCUN1D3_3**	105,14	99,54	91,78	113,46	102,48	7,92	-0,63	0,25	182,60	176,97	200,31	205,18	191,26	13,60	0,33	0,51
s11217	5624	**PROC_3**	77,81	128,84	103,27		103,30	25,51	-0,62	0,33	119,85	137,79	113,48		123,71	12,60	-0,73	0,22
s28892	54165	**DCUN1D1_3**	90,22	96,74	119,33	107,81	103,53	11,08	-0,62	0,26	164,44	181,70	184,06	214,91	186,28	21,00	0,26	0,61
s14601	7336	**UBE2V2_1**	120,33	93,15	103,00	98,94	103,86	10,13	-0,61	0,27	175,61	159,25	171,46	165,61	167,98	7,12	-0,03	0,96
s28891	54165	**DCUN1D1_2**	119,41	122,46	94,81	83,91	105,15	16,29	-0,59	0,28	98,85	104,66	105,18	100,37	102,27	3,14	-1,07	0,04
s33005	57407	**NMRAL1_2**	80,69	85,67	152,92		106,42	40,34	-0,58	0,37	75,32	75,86	94,98		82,05	11,20	-1,39	0,02
Non-Targeting siRNA		Plate1-NT#1	100,48	106,99	122,22	101,99	107,92	8,60	-0,55	0,32	95,68	98,13	109,81	112,42	104,01	8,34	-1,05	0,04
Non-Targeting siRNA		Plate4-NT#6	99,12	113,98	112,88		108,66	8,28	-0,54	0,40	106,33	110,02	102,84		106,39	3,59	-1,01	0,09
s41044	92912	**UBE2Q2_2**	147,49	106,87	82,54	100,47	109,34	23,76	-0,53	0,34	129,31	130,46	181,23	159,00	150,00	24,94	-0,32	0,55
s18779	9736	**USP34_1**	112,46	98,19	122,06	105,14	109,46	8,85	-0,53	0,34	106,67	121,40	137,95	122,94	122,24	12,79	-0,76	0,15
s9947	5021	**OXTR_2**	107,88	119,76	101,71		109,78	9,17	-0,53	0,41	162,64	168,72	140,84		157,40	14,66	-0,20	0,74
s30442	55208	**DCUN1D2_2**	102,39	103,35	128,40	105,02	109,79	10,78	-0,53	0,35	129,02	147,23	147,52	136,65	140,10	8,95	-0,47	0,36
s14576	7322	**UBE2D2_3**	116,69	113,98	105,77	106,22	110,67	4,77	-0,51	0,36	172,12	175,95	181,73	179,60	177,35	4,23	0,11	0,81
s38746	84259	**DCUN1D5_2**	99,16	109,25	115,11	119,21	110,68	7,53	-0,51	0,36	198,24	213,88	227,46	236,94	219,13	16,84	0,78	0,13
s39400	84749	**USP30_2**	111,86	113,85	108,29	113,64	111,91	2,23	-0,49	0,38	153,75	159,66	166,16	199,18	169,69	20,30	-0,01	1,00
s12386	6256	**RXRA_3**	103,57	85,00	150,96		113,18	34,01	-0,48	0,46	241,76	187,53	214,77		214,69	27,11	0,70	0,23
Non-Targeting siRNA		Plate2-NT#3	126,84	102,67	121,00	103,32	113,46	10,67	-0,47	0,40	122,23	113,49	105,34	104,67	111,43	8,24	-0,93	0,07
s846	19	**ABCA1_1**	134,81	93,09	113,05		113,65	20,87	-0,47	0,47	244,53	202,83	198,80		215,39	25,32	0,72	0,22
Non-Targeting siRNA		Plate2-NT#1	99,31	112,72	112,39	130,33	113,69	11,03	-0,47	0,41	104,94	106,06	103,28	120,65	108,73	8,03	-0,97	0,06
s14579	7323	**UBE2D3_3**	131,64	109,89	109,29	107,78	114,65	9,84	-0,45	0,42	170,87	210,36	169,08	171,21	180,38	20,01	0,16	0,74
s30441	55208	**DCUN1D2_1**	98,54	123,71	112,76	125,97	115,24	10,86	-0,44	0,43	142,89	166,73	146,60	156,99	153,30	10,76	-0,27	0,61
s3265	1269	**CNR2_3**	116,70	105,02	124,71		115,48	9,90	-0,44	0,50	178,08	179,43	198,50		185,34	11,42	0,24	0,68
s20571	10495	**ENOX2_1**	113,06	113,98	120,13		115,73	3,84	-0,44	0,50	142,61	144,86	138,00		141,82	3,50	-0,45	0,46
Non-Targeting siRNA		Plate1-NT#5	129,18	108,31	101,50	126,55	116,39	11,77	-0,43	0,45	106,37	100,76	95,42	102,05	101,15	4,51	-1,09	0,04
s10230	5154	**PDGFA_3**	94,55	129,58	125,86		116,66	19,24	-0,42	0,52	191,82	190,97	191,00		191,26	0,48	0,33	0,57
s47595	219333	**USP12_1**	113,67	117,81	97,46	137,97	116,73	14,43	-0,42	0,46	179,80	177,85	183,60	204,69	186,49	12,37	0,26	0,61
Non-Targeting siRNA		Plate3-NT#1	132,98	106,48	111,75		117,07	14,03	-0,42	0,53	108,84	95,23	97,21		100,43	7,35	-1,10	0,07
s31617	55832	**CAND1_2**	92,29	125,22	120,07	133,82	117,85	15,56	-0,41	0,48	217,77	216,78	214,67	228,51	219,43	6,19	0,78	0,13
s20031	10254	**STAM2_2**	125,06	111,21	130,14	106,52	118,23	9,68	-0,40	0,48	129,56	133,12	109,26	118,90	122,71	10,81	-0,75	0,15
s46284	161725	**OTUD7A_1**	124,59	123,64	124,42	103,07	118,93	9,17	-0,39	0,50	171,28	208,00	215,97	203,91	199,79	19,65	0,47	0,36

s18781	9736	**USP34_3**	106,45	132,82	125,22	115,62	120,03	9,93	-0,37	0,52	184,09	192,49	191,90	216,71	196,30	14,14	0,41	0,41
s30443	55208	**DCUN1D2_3**	128,18	117,33	132,87	108,03	121,60	9,66	-0,35	0,55	173,93	185,64	176,88	161,94	174,60	9,79	0,07	0,88
s24626	25853	**DCAF12_1**	103,61	124,34	129,36	132,65	122,49	11,29	-0,34	0,56	153,72	186,61	178,92	176,29	173,88	14,14	0,06	0,90
s26460	29089	**UBE2T_2**	126,12	134,15	126,18	104,23	122,67	11,13	-0,34	0,57	138,16	176,28	174,74	178,06	166,81	19,14	-0,05	0,93
s6173	2904	**GRIN2B_1**	140,07	130,13	98,57		122,92	21,67	-0,33	0,62	261,32	225,58	284,33		257,08	29,60	1,38	0,02
s20572	10495	**ENOX2_2**	133,42	106,89	130,72		123,68	14,60	-0,32	0,64	210,51	213,83	202,01		208,78	6,09	0,61	0,30
Non-Targeting siRNA		Plate3-NT#3	123,63	111,82	136,47		123,97	12,33	-0,32	0,64	88,43	99,80	100,93		96,39	6,91	-1,17	0,05
s21219	10800	**CYSLTR1_2**	114,55	136,16	123,08		124,60	10,88	-0,31	0,65	176,89	147,36	150,82		158,36	16,14	-0,19	0,76
s2277	773	**CACNA1A_2**	103,83	121,35	155,60		126,93	26,34	-0,27	0,70	211,91	176,67	160,28		182,95	26,38	0,20	0,72
Non-Targeting siRNA		Plate4-NT#1	125,99	113,51	142,51		127,34	14,55	-0,27	0,70	114,29	91,68	101,97		102,65	11,32	-1,07	0,07
s7635	3709	**ITPR2_2**	164,76	104,59	116,18		128,51	31,92	-0,25	0,72	222,87	210,46	195,41		209,58	13,75	0,62	0,29
s33006	57407	**NMRAL1_3**	107,88	153,72	124,02		128,54	23,25	-0,25	0,72	197,50	203,41	198,52		199,81	3,16	0,47	0,42
s560	7324	**UBE2E1_1**	116,39	125,97	140,27	132,85	128,87	8,80	-0,24	0,69	171,89	157,68	200,22	240,92	192,68	36,70	0,36	0,48
s9416	4734	**NEDD4_2**	172,10	118,98	111,15	114,62	129,21	24,92	-0,24	0,70	187,97	187,88	200,98	202,53	194,84	8,01	0,39	0,44
s25671	26994	**RNF11_2**	133,49	130,49	139,91	113,83	129,43	9,63	-0,24	0,70	203,66	227,75	253,62	294,50	244,88	38,86	1,18	0,02
s39401	84749	**USP30_3**	144,98	114,48	143,36	115,12	129,49	14,70	-0,23	0,70	168,55	157,93	172,09	200,67	174,81	18,26	0,07	0,88
s41045	92912	**UBE2Q2_3**	86,23	187,53	108,72	136,83	129,83	37,83	-0,23	0,71	165,48	190,03	195,90	212,20	190,90	19,37	0,33	0,52
s14724	7398	**USP1_2**	168,53	117,81	129,76	108,79	131,22	22,79	-0,21	0,74	190,19	223,33	210,35	213,59	209,36	13,92	0,62	0,22
s38745	84259	**DCUN1D5_1**	117,62	111,67	156,09	140,20	131,39	17,79	-0,21	0,75	116,32	132,77	117,48	114,73	120,32	8,38	-0,79	0,13
s24092	23558	**WBP2_1**	100,70	148,58	90,78	185,85	131,48	38,25	-0,21	0,75	131,51	140,80	125,82	164,18	140,58	16,90	-0,47	0,37
s44389	140739	**UBE2F_3**	112,38	127,66	148,56	137,58	131,55	13,31	-0,20	0,75	124,20	153,13	137,72	137,82	138,22	11,82	-0,50	0,33
s10228	5154	**PDGFA_1**	154,08	132,33	108,39		131,60	22,85	-0,20	0,78	129,88	114,33	98,91		114,38	15,49	-0,88	0,14
s16975	8883	**NAE1_1**	106,20	145,98	141,49	133,59	131,81	15,44	-0,20	0,75	163,88	178,26	214,55	187,06	185,94	21,34	0,25	0,62
s41001	92714	**ARRDC1_1**	115,23	132,68	159,84	122,35	132,52	16,95	-0,19	0,77	155,88	183,23	157,15	165,33	165,40	12,61	-0,07	0,89
s12384	6256	**RXRA_1**	108,67	130,83	162,60		134,03	27,11	-0,17	0,83	231,60	219,86	213,04		221,50	9,39	0,81	0,17
s7636	3709	**ITPR2_1**	118,93	149,89	133,42		134,08	15,49	-0,17	0,83	125,29	132,82	114,03		124,05	9,46	-0,73	0,23
s27293	51035	**UBXN1_3**	123,98	148,77	156,93	108,88	134,64	19,19	-0,16	0,82	164,95	186,97	206,78	216,22	193,73	22,73	0,37	0,46
s21339	10869	**USP19_1**	158,56	137,02	129,27	113,74	134,65	16,15	-0,16	0,82	165,81	209,19	187,82	188,14	187,74	17,71	0,28	0,58
s14725	7398	**USP1_3**	128,88	147,42	144,28	121,39	135,49	10,75	-0,15	0,84	159,03	171,24	160,54	167,20	164,50	5,73	-0,09	0,87
s21221	10800	**CYSLTR1_3**	156,33	116,97	136,19		136,50	19,68	-0,13	0,88	265,54	237,98	221,64		241,72	22,19	1,13	0,06
s16313	8567	**MADD_1**	137,10	121,95	151,94		136,99	15,00	-0,12	0,89	261,37	191,00	212,24		221,53	36,10	0,81	0,17
s23128	23142	**DCUN1D4_2**	134,75	134,04	138,25	147,93	138,74	5,54	-0,10	0,91	182,19	186,83	148,02	176,73	173,44	17,44	0,05	0,91
s24628	25853	**DCAF12_3**	110,73	125,22	184,32	138,53	139,70	27,57	-0,08	0,93	124,64	133,24	155,11	133,51	136,62	12,99	-0,53	0,31
s18780	9736	**USP34_2**	160,80	141,23	137,08	126,31	141,35	12,48	-0,06	0,97	143,06	160,51	163,63	142,77	152,49	11,13	-0,28	0,60
s12467	6300	**MAPK12_1**	114,47	169,43	143,71		142,53	27,50	-0,04	1,00	128,09	155,47	134,02		139,20	14,41	-0,49	0,42
s17229	9040	**UBE2M_1**	137,45	149,83	162,98	121,45	142,93	15,34	-0,04	1,00	91,05	79,23	70,36	66,57	76,80	10,88	-1,48	0,00
s16480	8658	**TNKS_1**	137,00	155,79	129,17	151,87	143,46	10,83	-0,03	0,98	256,87	291,72	224,89	273,58	261,77	28,41	1,45	0,00
s10229	5154	**PDGFA_2**	139,72	160,41	133,06		144,40	14,26	-0,01	0,97	145,55	134,20	126,18		135,31	9,73	-0,55	0,36

s27291	51035	UBXN1_1	215,67	151,00	108,72	102,53	144,48	45,14	-0,01	0,96	97,94	100,87	100,03	70,73	92,39	14,50	-1,23	0,02
s16977	8883	NAE1_3	125,95	141,37	154,56	160,92	145,70	13,41	0,00	0,93	181,39	203,77	163,48	196,39	186,26	17,81	0,26	0,61
s1538	367	AR_1	167,66	158,27	111,23		145,72	30,23	0,01	0,94	212,06	176,49	170,45		186,33	22,48	0,26	0,66
s14575	7322	UBE2D2_2	185,93	154,33	119,14	132,59	148,00	25,25	0,04	0,88	158,59	176,79	171,54	157,60	166,13	9,53	-0,06	0,91
s31618	55832	CAND1_3	110,43	141,66	155,43	187,23	148,69	27,59	0,05	0,87	225,79	221,11	254,17	266,30	241,84	21,89	1,13	0,03
s561	7324	UBE2E1_2	147,49	162,24	161,07	128,00	149,70	13,80	0,06	0,84	157,35	179,94	218,44	179,10	183,71	25,41	0,21	0,67
s5837	2743	GLRB_3	216,54	121,21	114,87		150,87	56,96	0,08	0,84	211,95	165,56	185,87		187,79	23,25	0,28	0,63
s1797	526	ATP6V1B2_1	158,88	123,06	170,81		150,92	24,85	0,08	0,84	267,62	276,52	278,50		274,22	5,80	1,65	0,01
s19997	10242	KCNMB2_1	128,10	155,32	169,46		150,96	21,02	0,08	0,84	204,31	216,41	165,93		195,55	26,36	0,40	0,49
s16315	8567	MADD_3	143,47	164,76	149,02		152,41	11,04	0,10	0,81	199,23	208,15	209,65		205,68	5,63	0,56	0,34
s14578	7323	UBE2D3_2	152,21	172,12	140,45	145,60	152,59	12,02	0,11	0,78	161,14	214,31	144,04	185,60	176,27	30,56	0,10	0,84
s23127	23142	DCUN1D4_1	146,70	112,49	207,87	144,04	152,77	34,54	0,11	0,78	186,96	221,51	219,54	215,06	210,77	16,10	0,64	0,21
s1798	526	ATP6V1B2_2	143,54	169,86	146,06		153,15	14,52	0,12	0,80	266,68	237,92	261,47		255,36	15,32	1,35	0,02
s24094	23558	WBP2_3	153,51	112,72	176,02	174,20	154,11	25,48	0,13	0,75	132,91	135,05	122,98	128,71	129,91	5,32	-0,64	0,22
s6175	2904	GRIN2B_3	148,70	122,49	193,21		154,80	35,75	0,14	0,77	168,68	176,55	153,55		166,26	11,69	-0,06	0,93
s19998	10242	KCNMB2_2	134,93	144,81	187,60		155,78	28,00	0,15	0,75	193,40	202,73	218,76		204,96	12,83	0,55	0,35
s9415	4734	NEDD4_1	146,23	135,96	180,92	161,34	156,11	16,93	0,16	0,70	213,79	221,87	268,48	259,57	240,93	27,12	1,12	0,03
s21341	10869	USP19_3	160,16	159,42	150,55	158,05	157,05	3,83	0,17	0,68	112,53	105,20	116,66	126,94	115,33	9,07	-0,87	0,10
s46285	161725	OTUD7A_2	204,55	169,27	130,59	125,01	157,36	32,14	0,18	0,68	151,10	164,13	144,49	148,27	151,99	8,53	-0,29	0,59
s6101	2875	GPT_1	138,17	193,62	140,39		157,39	31,39	0,18	0,72	302,04	307,95	336,52		315,50	18,44	2,30	0,00
s16976	8883	NAE1_2	177,61	154,64	152,62	147,68	158,14	11,52	0,19	0,66	169,45	171,77	140,17	137,55	154,74	18,39	-0,24	0,65
s24627	25853	DCAF12_2	165,34	150,15	167,09	151,13	158,43	7,82	0,19	0,65	135,64	120,79	121,85	131,03	127,32	7,20	-0,68	0,19
s42682	123879	DCUN1D3_1	140,31	151,10	183,33	169,45	161,05	16,55	0,23	0,60	114,85	126,84	145,79	129,59	129,27	12,74	-0,65	0,21
s6063	2859	GPR35_1	146,59	145,59	194,14		162,11	27,74	0,25	0,63	177,03	184,47	156,33		172,61	14,58	0,04	0,94
s31616	55832	CAND1_1	147,47	111,90	200,56	188,62	162,14	35,06	0,25	0,58	242,99	303,33	269,40	325,06	285,20	36,28	1,82	0,00
s2065	667	DST_1	110,28	153,99	212,31	175,80	163,10	36,93	0,26	0,56	186,94	196,16	226,87	228,54	209,63	21,22	0,62	0,22
s6938	3292	HSD17B1_1	163,41	132,33	196,35		164,03	32,01	0,28	0,60	208,93	211,37	180,41		200,23	17,21	0,48	0,42
s562	7324	UBE2E1_3	150,32	161,11	195,85	151,83	164,78	18,41	0,29	0,53	186,47	186,79	230,00	226,81	207,52	24,16	0,59	0,25
s46286	161725	OTUD7A_3	214,62	194,82	122,53	128,99	165,24	40,16	0,29	0,52	129,09	152,90	140,89	142,38	141,31	9,75	-0,46	0,38
s5835	2743	GLRB_1	164,98	158,90	173,24		165,71	7,20	0,30	0,57	249,18	196,62	215,29		220,36	26,65	0,79	0,18
s44387	140739	UBE2F_1	125,50	162,25	184,07	195,37	166,80	26,65	0,32	0,49	215,99	274,89	227,42	264,49	245,70	28,41	1,20	0,02
s12469	6300	MAPK12_3	146,59	194,85	170,74		170,73	24,13	0,37	0,49	211,87	235,94	200,77		216,19	17,98	0,73	0,22
s9946	5021	OXTR_1	173,75	141,71	204,47		173,31	31,38	0,41	0,45	176,93	180,19	167,08		174,73	6,82	0,07	0,89
s33305	57558	USP35_2	184,27	172,73	175,24	162,14	173,59	7,88	0,42	0,38	160,51	180,00	181,97	171,56	173,51	9,77	0,05	0,91
s7801	3783	KCNN4_1	166,26	177,25	181,71		175,07	7,95	0,44	0,42	137,75	133,28	140,02		137,02	3,43	-0,52	0,38
s14577	7323	UBE2D3_1	173,08	191,96	147,28	192,28	176,15	18,39	0,45	0,34	156,29	190,03	141,36	186,50	168,55	23,62	-0,02	0,97
s20573	10495	ENOX2_3	190,02	168,60	177,49		178,70	10,76	0,49	0,37	226,42	230,72	203,23		220,12	14,79	0,79	0,18
s6940	3292	HSD17B1_3	175,46	166,95	197,73		180,05	15,90	0,51	0,36	580,79	460,33	450,70		497,27	72,49	5,17	0,00

s8879	4323	MMP14_3	198,59	177,81	175,66		184,02	12,66	0,57	0,31	223,67	192,82	168,31		194,93	27,74	0,39	0,50
s33004	57407	NMRAL1_1	218,06	148,72	191,40		186,06	34,98	0,60	0,28	173,69	166,09	174,79		171,52	4,74	0,02	0,96
s14603	7336	UBE2V2_3	168,53	197,01	172,47	216,20	188,55	19,34	0,64	0,19	148,86	160,25	143,79	199,04	162,98	25,00	-0,11	0,84
s2278	773	CACNA1A_1	225,78	129,84	219,75		191,79	53,74	0,69	0,23	147,36	103,82	93,41		114,86	28,62	-0,87	0,15
s7061	3362	HTR6_3	216,54	145,77	216,73		193,01	40,92	0,70	0,21	159,84	124,97	140,68		141,83	17,47	-0,45	0,46
s16314	8567	MADD_2	194,93	197,22	188,14		193,43	4,72	0,71	0,21	225,05	192,82	175,21		197,69	25,27	0,44	0,46
s844	18	ABAT_2	231,13	194,63	160,02		195,26	35,56	0,74	0,19	248,61	190,40	179,78		206,26	37,06	0,57	0,33
s11215	5624	PROC_1	218,89	158,26	211,06		196,07	32,98	0,75	0,19	236,38	230,31	241,26		235,98	5,48	1,04	0,08
s7568	3685	ITGAV_1	195,68	174,39	218,41		196,16	22,01	0,75	0,19	261,92	251,46	229,83		247,74	16,37	1,23	0,04
s20030	10254	STAM2_1	139,55	191,18	243,55	224,42	199,68	39,45	0,80	0,10	163,86	175,52	163,20	179,80	170,59	8,35	0,01	0,98
s7634	3709	ITPR2_3	267,36	165,22	168,08		200,22	58,16	0,81	0,16	268,44	200,14	205,66		224,75	37,94	0,86	0,14
s24093	23558	WBP2_2	158,41	188,37	235,46	227,84	202,52	31,12	0,84	0,09	125,07	134,01	99,45	114,13	118,16	14,89	-0,82	0,11
s1799	526	ATP6V1B2_3	241,55	163,15	215,40		206,70	39,91	0,91	0,11	247,23	254,01	237,75		246,33	8,17	1,21	0,04
s8877	4323	MMP14_1	235,99	190,45	198,01		208,15	24,41	0,93	0,11	256,43	244,51	200,95		233,96	29,21	1,01	0,09
s1948	613	BCR_2	260,61	179,95	216,06		218,87	40,41	1,09	0,06	214,73	192,89	178,10		195,24	18,43	0,40	0,50
s843	18	ABAT_1	281,69	175,20	216,73		224,54	53,67	1,17	0,04	214,68	189,07	182,21		195,32	17,11	0,40	0,50
s6157	2898	GRIK2_3	242,17	211,15	234,06		229,13	16,09	1,24	0,03	291,71	262,07	246,40		266,73	23,01	1,53	0,01
s14574	7322	UBE2D2_1	157,61	279,48	184,09	299,87	230,26	60,58	1,25	0,01	161,96	202,30	162,09	254,36	195,18	43,79	0,40	0,43
s1540	367	AR_3	216,54	213,42	263,11		231,02	27,83	1,26	0,03	35,93	47,13	36,36		39,81	6,34	-2,06	0,00
s5831	2741	GLRA1_1	254,01	186,23	254,82		231,69	39,36	1,27	0,03	243,85	233,00	227,13		234,66	8,48	1,02	0,08
s3263	1269	CNR2_1	286,31	219,19	195,52		233,67	47,10	1,30	0,02	225,93	220,95	196,19		214,36	15,93	0,70	0,24
s11216	5624	PROC_2	248,74	216,38	237,21		234,11	16,40	1,31	0,02	117,05	115,24	119,12		117,13	1,94	-0,84	0,16
s223918	3480	IGF1R_3	239,68	193,79	272,26		235,24	39,42	1,33	0,02	169,37	142,73	140,17		150,76	16,17	-0,31	0,61
s6155	2898	GRIK2_1	299,29	165,54	241,02		235,28	67,06	1,33	0,02	233,93	181,06	192,51		202,50	27,81	0,51	0,38
s17718	9266	CYTH2_1	245,74	205,01	256,83		235,86	27,28	1,34	0,02	137,60	93,92	116,81		116,11	21,85	-0,85	0,15
s6174	2904	GRIN2B_2	251,73	203,00	256,25		236,99	29,53	1,35	0,02	226,56	203,26	211,17		213,67	11,85	0,69	0,24
s41043	92912	UBE2Q2_1	256,48	238,88	227,67	235,41	239,61	10,55	1,39	0,01	172,34	171,36	172,47	182,89	174,76	5,44	0,07	0,88
s848	19	ABCA1_3	285,64	206,80	230,28		240,91	40,48	1,41	0,02	140,33	144,09	126,11		136,84	9,49	-0,53	0,38
s6939	3292	HSD17B1_2	238,92	233,23	250,60		240,92	8,86	1,41	0,02	165,24	167,29	147,22		159,92	11,05	-0,16	0,79
s845	18	ABAT_3	318,23	181,76	236,83		245,61	68,66	1,48	0,01	249,62	187,66	181,29		206,19	37,75	0,57	0,33
s41002	92714	ARRDC1_2	203,02	205,12	345,01	241,21	248,59	57,70	1,52	0,00	137,14	144,43	140,53	142,75	141,21	3,15	-0,46	0,38
s17719	9266	CYTH2_2	256,66	216,07	274,11		248,95	29,78	1,53	0,01	137,22	135,30	142,74		138,42	3,86	-0,50	0,41
s21220	10800	CYSLTR1_1	314,68	199,23	239,27		251,06	58,62	1,56	0,01	265,37	221,30	233,30		239,99	22,78	1,10	0,06
s7211	3480	IGF1R_1	251,40	223,86	283,04		252,77	29,61	1,59	0,01	106,93	98,28	104,39		103,20	4,45	-1,06	0,08
s1949	613	BCR_1	279,90	197,01	289,44		255,45	50,84	1,63	0,01	272,54	226,78	212,01		237,11	31,56	1,06	0,07
s7212	3480	IGF1R_2	331,96	208,19	245,23		261,79	63,53	1,72	0,00	144,19	109,38	112,00		121,86	19,38	-0,76	0,20
s22708	22933	SIRT2_3	238,04	258,63	293,73		263,47	28,16	1,74	0,00	123,96	124,70	105,42		118,03	10,92	-0,82	0,17
s1539	367	AR_2	370,75	185,73	248,41		268,30	94,10	1,82	0,00	220,52	149,59	168,66		179,59	36,71	0,15	0,79

s5836	2743	GLRB_2	290,37	213,25	316,08		273,23	53,52	1,89	0,00	191,26	176,29	142,28		169,94	25,10	0,00	1,00
s16481	8658	TNKS_2	183,22	243,02	334,41	396,22	289,22	81,95	2,12	0,00	169,50	170,80	181,25	197,43	179,75	12,91	0,15	0,76
s12468	6300	MAPK12_2	279,75	287,41	300,76		289,31	10,63	2,13	0,00	180,66	175,06	180,45		178,72	3,17	0,14	0,81
s9417	4734	NEDD4_3	341,78	338,43	247,47	232,93	290,15	50,23	2,14	0,00	108,03	135,03	122,03	112,33	119,35	11,98	-0,80	0,12
s6064	2859	GPR35_2	245,14	326,76	330,62		300,84	48,27	2,30	0,00	67,22	97,16	89,07		84,48	15,49	-1,35	0,02
s47596	219333	USP12_2	369,11	387,81	364,64	327,00	362,14	22,07	3,20	0,00	46,61	62,38	63,72	61,86	58,64	8,06	-1,76	0,00
s9948	5021	OXTR_3	425,61	349,11	347,89		374,20	44,53	3,38	0,00	143,83	115,42	125,67		128,31	14,39	-0,66	0,27
s847	19	ABCA1_2	373,46	269,99	500,85		381,44	115,64	3,49	0,00	68,96	70,93	66,03		68,64	2,47	-1,60	0,01
s5830	2741	GLRA1_3	468,87	307,37	402,27		392,83	81,16	3,65	0,00	174,71	160,19	130,07		154,99	22,77	-0,24	0,70
s6102	2875	GPT_2	472,16	321,40	492,61		428,72	93,51	4,18	0,00	106,41	141,17	140,44		129,34	19,86	-0,64	0,28

Table 7.3. Host factor identified in HBV proteome analysis - LC-MS/MS results

The IBAQ scores (log2) of the host factors in Figure 3.2.12. are listed below.

Cell Line	Hep AD38	Hep AD38	Hep AD38	Hep AD38	Hep AD38	Hep AD38	Hep AD38	Hep AD38	Hep AD38	Hep AD38	Hep AD38	Hep AD38	Hep AD38	Hep AD38	Hep AD38	Hep AD38	Hep AD38	Hep AD38	Hep AD38	Hep AD38	Hep G2	Hep G2	Hep G2	Hep G2	HB2.7	HB2.7	HB2.7	HB2.7	HB2.7	HB2.7	HB2.7	HB2.7
Fraction	HBV	HBV	HBV	HBV	HBV	HBV	HBV	HBV	HBV	HBV	SVP	SVP	SVP	SVP	SVP	SVP	SVP	SVP	SVP	SVP	HBV	HBV	HBV	HBV	SVP	SVP	SVP	SVP	SVP	SVP	SVP	SVP
Anti-	HBS	HBS	HBS	HBS	HBS	IgG1	IgG1	IgG1	IgG1	IgG1	HBS	HBS	HBS	HBS	HBS	IgG1	IgG1	IgG1	IgG1	IgG1	HBS	HBS	HBS	HBS	HBS	HBS	HBS	HBS	IgG1	IgG1	IgG1	IgG1
Gene	Rep1	Rep2	Rep3	Rep4	Rep5	Rep1	Rep2	Rep3	Rep4	Rep5	Rep1	Rep2	Rep3	Rep4	Rep5	Rep1	Rep2	Rep3	Rep4	Rep5	Rep1	Rep2	Rep3	Rep4	Rep1	Rep2	Rep3	Rep4	Rep1	Rep2	Rep3	Rep4
HBV Envelope	28,9	29,1	29,0	30,0	31,7						28,7	29,2	28,7	31,2	30,2										33,0	32,3	32,9	32,8		21,0		
HBV core	27,6	27,5	28,6	29,4	31,4						22,7	23,6	21,5	28,3	24,3										20,4							
APOE	23,2	23,6	23,8	23,6	27,1	19,7		20,6	19,7	19,9	24,7	25,7	24,5	27,8	25,0	22,6	22,9	23,5	21,7	18,7					30,7	29,4	30,2	29,9	23,7	24,9	23,1	24,4
CYB5A	22,6	23,9	24,4	24,1	26,7						22,5	24,1		26,5	24,8										28,2	27,1	27,6	27,3				
RAN		22,1	21,4	23,5	25,5			19,3				22,1	21,3	25,0	22,0					21,7					27,3	25,0	26,3	27,6				
HBV pol	22,0	22,3	23,0	23,1	25,4						20,2	20,1	19,4	24,2	21,3																	
PPIA					24,9									25,2	20,4										26,6	25,3	26,2	26,4				
ACTB	23,4	24,8	22,9	23,7	24,9	22,2	22,1	22,0	21,8	21,9	22,6	22,3	22,8	24,5	22,8	22,3			22,4	22,6	23,3	23,3	23,3	23,1	26,9	25,5	26,5	26,3	22,7	22,4	22,4	22,1
MXRA7				20,9	24,8									22,7											22,0	21,8	23,5	24,4				
DCD		22,1	26,4		24,8	26,2	25,7	26,3	22,8	25,1	26,2	24,9	24,9	22,3		23,5	24,0	25,6	23,3							22,5	23,7	22,8	23,3	20,8		25,2
NUTF2					24,5									24,7	23,1										28,9	27,6	28,4	28,4				

APMAP				21,0	24,5							20,4		24,5	21,0									26,8	25,4	26,3	25,9							
APOC1					24,4					24,9	22,1		26,6		23,5									27,9	27,1	28,2	29,2		23,4					
LMO7		24,7	24,2		24,4		24,0									23,8		24,1									22,6							
MLF2				21,2	24,3								23,7	20,9										26,5	24,9	25,2	25,2							
UBC	22,6	23,0	21,1	22,9	24,1		18,7		18,1		21,0	22,3	21,3	24,5	23,8	19,4		20,3	20,4	21,0	18,0	19,2	19,2	21,1	26,3	25,0	24,8	24,5	20,0	21,0		20,2		
APOA1	20,3	20,4		20,2	24,0		19,7				23,7	22,3	21,1	23,5	19,9	21,5		21,3			18,7	19,4	19,1		25,2	24,6	25,2	24,7		21,9		19,8			
APOA2					23,9					23,1			23,7				22,5							26,8	25,7	26,2	25,6		24,0	21,9	22,4			
PDCD6					23,7						21,2		24,4											26,7	24,6	26,3	25,8							
CYSTM1					23,7																				22,7	23,4	23,0							
HNRNPC			21,3	20,6	23,5																													
GAPDH	20,4	29,0	21,7	22,0	23,3				21,1		19,7	23,1	19,9	19,2	22,7	19,8			19,5	19,1	20,2	21,4	21,2	21,2	22,0	21,8	21,3	21,5							
FKBP1A					23,2																			25,9	23,3	25,5	25,4							
LGALS3	20,8		20,7	21,9	23,1						20,7	19,5	23,6	21,1										26,6	25,4	25,5	25,1							
HSPB1	20,9	19,9	20,7	21,6	23,1					19,7	20,6	19,3	23,2	21,1	19,5			20,4				21,2			23,4	23,1	23,8	23,6							
RAB5C					23,1								22,8											26,1	24,5	25,3	25,0							
LMAN2				19,6	23,0								22,1											24,0	22,0	22,9	22,5							
GPC3			20,6	21,6	23,0								21,4											23,4		22,6	23,8							
CDIP1					22,9								22,5											23,7		23,5	25,3							
LGALS3BP		19,9	21,4	19,8	22,9		20,9	20,4		18,5	19,0							20,3			18,4			18,7	23,9	22,7	22,4	23,5	21,4					
ARF1		20,4			22,8								23,2	20,5										23,1	20,9	24,5	24,5							
RAB1B					22,8								21,8											25,9	22,1	25,3	24,0							
PEF1					22,7								21,7											26,3	23,7	24,4	25,0							
PFN1					22,6								21,5											24,6	23,9	24,8	24,7							
PEBP1					22,6								21,2											25,1	23,2	24,3	24,9							
NCEH1				20,1	22,5						17,6		21,0	17,9										23,6	22,7	24,1	24,1							
RAB11B					22,5								23,1	21,3										25,9	23,0	24,7	24,9							
APOC3		19,9	19,6	20,3	22,5					22,5			22,7		20,5			20,8							24,0	22,9	24,8	24,2							
RAB2A					22,3								22,4											24,9	23,4	24,8	24,7							
RAB1A					22,0																			24,7	23,4	24,0	24,7							
HSPA8		18,3	18,6	18,6	21,9							18,0	21,3	18,3										23,6	22,3	23,3	22,0							

EEF1A1	19,8	23,4			21,9			19,7						20,9				22,7	22,0	20,8			21,0		20,4							
SULT1A3					21,6																		22,6	19,7	21,6							
CSTA	22,5	23,0	25,1		21,6						22,5	24,3			22,2					21,5		22,0		22,3	21,7	22,4	22,1	24,4			
PGK1		24,9			21,5									21,0	18,5								24,0	22,8	23,6	23,7					
CSTB					21,5																		25,9	25,5	26,4	26,3					
RAB6A					21,5							18,6		20,7	21,3								25,0	22,0	23,6	24,3					
TXN	22,4		22,4	21,6	21,5						21,0	24,1		23,9	24,6			22,1				22,1	26,8	25,4	25,9	25,3		23,4			
SMPD4				18,4	21,4									20,7									23,7	22,1	24,2	23,2					
ANXA7				19,8	21,3									22,1									24,9	21,7	24,3	24,4					
PON2				19,9	21,2							19,5	18,5	22,0									25,7	24,6	24,8	25,4					
FABP1					21,1									23,9	21,3								24,9	23,2	24,7	23,3					
DNAJB12				19,4	21,1									20,7									23,0	21,8	22,7	23,5					
EPHX1					21,0																		22,5	22,4	21,5	22,6					
APOL2					21,0									21,0									23,3	21,1	22,2	22,9					
C3					20,8									15,8					15,6				21,4	20,1	20,5	21,6					
HSPA1B		18,7	19,3	18,8	20,7									20,8									23,6	22,5	22,6	22,7					
TPI1		25,5			20,6																	18,4	23,0	22,1	23,9	23,7					
PKM	19,6	26,3			20,6		18,6		20,5	19,4					20,0		18,5	18,9	22,2			19,0									
GDE1		20,2	20,6	21,3	20,5						19,5	20,7		23,1	20,2								26,4	25,0	26,1	26,2					
RAB14					20,5									20,7									23,0	21,2	23,0	22,9					
CANX				19,0	20,4							18,9	18,8	21,6	19,0								25,0	23,9	25,0	24,6					
TF				17,4	20,4									17,6									23,3	21,8	22,6	22,4					
HAX1					20,4									21,5									25,5	24,3	24,0	24,3					
PGRMC1					20,4									22,6									24,5	23,8	24,7	24,3					
SULT2A1					20,4																		21,2	20,2	21,4	20,5					
HSP90AB1		19,5			20,3		17,9		18,2	18,1					19,4				19,6													
DQX1					20,2																		23,5	20,9	21,9	22,0					
ENO1		21,9			20,1			19,6						21,1	22,8				21,0	19,2		19,3	20,5	25,2	24,9	25,2	25,9					
PCBP1					20,0									19,3									23,2	21,6	22,5	21,6					
NUP155				17,4	19,9									21,5	17,4								24,0	21,9	23,2	23,0					

TUBB4B		20,8			19,8																				19,5		18,1	18,8									
POR					19,8								19,5												24,6	24,4	24,4	24,9									
ARSE					19,6								19,9												23,7	21,9	23,3	23,8									
RAB21					19,6								21,5												24,5	22,0	23,7	23,6									
RAB10					19,3																				21,0	20,4	21,4	21,3									
TMX2					19,3								18,5												22,4	21,1	22,6	22,8									
GDI2					19,0								18,7												21,6	22,3	22,9	23,2									
CYP17A1					18,9																				19,4	19,0	21,4	21,6									
ACSL5					18,7																				21,5	19,1	21,3	18,9									
NSDHL					18,5								19,3												24,0	21,2	23,8	23,6									
HSPD1				16,1	17,6				18,2					18,0						17,7	21,4	19,6	18,2	19,1	17,9												
DHRS7																									21,3		21,3	20,9									
SAA2-SAA4													22,5												24,3	22,8	24,6	23,1									
CYP4F2																									21,5	20,2	21,4	20,2									
PLEKHB2																									22,8	21,3		19,9									
AKR1C3													19,8												22,9	20,7	22,5	22,2									
C4B															18,0			18,8							16,7		17,1	17,8									
DNAJB6																									23,7	20,4	21,5	22,0									
ILVBL																									19,5	18,5	19,1	19,2									
DDT																									21,9	21,0	22,0	22,1									
ANXA2	20,7	20,3	19,0	21,3			20,2		21,2		21,8	18,0	22,4	17,9	17,7	22,1	20,6		20,7	20,8	22,4	17,8	18,4	18,4	21,4		20,9	18,5									
CPNE1																									22,3	21,7	22,3	21,6									
ARL1																									21,6		21,1	20,9									
MAPK14																									21,7	19,2	21,9	20,7									
PMS1							21,7	21,6	22,0	21,8	21,9						21,1	21,2	21,1	21,9	22,1								21,2	21,0	20,9	21,4					
C9orf172		25,4	25,6	25,4								20,4	26,4	23,1		20,7						24,1	23,4	29,0	24,9	26,8	29,2	21,4	26,7									
PFN2																									22,3		22,0	22,0									
MAPKAPK3																									20,5		19,7	21,4									
FGG																						19,4				23,1		21,6	19,7								
CPLX2																									24,3	23,1	23,7										

SAR1B															22,9											24,5		24,0	24,9				
CYB5B																										23,5		22,9	22,9				
LYPLA1																										21,6	22,1	22,7	24,4				
GBE1																										23,4	21,5	22,3	23,0				
USP2																	20,9	21,6	21,9	22,3													21,5
CFL1																										20,7		21,5	21,4				
C11orf73																										24,1	21,0		21,6				
IFITM3															21,7											24,3		23,8	22,6				
CD63																										23,0		22,2	21,4				
CTTNBP2							21,5	21,4			22,2																						
GCA																										25,4	23,5	24,2	24,2				
SOD1													20,6													23,2	22,9	22,9	22,5				
ACTN1																										20,4	18,8	20,0	20,0				
CDKN2A																										21,3	20,6	22,2	20,9				
CLIC1																										23,0	19,8	22,3	21,3				
SDCBP																										23,4	22,0	22,5	21,7				
PGRMC2															19,3											23,6	21,0	21,0	22,6				
LYPLA2																										23,7	22,7	23,0	24,0				
LDHA		25,0																								21,6	20,4	22,1					
CYB5R3															20,2											21,9	21,1	21,4	22,7				
APOH							19,1	20,0			21,5						23,4		21,7	21,9	21,9							19,0		22,3	24,1	21,5	22,6
FN1																										17,9	17,1	18,9	20,9		16,8	16,4	
APOB																										20,3	18,8	20,9	19,5		14,5		
S100A9	23,7		22,2	27,1			21,2			20,1		21,7					20,7			21,8		20,4			23,2	22,6	23,4	21,7					
LGALS1																						19,4			21,5	21,9	20,1	20,6	21,2				
RNH1																										18,3		18,6	18,7				
MIF															24,0											26,3	25,0	26,4	26,5				
AKR1A1																										19,8	18,3	19,2	19,0				
DSP	17,8			17,2			14,4						19,9			21,7				18,4			18,9	16,3	19,9								
COMT																										21,1	21,2	22,7	22,7				

TGM2																										18,6	17,6		18,6				
S100A1																										27,1	27,0	27,6	27,4				
DNAJB2															20,9											23,3	22,9	23,7	23,6				
S100P																											23,6	24,0	24,2				
PRDX6															17,9											21,7	20,9	22,3	22,0				
CASP14	19,1	18,8	21,2	23,6									23,3			20,0									20,6								
NNMT																											20,9	21,1	21,0				
HINT1																										23,9	22,0	22,2	23,2				
KHK																										20,5	19,8	20,2					
EMD																										23,5	20,2	21,3	20,6				
RAB7A															21,6											24,4	23,3	24,2	24,2				
GALK1																											19,0	20,6	19,4				
ARSD																											18,1	19,5	19,5				
NAPA																										22,1	21,0	22,2	21,6				
DCAF7																										23,2		20,2	20,9				
GRB2																										23,1	20,7	22,6	22,3				
ACTA1		21,9																								21,9		18,7	21,5				
DSG1	21,0		20,7				19,4						23,3			24,1	20,0	17,9		20,8	20,5		21,6	19,0	22,6					19,4	20,4		
GLO1																										19,7		20,2	19,7				
CSTF1															18,8											23,8	21,2	22,3	20,8				
DSC1	20,3		20,1	18,7			18,8						23,5			23,7				20,7			21,8		22,1	18,4					20,5		
COASY																										20,0		19,5	19,4				
RAB32																										23,7	21,7	22,1	21,7				
APOF																										23,4	21,1	21,5					
BAAT																										23,1	20,5	22,1	23,6				
CWF19L2	20,2	18,8	20,2																														
PSMF1															22,1											23,3	21,8	22,3	21,0				
ASPHD1																										21,5		20,3	18,0				
SBSN	21,6	18,2	18,3	22,9								19,1	22,3			24,2				18,6											21,9		
RAB43																										22,5	20,0	21,6	20,0				

MAPK1IP1L																25,7	24,4	24,7	25,1				
ATL2																18,8	20,1	20,6	20,3				
RAB2B							18,3									18,9		20,4	20,3				
CCDC107																23,4	19,8		22,3				
NDRG1							19,0									24,4	22,5	23,9	24,6				
TNPO1																19,9	18,4	19,2					
TESC							21,8									23,3		21,7	21,9				
PDXP																19,6		19,1	19,6				
ERO1L																21,9	20,2	21,9	21,7				
VPS13A				21,0	20,4	21,6			18,8	20,4	19,9		21,5							20,6	20,0	20,4	20,5
DUSP9																22,2	19,7	21,1	20,2				
CPPED1																21,1	18,3	20,3	21,2				
AIFM2																22,0	20,7	20,9					
CARD9			23,4	23,4	23,0	22,6				22,8	23,0	23,2	23,1							23,1		23,4	
HSD3B7																22,3	20,3	20,4	19,6				
SAR1A																24,8	21,2	23,5	24,0				
MDN1		19,9	19,7		19,0	19,8			17,9	18,2	19,4	19,5	20,1			20,6				19,3		19,5	19,5